# Realization of a Kerr-lens mode-locked vertical-external-cavity surface-emitting laser

Dissertation

zur Erlangung des Doktorgrades der Naturwissenschaften
(Dr. rer. nat.)
dem Fachbereich Physik
der Philipps-Universität Marburg


vorgelegt von

**Mahmoud Abdelaziz Gaafar**

aus

Beheira, Ägypten

Marburg (Lahn), September 2015

Vom Fachbereich Physik der Philipps-Universität Marburg (Hochschulkennziffer 1180)
als Dissertation angenommen am: 20.11.2015

| | |
|---|---|
| Erstgutachter: | Prof. Dr. Martin Koch |
| Zweitgutacher: | Prof. Dr. Wolfgang Stolz |

Tag der mündlichen Prüfung: 30.11.2015

Dedicated to my father

# Acknowledgements

In this thesis, the work that I have carried out at the Department of Physics and Material Sciences Center, Philipps-University of Marburg, during the years 2012-2015 is introduced. In the first place, I want to express my gratitude to my supervisor, Professor Martin Koch, for giving me the opportunity to do my PhD in his group, as well as for his support during this work. I also gratefully acknowledge the considerable amount of help that I received from Dr. Arash Rahimi-Iman -the leader of our VECSEL team- throughout this work. My thank goes also to Prof. Dr. Wolfgang Stolz for innumerable valuable discussions and the help that he provided, as well as for providing me the quantum-well VECSEL-chip exploited in this work. Furthermore, I would like to acknowledge financial support from the Yousef Jameel scholarship funds.

Many thanks to all those colleagues that made work more pleasant by their company. In particular, to those who proof-read this thesis and contributed with their invaluable comments. I would like to thank (again) Dr. Arash Rahimi-Iman, Fan Zhang, Christoph Möller, Max Vauple and Mostafa El-demery.

External collaborators supported this work as well and I gratefully acknowledge: Prof. Dr. Edik Rafailov and Dr. Ksenia A. Fedorova, from Aston University in the United Kingdom, for providing the quantum-dot VECSEL-chips; Prof. Dr. Stephan Reitzenstein, Dr. Tobias

Heindel and Alexander Schlehahn, from the Institute of Solid-State Physics, Technical University of Berlin, for carrying out some experiments together. It has been an honor and pleasure to work with you.

A big thank goes to the whole Koch group for helping me through my PhD. I will always remember the people from the group as true friends: Dr. Matthias Wichmann, who was a great teacher in the lab. Fan Zhang and Christoph Möller for encouraging me to do things proper really helped me a lot. Dalia Al Nakdali, Mohammed Khaled Shakfa and Phillip Richter, who were supporting me in the lab. Oday Mazin and Muhanad Bilal for providing me the very valuable balance to the work-life. Furthermore, I would like to thank Dr. Jan Balzer and Norman Born for fruitful discussions as well as Dr. Bernd Heinen and Dr. Bernardette Kunert for the quantum-well VECSEL-chip processing.

Finally, I am deeply grateful to my parents, my sisters and my brothers for always encouraging and supporting me in everything I did. All the achievements in my life would not have been possible without the very close relation to my family. Furthermore, I thank my beloved wife Abeer Elgammal, who has been giving me so much that I can never pay back; also I thank my beautiful daughter, Nadin, for her love and understanding.

# Abstract

Besides continuous wave (cw) operation, where light is emitted continuously over time, specially designed lasers can also generate short or even ultrashort pulses of light, the latter referred to as ultrafast lasers. So far, ultrafast laser systems have been used in different industrial and research areas such as biology, metrology or medicine. But these systems are subject to high costs and great complexity, limiting their use in new application areas that demand for low-cost and compact ultrafast laser sources, such as the optical clocking of microprocessors or free-space data communication. Semiconductor lasers would be ideally suited to meet this demand, however conventional semiconductor lasers are edge-emitters and their power cannot simply be scaled. The same is true for microcavity-based surface-emitters. Moreover, the more powerful edge-emitters feature strongly asymmetric beam profiles, which makes them unsuitable for many ultrafast applications.

Vertical-external-cavity surface-emitting lasers (VECSELs), also known as semiconductor disk lasers (SDLs), are powerful and very flexible coherent light sources. They can be considered as a hybrid system between ion-doped solid state lasers and conventional semiconductor lasers. SDLs combines the advantages of semiconductor gain, e.g. wavelength versatility, high gain cross sections, and simple fabrication, with the benefits of the ion-doped bulk lasers, such as a high-Q external cavity and excellent beam quality. Furthermore, due to the 1-D heat flow, resulting from the arrangement as a thin film laser, very efficient heat

removal enables power scaling via the pump area as well as the mode size. SDLs have proved to be versatile lasers which allow for various emission schemes which on the one hand include remarkably high-power multimode or single-frequency cw operation, and on the other hand two-color as well as mode-locked emission.

Mode-locked SDLs offer numerous advantages over their solid-state pendants, such as their low-complexity, compactness, cost-efficiency, and an extremely wide range of accessible emission wavelengths (from visible to mid-infrared, based on the employed material system) and repetition rates. This makes ultrafast SDLs very interesting for various applications that rely on a compact, cost-efficient and mass-producible laser technology.

SDLs can be passively mode-locked using different mode-locking techniques. While previously saturable absorbers such as semiconductor saturable-absorber mirrors (SESAMs) - either external, or even internal, like in a mode-locked integrated external-cavity surface emitting laser (MIXSEL) - and recently novel-material-based carbon-nanotube or graphene saturable absorbers were employed. Up to date, the presented mode-locking techniques have led to a great enhancement in average powers, peak powers and repetition rates that can be achieved with passively mode-locked SDLs. However, the power-sensitive, complex and costly absorber mirrors, which have to be carefully designed for a certain wavelength range, naturally impose limitations on the device performance. Fortunately, on the other hand, a new mode-locking method was presented and discussed in recent years which is referred to as self-mode-locking (SML) or saturable-absorber-free operation of mode-locked SDLs.

In this context, motivated by the demand for overcoming the aforementioned limitations, the goal of this thesis was to further exploit the potential of mode-locked SDLs. Particularly, focus on the SML or saturable-absorber-free operation technique, which is consid-

ered a promising technique for the realization of compact, robust and cost-efficient mode-locked devices. In this thesis, experimental results of SML operation of SDLs in the sub-picosecond regime will be presented. We show that the SML scheme is not only applicable to quantum-well-based SDLs, but also to quantum-dot-based devices. Moreover, harmonic mode-locking with sub-ps pulses is demonstrated at discrete power levels. Furthermore, to extend the applications of ultrafast SDLs, we realized an ultra-bright single-photon-source by optically exciting a deterministically integrated single quantum-dot microlens using a mode-locked SDL. The compact and stable laser system allows for overcoming the limited repetition rates of commercial mode-locked Ti:sapphire lasers and to excite the single quantum-dot microlens with a pulse repetition rate close to 500 MHz and a pulse width of 4.2 ps at a wavelength of 508 nm, utilizing second-harmonic generation in an external nonlinear crystal.

# Kurzfassung

Neben dem Dauerstrichbetrieb (engl. continuous wave, kurz CW), bei dem Licht kontinuierlich emittiert wird, können speziell entwickelte Laser auch kurze oder sogar ultrakurze Lichtpulse erzeugen, wobei im letzteren Fall von Ultrakurzpulslasern die Rede ist. Bis jetzt wurden Ultrakurzpulslaser in verschiedenen Industrie- und Forschungsbereichen, wie der Biologie, Metrologie oder Medizin eingesetzt. Aber hohe Kosten und die große Komplexität dieser Systeme verhindern ihren Einsatz in neuen Anwendungsgebieten, in denen günstige und kompakte Ultrakurzpulslaser, wie zum Beispiel bei der optische Takterzeugung für Mikroprozessoren oder beim optischen Richtfunk, benötigt werden. Halbleiterlaser würden diesen Anforderungen genügen, jedoch sind konventionelle Halbleiterlaser Kantenemitter, deren Ausgangsleistung nicht ohne weiteres gesteigert werden kann. Auch Oberflächenemitter in einer Mikrokavität unterliegen dieser Beschränkung. Zudem besitzen die stärksten Kantenemitter eine stark asymmetrische Strahlcharakteristik, wodurch sie für viele Anwendungensbereiche von Ultrakurzpulslasern untauglich sind.

Oberflächenemittierende Halbleiterscheibenlaser mit externer Kavität (engl. Vertical-external-cavity surface-emitting lasers, kurz VECSEL), auch als Halbleiterscheibenlaser (engl. semiconductor disk lasers, kurz SDL) bezeichnet, sind leistungsstarke und sehr flexible koherente Lichtquellen. Sie können als Hybridsystem aus ionendotierten Festkörperlasern und konventionellen Halbleiterlasern betrachtet werden. SDLs kombinieren die Vorteile

eines aktiven Mediums aus Halbleitermaterialien, z.B. Flexibilität der Wellenlänge, hohen Gewinnquerschnitt und einfache Herstellung mit den Vorteilen eines ionendotierten Festkörperlasers, wie externe Resonatoren mit hoher Güte und exzellentem Strahlprofil. Zudem erlaubt der 1-D Wärmestrom, welcher aus dem Aufbau als Dünnschichtlaser resultiert und eine effiziente Kühlung ermöglicht, die Skalierung der Ausgangsleistung durch Veränderung von Anregungsbereich und Modengröße. SDLs haben sich als vielseitige Laser mit unterschiedlichen Betriebsmodi erwiesen, welche auf der einen Seite bemerkenswerte Ausgangsleistungen im multimoden oder einzelfrequenten CW-Betrieb und auf der anderen Seite zwei-Farben sowie modengekoppelte Emission beinhalten.

Modengekoppelte SDLs besitzen gegenüber Festkörperlasern viele Vorteile, wie ihre geringe Komplexität, Kompaktheit, Kostengünstigkeit und ein extrem weiter Bereich der möglichen Emissionswellenlängen (vom Sichtbaren bis zum mittleren Infrarotbereich, abhängig vom verwendeten Materialsystem) sowie hohe Wiederholraten. Dadurch werden Ultrakurzpuls-SDLs für verschieden Anwendungen sehr interessant, welche auf kompakte, günstige und massenfertigungstaugliche Lasertechnologie setzen.

SDLs können mit verschiedenen Modenkopplungstechniken zur passiven Modenkopplung gebracht werden. In der Vergangenheit wurden sättigbare Absorber, wie sättigbar absorbierende Halbleiterspiegel (engl. semiconductor saturable-absorber mirror, kurz SESAM) – entweder extern, oder sogar intern, wie bei dem modengekoppelten integrierten oberflächenemittierenden Halbleiterscheibenlaser (engl. mode-locked integrated external-cavity srface emitting laser, kurz MIXSEL)– und neuerdings auch auf neuen Materialsystemen beruhende sättigbare Absorber aus Kohlenstoff-Nanoröhrchen oder Graphen eingesetzt. Aktuell haben die vorhandenen Techniken zur Modenkopplung zu einer großen Steigerung von durchschnittlicher Ausgangsleistung, Spitzenleistung und Repetitionsrate geführt, welche mit passiv modengekoppelten SDLs erreicht werden können. Allerdings limitieren die leis-

tungssensitiven, komplexen und teuren sättigbar absorbierenden Spiegel, welche aufwändig für einen bestimmten Wellenlängenbereich hergestellt werden müssen, die Leistungsfähigkeit der Einheit. Erfreulicherweise wurde in den letzten Jahren neben diesen Methoden eine neue Methode der Modenkopplung präsentiert und diskutiert, welche als Selbst-Modenkopplung (engl. self-mode-locking, kurz SML) oder sättigbarer-Absorber-freier Betrieb (engl. saturable-absorber-free) von modengekoppelten SDLs bezeichnet wird.

In diesem Zusammenhang, motiviert durch den Bedarf die beschriebenen Limitierungen zu überwinden, war das Ziel dieser Arbeit das weitere Potential von modengekoppelten SDLs zu erforschen. Insbesondere lag der Fokus auf dem SML oder dem sättigbaren-Absorber-freien Betrieb, welcher als eine vielversprechende Technik zur Realisierung eines kompakten, robusten und kostengünstigen modengekoppelten Systems betrachtet wird. In dieser Arbeit werden die experimentellen Ergebnisse zum SML Betrieb eines SDLs im sub-Picosekunden Bereich präsentiert. Wir zeigen, dass der SML Betrieb nicht nur für Quantenfilm basierenden SDLs, sondern auch auf Quantenpunkt basierenden Systemen möglich ist. Des weiteren wird die Modenkopplung bei höheren Harmonischen mit sub-ps Pulsen bei diskreten Ausgangsleistungen gezeigt. Weiterhin wurde zur Erweiterung der Anwendungen von Ultrakurzpuls-SDLs eine ultrahelle Einzelphotonenquelle durch optische Anregung einer deterministisch integrierten Einzelquantenpunkt Mikrolinse mittels eines modengekoppelten SDL realisiert. Das kompakte und stabile Lasersystem erlaubt die überwindung der limitierten Repetitionsraten von kommerziellen, modengekopellten Ti:Sapphir Lasern und die Anregung der Einzelquantenpunkt Mikrolinse mit einer Pulswiederholrate nahe 500 MHz und einer Pulsdauer von 4,2 ps mit einer Wellenlänge von 508 nm, die durch Frequenzverdopplung in einem externen nichtlinearen Kristall erreicht wurde.

# Contents

# List of Figures

# List of Tables

# List of Acronyms

**AlGaAs** aluminium gallium arsenide

**CW** continuous wave

**CVD** chemical vapour deposition

**DBR** distributive Bragg reflector

**GDD** group delay dispersion

**GaAs** gallium arsenide

**KLM** Kerr lens mode-locking

**LCF** longitudinal confinement factor

**MOVPE** Metalorganic vapour phase epitaxy

**MIXSEL** mode-locked integrated external-cavity surface emitting laser

**OP** Optically-pumped

**QW** quantum well

**QD** quantum dot

**RPG** resonant periodic gain

**SML** self-mode-locking

**SESAM** semiconductor saturable-absorber mirror

**SDL** semiconductor disk laser

**TDL** thin disc laser

**TBWP** time-bandwidth product

**VECSEL** vertical-external-cavity surface-emitting laser

# 0

# Introduction

## Background

Since its invention in 1960 [1], different types of lasers have been developed, such as dye, solid-state, gas, and semiconductor lasers [2, 3]. Currently, a wide range of applications has been covered by lasers, particularly in industry, communication, medicine, spectroscopy, but also in many other fields. Typically, each kind of laser has its unique benefits for certain applications, however exhibiting inability for the others. Solid state lasers on the one hand can emit high output powers (hundreds of watts) with good beam quality (fundamental transverse mode) which are required for several applications that include metrology and remote sensing. But on the other hand, their accessible emission wavelengths are limited to some discrete values, due to the limitation of the available gain media [4, 5].

While conventional semiconductor lasers can access a wide emission wavelength range from the UV to the mid-IR [6, 7]. However, the good beam quality operation can be achieved only at output powers lower than 1 W. Notably, high power and good beam quality combination is required, such as for efficient nonlinear optical harmonic generation.

In the mid-1990s, the vertical-external-cavity surface-emitting lasers (VECSELs), also referred to as semiconductor disk lasers (SDLs), were developed, to overcome problems with conventional semiconductor lasers [8]. This new class of lasers may be considered as a hybrid system between solid state laser and semiconductor laser. It combines the advantages of semiconductor gain media, e.g. high gain cross sections, wavelength versatility and simple fabrication with the benefits of the ion doped bulk lasers such as a high-Q external cavity and excellent beam quality. A unique feature of semiconductor gain structures is that they can be pumped either electrically with a p-i-n configuration or optically with an external low-brightness pump. The first realization of an SDL was an electrically-pumped and it was reported in 1993 [8] which emitted several mW in $TEM_{00}$ operation. Optically-pumped (OP) SDLs, on the other hand, represent the cutting-edge of the vertical emitting lasers. The first of its kind was demonstrated in 1997 by Kuznetsov *et al.* [9] and thereafter - owing to their remarkable design flexibility and features - rise was given to a plethora of modifications and improvements towards more specific applications. Furthermore, the arrangement as a thin film laser offers very efficient heat removal due to the 1-D heat flow and thus enables power scaling. The optical pumping scheme holds an advantage, as the uniform distribution of excited carriers over the whole (large) gain area is easier to achieve by optical absorption than by current injection.

It has been shown, that careful thermal management enables high power operation for OP-SDLs with output powers exceeding 100 W [10] under multi-mode continuous wave (cw) operation, 20 W with a fundamental $TEM_{00}$-mode [11] and 23 W under single-frequency

operation [12]. An extremely wide operation range with respect to emission wavelength has been demonstrated for cw operation. SDLs were operated at emission wavelengths ranging from 244 nm to 5.3 $\mu$m [13–16]. Nowadays, the cw semiconductor lasers are widely spread over a vast range of applications; they can even be found in everyday devices such as laser printers, audio CD players, or barcode readers in supermarkets and many others.

On the other hand, lasers generating ultrashort pulses (with picosecond or femtosecond duration) enabled many breakthroughs since the early 1990s in both industrial applications and fundamental science [17–20]. Many experiments demonstrated that ultrafast lasers enable not only new applications but also improve the existing technologies in fields as diverse as medicine, manufacturing, biology, and communication.

Due to the power-scaling potential, wavelength versatility, broad gain bandwidth, and the numerous advantages offered from the vertical external-cavity geometry, SDLs caught the attention to serve as very compact, cheap and simple sources for ultrashort pulses. To date, mode-locked SDLs cover an extremely wide operation range with respect to repetition rates (between 85.7 MHz and 101.2 GHz) and emission wavelength (between 665 nm and 2 $\mu$m). This makes the ultrafast SDLs very interesting for various applications that rely on an inexpensive and mass-producible laser technology. Furthermore, because the semiconductor gain region exhibits a high gain cross section and a short upper state lifetime, therefore it is capable of supporting high repetition rates without suffering from Q-switching which is challenging for solid state lasers operation. lasers operating at multi-gigahertz (GHz) repetition rates are now becoming key elements for high-capacity telecommunication systems [21] and optical interconnects [22].

The realisation of the first mode-locked SDL dates back to the year 2000 and was demonstrated by Hoogland *et al.* for a central wavelength of 1 $\mu$m [23]. It did not take long and

SDLs were considered becoming cost-efficient, compact alternatives to commercial pulsed lasers with even enhanced tunability, and shorter pulses using resonator-integrated [23–47] or chip-integrated [48–52] semiconductor saturable-absorber mirrors (SESAMs). Recently, besides semiconductor-based materials, graphene [53, 54] as well as carbon-nanotubes [55] saturable absorbers have been employed for mode-locked operation of SDLs. However, mode-locking has also been reported to take place even without any additional saturable absorber—an effect called self-mode locking (SML) [56–65]. Up to date, the average output power of mode-locked SDLs has been increased to 10.2 W, the pulse durations decreased to 107 fs (fundamentally mode-locked) or even 60 fs in burst operation, the pulse repetition rate has been pushed beyond 100 GHz, and the peak power increased to 6.5 kW. To highlight progress in this field, the number of publications for mode-locked SDLs over the last 14 years is presented in Fig. 1. While initially, only a small amount of publications followed the demonstration of the first mode-locked SDL in 2000, a significant increase of publications was registered after 2005.

## Thesis outline

The main objective of this thesis was to develop the mode-locked operation of SDLs and to improve the process of pulse emission from such a device in terms of efficiency and speed. To achieve mode-locking, SDLs normally incorporate a saturable absorber in the laser cavity, most frequently in the form of a SESAM. The use of saturable absorbers is well understood in SDLs and once a suitable saturable absorber has been developed for a desired laser, a good pulsed source can be reliably produced. However, the use of saturable-absorbers also brings additional costs: they have to be carefully designed for a certain wavelength range and their production is costly. In addition, the saturable absorber parameters, such

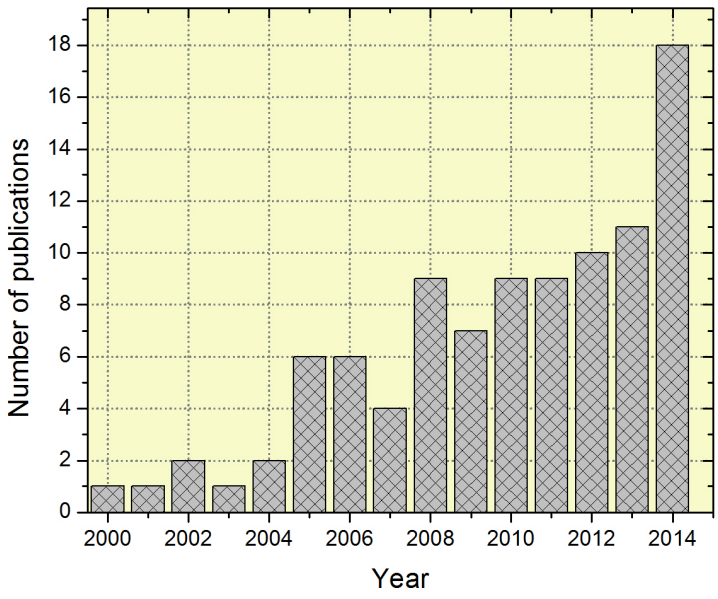


Figure 1: Number of publications per year for mode-locked semiconductor disk lasers.

as non-saturable loss, modulation depth, saturation fluence and the carrier lifetime impose limitations on the performance of the device. Therefore, exploring new mode-locking techniques for SDLs to overcome the aforementioned limitations will enhance the pulse emission performance from such a device. Therefore, throughout this thesis, we demonstrate that mode-locking of SDLs can also take place even without any additional saturable absorber, or intracavity element except an intracavity hard aperture. We show that the realization of SML for both quantum well (QW) and quantum dot (QD) based SDLs devices is possible. These results emphasize that this quite young technique—even though the mechanism behind the effect has not been well understood yet—is capable of enabling mode-locked operation for different gain media as well as cavity configurations.

This thesis is written in cumulative form and is structured as follows: Chapter 1 describes SDLs and their history; discusses how they are made and characterized; explains how the

SDL structure enables the SDL's basic properties. The fundamental principles of passively mode-locked SDLs are recapitulated in chapter 2. Since a complete theoretical discussion exceeds the scope of this thesis, only the most relevant concepts, that are directly linked to the covered topics, are discussed. This is followed by the description of the different SDL structures that were used in this thesis work. The research results are summarized in Chapter 3 as they are discussed in detail in the following publications that were published in the course of this work and are printed in full length in Chapter 4.

**List of publications:**

- M. Gaafar, C. Möller, M. Wichmann, B. Heinen, B. Kunert, A. Rahimi-Iman, W. Stolz, M. Koch: *Harmonic self-mode-locking of optically pumped semiconductor disc laser*. IET Electronics letters **50**, 542 (2014). (Section 4.1)

- M. Gaafar, D. Al Nakdali, C. Möller, K. A. Fedorova, M. Wichmann, M. K. Shakfa, F. Zhang, A. R-Iman, E. U. Rafailov, M. Koch: *Self-mode-locked quantum-dot vertical-external-cavity surface-emitting laser*. Optics letters **39**, 17 (2014). (Section 4.2)

- M. Gaafar, P. Richter, H. Keskin, C. Möller, M. Wichmann, W. Stolz, A. Rahimi-Iman, M. Koch: *Self-mode-locking semiconductor disk laser*. Optics Express **22**, 23 (2014). (Section 4.3)

- M. Gaafar, A. Rahimi-Iman, K. Fedorova, W. Stolz, E. Rafailov, M. Koch: *Mode-locked semiconductor disk lasers*. Under review (2015). (Section 4.4)

- D. Al Nakdali, M. K. Shakfa, M. Gaafar, M. Butkus, K. A. Fedorova, M. Zulonas, M. Wichmann, F. Zhang,B. Heinen, A. Rahimi-Iman, W. Stolz, E. U. Rafailov, M. Koch: *High-Power Quantum-Dot Vertical-External-Cavity Surface-Emitting Laser Exceeding 8 W*. IEEE Photonics Technology Letters **26**, 15 (2014). (Section 4.5)

- D. Al Nakdali, M. Gaafar, M. K. Shakfa, , F. Zhang, M. Vaupel, K. A. Fedorova, A. Rahimi-Iman, E. U. Rafailov, M. Koch: *High-Power Operation of Quantum-Dot Semiconductor Disk Laser at 1180 nm*. IEEE Photonics Technology Letters, 27, 1128 (2015). (Section 4.6)

- A. Schlehahn, M. Gaafar, M. Vaupel, M. Gschrey, P. Schnauber, J.-H. Schulze, S. Rodt, A. Strittmatter, A. Rahimi-Iman, T. Heindel, M. Koch, S. Reitzenstein: *Ultra-bright deterministic quantum-dot single-photon source triggered by mode-locked VECSEL*. Applied Physics Letters 107, 041105 (2015). (Section 4.7)

- A. Rahimi-Iman, M. Gaafar, D. Al Nakdali, C. Möller, F. Zhang, M. Wichmann, M. K. Shakfa, K. A. Fedorova, W. Stolz, E. U. Rafailov, M. Koch: *Recent advances in the field of vertical-external-cavity surface-emitting lasers*. In Proceedings of SPIE 9349, Vertical External Cavity Surface Emitting Lasers (VECSELs), Vol. 934906, (2015). (Section 4.8)

# 1

# Optically-pumped Semiconductor disk lasers

In the mid-1990s, SDLs were developed [9, 66] to overcome a key problem with conventional semiconductor lasers: how to generate watt-level optical powers with good beam quality. Although edge-emitting semiconductor lasers are capable of producing tens of watts of output power, the beams are highly multimode [67, 68]. In contrast, vertical-cavity surface-emitting lasers can achieve single transverse mode operation, but only with powers up to several milliwatts [69]. Therefore obtaining semiconductor lasers with both good beam quality and high optical power simultaneously has always been a challenging task, till the invention of SDLs. This combination is the key for many important commercial and scientific laser applications.

Compared with other semiconductor laser types, SDLs hold a number of advantages, such as:

1. The extension of the cavity by using external mirrors allows for
    - Excellent beam quality,
    - External laser mode control,
    - Employment of intracavity elements, such as
        - Saturable absorbers for mode-locking,
        - Nonlinear elements for frequency conversion,
        - Birefringent filters and etalons for wavelength tuning, dual wavelength emission, and single frequency generation.
2. The heat flow in the gain structure becomes one-dimensional and is directed perpendicularly to the semiconductor disk surface, resulting in marvelous heat removal, particularly in combination with a diamond heat spreader.
3. Remarkably high output powers (up to tens of Watts) are achievable:
    - With single-transverse mode,
    - With a single-longitudinal mode,
    - Or simply in a multimode regime.
4. High intracavity powers allow for efficient intracavity frequency conversion, including:
    - Higher harmonic generation,
    - Sum/difference frequency generation.

On the other hand, SDLs resemble a diode-pumped solid state thin disc lasers (TDLs) with respect to its construction [70], except that the dielectric laser disc is replaced by a surface-emitting semiconductor active mirror structure, which may be electrically or optically pumped. However, they also have several disparities. For instance:

1. The emission wavelength of SDLs can be tailored to match specific applications because it is determined by bandgap engineering. Whereas, the operation wavelength of solid state TDLs is limited to the discrete emission lines of the available materials.

2. Due to the poor pump light absorbtion in a single pass through the 100-300 $\mu$m thick gain section of solid state TDLs, it requires optics for recirculating the residual pump radiation [71, 72]. SDLs do not require these arrangements, because pump radiation can be absorbed efficiently on a single or double pass of even a very thin active region (2 $\mu$m).

3. Solid state lasers require pumping at specific wavelengths that correspond to the narrow absorption lines of the gain materials. This does not hold for SDLs, because the pump photon energy only needs to exceed the bandgap of the pump absorbing layers [73].

To summarize, SDLs may be considered as a hybrid system between solid state lasers and semiconductor lasers. They combine the high Q external cavity and excellent beam quality with wavelength versatility, high gain cross sections, and simple fabrication.

The SDL concept is based on a semiconductor region providing gain to the laser in a direction normal to the semiconductor wafer surface. The thin semiconductor disk, which is a stack of alternating semiconductor layers, can be subdivided into three regions: a multilayer high-reflectivity distributive Bragg reflector (DBR) mirror, a gain medium contain-

ing multi quantum wells (QWs) or planes of quantum dots (QDs), and the cap layer. For efficient heat removal, the thin disk is usually bonded either onto an chemical vapour deposition (CVD) diamond heat spreader or to an intracavity diamond heat spreader. The laser cavity consists of the on-chip mirror and an external spherical mirror, which serves as the output coupler. The external laser cavity enforces output in a circular, low-divergence, near-diffraction-limited beam of high quality. For more specific applications like single frequency generation, mode-locking, etc., other intracavity optical elements can also be used. The active region can be pumped either optically by a low cost, low brightness laser or electrically using a p-i-n diode configuration. Figure 1.1 (a) shows a scheme of the simplest straight cavity configuration of an OP-SDL. Here, the semiconductor part of the SDL is bonded to the heatsink to dissipate the heat. A zoom in of the SDL's layered structure is shown in Fig. 1.1 (b). Up to date, output powers exceeding 100 W [10] in multi-mode operation has been achieved from QW-gain medium SDLs. Moreover, an extremely wide operation range with respect to emission wavelength has been demonstrated in cw operation. SDLs were operated at emission wavelengths ranging from the visible to mid-infrared regime. Through frequency conversion, the spectral coverage extends further to ultraviolet light.

The power scaling is not only limited to QW-based SDLs, but also QD-based SDLs provide versatile systems similar to QW pendants with even broader gain bandwidth [74]. However, their output power is significantly lower. Nevertheless, up to a few Watts output power were demonstrated for various operation wavelengths ranging from 654 nm up to 1.3 $\mu$m [75–78]. Using second harmonic generation, even wavelengths down to 514 nm were presented [79]. The highest output power for QD-SDLs has been obtained to be 8.4 W in multi-mode operation [80] from a single-chip at 1040 nm wavelength. While 6 W output power in fundamental $TEM_{00}$-mode operation has been demonstrated employing a dual-

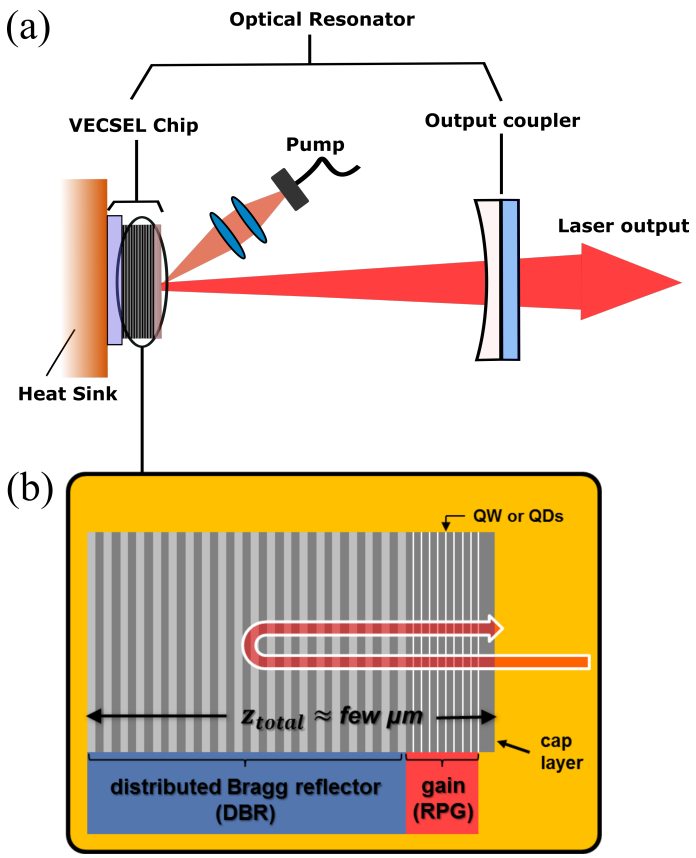


Figure 1.1: (a) Scheme of an optically-pumped VECSEL. Here, a linear cavity is shown. The pumping light is directed to the VECSEL via an optical fiber combined with a lens system for collimation and focusing. (b) A schematic of the SDL's chip structure.

chip VECSEL at the same wavelength [81]. Extensive reviews on the results obtained at the wavelengths demonstrated to date can be found in the scientific literature [82–86].

## 1.1 Semiconductor disk laser configuration

Having briefly reviewed the properties of the SDLs and their applications in the aforementioned section, it is now the time to discuss the operational principles of the SDL more thoroughly. In this section, all basic components of the SDL device will be reviewed. As mentioned before, the semiconductor structure of SDLs consists of a cap layer, and an ac-

tive region (gain region) grown on a fully reflecting DBR. The semiconductor structure as a whole typically has a total thickness of only a few micrometers (not including the semiconductor substrate), and is mounted on a heat spreader. Whereas the functionality of the cap layer will become clear at the end of this section, the functionality of the DBR and the active region are more apparent. The gain section, the DBR section and the cap layer also form a so-called resonant periodic gain (RPG) structure. These concepts are introduced in the following sections.

### 1.1.1 The gain region

The semiconductor gain region is by far the most important part of the SDL. It consist of multiple QW or QD layer structure grown on top of the DBR. In this chapter, only QW layers will be considered, however, most of the design is similar for QD based SDLs. Basic operation principles of SDLs are illustrated in Fig. 1.2 (a), which shows the conduction and valence band energy levels across the semiconductor hetero-structure.

Upon non-resonant pumping, incident pump photons with high-enough photon energies are absorbed in separate pump-absorbing layers that also serve as the QW barriers. The generated free carriers, electrons and holes, in the barrier layers diffuse into the lower energy states in the QWs. The electrons then recombine with holes in the valence band radiatively, generating photons at a wavelength corresponding to the QW energy. A higher bandgap window layer on the top of the structure prevents carriers from reaching the semiconductor gain structure's surface, where they could recombine non-radiatively, and thus deplete laser gain. Some structures also include a thin (5-20 nm) cap layer to protect the window layer from oxidation. Figure 1.2 (b) presents the spatial profile of the conduction and valence band edges at one of the quantum wells. The energies of electrons and holes

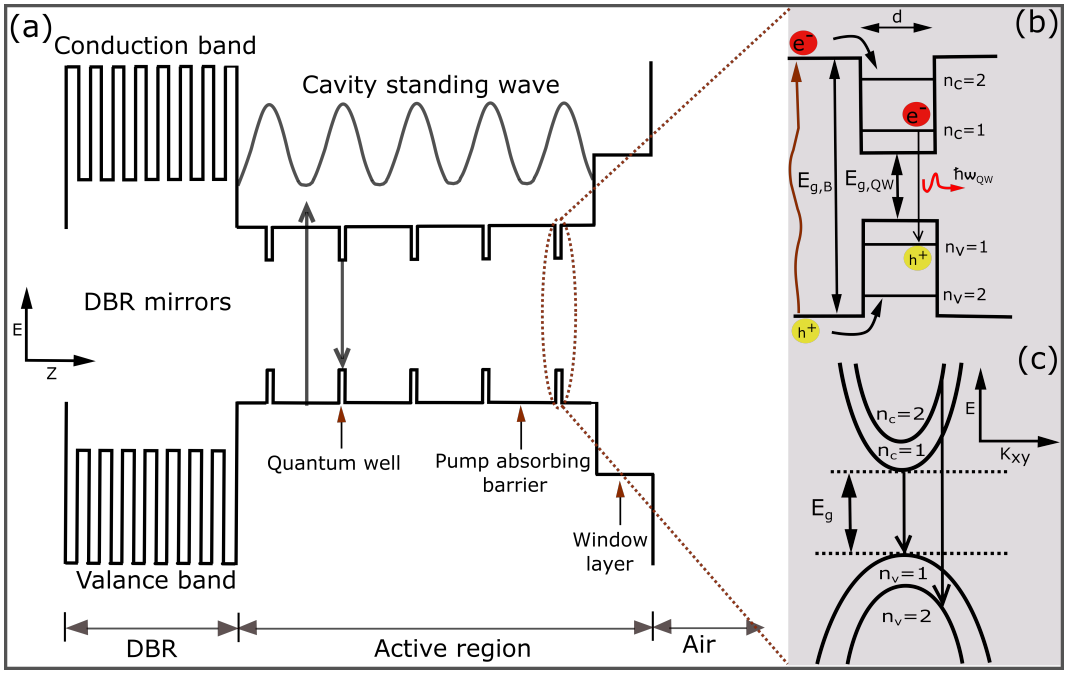


Figure 1.2: (a) Schematic drawing of potential energy bands in a typical SDL. (b) Energy diagram of a typical QW and its surrounding barriers. (c) Energies of electrons and holes in the plane of the QW.

in the plane of the QW have an approximately parabolic dependence on the momentum as shown in Fig. 1.2 (c).

### 1.1.2 The DBR section

The reflectivity of the SDL chip is an important quantity, since intracavity losses have to be kept at a minimum for efficient laser operation. Thus, the multilayer DBR is a critical component of the SDL semiconductor chip which serves as one of the mirrors of the laser cavity. DBRs are dielectric mirrors consisting of pairs of $\lambda_R/4$ thick layers with high and low refractive indices denoted by $n_H$ and $n_L$, where $\lambda_R$ is the design wavelength where the

reflection is the highest, the thicknesses of the DBR layers are given by:

$$d = \frac{\lambda_R}{4n(\lambda_R)}. \tag{1.1}$$

Operation of the DBR is based on constructive interference of waves Fresnel-reflected from the layer boundaries. Light reflected within the high refractive index layers will not suffer any phase change on reflection, while, on the other hand, that reflected within the low refractive index layers will experience a $180^\circ$ phase shift. Therefore, the various components of the incident light reflected at successive boundaries throughout the DBR section will reappear at the front surface all in phase. They will interfere constructively, thus creating a high reflectivity stop band. As QDs have quite a low gain, high reflectivity DBRs are particulary needed to have a low operation threshold and to optimize the performance of the device. If the DBR is formed on a substrate with a refractive index $n_s$, the DBR reflectivity at the center wavelength $\lambda_R$ is given by:

$$R_{2N}(\lambda_R) = \left( \frac{1 - (\frac{n_s}{n_i})(\frac{n_H}{n_L})^{2N}}{1 + (\frac{n_s}{n_i})(\frac{n_H}{n_L})^{2N}} \right)^2. \tag{1.2}$$

for a structure with an even number of layers (2N), and by

$$R_{2N+1}(\lambda_R) = \left( \frac{1 - (\frac{n_H}{n_i})(\frac{n_H}{n_s})(\frac{n_H}{n_L})^{2N}}{1 - (\frac{n_H}{n_i})(\frac{n_H}{n_s})(\frac{n_H}{n_L})^{2N}} \right)^2. \tag{1.3}$$

for a structure with an odd number (2N+1) of layers. Here $n_i$ denotes the refractive index of the surrounding medium and N refers to the number of DBR layers. For a maximum reflectivity, the DBR should begin and end with a layer that provides the highest refractive index contrast to the substrate and to the surrounding material, respectively. The bandwidth of the DBR is determined by the refractive index contrast between the DBR layers,

and is given by [87]:

$$\Delta\lambda_R = \frac{4\lambda_R}{\pi} \arcsin\left(\frac{1-(\frac{n_L}{n_H})}{1+(\frac{n_L}{n_H})}\right). \tag{1.4}$$

As the DBR multi-layers are placed between the active region and substrate or heatsink, the thermal impedance must be considered as pump induced heat in the active region dissipates through the DBR layers. Therefore, the thickness of the mirror should be kept to a minimum while maintaining a high reflectivity value. Further details about thermal management in SDLs will be discussed in more detail in section 1.1.4.

### 1.1.3 Resonant periodic gain structure

In SDLs, multiple reflections are formed not only between the Bragg mirror and the end mirror of the external cavity, but also in the chip structure between Bragg mirrors and semiconductor air interface. The SDL chip itself thus represents a Fabry-Perot microcavity whose spectral filtering action significantly affects the behavior of the entire laser. In the active region, the electrical field forms a standing wave pattern as shown in Fig. 1.2. In order to improve the performance of lasing, the gain structure has to be optimized in order to maximize the overlap between the QWs and the peaks of the standing wave pattern at the target wavelength ($\lambda_t$). Such design is commonly known as the aforementioned RPG. The microcavity can be either resonant or antiresonant at the design wavelength. In both cases, the field distribution differs considerably within the chip structure. It is therefore necessary to define the modal gain per unit time of the structure. Following [88], it can be written as:

$$\langle g \rangle = \frac{\int g|E^+ + E^-|^2 dV}{\int [|E^+|^2 + |E^-|^2] dV} \tag{1.5}$$

Where $g$ is the intrinsic material gain, and $E^+$ as well as $E^-$ represent the electric fields of the incident and back reflected waves in the resonator. The integral in the numerator extends over the entire active region, while the denominator is calculated over the entire resonator. For an SDL the expression can be rewritten as:

$$\langle g \rangle = g\Gamma_z\Gamma_t V^{-1} \tag{1.6}$$

with

$$\Gamma_z = \frac{\sum_i |E^+(z_i) + E^-(z_i)|^2}{|E_0^+|^2 + |E_0^-|^2} \tag{1.7}$$

where the volume of the resonator is expressed by V. The modal gain per unit time is thus represented by multiplication of the intrinsic material gain by the longitudinal and transversal confinement factors $\Gamma_z$ and $\Gamma_t$, respectively. The longitudinal confinement factor (LCF) $\Gamma_z$, also named enhancement-factor (defined as the proportion of the confined optical energy in the QWs relative to the optical energy in the whole structure) controls the performance of the gain chip in the following important ways:

- Firstly, as in Eq. 1.6, it determines the overall modal gain of the chip, where $g$ is assumed to be constant for all the QWs in the structure. And therefore it has an impact on the laser threshold.

- Secondly, it is wavelength dependent, and therefore acts as an intracavity spectral filter, with important consequences for the performance of the laser.

The transverse confinement factor essentially describes the overlap of the transverse distribution of charge carriers with the laser mode. Since the carrier distribution is dependent on the pump light, the transverse confinement can be described as the overlap between pump

and laser modes.

In order to make the RPG structure resonant at $\lambda_t$, the optical length of the structure is often chosen as a multiple of $\lambda_t/2$ . Such structure provides the highest gain, because it increases the optical field confinement within the RPG structure. In this structure, the efficient operation is obtained when the QW emission, the resonance wavelength and the DBR center wavelength correspond to the same wavelength, $\lambda_t$ [82]. Here, the LCF exhibits a resonance peak at the operation wavelength. However, the disadvantage of this design is the narrow spectral width, which increases the thermal sensitivity of the device, and restricts the gain bandwidth for mode-locking or frequency tuning [89]. Furthermore, the standing-wave profile has an anti-node located on the surface of the output window, just where surface contamination will cause great local scattering losses. In addition, from the point of view of mode-locking, a resonant design also introduces high group delay dispersion (GDD).

A representation of the resonant chip-design is shown in Fig. 1.3. These simulations are shown for a gain medium which consists of 10 InGaAs QWs equally spaced by $\lambda/2$ GaAsP barrier layers and 24.5 pairs of $\lambda/4$ GaAs/AlGaAs layers of DBR. Both, QWs and DBR are designed for a laser emission at 1010 nm. The thickness of the GaInP cap layer is etched down to a thickness of $\lambda/2$. Figure 1.3 (a) shows the refractive indices (top) and the standing wave pattern (bottom) of the multilayer structure. The simulated reflectivity (black line) and LCF (blue line) of this resonant structure as a function of the wavelength are plotted in Fig. 1.3 (b). The transmission peak is at the center of the design wavelength, therefore, the structure enhances the gain intensity in the middle of the bandwidth and reduces it at the wings. In such a configuration, the electric field is higher in the subcavity region, and thus, the design is favorable for low threshold or low gain devices.

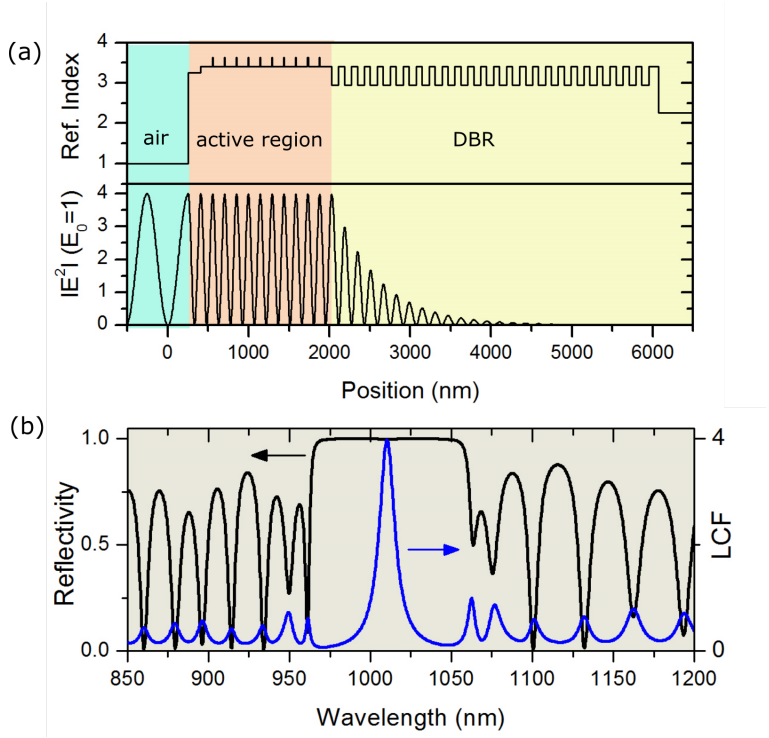


Figure 1.3: Representations of the resonant chip-design (a) Refractive index of the layers (top) and the electric-field distribution of a standing optical wave inside the structure (bottom) for a design wavelength of 1010 nm and 10 QWs. The standing wave intensity is normalized to the input intensity. (b) The wavelength-dependent reflectivity spectrum (left axis) and the light intensity (represented by the longitudinal confinement factor) in the QWs (right axis).

At the other extreme, the cavity can be made antiresonant if the overall thickness of the RPG is chosen to be a multiple of $\lambda_t/4$. In such design, the amplitude of the standing wave antinodes at the QWs is reduced and less gain than for the aforementioned RPG structure is exhibited, but the spectral bandwidth is increased. Such a broad gain bandwidth configuration is favourable for mode-locking as well as wavelength tunability. Here, since a node is located at the semiconductor-air interface, scattering losses play a less important role. However, compared to the resonant design, the gain is significantly decreased and therefore the introduction of intracavity elements is more difficult. A representation of the near-antiresonant chip-design is shown in Fig. 1.4. The simulations are made for the same aforementioned structure except that the thickness of the GaInP cap layer is etched down

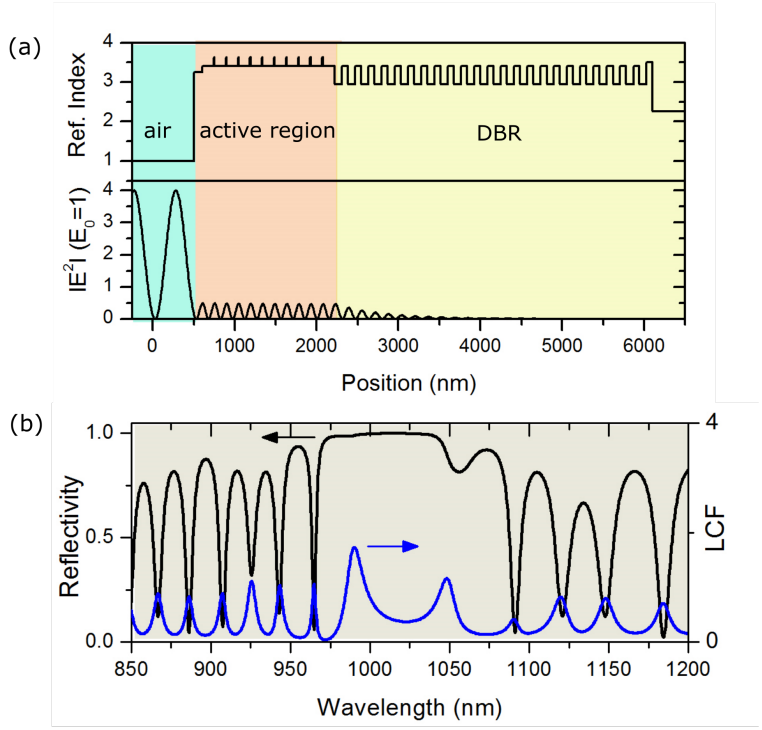


Figure 1.4: Representations of near-antiresonant chip-design (a) Refractive index of the layers (top) and the electric-field distribution of a standing optical wave inside the structure (bottom) for a design wavelength of 1010 nm and 10 QWs. The standing wave intensity is normalized to the input intensity. (b) The wavelength-dependent reflectivity spectrum (left axis) and the light intensity in the QWs (right axis).

to a thickness of 1.25.$\lambda/4$. The refractive indices (top) and the standing wave pattern (bottom) of the multilayer structure are presented in Fig. 1.4 (a), while the simulated reflectivity (black line) and LCF (blue line) of this structure are plotted in Fig. 1.4 (b). In contrast to the resonant-design, it can be seen that, the transmission of the micro-cavity is at a minimum at the design wavelength.

### 1.1.4 Thermal management

High output power is one of the most attractive features of SDLs. However it is strongly limited by a few effects. The main, but not the only, limit is the heat dissipation from the

active region. Additional effects limiting the output power are diffraction losses due to the surface roughness and amplified spontaneous emission in the lateral direction [90]. However those effects are considered to be minor compared to the heating of the active region. The main heat sources in SDLs are the quantum defect, which refers to the energy difference between the pump and the laser photons, and non-radiative recombination [90, 91]. In SDLs, an increase of the temperature of SDLs with increasing pump power will lead to:

- A shift of the QW emission peak to longer wavelengths by $\sim$ 0.3-0.5 nm/K.

- A shift of the microcavity resonance at a rate of $\sim$ 0.1-0.2 nm/K.

Consequently, the RPG resonance wavelengths cannot match the QW peak gain wavelength at low pump power levels. Therefore, the QW emission wavelength is designed to locate at shorter wavelengths than the microcavity resonance at room temperature, so that they coincide at the typical SDL operating temperature [92, 93]. Otherwise, the gain is reduced at low pump powers as well as the output power remains low.
The relation between the wavelength shift due to the dissipated power (calculated as the difference of input power and output power) $\partial\lambda/\partial P$, and due to the temperature $\partial\lambda/\partial T$ is described by the thermal resistance:

$$R_{th} = \frac{\partial\lambda/\partial P}{\partial\lambda/\partial T}. \tag{1.8}$$

Since it is not possible to obtain the temperature in the SDL chip directly from a measurement, the thermal resistance has to be measured indirectly. Several techniques for the determination of the thermal resistance are discussed in [19]. An important result of [19] is, that the roll over temperature $T_{ro}$ is independent on the heat sink temperature $T_{HS}$ of the

SDL device. Furthermore, the following equation is derived:

$$T_{HS} = -R_{th}.P_{d,ro} + T_{ro} \tag{1.9}$$

in which $P_{d,ro}$ is the dissipated power at the roll over point. It can be seen that a lower thermal resistance allows for higher pump powers before the roll over point is reached. As a consequence, higher SDL output powers can be reached. Therefore, a low thermal resistance is desired.

One feature of the SDL's configuration is the thin disk approach. This configuration enables efficient cooling of the device, because the cooled area of the gain element is large with respect to its volume. Therefore, the heat flow occurs mainly along the thickness of the disk and is nearly one-dimensional. Heat dissipation from the SDL's active region is often achieved by the heat spreader connected to the heat sink: either a soldered heat spreader below the DBR is employed, or a transparent heat spreader bonded on top of the emitting surface of the SDL. These principles are called the flip-chip approach and the intracavity diamond approach, respectively. An illustrations of both approaches are shown in Fig. 1.5.

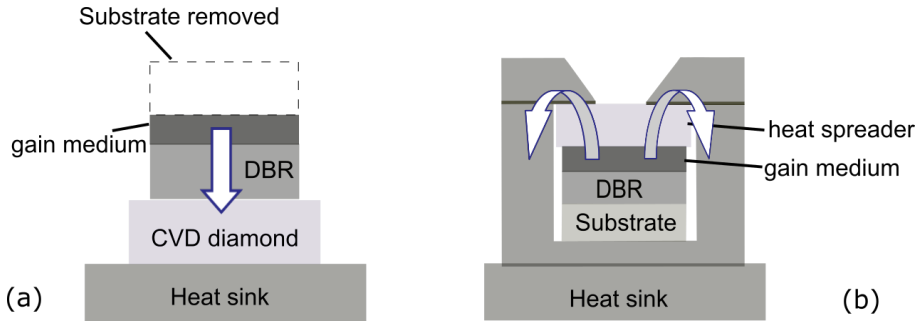


Figure 1.5: (a) Flip-chip bonded device with removed semiconductor substrate. (b) The intracavity diamond heat spreader configuration. Direction of the heat flow is presented by the arrows.

*In the flip-chip approach*, the SDL structure is bonded onto a CVD diamond heat spreader as can be seen in Fig. 1.5 (a). The substrate is then removed from the top of the structure

and the diamond-SDL assembly is consequently bonded onto a water-cooled copper heat sink. The excess heat in the active region in this configuration is extracted through the DBR section, so the thermal conductivity of the DBR section is critical.

*In the intracavity diamond heat spreader configuration*, as shown in Fig. 1.5 (b): The structure growth is capillary bonding to the diamond heat spreaders using water or alcohol at room temperature [94]. Here, the excess heat is extracted directly from the active region, therefore the thermal conductivity of the DBR is less critical. Additionally, the top surface of the intracavity diamond is often coated with an anti-reflection (AR) material in order to reduce the pump reflections.

# 2

# Passively Modelocked Semiconductor disk lasers

Lasers can be operated in different operation modes. Beside cw emission, pulsed operation is also possible. However, the properties of the emitted light are fundamentally different. In case of a cw laser, the output can be optimized for being very well-defined in the optical frequency domain but not in time. On the other hand, a pulsed laser output is confined in time (i.e. the energy is concentrated in a short time) and exhibits a broad spectrum. Pulsed laser sources are a key component in many applications, like frequency comb metrology [95], communication applications [21], laser ablation and many others.

There are various techniques for achieving pulsed operation. One way is to modulate the quality factor (Q-factor) of the laser cavity, this method is referred to as Q-switching [96]. In this method, the modulation of the Q-factor can be done for example with a shutter, which blocks the cavity when it is closed and does not affect the cavity when it is open. When

the cavity is blocked a high level of inversion can be achieved in the gain, which is then suddenly released, once the shutter is opened. With this technique, highly energetic pulses with pulse durations down to values below 100 ps can be obtained.

On the other hand, much shorter pulses as short as a few femtoseconds can be obtained with mode-locking techniques. In this method, a train of pulses is formed, by constructive interference of the different longitudinal modes in the laser cavity. It was first described by DiDomenico [97], Hargrove *et al*. [98] and Yariv [99].

## 2.1 Active and passive mode-locking

In a laser cavity, only discrete optical frequencies are supported. Such frequencies are called resonator modes, and are separated by Fabry-Perot intermodal spacing (free spectral range of a Fabry-Perot):

$$\nu_F = \frac{c}{2L} \tag{2.1}$$

where $c$ is the speed of light in the medium of resonator, and $L$ is the resonator length. In cw operation, these modes oscillate independently and therefore their phases have a random phase relationship between each other. The superposition of their plane waves is noisy (see Fig. 2.1 (b)). On the other hand, while the phase relationship between all the longitudinal modes can be fixed or locked by external means. In this case, destructive interference of the waves will cancel out each other except at regular temporal positions where the waves interfere and add up constructively (see Fig. 2.1 (a)). The more modes that are locked to each other, the broader the spectral bandwidth and the shorter the resulting pulse duration. Such a laser is said to be mode-locked and the result are intense pulses. The modes can be

described as parts of a Fourier-series expansion of a periodic function with time period

$$T_F = \frac{1}{\nu_F} = \frac{2L}{c} = T_R \tag{2.2}$$

which results in a continuous pulse train, spaced by the cavity roundtrip time $T_R$.

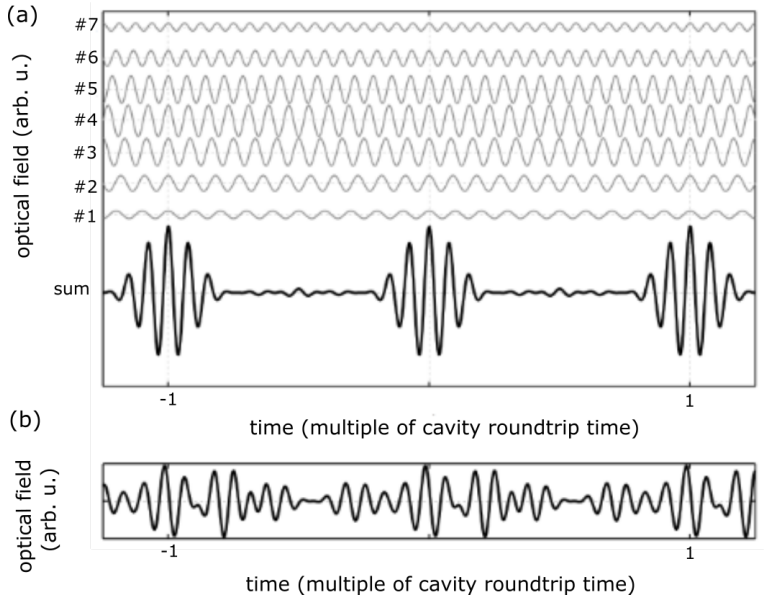


Figure 2.1: Superposition of plane waves at different wavelengths: a) When all modes are locked in phase, they sum up to a light pulse, b) If these modes have random phases, the superposition will lead to a noisy signal.

But the question arising now is, how this modes can be locked together to have the same phase. This can be done by inserting a loss modulator inside the laser cavity, which can be either active or passive. Figure 2.2 shows the laser cavity and loss modulation for an actively and passively mode-locked laser.

*In case of active mode-locking*, the losses in the cavity are modulated by an externally driven element like an electro-optic or acousto-optic modulator. The signal which is electronically driven results in a sinusoidal loss modulation with a period given by the cavity round trip time $T_R$ (see Fig. 2.2 (a)). Around the minimum of the sinusoidal loss modulation, a net

gain is accumulating which leads to opening a window for pulsed operation. The pulses are therefore significantly shorter than $T_R$.

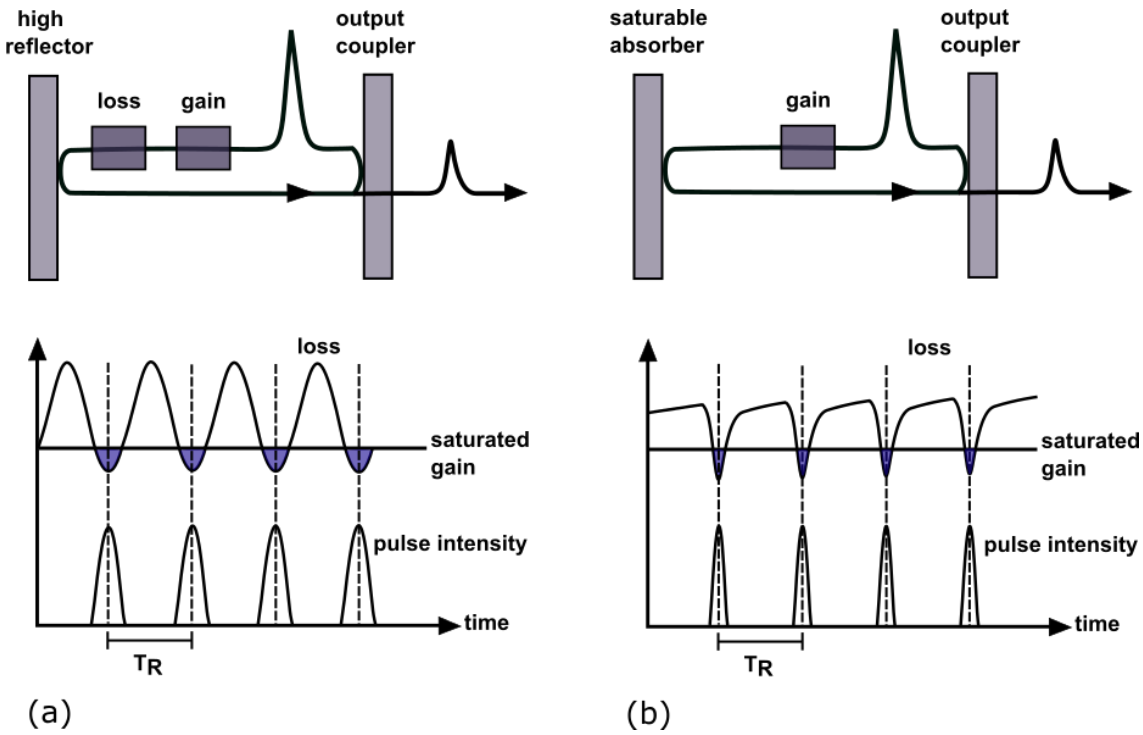


Figure 2.2: a) Active mode-locking: The losses are modulated by an optical switch driven by an externally applied signal. The signal produces a sinusoidal loss modulation. Only around the minimum of the losses a net gain is obtained which opens the window for pulsed operation. b) Passive mode-locking: A saturable absorber is used as an end mirror. The loss of the saturable absorber are modulated by the pulse itself.

*In case of passive mode-locking*, an intracavity element with an intensity-dependent loss is required, like a saturable absorber. In this case, the loss of the saturable absorber is modulated by the pulse itself (see Fig. 2.2 (b)). For low intracavity intensities, the larger the losses of the saturable absorber, the smaller intensities are and vice versa. Therefore, the optical losses in cw operation are much higher than that of an optical pulse. As a result, the behaviour of the losses becomes nonlinear, and the laser favours mode-locked over cw operation. This method produces much shorter pulses, because of the recovery time of the saturable absorber is usually much shorter than the oscillation of an electronic signal used

for active mode-locking.

## 2.2 Mechanisms of passive mode-locking

Depending on the recovery time of the absorber, passive mode-locking can be classified by three different mechanisms [100], shown in Fig. 2.3 and briefly summarized in the following:

- Fast saturable absorber with weak gain saturation.
- Slow saturable absorber with weak gain saturation.
- Slow saturable absorber with strong gain saturation.

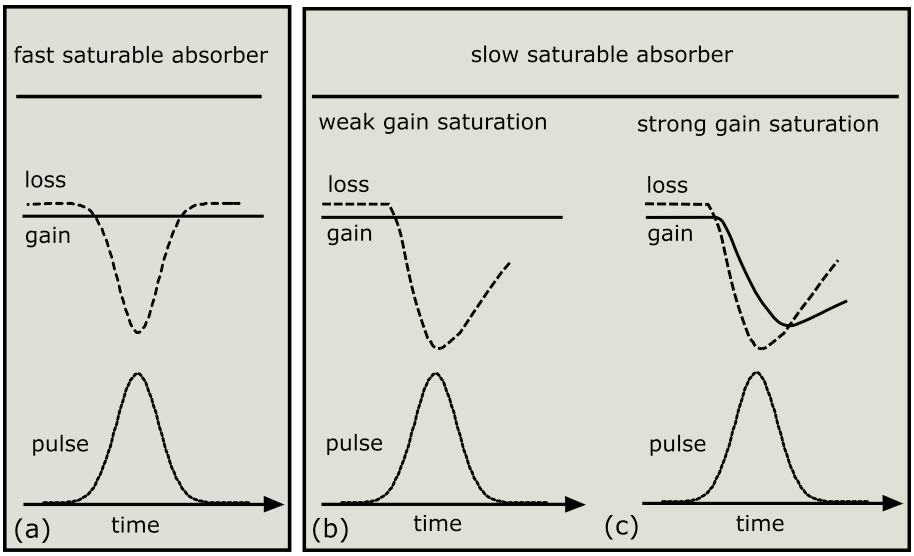


Figure 2.3: Three typical passive mode-locking mechanisms: (a) A fast saturable absorber with a recovery time shorter than the pulse duration; (b) A slow saturable absorber opens a long time window of positive net gain; (c) A slow saturable absorber in combination with dynamic gain saturation.

### 2.2.1 Fast saturable absorber

A fast saturable absorber means that its recovery time is much shorter than the pulse duration. Constant gain is assumed and the recovery time of the absorber dominates the pulse characteristics, as can be seen in Fig. 2.3 (a). An example of this mode-locking mechanism is Kerr lens mode-locking (KLM) [101, 102]. The loss modulation follows the pulse shape, and the positive net gain window is closed immediately after the pulse has passed. Here, the Kerr non-linearity leads to an intensity-dependent lensing effect of the gain medium, also referred to as self-focusing. The self-focusing in combination with an aperture leads to a reduction in losses and thus favors mode-locked operation. One disadvantage of KLM is, that a significant change in mode size from the Kerr effect is achieved only if the laser cavity is operated near the stability limit, making operation more sensitive to temperature changes and mechanical drift. On the other hand, the very fast response and recovery time (in the range of few a femtoseconds) for this effect enabled the shortest pulses directly generated by a laser oscillator; pulse durations down to 5 fs were obtained using the Ti:sapphire gain material [103, 104].

### 2.2.2 Slow saturable absorber with weak gain saturation

In case of a slow saturable absorber, the recovery time is slow compared to the pulse duration. One can distinguish two dynamic situations, which depend on the gain medium used in the laser system. If the upper state gain-medium lifetime is longer than the cavity roundtrip time, a weak gain saturation is resulted and the gain can be considered as nearly constant over time. This is mostly the case for ion-doped solid-state gain media that have typical cross sections more than $10^5$ times smaller than semiconductor or dye lasers [5]. On the other hand, semiconductors, have a high gain cross sections, and significant dynamic

gain saturation can occur during the amplification of the pulse. Figure 2.3 (b) shows the combination of constant gain with a slow saturable absorber.

Due to the slow recovery of the absorber, a wide net gain is resulting even after the pulse. At the first glance, it is surprising that stable operation can be obtained because any fluctuations after the pulse can be amplified (due to the constant gain) and might introduce instabilities. Nevertheless, stable mode-locked operation can be achieved in this regime even if the pulse duration is shorter than the net gain window. This result is simply obtained, because the leading edge of the pulse is absorbed by the saturable absorber much stronger than the trailing edge on each cavity roundtrip time. Thereby, constantly shifting the pulse slightly backwards in time, such that the pulse itself is swallowing any amplified noise behind it. Depending on the recovery time of the saturable absorber, pulse durations in the picoseconds regime can be achieved with this mode-locking scheme. To obtain sub-ps pulses in this mode-locking regime, additional pulse shaping mechanisms are required, most commonly found is soliton-modelocking.

### Soliton mode-locking

Briefly summarized, soliton mode-locking refers to the case when femtosecond solid-state lasers with soliton-like pulse shaping can be mode-locked by a slow saturable absorber with a recovery time much longer than the pulse width without any additional dynamic gain saturation. Soliton mode-locking is based on an interplay of self-phase modulation (SPM) and negative GDD [105]. The phase $\Delta\varphi$ introduced for a wave travelling through an optical Kerr medium with a nonlinear refractive index $n_2$ and a thickness $d$ is

$$\Delta\varphi = n_2 I k_0 d. \tag{2.3}$$

where $k_0$ is the wavenumber and $I$ is the optical intensity [105]. In case of an optical pulse, the Kerr effect causes a time-dependent phase shift according to the time-dependent pulse intensity. In this way, an initial unchirped optical pulse acquires a so-called chirp, i.e., a temporally varying instantaneous frequency.

$$\Delta\varphi(t) = n_2 I(t) k_0 d. \tag{2.4}$$

For a gaussian beam with a radius $\omega$, Eq. 2.4 can be written as:

$$\Delta\varphi(t) = 2n_2 \frac{P(t)}{\omega^2 \pi} \frac{2\pi}{\lambda} d = \frac{4n_2 d}{\omega^2 \lambda} P(t) = \gamma_{SPM} P(t), \tag{2.5}$$

wherein $\gamma_{SPM}$ is the SPM coefficient (in rad/W). Therefore it is possible to calculate the instantaneous frequency of the pulse by

$$\Delta\omega_i(t) = -\frac{dP(t)}{dt} \gamma_{SPM}. \tag{2.6}$$

Since $\frac{dP(t)}{dt} < 0$, the frequencies are higher in the trailing edge (back of the pulse), while lower in the leading edge (front of the pulse). Therefore, SPM introduces a so called up-chirp, i.e. the instantaneous frequency increases during the pulse. On the other hand, a negative GDD causes the high frequency components of the pulse to travel faster than the low frequency components, therefore, the pulse gets down-chirped. In this case, if GDD and SPM are properly balanced, they compensate each other in such a way that the soliton shape ($\text{sech}^2$-pulse, hyperbolic secant squared envelope) is maintained in the time and frequency domain. Nevertheless, the saturable absorber still plays an important role, it starts the mode-locking operation and prevents the cw background from growing. A

soliton pulse can be achieved with

$$\tau_p \approx 1.76 \frac{2 \mid D \mid}{\mid \gamma_{SPM} \mid E_p}, \tag{2.7}$$

where $\tau_p$ is the full-width half maximum pulse duration, $E_p$ is the intracavity pulse energy and $D$ is the total negative dispersion per roundtrip. The quantities $\gamma_{SPM}$ and $D$ must have opposite signs [105]. Equation 2.7 is a good approximation if the action of the absorber is weak, so that the pulses effectively see only the average dispersion and nonlinearity. With too-low nonlinear phase changes, the solitons are strongly disturbed by other effects such as the action of the absorber, while excessive nonlinear phase shifts can cause pulse break-up [105]. Pulses as short as 46 fs have been achieved with this technique [106]. With shorter pulses, this model fails, since higher order dispersion influences the pulse as well.

### 2.2.3 Slow saturable absorber with strong gain saturation

In contrast to ion-doped solid-state gain media, semiconductor lasers as well as dye lasers exhibit a high gain cross sections and a short carrier recombination times, which is on the order of ns [7]. As a result, the saturation energies of the gain media are relatively low and the excited state can be almost totally depleted by an incoming pulse. For this mode-locking mechanism, the time-dependent net gain plays an important role for providing a pulse shortening. Fig. 2.3 (c) shows schematically the pulse-shortening mechanism in this case. Before the pulse the loss exceeds the gain. As the pulse arrives, it saturates the absorber so that the loss line drops below the gain. At this point, the pulse experiences an amplification. Later in, the gain begins to saturate, and as a result, the gain drops below the loss.

## 2.3 Theories of pulse formation in passively mode-locked SDLs

No systematic investigation of pulse formation in passively mode-locked SDLs was performed until 2002 by Paschotta *et al*. [107]. Here, short pulse operation was accounted for by a balanced interplay between SPM from refractive index changes in the semiconductor structures and the normal cavity dispersion, in analogy to the soliton mode-locking frequently observed in solid-state and fiber lasers.

Since then, many theoretical considerations have been devoted to the explanation of the occurrence of sub-ps pulses in SESAM mode-locked SDLs. Mechanisms such as the optical Stark effect [108–110] and spectral hole burning [111] have been proposed as being responsible for pulse shortening. Up to now, neither a numerical nor an analytical approach for the modelling of passively mode-locked SDLs that includes all the above mentioned phenomena has been introduced. In addition, investigations of picosecond pulse dynamics in the multiple pulses regime and with a weak saturation of the absorber have been performed in Refs. [112, 113].

### 2.3.1 Pulse shaping in SESAM-mode-locked SDLs

Since the SDL gain chips consist of semiconductor materials, the corresponding mechanism of mode-locking is based on a slow saturable absorber in combination with strong dynamic gain saturation. Semiconductor materials have a short gain lifetime of the excited state (in the order of nanoseconds) which results in a relatively high gain cross section [7]. As a result, the saturation energy of the gain is relatively low and the excited state can be almost totally depleted by an incoming pulse. In this mode-locking scheme, the net gain window for a pulse opens if the absorber saturates faster than the gain, i.e., if the saturation energy of

the absorber is much lower than that of the gain. The net gain window remains open until the gain is saturated to a level where the losses exceed gain. In order to obtain a net gain and stable mode-locked operation in this regime, the saturation energy of the gain must be about an order of magnitude larger than the saturation energy of the absorber [114], i.e.

$$\frac{E_{sat,abs}}{E_{sat,gain}} = \frac{A_{abs} \cdot F_{sat,abs}}{A_{gain} \cdot F_{sat,gain}} \ll 1. \tag{2.8}$$

where

$E_{sat,abs}$: the saturation energy of the absorber,

$E_{sat,gain}$: the saturation energy of the gain,

$A_{abs}$: the cavity mode area on the absorber,

$A_{gain}$: the cavity mode area on the gain,

$F_{sat,abs}$: the saturation fluence of the absorber,

$F_{sat,gain}$: the saturation fluence of the gain.

This equation can be satisfied by either using a smaller spot size on the saturable absorber or by choosing an absorber with a lower saturation fluence than the gain. In the absence of additional pulse shaping mechanisms, the pulse duration relates to the width of the net gain window determined by the interplay of gain depletion and absorber saturation.

### 2.3.2 Pulse shaping in femtosecond SESAM-mode-locked SDLs

Pulses much shorter than the interband recombination time of the saturable absorber can be achieved in mode-locked SDLs if additional mechanisms contribute to pulse shortening,

such as spectral hole burning and the optical Stark effect, in order to switch the semiconductor elements into effectively fast pulse shapers [108, 109, 111]. Additionally, a necessary condition for ultrashort pulse generation is the minimization of the chirp, which is easily provided for SDLs by soliton-like mode-locking [107].

### Quasi-soliton mode-locking

As described before in Section 2.2.2, in ion-doped solid-state lasers, for which no significant dynamic gain saturation takes place, the most common mode-locking mechanism to obtain short pulses with slow saturable absorber is soliton-mode-locking. Here, SPM introduces a phase shift proportional to the instantaneous power, according to Eq. 2.5. This phase changes can be compensated by negative dispersion. On the other hand, semiconductor lasers can exhibit a large gain depletion during the pulse transit through the gain medium. Further, this dynamic gain saturation is followed by a fast gain recovery between pulses. In a semiconductor saturable absorber, a change of opposite sign compared to that in the gain is created in the excited carrier density when a pulse bleaches the absorber. From the Kramers-Kronig relation, the changes in the excited carrier density are directly related to changes of the refractive index of the semiconductor material through the linewidth enhancement factor [115]:

$$\alpha = 2k\frac{dn/dN}{dg/dN}, \tag{2.9}$$

where $k$ is the wavenumber, $N$ is the carrier density, $n$ is the refractive index and $g$ is the power gain. These changes in the refractive indices result in a nonlinear phase change. This

phase change due to the gain change is given by

$$\Delta\varphi = -\frac{\alpha}{2} \cdot g(t). \tag{2.10}$$

In Fig. 2.4 (a), the changes in reflectivity of the SESAM (dashed black) as well as the gain (solid black) are illustrated for an incoming 1-ps pulse. The resulting phase changes are shown in Fig. 2.4 (b). Due to the requirement and fact, that the SESAM has to saturate faster than the gain (Eq. 2.8), the phase change from the SESAM (dashed black), which is negative, decreases mainly in the leading edge of the pulse. On the other hand, the phase change of the gain is positive and rises slowly during the pulse (solid black).

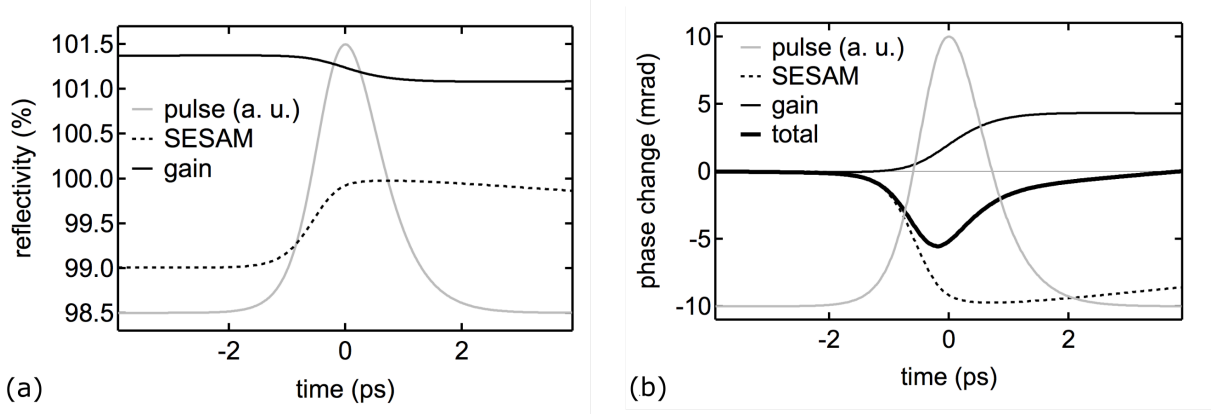


Figure 2.4: (a) Dynamic saturation of the gain and the SESAM within the pulse duration, represented by an optical pulse in arbitrary units. (b) Phase changes of the gain and the SESAM induced by saturation effects resulting in a total phase change which is similar to the phase change induced by SPM. Copied from [116].

The total phase change (bold black) results from the phase change of the SESAM and the phase change of the gain. The total phase change is similar to the phase change of SPM in case of soliton mode-locked lasers, but with an opposite sign. As a result, positive dispersion is needed to balance these phase shifts in order to obtain stable mode-locked operation. This mechanism is referred to as quasi-soliton mode-locking. The quasi-soliton mechanism

was experimentally verified in the picosecond regime [117] as well as in the femtosecond regime [118] by comparing pulse propagation simulations with real experiments.

### 2.3.3 Other SDL mode-locking mechanisms

In addition to the standard SESAM mode-locking techniques, other SDL mode-locking techniques have been introduced. In 2013, Zaugg *et al*. presented an SDL mode-locked with a single layer graphene saturable absorber mirror [53]. They demonstrated a very broad tunable operation bandwidth of 46 nm and a very fast absorber recovery time. However, a limited average power in the milliwatt regime has been obtained, which is caused by excessive nonsaturable losses. One year later, output power levels of up to 10 W have been obtained by Husaini *et al*., but with double pulses operation [54]. On the other hand, another mode-locking mechanism reported recently is the so-called SML-SDLs or the KLM-SDLs [56–63]. In that case, mode-locking takes place without any additional saturable absorber in the system while a hard aperture is inserted in front of the output coupler. In analogy to solid-state lasers, the mode-locking mechanism was initially explained by the Kerr lensing effect in the gain region.

## 2.4 Self-mode-locking SDLs

The first SESAM-free mode-locked SDL has been reported by Chen *et al*. in classical straight cavity configuration [56]. In that work, the authors suggested that mode-locking results from saturable absorption in the unpumped QWs, in analogy to the MIXSEL. Pulses as short as 654 fs have been generated with an average output power of 0.45 W at a repetition rate of 2.17 GHz. One year later, Kornaszewski *et al*. demonstrated the SML in a folded

six-mirror SDL-cavity configuration [57]. However, they attributed the origin of pulsed operation to the intensity dependent Kerr lensing effect arising in the semiconductor gain medium. In that work, the mode-locked operation has been shown in two different configurations. Firstly, stable mode-locking was observed when the cavity was operated near its stability limit. In such configuration, single pulses with durations of 1.5 ps at an average output power of 700 mW at 200 MHz repetition rate could be achieved. Secondly, mode-locked operation could also be achieved by operating the cavity in its stability region and by inserting a hard aperture near the output. Pulses with durations of 930 fs could be achieved at a 210 MHz repetition rate.

It did not take long time and other groups observed the SML phenomena. Albrecht *et al*. also predicted KLM operation for both soft and hard apertures placed at the optimal intra-cavity positions [58]. Their system delivered pulses with durations of below 500 fs at 1 GHz repetition rate. Nevertheless, in their measurements, they observed a residual background or pedestal which can be attributed to CW background; in addition the pulse train fluctuated over a time scale of some microseconds. Alternatively, in [60] Moloney *et al*. claimed to enhance the Kerr lensing effect with an extra Kerr medium inside the cavity. For this, they utilized an yttrium orthvanadate crystal which exhibits a nonlinear refractive index three times higher than that of titanium sapphire. However, a pulse duration of about 850 fs sits on a high background pedestal indicating a strong quasi-CW component in the emission. On the other hand, Liang *et al.* (in the Chen-group) [61] supposed that the occurrence of SML can be assisted by the existence of high-order transverse modes. Liang *et al.* observed a threshold for SML which coincided with the threshold of high-order transverse modes.

### 2.4.1 Kerr-lensing in an SDL gain chip

As discussed before in section 2.2.1, in the majority of solid state lasers, KLM originates from the optical Kerr effect in the gain-medium hosting crystal, while it is possible that the Kerr medium is separate from the gain structure itself. On the other hand, Albrecht *et al.* analyzed the potential for KLM operation in a simple SDL cavity as a consequence of the ultrafast Kerr nonlinearity in the semiconductor gain chip itself [58]. They considered a typical linear SDL cavity of length $d$, consisting of a curved mirror with radius $R$, and a flat end mirror with the gain (Kerr) medium.

Using standard text book ABCD matrix formalism, they calculated the modulation (relative change in beam radius) at any point (z) in the cavity as:

$$\frac{\omega(z, P_{peak}) - \omega(z, 0)}{\omega(z, 0)} \approx \gamma(z_k) \frac{P_{peak}}{P_c} \frac{L}{2 z_0 n_0} \frac{1 - z^2/z_0^2}{1 + z^2/z_0^2}. \tag{2.11}$$

where $L$ is the Kerr medium thickness, $P_{peak}$ is the intracavity peak power, $z_0 = (dR(1 - d/R))^{1/2}$ is the Rayleigh rang of the linear cavity, $P_c \approx a\lambda^2/8\pi n_0 n_2$ is the self-focusing critical power, and $n_2$ is the nonlinear refractive index, while $\gamma$ is a geometric cavity parameter given by:

$$\gamma(z_k) = -\frac{R/z_0}{2(1 + z_k^2/z_0^2)} + \frac{(d/z_0)(1 - z_k/d)^2}{(1 + z_k^2/z_0^2)^2}. \tag{2.12}$$

Next, Albrecht *et al.* explored the feasibility of KLM operation in SDLs for typical experimental parameters of $P_{peak} = 10$ kW, $L = 4\mu m$, and $n_2 = -1 \times 10^{-12} cm^2/W$. Figure 2.5 depicts essentially an intracavity z-scan, where the calculated change in the beam radius (from Eq. 2.11) at the locations of gain chip and the curved mirror are shown as a function

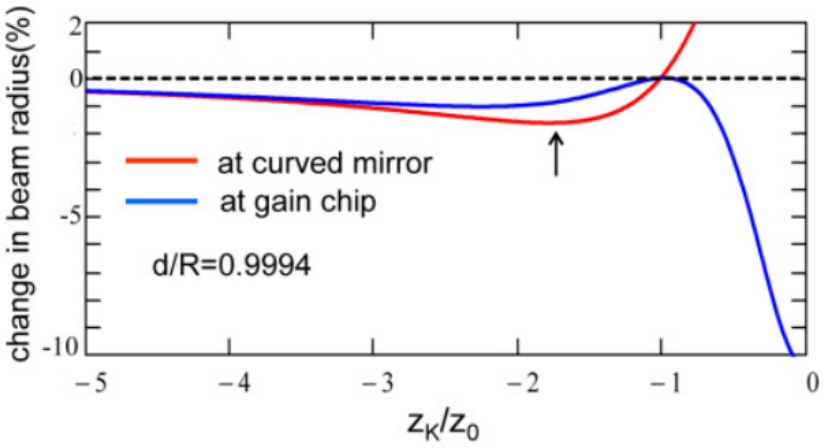


Figure 2.5: Calculated beam-radius modulation (using Eq. 2.11) at the gain chip (blue) and the curved mirror (red) as a function of the distance of the gain medium from the flat mirror. Negative change (in y-axis) implies beam narrowing. Reproduced with permission [58]. Copyright 2013, Optical Society of America.

of position of the Kerr medium. The negative sign, implying beam narrowing, can therefore be exploited for mode-locking. As shown in the figure, the beam narrowing due to the negative Kerr effect at the gain chip occurs for all positions of the gain chip.

### 2.4.2 Z-scan measurements of SDL gain medium nonlinear refractive index

As was mentioned before, the mechanism responsible for SML has not been identified yet, with some proponents suggesting that Kerr lensing in the gain medium is responsible and others suggesting that mode-locking results from saturable absorption in unpumped quantum wells. Motivated by this uncertainty and for the sake of a deeper analysis, Quarterman *et al*. described measurements of the nonlinear refractive index ($n_2$) of an SDL gain medium and demonstrated that the magnitude of the resulting Kerr lens is sufficiently large to cause an appreciable perturbation in a typical SDL cavity [119].

The authors of that study measured $n_2$ of an antiresonant 1050 nm SDL gain medium with

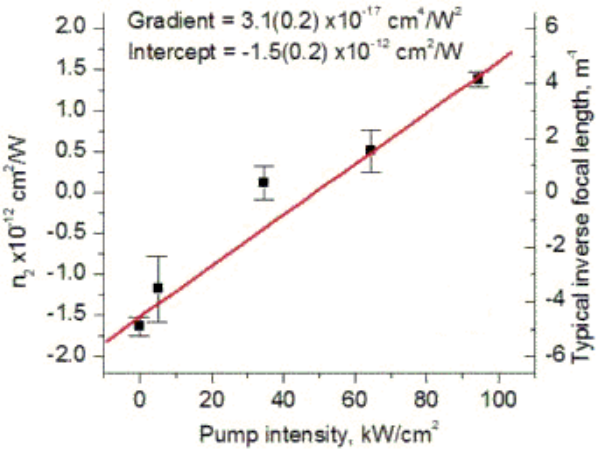


Figure 2.6: Extracted values of $n_2$ as a function of pump intensity shown on the left-hand y-axis, and the corresponding inverse focal lengths of nonlinear lenses shown on the right-hand y-axis. Reproduced with permission [119]. Copyright 2015, AIP publishing LLC

11 InGaAs QWs using a reflection-type z-scan system, with a 1064 nm, 10-ps-pulse laser as a probe, and a fiber-coupled 808 nm diode pump laser for carrier injection. They found, that $n_2$ depends approximately linearly on the applied pump intensity, having a value of $-1.5(0.2) \times 10^{-12} cm^2/W$ at zero excitation but increasing to take on positive values at typical SDL operating conditions. The focal lengths of corresponding Kerr lenses were calculated using typical SDL pulse intensities, which turned out to be sufficiently short to be comparable to the SDL's cavity mirror distances, implying that KLM may be responsible for the observation of SML in SDLs. The obtained values of $n_2$ are plotted in Fig. 2.6 as a function of incident pump intensity. In the chart, the nonlinear refractive index increases approximately linearly with increasing pump power. It should be noted, that theoretical predictions of $n_2$ in active semiconductor structures are difficult to obtain, owing to the large number of effects which can contribute to $n_2$. Notice that, the presented values of $n_2$ are many orders of magnitude larger than in solid state gain-medium hosting crystals, such as sapphire. This large value of $n_2$ is however compensated by the small thickness of the semiconductor gain medium, which is typically of the order of a few $\mu m$.

## 2.5 Employed gain mirror structures and cavity designs in this thesis

### 2.5.1 Gain mirror structures

In this section the design of the employed chip structures used in this thesis will be discussed. A brief overview of two different structures is given in Table 2.1.

Table 2.1: Overview of the semiconductor disk laser gain mirrors used in this thesis.

| | Chip 1 | Chip 2 |
|---|---|---|
| Design wavelength (nm) | 1010 | 1040 |
| Gain type | QW | QD |
| Gain layers | 10 single QWs | 35 QD layers |
| Active material | InGaAs | InGaAs |
| Quantum-film thickness (nm) | 8 | 79.5 |
| Barrier | GaAsP | GaAs |
| Mirror pairs per DBR | 24.5 | 29.5 |
| Resonance | Anti-resonant | Anti-resonant |
| Heat spreader | CVD diamond below DBR | Intracavity diamond |

*Structure 1* is an MOVPE grown VECSEL chip with 10 InGaAs QWs equally spaced by $\lambda/2$ GaAsP barrier layers. The DBR consists of 24.5 pairs of $\lambda/4$ GaAs/AlGaAs layers and is transparent to the wavelength of the fibre-coupled 808 nm diode pump laser. The structure was grown bottom-up and flip-chip bonded with Au-In solid-liquid interdiffusion onto a 350 $\mu$m-thick CVD diamond heat spreader. Originally, the chip was designed as a resonant chip and exhibits the micro-cavity resonance at the quantum well gain peak at 1010 nm. For the purpose of mode-locking, the cap layer thickness was reduced from $\lambda/2$ to $\lambda/4$ via

wet etching in order to obtain an anti-resonant micro-cavity with minimized GDD and a spectrally broadened effective gain of the structure. A schematic drawing of the SDL chip as well a zoom in for the chip structure are shown in Fig. 2.7 (a) and Fig. 2.7 (b), respectively.

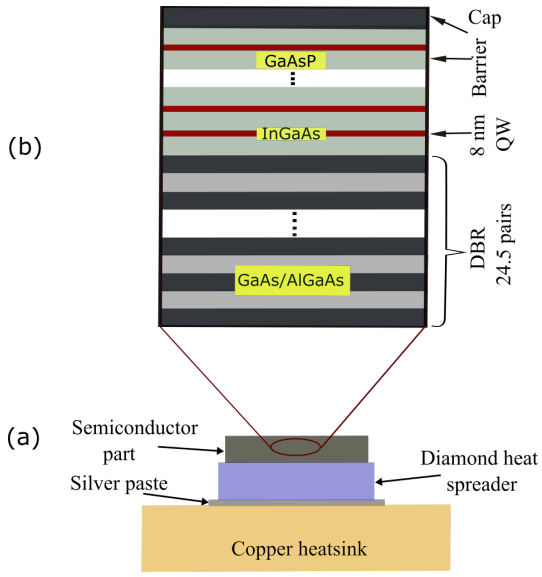


Figure 2.7: (a) Scheme of flip-chip bonded *Structure 1* onto a diamond heat spreader. (b) Schematic zoom-in view for this QW-VECSEL chip structure.

*Structure 2* was grown by molecular-beam epitaxy. It consists of 35 layers of Stranski-Kranstanow grown InGaAs QDs within GaAs spacers, organized as five stacks of seven QD layers. These stacks are distributed within the cavity to be located at standing-wave electric field antinodes of the optical mode for an optimum gain. As in *structure 1*, a ternary DBR was grown, which consists of 29.5 pairs of GaAs/AlGaAs and is transparent to the wavelength of the fiber-coupled 808 nm pump laser. Both, the QDs and the DBR, are designed for an emission wavelength of 1040 nm. The SDL chip is capillary bonded to an intracavity diamond heat spreader with an anti-reflection coating, which also minimizes the GDD at the design wavelength. A schematic drawing of the SDL chip as well as a zoom in for the

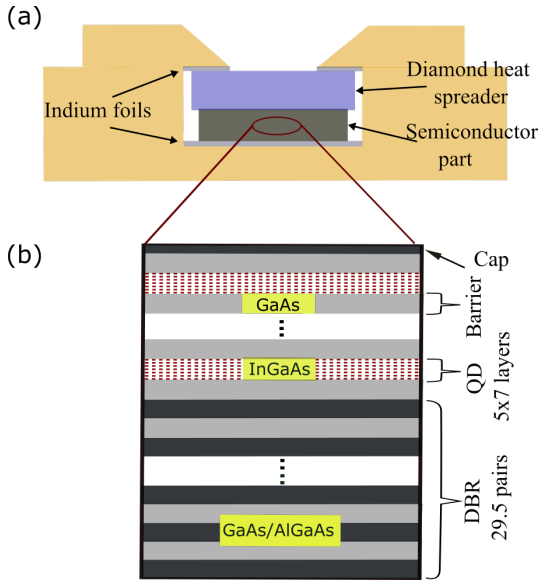


Figure 2.8: (a) Scheme of top emitting *Structure 2* with an intracavity diamond heat spreader (b) Schematic zoom-in view for the QD-VECSEL chip structure.

chip structure are shown in Fig. 2.8 (a) and Fig. 2.8 (b), respectively.

### 2.5.2 Cavity designs

While the cavity geometry of the presented SML SDLs vary slightly, the principle which allows for mode-locking remains the same. Here, the laser setups for a QW and a QD-VECSELs are schematically shown in Figs. 2.9 (a) and 2.10 (a), respectively. As the diamond heat spreader of the QW-VECSEL is attached to the chip's DBR structure, the VECSEL chip is directly mounted on a water-cooled copper heat sink. The laser resonator can be seen as a Z-shaped cavity, which is formed by a flat output coupler (OC) with a transmittance of $1.6\%$, the gain chip itself, and a highly reflective (HR) curved mirror (CM) with a radius of curvature of 150 mm as well as a plane HR mirror. With a total cavity length amounting to 30 cm, a free spectral range of approximately 0.5 GHz is determined. The cavity is optimized for mode-locked operation assuming negative Kerr-lensing inside the VECSEL

chip structure. Therefore, a variable slit is placed directly in front of the HR end mirror. An 808 nm fiber-coupled diode laser, which can deliver up to 35 W output power, is used to pump the system. The beam waist variation over the cavity elements is shown in Fig. 2.9 (b). An overview of the setup parameters and cavity results obtained from such laser cavity is illustrated in Table 2.2.

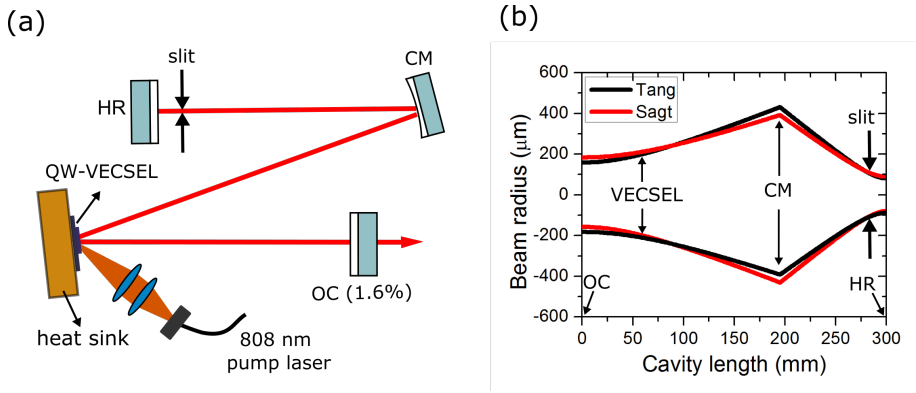


Figure 2.9: (a) Schematic drawing of the Z-cavity setup used to realize SML for the QW-SDL. (b) Illustration for the variation of the mode sizes on the different cavity elements.

For the QD-VECSEL setup, the copper heat sink is attached to both the outer region of the intracavity diamond heat spreader on the top of the gain mirror and the DBR structure on the reverse side of the VECSEL chip. A thermoelectric cooler is employed to extract excess heat from the copper heat sink and to transfer it to the closed-cycle water-cooling mount. To complete the laser cavity, a concave OC mirror with a transmittance of $0.6\%$ and radius of curvature of 100 mm is placed at a position 97 mm away from the gain chip. Thereby, a linear cavity is formed with a free spectral range of approximately 1.5 GHz. Figure 2.10 (b) shows the beam waist variation over the cavity length. An overview of the setup parameters and cavity results obtained from this laser cavity is illustrated in Table 2.3.

Table 2.2: Overview of the setup parameters and cavity results for a Z-cavity design using a QW-based gain structure.

| Parameter | | | Value |
|---|---|---|---|
| Cavity Results | | | |
| | Fundemental ML | $2_{nd}$ harmonic | $3_{rd}$ harmonic |
| Pulse duration (fs) | 860 | 1120 | 950 |
| Average output power (W) | 0.46 | 0.96 | 1.23 |
| Repetition rate (GHz) | 0.504 | 1.008 | 1.512 |
| Peak power (W) | 948 | 752 | 754 |
| Central wavelength (nm) | 1013.8 | 1014.2 | 1014.5 |
| TBWP | 0.69 | 0.73 | 0.72 |
| Setup Parameters | | | |
| Cavity length (mm) | | | 300 |
| OC transmission (%) | | | 1.6 |
| Heat sink temperature ($°C$) | | | 18 |
| Pump mode radius ($\mu m$) | | | 160 |

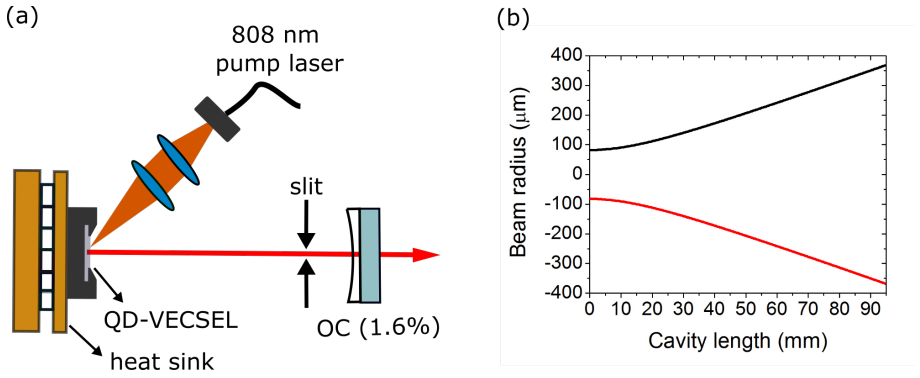


Figure 2.10: (a) Schematic drawing of the linear-cavity setup used to realize SML for the QD-SDL. (b) Illustration for the variation of the mode sizes on the different cavity elements.

Table 2.3: Overview of the setup parameters and cavity results for a linear-cavity design using a QD-based gain structure.

| Parameter | value |
|---|---|
| Cavity Results | |
| Pulse duration (fs) | 950 |
| Average output power (W) | 0.76 |
| Repetition rate (GHz) | 1.5 |
| Peak power (W) | 460 |
| Central wavelength (nm) | 1040 |
| TBWP | 1.07 |
| Setup Parameters | |
| Cavity length (mm) | 97 |
| OC transmission ($\%$) | 0.6 |
| Heat sink temperature ($^{\circ}C$) | 5 |
| Pump mode radius ($\mu m$) | 65 |

# 3

# Summary and outlook

This dissertation presents results on ultrashort pulse generation in optically-pumped SDLs using a saturable-absorber-free mode-locking technique. In this context, we highlight the demonstration of SML-SDLs as a variation of mode-locked SDLs which do not require a saturable-absorber mirror for pulsed operation, and thus circumvent some limitations set by saturable absorbers.

In this work, SML operation has been demonstrated for quantum well (QW) based SDLs. The used cavity was designed by assuming a Kerr-lensing in the laser gain region. Short pulses down to 860 fs with a peak power of 948 W has been obtained at a repetition rate of 500 MHz. Furthermore, a clear evidence of mode-locking under SML conditions is presented. Green light originating from second-harmonic generation in an external BBO crystal was demonstrated using the out-coupled laser beam, unobtainable under cw operation

at equivalent average-power levels. In addition, long-time-span pulse trains as well as radiofrequency spectra measurements were presented for the sub-ps pulses which indicate the stable pulse operation of our device. Moreover, a long-time-span autocorrelation trace, which emphasizes the absence of a pedestal or double pulses, was shown. A beam-profile measurement revealed the excellent beam quality of the device with an M-square factor of less than 1.1 for both axes, showing that SML can be achieved for the fundamental transverse mode.

Additionally, our SESAM-free mode-locked SDL device is not only demonstrated for a single pulse operation, but also for the second and third harmonic mode-locking. In contrast to SESAM mode-locking, stable harmonic mode-locking is achieved only at nearly-discrete pump-power levels. For the second and the third harmonic operations, we obtain pulse durations of 1.12 ps and 950 fs with peak powers of 752 and 754 W, respectively.

On the other hand, quantum dot (QD) based SDLs also attracted much attention in mode-locking experiments due to the novel properties of QDs. They have shown their potential for realizing low thresholds and a lower thermal sensitivity. In addition, the QD gain layers inherently exhibit strong inhomogeneous gain broadening and ultrafast carrier dynamics. In this thesis, we presented the first passively SML QD-based SDL. The measurements indicated sub-picosecond duration of the laser pulses with 750 mW average output power at 1.5 GHz repetition rate.

To summarize, SML results are presented for a QW as well as a QD device to emphasize that this quite young technique—even though the mechanism behind the effect has yet not been well understood—is capable of enabling mode-locked operation for different gain media as well as cavity configurations.

Even though the driving mechanism for SML has to be studied with care in future inves-

tigation for an efficient use of the underlying effects, we believe that in the near future SML-SDLs, which combine the advantages of solid-state and semiconductor devices, can become robust, compact and low-cost sources of fs-pulsed laser light. Future work in the field of ultrafast SDLs will involve the further improvement of the oscillators, the search for novel applications and the development of prototype sources. Furthermore, pushing the limits of mode-locked SDLs towards 100 fs pulse durations at watt-level average output power will allow for omitting external power amplification and compression stages in such ultrafast lasers.

# 4

# Publications

## 4.1 Harmonic self-mode-locking of optically pumped semiconductor disc laser

M. Gaafar, C. Möller, M. Wichmann, B. Heinen, B. Kunert, A. Rahimi-Iman, W. Stolz, M. Koch, IET Electronics letters **50**, 542 (2014). DOI:10.1049/el.2014.0157.

**Abstract**

A saturable-absorber-free vertical-external-cavity surface-emitting laser is presented which is harmonically mode-locked. Mode-locking is initiated via fine-tuning of an aperture which is placed near one of the cavity end mirrors. Fundamental mode-locking is observed along with the second and third harmonic operations for increased optical pump powers.

The system features pulse durations penetrating the femtosecond regime at a wavelength of 1014 nm.

**The author's contribution**

This work was planned and conducted by myself, with the guidance of Prof. Dr. M. Koch. I carried out all experiments by myself, with the support of the coauthors, who also helped to interpret the data. The manuscript was primarily written by myself with the help of Dr. A. Rahimi-Iman, Dr. M. Wichmann and C. Möller. All co-authors contributed with fruitful discussions and important ideas. The VECSEL chip was designed and provided by B. Heinen, B. Kunert, and Prof. Dr. W. Stolz.

# Harmonic self-mode-locking of optically pumped semiconductor disc laser

M. Gaafar, C. Möller, M. Wichmann, B. Heinen, B. Kunert, A. Rahimi-Iman, W. Stolz and M. Koch

A saturable-absorber-free vertical-external-cavity surface-emitting laser is presented which is harmonically modelocked. Modelocking is initiated via fine-tuning of an aperture which is placed near one of the cavity's end mirrors. Fundamental modelocking is observed along with the second and third harmonic operations for increased optical pump powers. The system features pulse durations penetrating the femtosecond regime at a wavelength of 1014 nm.

*Introduction:* In recent years, considerable efforts have been undertaken to study and optimise modelocking (ML) for the vertical-external-cavity surface-emitting lasers (VECSELs). ML in VECSELs is mainly achieved by the use of semiconductor saturable absorber mirrors (SESAMs). Therefore, the involved ML mechanisms have been explored extensively [1]. SESAMs and VECSELs have to be attuned carefully to provide the desired parameters for the shortest pulse durations and the highest peak powers. To date, the record pulse durations have even undercut 100 fs [2], while the record peak powers amount to a few kilowatts [3, 4].

Recently, ML was also reported to take place in VECSELs even without any saturable absorber medium within the laser resonator [5–7]. In this context, different driving mechanisms for the ML operation were proposed and discussed within the community. On the one hand, Chen *et al.* [5] suppose that the gain region of the VECSEL itself acts as a saturable absorber. On the other hand, Kornaszewski *et al.* [6] as well as Albrecht *et al.* [7] propose Kerr-lensing in the gain region as the underlying effect. However, it is still unclear which of these scenarios holds true. Although the underlying ML mechanism has not been revealed yet, the phenomenon attracts considerable attention since the output powers and the pulse durations already compete with the latest records achieved by the SESAM-based devices. In particular, a SESAM-free self-ML of VECSELs circumvents the device limitations accompanied by the use of such absorbers, thus potentially providing an easier access to pulsed operation with a significantly broader spectral coverage [8].

In this Letter, we present a SESAM-free harmonically modelocked VECSEL. As in [6, 7], ML is initiated by introducing a slit near the high reflective (HR) end mirror of our Z-shaped laser cavity. Besides a single pulse operation, we observe the second as well as the third harmonic ML for the higher powers. Nevertheless, this feature is only found in the nearly discrete pump levels. For a single pulse operation, we obtain a pulse duration of 860 fs with a peak power of 948 W. For the second and the third harmonic operations, we obtain pulse durations of 1.12 ps and 950 fs with peak powers of 752 and 754 W, respectively.

*Experimental setup:* We employ an MOVPE grown VECSEL chip with 10 (InGa)As quantum wells (QWs) equally spaced by $\lambda/2$ (GaP)As barrier layers. The distributed Bragg reflector (DBR) consists of 24½ pairs of quarter wavelength GaAs/(AlGa)As layers and is transparent to the wavelength of the fibre-coupled 808 nm diode pump laser. Both the QWs and the DBR are designed for an emission at 1010 nm. We choose an antiresonant microcavity in order to minimise the group delay dispersion (GDD) and to spectrally broaden the effective gain of the structure. The semiconductor structure is flip-chip-bonded with an Au–In solid–liquid interdiffusion onto a 350 µm-thick CVD diamond heat spreader for optimal temperature management. Then, the substrate is removed by polishing and wet etching. Finally, the chip is mounted onto a water cooled copper heatsink which is held at 18.5°C during our experiments.

Fig. 1 shows a schematic drawing of the setup. Our VECSEL chip acts as one of the two folding mirrors. The device is pumped under an angle of incidence of 30°. The pump optics are carefully adjusted to ensure a good matching between the pump spot and the laser mode on the chip which is estimated to have a radius of 210 µm. The angle of incidence on the HR curved mirror was kept below 15° to avoid excessive astigmatism. Furthermore, the transmittance of the output coupler is 1.6%. The cavity is designed by assuming a Kerr-lensing in the VECSEL chip. Hence, a variable slit is placed directly in front of the HR end mirror. A negative Kerr-lensing in the VECSEL chip will lead to a decrease of the laser mode at the slit position which will initiate the ML process.

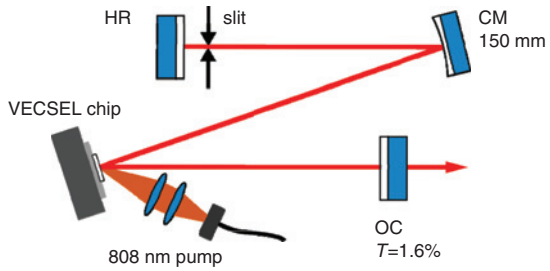


**Fig. 1** *Schematic drawing of experimental setup*

*Results:* ML is initiated when the slit is moved or the slit width is narrowed. In the fundamental modelocked operation, the slit can be opened completely without disturbing the ML process. In a harmonic operation, a self-sustaining ML is only achieved with the slit partially closed.

In contrast to the SESAM ML [9], a stable ML is achieved only at the nearly discrete pump power levels. The error bars in Fig. 2 represent the pump regions in which a stable ML was accomplished in repeated investigations. As is usual for a harmonic ML, an increased pump power is required to achieve higher harmonics. As a consequence, the average output power is increased as well. We find that the peak power is fairly constant for the fundamental (948 W), second (752 W) and third harmonic ML (754 W). This indicates that a certain intracavity power is needed for the underlying ML mechanism.

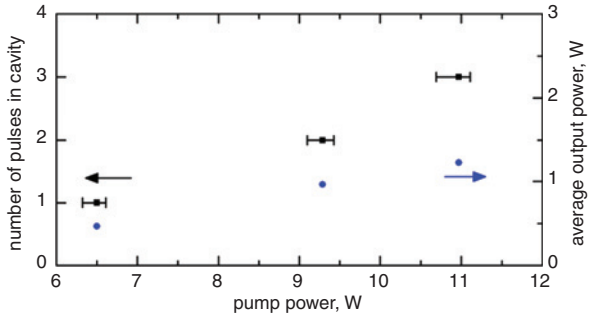


**Fig. 2** *Optical pump power against number of pulses in cavity (black, left axis) and average output power (blue, right axis)*

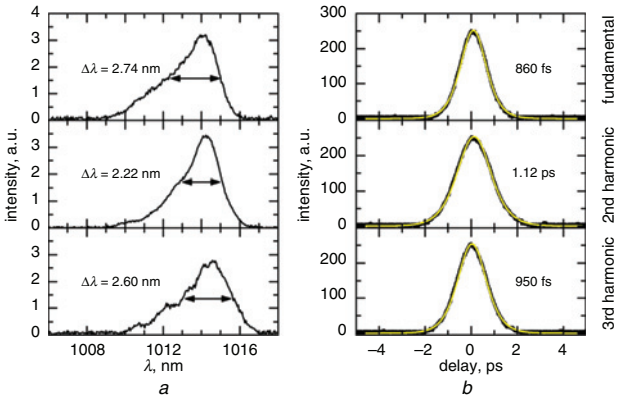


**Fig. 3** *Optical spectra and autocorrelation traces for fundamental, second and third harmonic ML*

*a* Optical spectra
*b* Autocorrelation traces (black) with sech² fits (yellow)

We used an Ando AQ-6315A optical spectrum analyser and an A.P.E t5050 autocorrelator for the measurement of the optical spectra and the autocorrelation traces which are shown in Fig. 3. The pulse durations are determined by assuming the sech² shaped pulses. The time bandwidth products of 0.69 (first), 0.73 (second) and 0.72 (third) reveal that our results are not transform limited which can be attributed to the remaining GDD caused by the VECSEL chip.

Fig. 4 shows the RF spectra of the observed ML states. The spectra have been recorded using an electrical spectrum analyser with a bandwidth of 22 GHz (HP 8566A) and an InGaAs photodetector with a 3 dB bandwidth of 1.2 GHz. The repetition rates of 504, 1008 and 1512 MHz for the fundamental, second and third harmonic ML correspond to the total cavity length of about 30 cm. The drop in the amplitude of the third harmonic is attributed to the limited bandwidth of the photodetector.

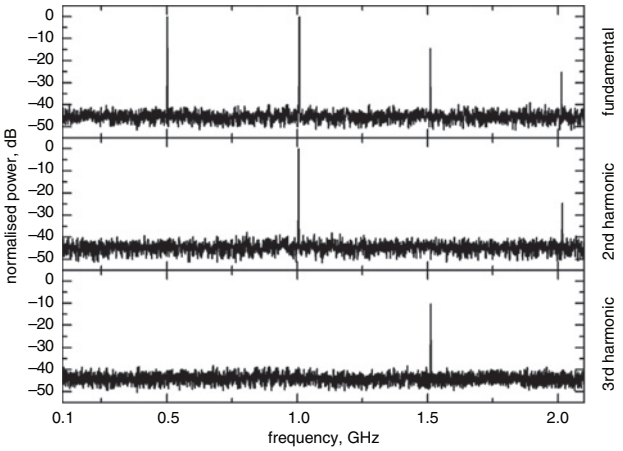


**Fig. 4** *Corresponding RF spectra for fundamental, second and third harmonic ML*

*Conclusion:* We have demonstrated a self-modelocked VECSEL operation in the fundamental as well as in a higher harmonic ML regime. Therefore, the cavity was designed by assuming a negative Kerr-lensing in the laser gain region. ML is initiated by using a variable slit in front of one end mirror. In contrast to previous reports, our SESAM-free modelocked VECSEL is not only demonstrated for a single pulse operation, but also for the second and third harmonic ML.

The presented results with the peak powers close to 1 kW and with the pulse durations below 1 ps are close to the latest results based on the SESAM-assisted ML. In our future investigations, we will employ different VECSEL chip designs and resonator arrangements with a dispersion compensation in order to reduce the time bandwidth product.

*Acknowledgments:* We acknowledge the financial support by the DFG through GRK1782. M. Gaafar acknowledges support from the Yousef Jameel scholarship funds.


*15 January 2014*
doi: 10.1049/el.2014.0157
One or more of the Figures in this Letter are available in colour online.

M. Gaafar, C. Möller, M. Wichmann, B. Heinen, A. Rahimi-Iman, W. Stolz and M. Koch (*Material Sciences Center and Department of Physics, Philipps-Universität Marburg, Marburg D-35032, Germany*)

E-mail: mahmoud.gaafar@physik.uni-marburg.de

B. Kunert (*NAsP III/V GmbH, Am Knechtacker 19, Marburg D-35041, Germany*)

## References

1 Tropper, A., and Hoogland, S.: 'Extended cavity surface-emitting semiconductor lasers', *Prog. Quantum Electron.*, 2006, **30**, (1), pp. 1–43
2 Quarterman, A.H., Wilcox, K.G., Apostolopoulos, V., Mihoubi, Z., Elsmere, S.P., Farrer, I., *et al.*: 'A passively mode-locked external-cavity semiconductor laser emitting 60-fs pulses', *Nat. Photonics*, **3**, (12), pp. 729–731
3 Wilcox, K.G., Tropper, A.C., Beere, H.E., Ritchie, D.A., Kunert, B., Heinen, B., *et al.*: '4.35 kW peak power femtosecond pulse mode-locked VECSEL for supercontinuum generation', *Opt. Express*, 2013, **21**, (2), pp. 1599–1605
4 Scheller, M., Wang, T.-L., Kunert, B., Stolz, W., Koch, S.W., and Moloney, J.V.: 'Passively modelocked VECSEL emitting 682 fs pulses with 5.1 W of average output power', *Electron. Lett.*, 2012, **48**, (10), pp. 588–589
5 Chen, Y.F., Lee, Y.C., Liang, H.C., Lin, K.Y., Su, K.W., and Huang, K.F.: 'Femtosecond high-power spontaneous mode-locked operation in vertical-external cavity surface-emitting laser with gigahertz oscillation', *Opt. Lett.*, 2011, **36**, (23), pp. 4581–4583
6 Kornaszewski, L., Maker, G., Malcolm, G.P.A., Butkus, M., Rafailov, E.U., and Hamilton, C.J.: 'SESAM-free mode-locked semiconductor disk laser', *Laser Photonic Rev.*, 2012, **15**, (6), pp. 20–23
7 Albrecht, A.R., Seletskiy, D.V., Cederberg, J.G., and Sheik-Bahae, M.: 'Self-mode-locked vertical external-cavity surface-emitting laser (VECSEL)'. Proc. CLEO, San Jose, CA, USA, June 2013
8 Okhotnikov, O.: 'Semiconductor disk lasers: physics and technology' (Wiley-VCH, 2010, 1st edn)
9 Saarinen, E.J., Lyytikäinen, J., and Okhotnikov, O.G.: 'Hysteresis and multiple pulsing in a semiconductor disk laser with a saturable absorber', *Phys. Rev. E, Stat. Nonlinear Soft Matter Phys.*, 2008, **78**, (1), p. 016207

## 4.2 Self-mode-locked quantum-dot vertical-external-cavity surface-emitting laser

M. Gaafar, D. Al Nakdali, C. Möller, K. A. Fedorova, M. Wichmann, M. K. Shakfa, F. Zhang, A. R-Iman, E. U. Rafailov, M. Koch, Optics letters **39**, 17 (2014). DOI: 10.1364/OL.39.004623.

**Abstract**

We present the first self-mode-locked optically pumped quantum-dot semiconductor disk laser. Our mode-locked device emits sub-picosecond pulses at a wavelength of 1040 nm and features a record peak power of 460 W at a repetition rate of 1.5 GHz. In this work, we also investigate the temperature dependence of the pulse duration as well as the time-bandwidth product for stable mode locking.

**The author's contribution**

Similar to the previous publication, the design of experiments and all the practical steps of this study were carried mainly by myself. D. Al-Nakdali helped me partially to achieve these results for a QD-VECSEL chip. The semiconductor laser chip was designed and provided by the group of Prof. Dr. E. U. Rafailov, currently located at Aston University in the United Kingdom. All co-authors contributed to the experimental achievements, and helped to prepare the manuscript, which was primarily written by myself.

# Self-mode-locked quantum-dot vertical-external-cavity surface-emitting laser

**Mahmoud Gaafar,[1,*] Dalia Al Nakdali,[1] Christoph Möller,[1] Ksenia A. Fedorova,[2] Matthias Wichmann,[1] Mohammad Khaled Shakfa,[1] Fan Zhang,[1] Arash Rahimi-Iman,[1] Edik U. Rafailov,[2] and Martin Koch[1]**

[1]*Department of Physics and Material Sciences Center, Philipps University of Marburg, Renthof 5, D-35032 Marburg, Germany*

[2]*School of Engineering and Applied Science, Aston University, Aston Triangle, Birmingham B4 7ET, UK*

**Corresponding author: mahmoud.gaafar@physik.uni-marburg.de*

Received June 5, 2014; revised June 27, 2014; accepted July 4, 2014;
posted July 7, 2014 (Doc. ID 213575); published July 31, 2014

We present the first self-mode-locked optically pumped quantum-dot semiconductor disk laser. Our mode-locked device emits sub-picosecond pulses at a wavelength of 1040 nm and features a record peak power of 460 W at a repetition rate of 1.5 GHz. In this work, we also investigate the temperature dependence of the pulse duration as well as the time-bandwidth product for stable mode locking. © 2014 Optical Society of America

*OCIS codes:* (140.4050) Mode-locked lasers; (140.5960) Semiconductor lasers; (140.7270) Vertical emitting lasers; (250.5590) Quantum-well, -wire and -dot devices.

http://dx.doi.org/10.1364/OL.39.004623

An optically pumped vertical-external-cavity surface-emitting laser (VECSEL), also named semiconductor disk laser, is a versatile type of laser whose emission wavelength can be tailored according to the demands of a specific application [1]. VECSELs can offer not only high average output powers in continuous-wave (CW) multimode [2] or single-frequency [3] operation, but also in a mode-locked (ML: also "mode locking") regime [4–6]. In addition, VECSELs can provide excellent output beam quality with $M^2$ values smaller than 1.2 [7,8]. Interestingly, ML VECSELs, which can be employed for a variety of applications ranging from material processing to biophysical imaging, have been demonstrated by exploiting various methods to establish pulsed operation.

Typically, external semiconductor saturable-absorber mirrors (SESAMs) are employed, which exhibit intensity-dependent absorption [9,10] and have to be designed carefully for each wavelength and application—a cost-driving and limiting factor in the development of ML VECSELs. These SESAMs, usually based on quantum-well (QW) or quantum-dot (QD) structures, can even be integrated directly into the chip, resulting in a so-called ML integrated external-cavity surface-emitting laser (MIXSEL) [11]. Since MIXSELs combine both QD and QW technology, this approach is rather complex. A SESAM-free mode-locking technique potentially produces higher output powers because of the absence of nonradiative absorption, which usually is a power-limiting factor in SESAMs. Besides semiconductor materials, graphene [12] as well as carbon nanotube [13] saturable absorbers have been employed for ML operation of VECSELs. However, mode-locking has also been reported to take place even without any additional saturable absorber—an effect called self-mode locking (SML) [14–17]. Different driving mechanisms for the phenomenon of SML were proposed [14–16], but up to now, it is still unclear which mechanism is in force.

Due to the nature of their density of states, QD-based semiconductor lasers have shown their potential for realizing low thresholds and high characteristic temperatures [18]. In addition, the QD gain layers inherently exhibit strong inhomogeneous gain broadening, ultrafast carrier dynamics, and low absorption saturation [19]. Previously, it was demonstrated that the carrier recovery time in such a QD structure is less than 1 ps [20]. VECSELs based on QD gain regions have been reported in CW operation at emission wavelengths between 654 nm [21] and 1300 nm [8,22]. Currently, the highest output power achieved is 8.4 W for 1040 nm [23].

In the year 2008, the first ML QD-VECSEL had been demonstrated to generate 18-ps pulses with an average output power of 27 mW [24], whereas the demonstration of a Watt-level femtosecond QD-VECSEL with 200 W peak power was achieved recently [10]. This elucidates the significant improvements in this field.

In this Letter, we report on the first passively self-mode-locked QD-VECSEL, emitting at 1040 nm. The self-mode-locked VECSEL device was set up in a standard linear cavity geometry in which the VECSEL chip itself and a curved output coupler (OC) formed the laser resonator with a total length of 97 mm [see Fig. 1(a)]. Mode locking was initiated by introducing a slit acting as the intracavity mode aperture. The slit was placed closely in front of the OC mirror, which exhibited a transmittance of 0.6% and a radius of curvature of 100 mm. Stable pulses of sub-picosecond duration with an average output power up to 750 mW have been obtained. This corresponds to a record peak power of 460 W at a repetition rate of 1.5 GHz. Moreover, we investigate the dependence of the time-bandwidth product (TBWP) on the heat sink temperature of the QD-VECSEL device.

The chip structure employed in this study was grown by molecular-beam epitaxy on a GaAs substrate and exhibited an antiresonant design. A ternary distributed Bragg reflector (DBR) is grown, which consists of 29.5 pairs of GaAs-$Al_{0.9}Ga_{0.1}As$. Furthermore, the DBR is transparent to the wavelength of the fiber-coupled 808 nm pump laser. The active gain medium in the structure consists of 35 layers of Stranski–Krastanow grown InGaAs QDs within GaAs spacers, organized as five stacks of seven QD layers each that are placed at the standing-wave electric field antinodes inside the cavity. Both QDs and the DBR are designed for an emission wavelength of 1040 nm. In order to prevent surface

 

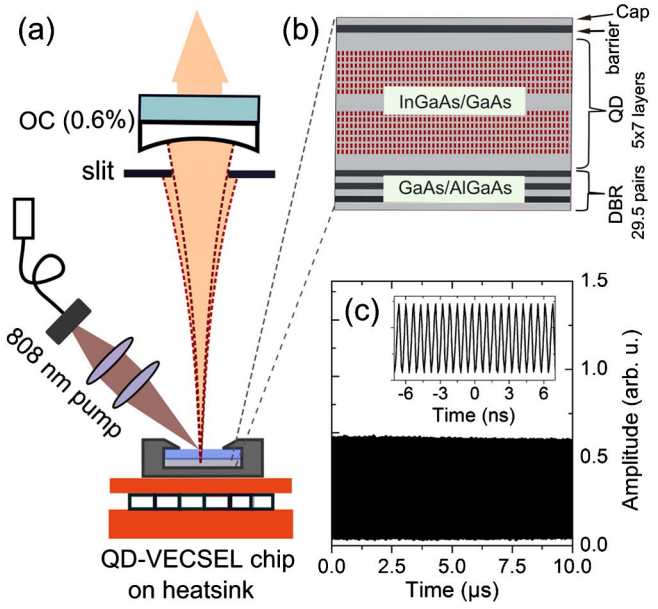


Fig. 1. (a) Schematic drawing of the optically pumped self-mode-locked QD-VECSEL setup. (b) Structure of the QD-VECSEL chip (top right). (c) Oscilloscope time trace of the VECSEL output for a time window of 10 μs and a few nanoseconds (inset), respectively.

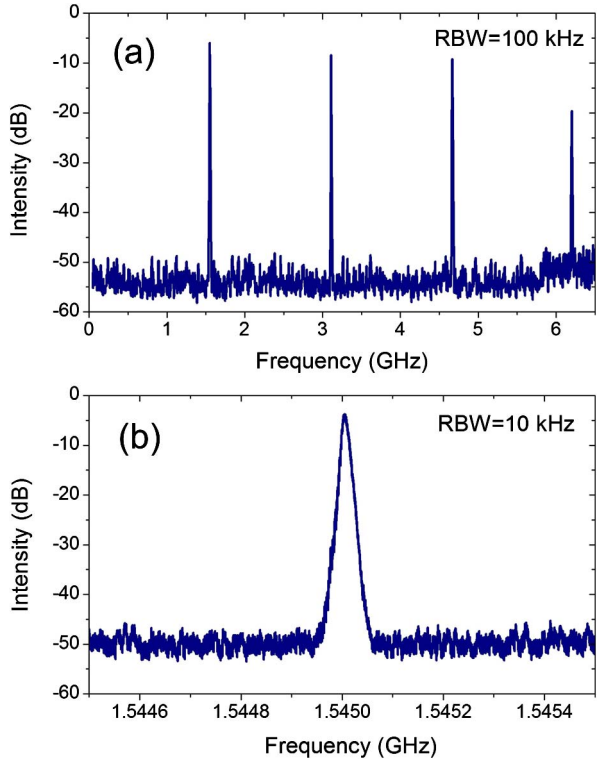


Fig. 2. RF spectra measured over (a) a span of 6.5 GHz and a RBW of 100 kHz, showing the first four harmonics, and (b) a span of 1 MHz and a RBW of 10 kHz. RF signal centered around 1.545 GHz.

recombination of the excited carriers and to avoid oxidation, the structure is capped by an $Al_{0.1}Ga_{0.9}As$ barrier layer followed by a GaAs layer. A schematic drawing of the VECSEL chip's structure is shown in Fig. 1(b).

The VECSEL chip is capillary bonded to an intracavity diamond heat spreader, which is employed for thermal management, and is mounted on a thermoelectrically cooled copper heat sink. The excess heat, generated during operation, is dissipated via closed-cycle water cooling.

Our VECSEL chip is optically pumped by an 808 nm diode laser under an incident angle of 30°. The pump optics is adjusted carefully to ensure good matching between the pump spot and the laser mode on the chip. The latter is estimated to have a radius of ~80 μm. Mode locking is initiated when the slit is moved or its width is varied [17]. Initially, ML operation was not stable and the resonator length was varied carefully by moving the OC in order to stabilize pulsing. Thereby, an improved operation is achieved at a certain cavity length (~97 mm). Stable ML operation was observed at a certain net pump power of about 16 W; otherwise, unstable mode-locking was observed. A representative long-span pulse train of the QD-VECSEL output is shown in Fig. 1(c): the signal was recorded for both a time window of 10 μs and a few nanoseconds (inset), respectively, via an InGaAs photodetector (PD) with a 3 dB bandwidth of 5 GHz and a digital oscilloscope with an analog bandwidth of 2 GHz.

Radiofrequency (RF) spectra measurements are presented in Fig. 2 with a signal-to-noise ratio of 45 dB at 1.5 GHz. For this, the PD is connected to an electrical spectrum analyzer exhibiting a bandwidth of 22 GHz (HP 8566A). Figure 2(a) presents an RF signal measured over a span of 6.5 GHz using a resolution bandwidth (RBW) of 100 kHz. The reduction in the amplitude of the fourth harmonic is attributed to the limited bandwidth of the PD. The corresponding RF spectrum of the fundamental repetition rate measured over a span of 1 MHz using a RBW of 10 kHz is shown in Fig. 2(b). Here, a clear peak at 1.5 GHz is observed corresponding to the total cavity length of 97 mm.

In order to analyze the ML operation further, autocorrelation traces and optical spectra were recorded, which are presented in Figs. 3(a) and 3(b), respectively. Corresponding measurements were performed with an A.P.E. t5050 autocorrelator and an Ando AQ-6315A optical spectrum analyzer. The pulse durations are determined by assuming $sech^2$ shaped pulses in the autocorrelation traces. The optical spectrum of the laser is centered at 1038 nm. The distinct periodically spaced peaks in the spectrum are caused by the spectral filtering induced by the etalon, which is formed by the intracavity diamond heat spreader. The inset in Fig. 3(b) displays a CCD image of the $TEM_{00}$ transverse mode profile of the laser output beam. The laser output is polarized linearly with a horizontal orientation.

As former investigations revealed, ML QD lasers exhibit strong temperature dependence of their mode locking properties [25]. Therefore, as the last part of our study, the performance of the self-mode-locked QD-VECSEL is investigated as a function of operation temperature. Pulse durations are measured in a stable ML regime for several temperatures. Figure 4(a) shows the expected increase of average/peak power (left/right axis) with decreasing temperature, with a peak power of 460 W obtained at 5°C. To our knowledge, this is the highest peak power obtained from a ML QD-VECSEL. Figure 4(b) depicts the decrease of pulse duration with

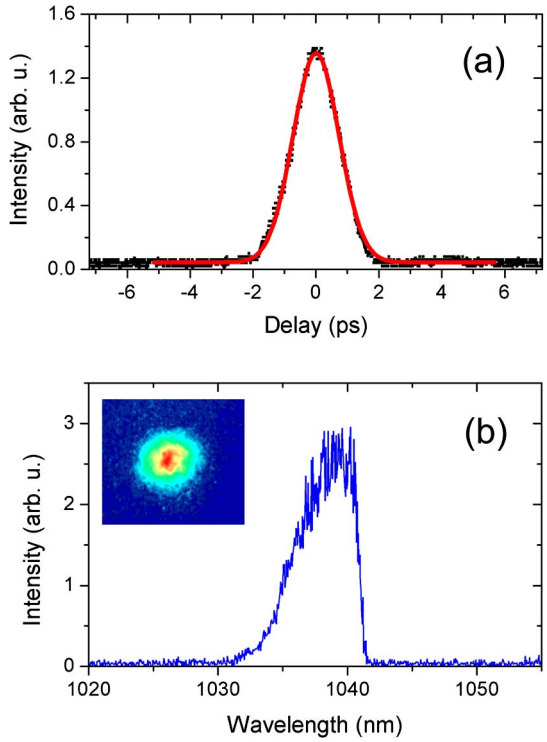


Fig. 3. (a) Autocorrelation trace of the self-mode-locked QD-VECSEL measured at 5°C. Black dots: experimental data. Red line: fit curve assuming a sech$^2$ pulse. (b) Corresponding optical spectrum. Inset: output beam profile in a false color map.

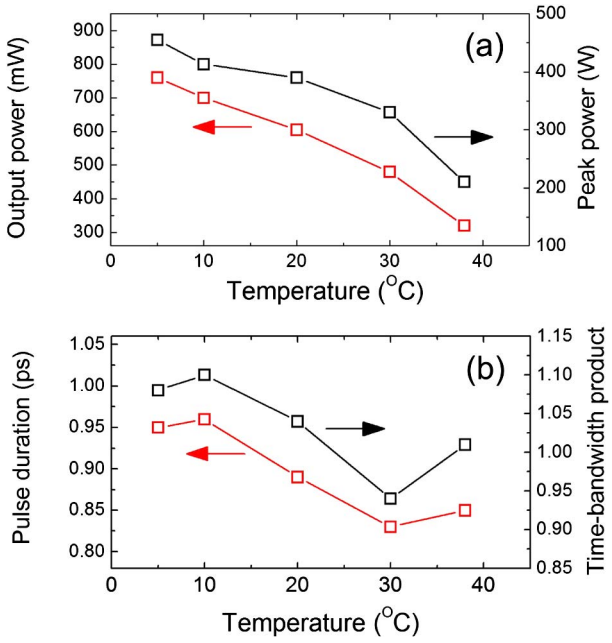


Fig. 4. (a) Average and peak output powers as a function of temperature (left/right axis). (b) Temperature-dependent pulse duration and time-bandwidth product for a sech$^2$-pulse shape. The optimum TBWP is 0.315.

increasing temperature (left axis). This trend might occur due to a temperature-dependent change of the dispersion inside the gain medium. Here, both output power and pulse duration measurements were performed at a constant net pump power of 16 W. In addition, a slight decrease of the TBWP could be observed as the temperature was increased, as revealed in Fig. 4(b) (right axis). The pulses measured are 3.0 to 3.4 times the transform limit of an ideal sech$^2$ pulse, confirming that the pulses are still strongly frequency-chirped due to the dispersion within the microcavity. The observed decrease of the TBWP in ML QD lasers has been investigated previously in the literature and several possible reasons have been suggested [25]: on the one hand, this feature implies an increase in the homogeneous linewidth [26], whereas on the other hand, it can be seen as the consequence of a decreased population inversion over the entire gain spectrum due to thermal coupling to the wetting layer, which would reduce the number of modes that reach the threshold [27]. It is worth to note that in our case, the decrease of TBWP is rather small compared with that in the references cited. We should mention that the present average output power and pulse durations are comparable with the results obtained using traditional saturable-absorber mirrors [10].

In conclusion, we have demonstrated the SML of an optically pumped QD-VECSEL. Sub-picosecond pulses with pulse duration as short as 830 fs at 1040 nm and a repetition rate of 1.5 GHz were obtained. Moreover, a record peak power of up to 460 W was demonstrated. A temperature-dependent study of the VECSEL's mode locking properties revealed that the pulse duration as well as the TBWP could be improved if the system is operated at increased temperatures.

The authors acknowledge the financial support by the DFG (GRK1782 and SFB 1083) and the EU FP7 program through the FAST-DOT project (contract no. 224338). M. Gaafar acknowledges the support from the Yousef Jameel scholarship funds. The authors would like to thank Innolume GmbH for the fabrication of the VECSEL chip and G. Bastian for providing the fast oscilloscope.

**References**

1. M. Kuznetsov, F. Hakimi, R. Sprague, and A. Mooradian, IEEE Photon. Technol. Lett. **9**, 1063 (1997).
2. B. Heinen, T. L. Wang, M. Sparenberg, A. Weber, B. Kunert, J. Hader, S. W. Koch, J. V. Moloney, M. Koch, and W. Stolz, Electron. Lett. **48**, 516 (2012).
3. F. Zhang, B. Heinen, M. Wichmann, C. Möller, B. Kunert, A. Rahimi-Iman, W. Stolz, and M. Koch, Opt. Express **22**, 12817 (2014).
4. S. Husaini and R. G. Bedford, Appl. Phys. Lett. **104**, 161107 (2014).
5. K. G. Wilcox, M. Butkus, I. Farrer, D. A. Ritchie, A. Tropper, and E. U. Rafailov, Appl. Phys. Lett. **94**, 251105 (2009).
6. M. Butkus, E. A. Viktorov, T. Erneux, C. J. Hamilton, G. Maker, G. P. A. Malcolm, and E. U. Rafailov, Opt. Express **21**, 25526 (2013).
7. J. Rautiainen, I. Krestnikov, M. Butkus, E. U. Rafailov, and O. G. Okhotnikov, Opt. Lett. **35**, 694 (2010).
8. M. Butkus, J. Rautiainen, O. G. Okhotnikov, C. J. Hamilton, G. P. A. Malcolm, S. S. Mikhrin, I. L. Krestnikov, D. A. Livshits, and E. U. Rafailov, IEEE J. Sel. Top. Quantum Electron. **17**, 1763 (2011).
9. A. A. Lagatsky, C. G. Leburn, C. T. A. Brown, W. Sibbett, S. A. Zolotovskaya, and E. U. Rafailov, Prog. Quantum Electron. **34**, 1 (2010).
10. M. Hoffmann, O. D. Sieber, V. J. Wittwer, I. L. Krestnikov, D. A. Livshits, Y. Barbarin, T. Südmeyer, and U. Keller, Opt. Express **19**, 8108 (2011).

11. M. Mangold, V. J. Wittwer, C. A. Zaugg, S. M. Link, M. Golling, B. Tilma, and U. Keller, Opt. Express **21**, 24904 (2013).
12. C. A. Zaugg, Z. Sun, V. J. Wittwer, D. Popa, S. Milana, T. S. Kulmala, R. S. Sundaram, M. Mangold, O. D. Sieber, M. Golling, Y. Lee, J. H. Ahn, A. C. Ferrari, and U. Keller, Opt. Express **21**, 31548 (2013).
13. K. Seger, N. Meiser, S. Y. Choi, B. H. Jung, D. I. Yeom, F. Rotermund, O. Okhotnikov, F. Laurell, and V. Pasiskevicius, Opt. Express **21**, 17806 (2013).
14. Y. F. Chen, Y. C. Lee, H. C. Liang, K. Y. Lin, K. W. Su, and K. F. Huang, Opt. Lett. **36**, 4581 (2011).
15. L. Kornaszewski, G. Maker, G. P. A. Malcolm, M. Butkus, E. U. Rafailov, and C. J. Hamilton, Laser Photon. Rev. **6**, L20 (2012).
16. L. Kornaszewski, G. Maker, G. P. A. Malcolm, M. Butkus, E. U. Rafailov, and C. J. Hamilton, Laser Photon. Rev. **7**, 555 (2013).
17. M. Gaafar, C. Möller, M. Wichmann, B. Heinen, B. Kunert, A. Rahimi-Iman, W. Stolz, and M. Koch, Electron. Lett. **50**, 542 (2014).
18. A. R. Kovsh, N. N. Ledentsov, S. S. Mikhrin, A. E. Zhukov, D. A. Livshits, N. A. Maleev, M. V. Maximov, V. M. Ustinov, A. E. Gubenko, I. M. Gadjiev, E. L. Portnoi, J. S. Wang, J. Chi, D. Ouyang, D. Bimberg, and J. A. Lott, Proc. SPIE **5349**, 31 (2004).
19. E. U. Rafailov, M. A. Cataluna, and W. Sibbett, Nat. Photonics **1**, 395 (2007).
20. E. U. Rafailov, S. J. White, A. A. Lagatsky, A. Miller, W. Sibbett, D. A. Livshits, A. E. Zhukov, and V. M. Ustinov, IEEE Photon. Technol. Lett. **16**, 2439 (2004).
21. T. Schwarzbäck, R. Bek, F. Hargart, C. A. Kessler, H. Kahle, E. Koroknay, M. Jetter, and P. Michler, Appl. Phys. Lett. **102**, 092101 (2013).
22. J. A. Lott, A. R. Kovsh, N. N. Ledentsov, and D. Bimberg, in *Proceedings of the CLEO* (2005), pp. 160–161.
23. D. Al Nakdali, M. K. Shakfa, M. Gaafar, M. Butkus, K. A. Fedorova, M. Zulonas, M. Wichmann, F. Zhang, B. Heinen, A. Rahimi-Iman, W. Stolz, E. U. Rafailov, and M. Koch, IEEE Photon. Technol. Lett. **26**, 1561 (2014).
24. M. Hoffmann, Y. Barbarin, D. J. H. C. Maas, M. Golling, I. L. Krestnikov, S. S. Mikhrin, A. R. Kovsh, T. Südmeyer, and U. Keller, Appl. Phys. B **93**, 733 (2008).
25. M. A. Cataluna, E. A. Viktorov, P. Mandel, W. Sibbett, D. A. Livshits, J. Weimert, A. R. Kovsh, and E. U. Rafailov, Appl. Phys. Lett. **90**, 101102 (2007).
26. A. Sakamoto and M. Sugawara, IEEE Photon. Technol. Lett. **12**, 107 (2000).
27. H. Huang and D. G. Deppe, IEEE J. Quantum Electron. **37**, 691 (2001).

## 4.3 Self-mode-locking semiconductor disk laser

M. Gaafar, P. Richter, H. Keskin, C. Möller, M. Wichmann, W. Stolz, A. Rahimi-Iman, M. Koch, Optics Express **22**, 23 (2014). DOI: 10.1364/OE.22.028390.

**Abstract**

The development of mode-locked semiconductor disk lasers received striking attention in the last 14 years and there is still a vast potential of such pulsed lasers to be explored and exploited. While for more than one decade pulsed operation was strongly linked to the employment of a saturable absorber, self-mode-locking emerged recently as an effective and novel technique in this field - giving prospect to a reduced complexity and improved cost-efficiency of such lasers. In this work, we highlight recent achievements regarding self-mode-locked semiconductor devices. It is worth to note, that although nonlinear effects in the active medium are expected to give rise to self-mode-locking, this has to be investigated with care in future experiments. However, there is a controversy whether results presented with respect to self-mode-locking truly show mode-locking. Such concerns are addressed in this work and we provide a clear evidence of mode-locking in a saturable-absorber-free device. By using a BBO crystal outside the cavity, green light originating from second-harmonic generation using the out-coupled laser beam is demonstrated. In addition, long-time-span pulse trains as well as radiofrequency-spectra measurements are presented for our sub-ps pulses at 500 MHz repetition rate which indicate the stable pulse operation of our device. Furthermore, a long-time-span autocorrelation trace is introduced which clearly shows absence of a pedestal or double pulses. Eventually, a beam-profile

measurement reveals the excellent beam quality of our device with an M-square factor of less than 1.1 for both axes, showing that self-mode-locking can be achieved for the fundamental transverse mode.

**The author's contribution**

This work was inspired by direct feedback from the VECSEL community on previous publications about self-mode-locking, which allowed the team in Prof. Dr. M. Koch's group to plan and conduct the experiments under supervision of Dr. A. Rahimi-Iman. In this context, I carried out all practical steps of the experimental work with the partial help of P. Richter, who built and tested a long-time-span intensity autocorrelator for this study under my supervision, and H. Keskin, who carried out some of the experiments in the laboratory together with me. All co-authors helped to interpret the data and to improve the manuscript that was written by me and Dr. A. Rahimi-Iman.

# Self-mode-locking semiconductor disk laser

**Mahmoud Gaafar,[1,*] Philipp Richter,[1] Hakan Keskin,[2] Christoph Möller,[1] Matthias Wichmann,[1] Wolfgang Stolz,[1,3] Arash Rahimi-Iman,[1] and Martin Koch[1]**

[1]*Department of Physics and Materials Sciences Center, Philipps-Universität Marburg, Renthof 5, 35032 Marburg, Germany*

[2]*Department of Physics, Middle East Technical University, Ankara, 06800, Turkey*

[3]*NAsP III/V GmbH, Am Knechtacker 19, 35041 Marburg, Germany*

**mahmoud.gaafar@physik.uni-marburg.de*

**Abstract:** The development of mode-locked semiconductor disk lasers received striking attention in the last 14 years and there is still a vast potential of such pulsed lasers to be explored and exploited. While for more than one decade pulsed operation was strongly linked to the employment of a saturable absorber, self-mode-locking emerged recently as an effective and novel technique in this field – giving prospect to a reduced complexity and improved cost-efficiency of such lasers. In this work, we highlight recent achievements regarding self-mode-locked semiconductor devices. It is worth to note, that although nonlinear effects in the active medium are expected to give rise to self-mode-locking, this has to be investigated with care in future experiments. However, there is a controversy whether results presented with respect to self-mode-locking truly show mode-locking. Such concerns are addressed in this work and we provide a clear evidence of mode-locking in a saturable-absorber-free device. By using a BBO crystal outside the cavity, green light originating from second-harmonic generation using the out-coupled laser beam is demonstrated. In addition, long-time-span pulse trains as well as radiofrequency-spectra measurements are presented for our sub-ps pulses at 500 MHz repetition rate which indicate the stable pulse operation of our device. Furthermore, a long-time-span autocorrelation trace is introduced which clearly shows absence of a pedestal or double pulses. Eventually, a beam-profile measurement reveals the excellent beam quality of our device with an M-square factor of less than 1.1 for both axes, showing that self-mode-locking can be achieved for the fundamental transverse mode.



**OCIS codes:** (140.4050) Mode-locked lasers; (140.5960) Semiconductor lasers; (140.7270) Vertical emitting lasers.

## References and links

1. M. Kuznetsov, F. Hakimi, R. Sprague, and A. Mooradian, "High-power (>0.5-W CW) diode-pumped vertical-external-cavity surface-emitting semiconductor lasers with circular TEM00 beams," IEEE Photon. Technol. Lett. **9**(8), 1063–1065 (1997).
2. B. Heinen, T. L. Wang, M. Sparenberg, A. Weber, B. Kunert, J. Hader, S. W. Koch, J. V. Moloney, M. Koch, and W. Stolz, "106 W continuous-wave output power from vertical-external-cavity surface-emitting laser," Electron. Lett. **48**(9), 516–517 (2012).
3. F. Zhang, B. Heinen, M. Wichmann, C. Möller, B. Kunert, A. Rahimi-Iman, W. Stolz, and M. Koch, "A 23-watt single-frequency vertical-external-cavity surface-emitting laser," Opt. Express **22**(11), 12817–12822 (2014).
4. M. Wichmann, M. K. Shakfa, F. Zhang, B. Heinen, M. Scheller, A. Rahimi-Iman, W. Stolz, J. V. Moloney, S. W. Koch, and M. Koch, "Evolution of multi-mode operation in vertical-external-cavity surface-emitting lasers," Opt. Express **21**(26), 31940–31950 (2013).
5. U. Keller and A. C. Tropper, "Passively modelocked surface-emitting semiconductor lasers," Phys. Rep. **429**(2), 67–120 (2006).
6. T. Schwarzbäck, H. Kahle, M. Eichfelder, R. Roßbach, M. Jetter, and P. Michler, "Wavelength tunable ultraviolet laser emission via intra-cavity frequency doubling of an AlGaInP vertical external-cavity surface-emitting laser down to 328 nm," Appl. Phys. Lett. **99**(26), 261101 (2011).

#224198 - $15.00 USD Received 1 Oct 2014; revised 22 Oct 2014; accepted 24 Oct 2014; published 7 Nov 2014

7. M. Scheller, J. M. Yarborough, J. V. Moloney, M. Fallahi, M. Koch, and S. W. Koch, "Room temperature continuous wave milliwatt terahertz source," Opt. Express **18**(26), 27112–27117 (2010).
8. M. Wichmann, M. Stein, A. Rahimi-Iman, S. W. Koch, and M. Koch, "Interferometric Characterization of a Semiconductor Disk Laser driven Terahertz Source," J. Infrared Milli. Terahz. Waves **35**(6-7), 503–508 (2014).
9. S. Hoogland, S. Dhanjal, A. C. Tropper, S. J. Roberts, R. Häring, R. Paschotta, and U. Keller, "Passively mode-locked diode-pumped surface-emitting semiconductor laser," IEEE Photon. Technol. Lett. **12**(9), 1135–1137 (2000).
10. R. Haring, R. Paschotta, E. Gini, F. Morier-Genoud, D. Martin, H. Melchior, and U. Keller, "Picosecond surface-emitting semiconductor laser with> 200 mW average power," Electron. Lett. **37**(12), 766–767 (2001).
11. A. Gamache, S. Hoogland, A. Trooper, I. Sagnes, G. Saint-Girons, and J. S. Roberts, "Sub-500-fs soliton-like pulse in a passively mode-locked broadband surface-emitting laser with 100 mW average power," Appl. Phys. Lett. **80**(21), 3892–3894 (2002).
12. R. Haring, R. Paschotta, A. Aschwanden, E. Gini, F. Morier-Genoud, and U. Keller, "High-power passively mode-locked semiconductor lasers," IEEE J. Quantum Electron. **38**(9), 1268–1275 (2002).
13. D. Lorenser, H. J. Unold, D. J. H. C. Maas, A. Aschwanden, R. Grange, R. Paschotta, D. Ebling, E. Gini, and U. Keller, "Towards wafer-scale integration of high repetition rate passively mode-locked surface-emitting semiconductor lasers," Appl. Phys. B **79**(8), 927–932 (2004).
14. S. Hoogland, A. Garnache, I. Sagnes, J. S. Roberts, and A. C. Tropper, "10-GHz train of sub-500-fs optical soliton-like pulses from a surface-emitting semiconductor laser," IEEE Photon. Technol. Lett. **17**(2), 267–269 (2005).
15. O. Casel, D. Woll, M. A. Tremont, H. Fuchs, R. Wallenstein, E. Gerster, P. Unger, M. Zorn, and M. Weyers, "Blue 489-nm picosecond pulses generated by intracavity frequency doubling in a passively mode-locked optically pumped semiconductor disk laser," Appl. Phys. B **81**(4), 443–446 (2005).
16. D. Lorenser, D. J. H. C. Maas, H. J. Unold, A. R. Bellancourt, B. Rudin, E. Gini, D. Ebling, and U. Keller, "50-GHz passively mode-locked surface-emitting semiconductor laser with 100-mW average output power," IEEE J. Quantum Electron. **42**(8), 838–847 (2006).
17. E. J. Saarinen, A. Härkönen, R. Herda, S. Suomalainen, L. Orsila, T. Hakulinen, M. Guina, and O. G. Okhotnikov, "Harmonically mode-locked VECSELs for multi-GHz pulse train generation," Opt. Express **15**(3), 955–964 (2007).
18. M. Hoffmann, Y. Barbarin, D. Maas, M. Golling, I. L. Krestnikov, S. S. Mikhrin, A. R. Kovsh, T. Südmeyer, and U. Keller, "Modelocked quantum dot vertical external cavity surface emitting laser," Appl. Phys. B **93**(4), 733–736 (2008).
19. K. G. Wilcox, M. Butkus, I. Farrer, D. A. Ritchie, A. Tropper, and E. U. Rafailov, "Subpicosecond quantum dot saturable absorber mode-locked semiconductor disk laser," Appl. Phys. Lett. **94**(25), 251105 (2009).
20. K. G. Wilcox, A. H. Quarterman, H. Beere, D. A. Ritchie, and A. C. Tropper, "High Peak Power Femtosecond Pulse Passively Mode-Locked Vertical-External-Cavity Surface-Emitting Laser," IEEE Photon. Technol. Lett. **22**(14), 1021–1023 (2010).
21. A. H. Quarterman, A. Perevedentsev, K. G. Wilcox, V. Apostolopoulos, H. E. Beere, I. Farrer, D. A. Ritchie, and A. C. Tropper, "Passively harmonically mode-locked vertical-external-cavity surface-emitting laser emitting 1.1 ps pulses at 147 GHz repetition rate," Appl. Phys. Lett. **97**(25), 251101 (2010).
22. M. Hoffmann, O. D. Sieber, D. J. H. C. Maas, V. J. Wittwer, M. Golling, T. Südmeyer, and U. Keller, "Experimental verification of soliton-like pulse-shaping mechanisms in passively mode-locked VECSELs," Opt. Express **18**(10), 10143–10153 (2010).
23. P. Klopp, U. Griebner, M. Zorn, and M. Weyers, "Pulse repetition rate up to 92 GHz or pulse duration shorter than 110 fs from a mode-locked semiconductor disk laser," Appl. Phys. Lett. **98**(7), 071103 (2011).
24. M. Hoffmann, O. D. Sieber, V. J. Wittwer, I. L. Krestnikov, D. A. Livshits, Y. Barbarin, T. Südmeyer, and U. Keller, "Femtosecond high-power quantum dot vertical external cavity surface emitting laser," Opt. Express **19**(9), 8108–8116 (2011).
25. K. G. Wilcox, A. H. Quarterman, V. Apostolopoulos, H. E. Beere, I. Farrer, D. A. Ritchie, and A. C. Tropper, "175 GHz, 400-fs-pulse harmonically mode-locked surface emitting semiconductor laser," Opt. Express **20**(7), 7040–7045 (2012).
26. M. Scheller, T. L. Wang, B. Kunert, W. Stolz, S. W. Koch, and J. V. Moloney, "Passively modelocked VECSEL emitting 682 fs pulses with 5.1 W of average output power," Electron. Lett. **48**(10), 588–589 (2012).
27. C. A. Zaugg, M. Hoffmann, W. P. Pallmann, V. J. Wittwer, O. D. Sieber, M. Mangold, M. Golling, K. J. Weingarten, B. W. Tilma, T. Südmeyer, and U. Keller, "Low repetition rate SESAM modelocked VECSEL using an extendable active multipass-cavity approach," Opt. Express **20**(25), 27915–27921 (2012).
28. O. D. Sieber, M. Hoffmann, V. J. Wittwer, M. Mangold, M. Golling, B. W. Tilma, T. Südmeyer, and U. Keller, "Experimentally verified pulse formation model for high-power femtosecond VECSELs," Appl. Phys. B **113**(1), 133–145 (2013).
29. M. Butkus, E. A. Viktorov, T. Erneux, C. J. Hamilton, G. Maker, G. P. A. Malcolm, and E. U. Rafailov, "85.7 MHz repetition rate mode-locked semiconductor disk laser: fundamental and soliton bound states," Opt. Express **21**(21), 25526–25531 (2013).
30. C. A. Zaugg, A. Klenner, M. Mangold, A. S. Mayer, S. M. Link, F. Emaury, M. Golling, E. Gini, C. J. Saraceno, B. W. Tilma, and U. Keller, "Gigahertz self-referenceable frequency comb from a semiconductor disk laser," Opt. Express **22**(13), 16445–16455 (2014).

#224198 - $15.00 USD Received 1 Oct 2014; revised 22 Oct 2014; accepted 24 Oct 2014; published 7 Nov 2014

31. D. J. H. C. Maas, A.-R. Bellancourt, B. Rudin, M. Golling, H. J. Unold, T. Südmeyer, and U. Keller, "Vertical integration of ultrafast semiconductor lasers," Appl. Phys. B **88**(4), 493–497 (2007).
32. M. Mangold, V. J. Wittwer, C. A. Zaugg, S. M. Link, M. Golling, B. W. Tilma, and U. Keller, "Femtosecond pulses from a modelocked integrated external-cavity surface emitting laser (MIXSEL)," Opt. Express **21**(21), 24904–24911 (2013).
33. C. A. Zaugg, Z. Sun, V. J. Wittwer, D. Popa, S. Milana, T. S. Kulmala, R. S. Sundaram, M. Mangold, O. D. Sieber, M. Golling, Y. Lee, J. H. Ahn, A. C. Ferrari, and U. Keller, "Ultrafast and widely tuneable vertical-external-cavity surface-emitting laser, mode-locked by a graphene-integrated distributed Bragg reflector," Opt. Express **21**(25), 31548–31559 (2013).
34. S. Husaini and R. G. Bedford, "Graphene saturable absorber for high power semiconductor disk laser mode-locking," Appl. Phys. Lett. **104**(16), 161107 (2014).
35. K. Seger, N. Meiser, S. Y. Choi, B. H. Jung, D.-I. Yeom, F. Rotermund, O. Okhotnikov, F. Laurell, and V. Pasiskevicius, "Carbon nanotube mode-locked optically-pumped semiconductor disk laser," Opt. Express **21**(15), 17806–17813 (2013).
36. Y. F. Chen, Y. C. Lee, H. C. Liang, K. Y. Lin, K. W. Su, and K. F. Huang, "Femtosecond high-power spontaneous mode-locked operation in vertical-external cavity surface-emitting laser with gigahertz oscillation," Opt. Lett. **36**(23), 4581–4583 (2011).
37. L. Kornaszewski, G. Maker, G. P. A. Malcolm, M. Butkus, E. U. Rafailov, and C. J. Hamilton, "SESAM-free mode-locked semiconductor disk laser," Laser Photonics Rev. **6**(6), L20–L23 (2012).
38. A. R. Albrecht, Y. Wang, M. Ghasemkhani, D. V. Seletskiy, J. G. Cederberg, and M. Sheik-Bahae, "Exploring ultrafast negative Kerr effect for mode-locking vertical external-cavity surface-emitting lasers," Opt. Express **21**(23), 28801–28808 (2013).
39. M. Gaafar, C. Möller, M. Wichmann, B. Heinen, B. Kunert, A. Rahimi-Iman, W. Stolz, and M. Koch, "Harmonic self-mode-locking of optically pumped semiconductor disc laser," Electron. Lett. **50**(7), 542–543 (2014).
40. M. Gaafar, D. A. Nakdali, C. Möller, K. A. Fedorova, M. Wichmann, M. K. Shakfa, F. Zhang, A. Rahimi-Iman, E. U. Rafailov, and M. Koch, "Self-mode-locked quantum-dot vertical-external-cavity surface-emitting laser," Opt. Lett. **39**(15), 4623–4626 (2014).
41. H. C. Liang, C. H. Tsou, Y. C. Lee, K. F. Huang, and Y. F. Chen, "Observation of self-mode-locking assisted by high-order transverse modes in optically pumped semiconductor lasers," Laser Phys. Lett. **11**(10), 105803 (2014).
42. K. G. Wilcox and A. C. Tropper, "Comment on SESAM-free mode-locked semiconductor disk laser," Laser Photonics Rev. **7**(3), 422–423 (2013).
43. L. Kornaszewski, G. Maker, G. P. A. Malcolm, M. Butkus, E. U. Rafailov, and C. J. Hamilton, "Reply to comment on SESAM-free mode-locked semiconductor disk laser," Laser Photonics Rev. **7**(4), 555–556 (2013).
44. A. Weiner, *Ultrafast Optics* (Wiley, 2009).

## 1. The path to self-mode-locking

Semiconductor disk lasers (SDLs), also known as vertical-external-cavity surface-emitting lasers (VECSELs), are versatile lasers which serve as an excellent platform for the realization of various emission schemes. The first of its kind was demonstrated in 1997 by Kuznetsov *et al.* [1] and thereafter - owing to their remarkable design flexibility and features – rise was given to a plethora of modifications and improvements towards more specific applications. In recent years, not only high-power multi-mode [2] or single-frequency [3] continuous-wave operation schemes have been achieved, but also two-color [4] as well as mode-locked [5] emission. Particularly, their external resonator is predestined to be exploited for intra-cavity frequency conversion via nonlinear elements which expands the accessible wavelength range drastically. While second-harmonic generation pushes the boundaries into the UV [6], even terahertz frequencies can be reached using difference-frequency generation inside a two-color VECSEL [7, 8] - to name a few remarkable achievements in this field.

Within the last decade, VECSELs have become particularly appealing sources of pulsed laser light, because they can typically provide a high output power and an outstanding beam quality. The demonstration of the first mode-locked (ML) VECSEL dates back to the year 2000 and was achieved by Hoogland *et al.* for a central wavelength of 1 µm with 22 ps long pulses [9]. It did not take long and VECSELs were considered becoming compact, cost-efficient alternatives to commercial mode-locked lasers with ever shorter pulses, higher peak powers and enhanced tunability using resonator-integrated [10–30] or even chip-integrated [31, 32] semiconductor saturable-absorber mirrors (SESAMs). However, the complex, power-sensitive and costly SESAMs, which have to be carefully designed for a certain wavelength

#224198 - $15.00 USD Received 1 Oct 2014; revised 22 Oct 2014; accepted 24 Oct 2014; published 7 Nov 2014

range, naturally impose limitations on the performance of the device. Currently, besides semiconductor materials, graphene [33, 34] as well as carbon nanotubes [35] saturable absorbers have been employed for ML operation of VECSELs. However, mode-locking has also been reported to take place even without any additional saturable absorber—an effect called self-mode locking (SML) [36–41].

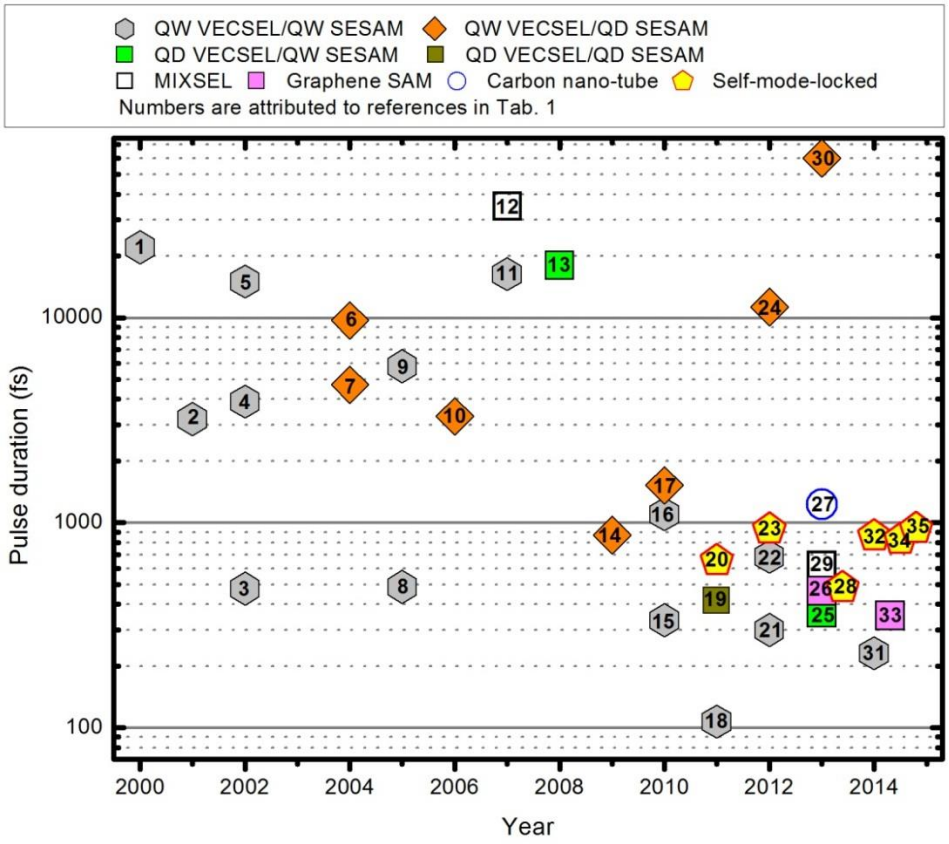


Fig. 1. Overview of pulse durations of mode-locked optically pumped VECSELs emitting around 1µm wavelength. More details including references are presented in Table 1.

In this work, light is shed on recent demonstrations of SESAM-free VECSELs which are operated under SML conditions. It was recently demonstrated that the SML scheme is not only applicable to quantum-well VECSELs [36–39, 41], but also to quantum-dot devices [40]. Furthermore, SML can be used for passively harmonically mode-locked devices with sub-ps-pulsed operation demonstrated at discrete power levels up to the third harmonic [39]. Inherently, this novel and effective technique allows for a maximum degree of wavelength flexibility and a reduction of device complexity. However, the mechanism of SML, which could give access to an exhaustive utilization of the occurring effects, is not fully understood yet and will be subject to future studies - noting that different driving mechanisms for SML were proposed [36–38, 41]. Nevertheless, an optimization of the dispersion management as well as the thermal management in an optimistic view promises the achievement of shorter pulses in the sub-100-fs range and significantly higher peak powers exceeding the current values at repetition rates ranging from a few hundreds of MHz to a few GHz.

In Fig. 1, an overview of all mode-locking techniques of optically pumped VECSELs around a wavelength of 1 µm is shown. More details and the attribution of numbers to references can be found in Table 1.

#224198 - $15.00 USD Received 1 Oct 2014; revised 22 Oct 2014; accepted 24 Oct 2014; published 7 Nov 2014

**Table 1. Overview of fundamentally mode-locked optically pumped VECSELs emitting around 1 µm wavelength**

| Number in Fig. 1 | Year | Type | Pulse duration | Repetition rate (GHz) | Average output power (W) | Reference |
|---|---|---|---|---|---|---|
| 1 | 2000 | QW-VECSEL/QW-SESAM | 22 ps | 4.4 | 0.022 | [9] |
| 2 | 2001 | QW-VECSEL/QW-SESAM | 3.2 ps | 2.06 | 0.213 | [10] |
| 3 | 2002 | QW-VECSEL/QW-SESAM | 477 fs | 1.21 | 0.1 | [11] |
| 4 | 2002 | QW-VECSEL/QW-SESAM | 3.9 ps | 5.95 | 0.53 | [12] |
| 5 | 2002 | QW-VECSEL/QW-SESAM | 15 ps | 6 | 0.95 | [12] |
| 6 | 2004 | QW-VECSEL/QD-SESAM | 4.7 ps | 30 | 0.025 | [13] |
| 7 | 2004 | QW-VECSEL/QD-SESAM | 9.7 ps | 21 | 0.055 | [13] |
| 8 | 2005 | QW-VECSEL/QW-SESAM | 486 fs | 10.01 | 0.0303 | [14] |
| 9 | 2005 | QW-VECSEL/QW-SESAM | 5.8 ps | 1.88 | 0.083 | [15] |
| 10 | 2006 | QW-VECSEL/QD-SESAM | 3.3 ps | 50 | 0.1 | [16] |
| 11 | 2007 | QW-VECSEL/QW-SESAM | 16.3 ps | 0.35 | 0.013 | [17] |
| 12 | 2007 | MIXSEL | 35 ps | 2.8 | 0.04 | [31] |
| 13 | 2008 | QD-VECSEL/QW-SESAM | 18 ps | 2.57 | 0.027 | [18] |
| 14 | 2009 | QW-VECSEL/QD-SESAM | 870 fs | 0.9 | 0.045 | [19] |
| 15 | 2010 | QW-VECSEL/QW-SESAM | 335 fs | 1 | 0.12 | [20] |
| 16 | 2010 | QW-VECSEL/QW-SESAM | 1.1 ps | 147 | 0.04 | [21] |
| 17 | 2010 | QW-VECSEL/QD-SESAM | 1.52 ps | 4.2 | 0.03 | [22] |
| 18 | 2011 | QW-VECSEL/QW-SESAM | 107 fs | 5.14 | 0.003 | [23] |
| 19 | 2011 | QD-VECSEL/QD-SESAM | 416 fs | 4.5 | 0.143 | [24] |
| 20 | 2011 | QW-self-mode-locking | 654 fs | 2.17 | 0.45 | [36] |
| 21 | 2012 | QW-VECSEL/QW-SESAM | 300 fs | 169 | 0.02 | [25] |
| 22 | 2012 | QW-VECSEL/QW-SESAM | 682 fs | 1.71 | 5.1 | [26] |
| 23 | 2012 | QW-self-mode-locking | 930 fs | 0.21 | 1.5 | [37] |
| 24 | 2012 | QW-VECSEL/QD-SESAM | 11.3 ps | 0.253 | 0.4 | [27] |
| 25 | 2013 | QD-VECSEL/QW-SESAM | 364 fs | 3.97 | 0.07 | [28] |
| 26 | 2013 | Graphene SAM | 466 fs | 2.48 | 0.013 | [33] |
| 27 | 2013 | Carbon nano-tube | 1.23 ps | 0.613 | 0.136 | [35] |
| 28 | 2013 | QW-self-mode-locking | 482 fs | 1 | 1 | [38] |
| 29 | 2013 | MIXSEL | 620 fs | 4.8 | 0.101 | [32] |
| 30 | 2013 | QW-VECSEL/QD-SESAM | 60 ps | 0.085 | 0.36 | [29] |
| 31 | 2014 | QW-VECSEL/QW-SESAM | 231 fs | 1.75 | 0.1 | [30] |
| 32 | 2014 | QW-self-mode-locking | 860 fs | 0.504 | 0.47 | [39] |
| 33 | 2014 | Graphene SAM | 353 fs | 1.76 | 10.2 | [34] |
| 34 | 2014 | QD-self-mode-locking | 900 fs | 1.5 | 0.75 | [40] |
| 35 | 2014 | QW-self-mode-locking | 935 fs | 1.8 | — | [41] |

Yet, the mode-locking semiconductor-laser community doubts that previous publications about SML truly show mode-locked devices. In our work, we intend to address concerns that have been discussed recently. Most prominent is the discussion presented in Refs [42, 43] triggered by a report on SESAM-free ML-VECSEL [37]. In the following, we provide clear evidence of SML by a variety of measurements: Green light originating from second-harmonic generation using the out-coupled laser beam is observed when our device is running in the ML regime. Furthermore, by presenting long-time-span pulse trains as well as radiofrequency-spectra measurements for our sub-ps pulses at 500 MHz repetition rate we highlight the stability of our device. In addition, a long-time-span autocorrelation trace shows absence of a pedestal or double pulses. Finally, we show a beam-profile measurement which reveals the excellent beam quality of our device with an M-square factor of less than 1.1 for both axes.

#224198 - $15.00 USD Received 1 Oct 2014; revised 22 Oct 2014; accepted 24 Oct 2014; published 7 Nov 2014

## 2. VECSEL chip design and setups

The VECSEL chip used in our experiments is grown by metal-organic-vapour-phase-epitaxy. The gain medium consists of 10 (InGa)As quantum wells (QWs) equally spaced by $\lambda/2$ GaAsP barrier layers. 24½ pairs of quarter wavelength GaAs/AlGaAs layers form a distributed Bragg reflector (DBR). Both, QWs and DBR are designed for a laser emission at approximately 1010 nm. The semiconductor structure is flip-chip-bonded using Au-In solid-liquid inter-diffusion bonding onto a 350 µm thick CVD-diamond heat spreader before wet etching to remove the substrate.

An anti-resonant micro-cavity design is chosen in order to minimize the group delay dispersion (GDD) and to spectrally broaden the effective gain of the structure. Therefore, the (InGa)P cap layer is etched down to a thickness of $1.25*\lambda/4$, which theoretically results in a negligible GDD at the design wavelength. The electric-field (E-field) distribution inside the gain medium is shown in Fig. 2(a). The positions of the quantum wells are represented by the vertical red lines. The laser setup is schematically shown in Fig. 2(b): The cavity is optimized for mode-locked operation assuming Kerr-lensing inside the VECSEL chip structure [38]. Therefore, a variable slit is placed directly in front of a highly reflective end mirror (HR). The Z-shaped cavity consists of a flat output coupler (OC) with a transmittance of 1.6%, the gain chip itself, and a highly reflective curved mirror (CM) with a radius of curvature of 150 mm as well as the HR mirror. With a total cavity length amounting to 30 cm a free spectral range of approximately 0.5 GHz is determined. The laser chip is mounted onto a water-cooled copper heat sink and pumped under an incident angle of 30° using an 808 nm fiber-coupled diode laser which is focused onto the chip and ensures a pump mode of adjustable size. The angle of incidence on the curved mirror was kept below 10° in order to avoid excessive astigmatism.

## 3. Evidence of self-mode-locked operation

In our VECSEL, mode-locking is initiated when the slit in front of the HR end mirror is moved or the slit width is narrowed. Furthermore, the cavity length was fine-tuned to stabilize SML operation (cf [39, 40].). In order to clearly demonstrate mode-locked operation employing the SML technique, different measurements have to be carried out [42]. Usually radiofrequency (RF) spectra, optical spectra, autocorrelation traces are sufficient for the characterization of mode-locking operation. However, if a new mode-locking technique is introduced, further measurements are required in order to exclude artificial effects and the standard characterization methods cannot serve as an unambiguous evidence of mode-locking. One of these artificial effects that could give the impression of a ML device is mode-beating which could result in an RF spectrum similar to which is recorded with a ML device. This was clearly demonstrated in [42]. Moreover, an autocorrelation trace can also be misleading as a CW signal may result in a time trace which gives rather information about the coherence length than about a pulse duration [44]. The possibility that both RF spectra and autocorrelation traces, which are presented in the next section, are misapprehended can be banned by recording externally the second-harmonic generation (SHG) signal of our SML-VECSEL.

#224198 - $15.00 USD Received 1 Oct 2014; revised 22 Oct 2014; accepted 24 Oct 2014; published 7 Nov 2014

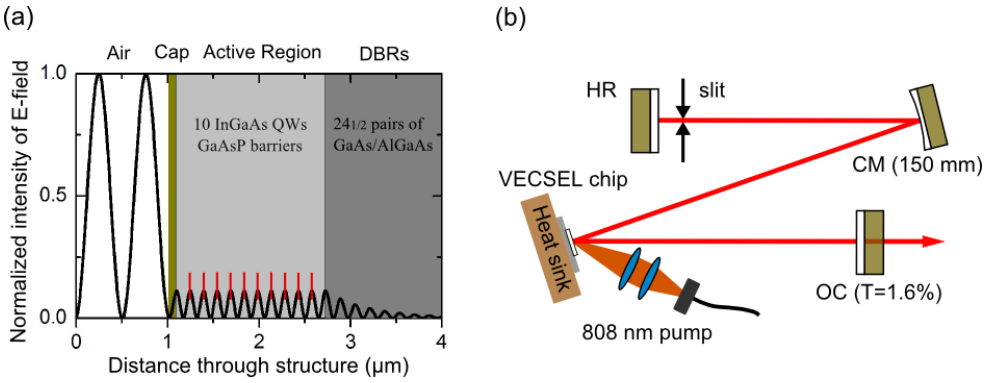


Fig. 2. (a) E-field distribution inside the near-antiresonant gain structure, normalized to the input intensity. The positions of the quantum wells are represented by the vertical red lines. (b) Schematic drawing of the setup of SML optically pumped VECSEL.

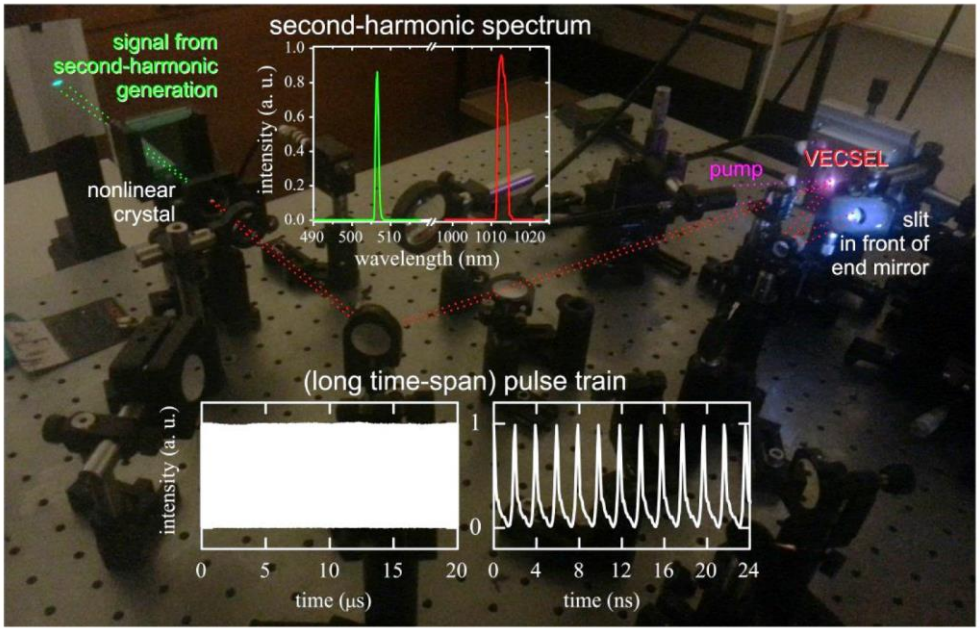


Fig. 3. Self-mode-locked quantum-well semiconductor disk laser: Green light is externally produced via second-harmonic generation with the infrared pulsed laser light. Inset: The spectrum shows the frequency-doubled signal originating from SHG using the out-coupled VECSEL beam (top). The diagram of the long-span pulse train of this device is shown at the bottom (left). The close-up of the pulse train reveals a 500-MHz repetition rate for the fundamental mode (right).

A nonlinear frequency conversion in a BBO crystal is performed using an SML VECSEL for the first time, to the best of our knowledge. Therefore, the out-coupled laser beam of the VECSEL is directed into the nonlinear crystal, as seen in Fig. 3, so that green light is externally produced via SHG with the infrared pulsed laser light. In case of continuous-wave operation no SHG signal is observed whereas a clear spectrum of the SHG signal can be measured if the laser is mode-locked, since SHG is an intensity-dependent nonlinear effect. The top inset of Fig. 3 shows the corresponding spectrum of the frequency-doubled signal (507 nm) originating from SHG using the out-coupled SML VECSEL beam (1013 nm). The photo shown in Fig. 3 presents the actual setup used for this experiment with colored dotted lines indicating the beam path inside and outside the VECSEL. The slit is highlighted by flash

#224198 - $15.00 USD Received 1 Oct 2014; revised 22 Oct 2014; accepted 24 Oct 2014; published 7 Nov 2014

light and is placed directly in front of the HR mirror of the cavity. A lens is used to focus the VECSEL output into the nonlinear crystal, as shown in the left part of the photo.

To highlight stable mode-locked operation of our QW VECSEL, a representative long-span pulse-train of the output is shown as inset on the bottom of Fig. 3. The signal was recorded for both a time window of 20 μs (bottom-left) and a few ns (bottom-right), respectively, via an InGaAs photodetector (PD) with a 3 dB bandwidth of 5 GHz and a digital oscilloscope with an analog bandwidth of 2 GHz. Stable mode-locking can be derived from this measurement as the pulse train with approximately 500 MHz repetition rate exhibits no intensity modulations.

## 4. Characterization of the emission features

In this section, we present RF-spectra measurements as well as time-resolved autocorrelation data of a VECSEL operated under SML conditions. Moreover, a beam-profile measurement is performed in order to reveal the excellent beam-quality of our device. Since RF-spectra measurements provide information on the frequency stability of the generated pulses, measurements are performed with a 3-dB bandwidth of a 5-GHz PD coupled to a 22-GHz-bandwidth electrical spectrum analyzer (HP 8566A). Figure 4 shows the RF spectrum of the fundamental repetition rate measured using a 10 kHz resolution bandwidth (RBW). Here, a clear peak at 504 MHz with a signal to noise ratio of about 50 dB is observed. The RF linewidth is less than 30 kHz, which highlights the stable operation of our mode-locked system. This result is similar to those obtained from SESEAM mode-locked VECSELs [12, 27]. The inset of Fig. 4 presents the RF spectrum of the first 9 harmonics indicating a stable pulse generation with no parasitic sidebands around the fundamental and higher harmonics frequencies.

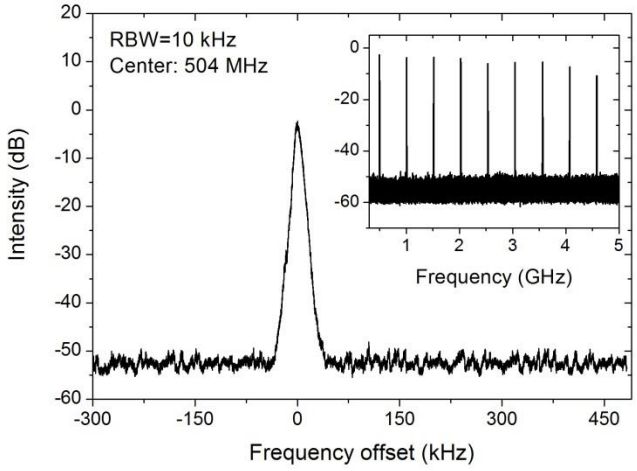


Fig. 4. RF spectrum of the fundamental repetition rate recorded with a 10 kHz resolution bandwidth (RBW). Inset: 5 GHz span showing the first 9 harmonics of the self-mode-locked device.

The mode-locked pulse duration was measured with a self-made intensity autocorrelator with a scan range of ~130 ps. Figure 5(a) shows a long-delay autocorrelation trace for fundamental mode-locking confirming the single-pulse operation. To complement the information, a short-delay autocorrelation trace with $\text{sech}^2$-fit is shown in Fig. 5(b) which yields a pulse duration of 860 fs. The corresponding optical spectrum was measured using an Ando AQ-6315A optical spectrum analyzer. The spectrum has a full width at half maximum of 2.7 nm, resulting in a time bandwidth product (TBWP) of 0.68 (Fig. 5(c)). The average

#224198 - $15.00 USD Received 1 Oct 2014; revised 22 Oct 2014; accepted 24 Oct 2014; published 7 Nov 2014

output power was measured to be 460 mW for this QW VECSEL which leads to a peak power of 950 W.

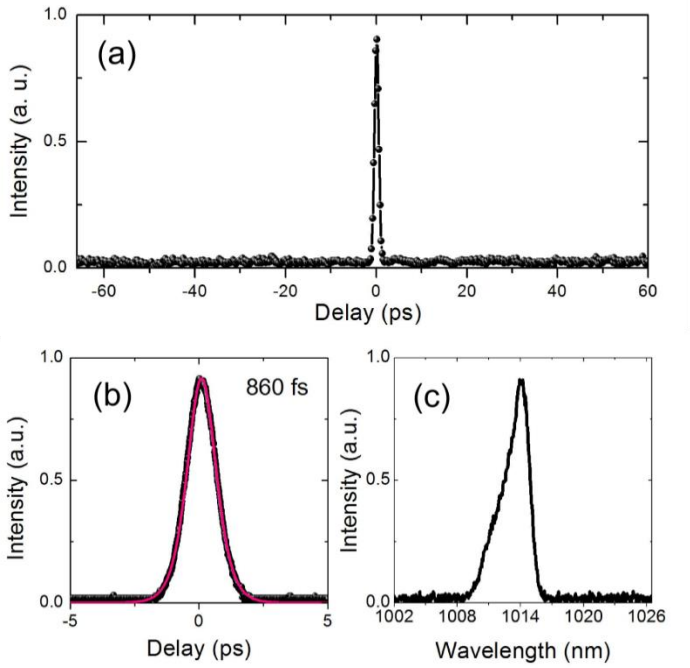


Fig. 5. (a) A long-delay autocorrelation trace for fundamental mode-locking confirming the single pulse operation. (b) A short delay autocorrelation trace with $sech^2$-fit precisely determines the pulse duration of 860 fs. (c) The corresponding optical spectrum centered at 1014 nm.

Finally, the beam quality was measured for an average output power of 450 mW, see Fig. 6: Excellent M-square values of 1.07 and 1.08 in the horizontal and vertical directions respectively have been obtained, confirming lasing in the fundamental transverse mode with nearly ideal Gaussian characteristics. The inset shows a corresponding beam-profile under SML operation. While Liang *et al*. [41] supposed that the occurrence of SML can be assisted by the existence of high-order transverse modes, our results are in contrast to these findings. Liang et al. observed a threshold for SML which coincided with the threshold of high-order transverse modes. With our results we rule out a dependence of SML on high-order transverse modes and demonstrate an excellent beam quality of our SML VECSEL with fundamental-transverse-mode profile.

#224198 - $15.00 USD Received 1 Oct 2014; revised 22 Oct 2014; accepted 24 Oct 2014; published 7 Nov 2014

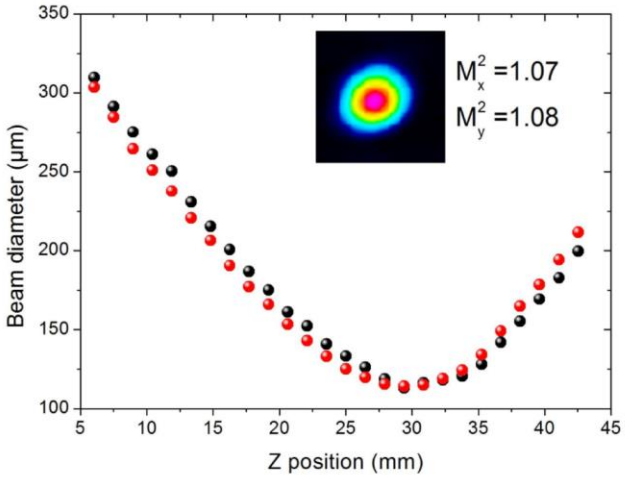


Fig. 6. Beam quality measurement confirming operation in fundamental-transverse mode with $M^2$ values less than 1.1 for both axes.

## 5. Conclusion

To summarize, we highlighted recent achievements in the field of ML and in particular SML VECSEL and presented a clear evidence of mode-locking for a QW device under SML conditions. Green light originating from second-harmonic generation in an external BBO crystal was demonstrated using the out-coupled laser beam. In addition, long-time-span pulse trains as well as radiofrequency spectra measurements were presented for our sub-ps pulses at 500 MHz repetition rate which indicate the stable pulse operation of our device. Furthermore, a long-time-span autocorrelation trace, which emphasizes the absence of a pedestal or double pulses, was shown. Additionally, a beam-profile measurement revealed the excellent beam quality of the device with an M-square factor of less than 1.1 for both axes. Even though the driving mechanism for SML has to be studied with care in future investigation for an efficient use of the underlying effects, we believe that in the near future SML VECSELs, which combine the advantages of solid-state and semiconductor devices, can become robust, compact and low-cost sources of fs-pulsed laser light.

## Acknowledgment

The authors acknowledge financial support from the German Science Foundation (DFG: GRK 1782, SFB 1083). M. Gaafar acknowledges support from the Yousef Jameel scholarship funds. H. Keskin acknowledges financial support from COST Action MP1204 as well as The Scientific and Technical Research Council of Turkey under grant #111T748 via H. Altan. The authors would like to thank E. U. Rafailov, K. A. Fedorova and A. A. Gorodetsky for fruitful discussions and G. Bastian for providing the fast oscilloscope. The authors further would like to thank B. Heinen and B. Kunert for VECSEL-chip processing.

## 4.4 Mode-locked semiconductor disk lasers

M. Gaafar, A. Rahimi-Iman, K. Fedorova, W. Stolz, E. Rafailov, M. Koch. Under review.

**Abstract**

This paper will review the recent advances in the field of ultrashort pulse generation from optically-pumped vertical-external-cavity surface-emitting lasers (VECSELs). In this review, we will summarize the most significant results presented over the last 15 years, before highlighting recent breakthroughs related to mode-locked VECSELs by different research groups. Different mode-locking techniques for optically pumped VECSELs are described in detail. While previously saturable absorbers such as semiconductor saturable absorber mirrors (SESAMs) - external, or internal like in mode-locked integrated external-cavity surface emitting laser (MIXSEL) - and recently novel-material-based carbon-nanotube or graphene saturable absorbers were employed, a new mode-locking method was presented and discussed in recent years which is referred to as self-mode-locking or saturable-absorber-free operation of mode-locked VECSELs. In this context, we particularly focus on achievements regarding self-mode-locking which is considered a promising technique for the realization of compact, robust and cost-efficient mode-locked devices. Up to date, the presented mode-locking techniques have led to a great enhancement in average powers, peak powers and repetition rates that can be achieved with passively mode-locked VECSELs.

**The author's contribution**

This review article was planned by all coauthors, who helped to discuss the featured topics and to improve the manuscript, which was to a large extend written by me.

# Mode-Locked Semiconductor Disk Lasers

*Mahmoud A. Gaafar[1], Arash Rahimi-Iman[1], Ksenia A. Fedorova[2], Wolfgang Stolz[1,3], Edik U. Rafailov[2], and Martin Koch[1]*

[1]Department of Physics and Material Sciences Center, Philipps-Universität Marburg, Renthof 5, D35032 Marburg, Germany
[2]Optoelectronics and Biomedical Photonics Group, School of Engineering and Applied Science, Aston University, Aston Triangle, Birmingham B4 7ET, UK
[3]NAsP III/V GmbH, Am Knechtacker 19, 35041 Marburg, Germany

## Abstract

This paper will review the recent advances in the field of ultrashort pulse generation from optically-pumped vertical-external-cavity surface-emitting lasers (OP-VECSELs). In this review, we will summarize the most significant results presented over the last 15 years, before highlighting recent breakthroughs related to mode-locked VECSELs by different research groups. Different mode-locking techniques for optically pumped VECSELs are described in detail. While previously saturable absorbers such as semiconductor saturable absorber mirrors (SESAMs) - external, or internal like in mode-locked integrated external-cavity surface emitting laser (MIXSEL) - and recently novel-material-based carbon-nanotube and graphene saturable absorbers were employed. A new mode-locking method was presented and discussed in recent years, which is referred to as self-mode-locking or saturable-absorber-free operation of mode-locked VECSELs. In this context, we particularly focus on achievements regarding self-mode-locking which is considered a promising technique for the realization of high power compact, robust and cost-efficient ultrashort pulse lasers. Up to date, the presented mode-locking techniques have led to a great enhancement in average powers, peak powers and repetition rates that can be achieved with passively mode-locked VECSELs.

## 1. Introduction

To date, ultrafast optical pulse generation [1] has opened the door for a wide range of different applications in biology, medicine, manufacturing, and metrology [2, 3]. The achieved ultrashort pulse durations have allowed for high-resolution measurements in the time-domain [4], a remarkable spatial precision in the field of material processing [5] and the peak powers satisfy for multiphoton-absorption-based technologies [3]. Moreover, lasers operating at multi-gigahertz repetition rates are now becoming key elements for optical interconnects [6] and high-capacity telecommunication systems [7]. In addition, focusing pulses with high peak power on nonlinear fibers creates a broad optical spectrum, which can cover a several hundred nanometers spectral range. This can be advantageous for applications such as optical coherence tomography, where a broad spectrum supports good spatial resolution.

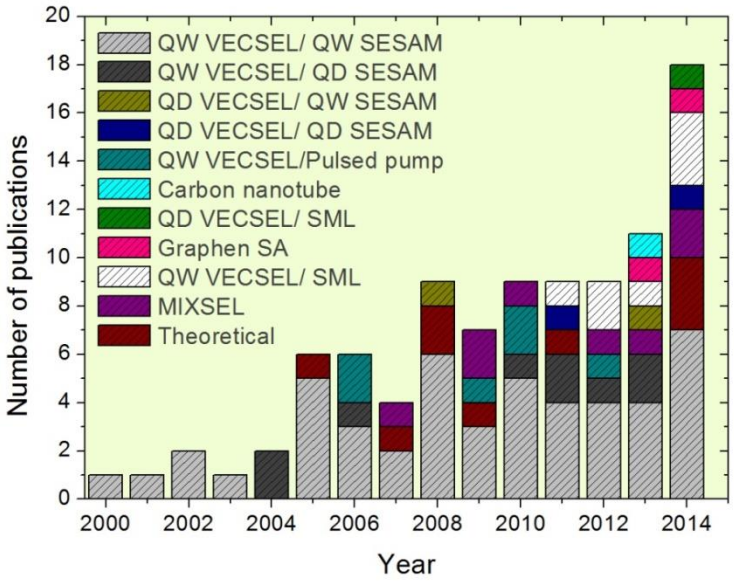


**Figure 1.** Number of publications per year for mode-locked semiconductor disk lasers.

In this context, it is natural to shed light on a class of lasers which turned up with ultrashort pulses within the last 15 years. Ultrafast semiconductor disk lasers (SDLs), also referred to as vertical external-cavity surface-emitting lasers (VECSELs) are indeed promising for those aforementioned applications.

SDLs combine the advantages of both semiconductor lasers, e.g. band-gap engineering based on available laser-proof materials and high gain cross sections, and ion-doped bulk lasers, such as a high-Q external cavity and an excellent beam quality [8]. Furthermore, mode-locked (ML, also 'mode-locking') SDLs offer numerous advantages over their solid-state pendants, such as their low-complexity, cost-efficiency, compactness and an extremely wide range of accessible emission wavelengths (from visible to mid-infrared, based on the employed material system) and repetition rates. This makes ultrafast SDLs very interesting for various applications that rely on a compact, cost-efficient and mass-producible laser technology.

To highlight progress in this field, the number of publications for mode-locked SDLs over the last 14 years is presented in Fig. 1. While initially, only a small amount of publications followed the demonstration of the first mode-locked VECSEL by Hoogland et al. in 2000 [9], a significant increase of publications was registered after 2005. To acknowledge various efforts made up to now, we are going to review various approaches for ultrashort pulsing, and the most relevant aspects of mode-locked VECSELs in the following.

## 2. Optically pumped semiconductor disk lasers

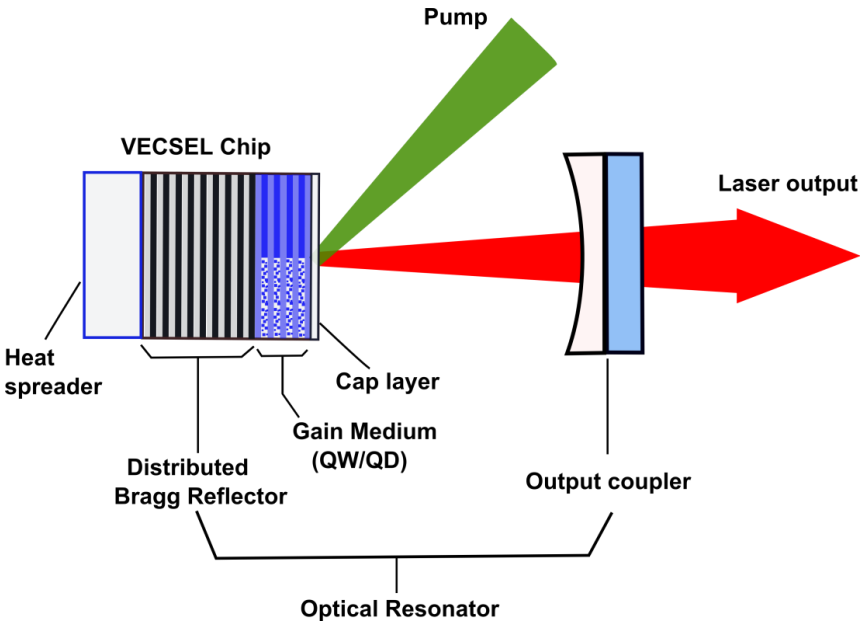


**Figure 2.** Schematic drawing of an OP-SDL device.

The SDL concept is based on a semiconductor region providing gain to the laser in a direction normal to the semiconductor wafer surface [8, 10]. The thin semiconductor disk, which is a stack of alternating semiconductor layers, can be subdivided into three regions: a multilayer high-reflectivity distributed Bragg reflector (DBR) mirror, a gain medium containing multi quantum wells (QWs) or layers of quantum dots (QDs), and the cap layer. For efficient heat dissipation, the thin disk has to be bonded either onto a CVD diamond heat spreader, which links the chip and a water-cooled copper heat sink thermally, or to an intra-cavity diamond heat spreader, which is typically clamped by a copper aperture. The laser cavity consists of the on-chip mirror and at least an external spherical mirror, which also serves as the output coupler. The active region can be pumped either optically by a low cost, low brightness lasers or electrically using a p-i-n configuration. Figure 2 shows a scheme of a linear cavity configuration – as described above – of an optically pumped semiconductor disk laser (OP-SDL), with the SDL-chip structure also schematically presented. The discussion of electrically-pumped VECSELs is out of the scope of this review, but examples can be found in the literature [11-13].

It has been shown, that careful thermal management enables high power operation for single-QW-chip VECSELs with output powers exceeding 100 W in multi-mode [14], 20 W in fundamental-$TEM_{00}$-mode [15] and 23 W in single-frequency [16] operation. Power scaling for VECSELs is also achieved by employment of multiple chips inside the resonator which is exploited for frequency-doubled 532 nm devices with output powers exceeding 60 W [17]. An extremely wide access to obtainable emission wavelengths has been demonstrated in the continuous wave (CW) operation. SDLs were operated at emission wavelengths ranging from 615 nm to 5.3 µm [18-22], and even down to 244 nm by exploiting higher harmonics generation [23]. However, power scaling is not limited to QW-gain VECSELs. Also QD-gain VECSELs provide versatile systems similar to their QW pendants, yet with an even broader gain bandwidth [24]. However, owing to the nature of the gain medium – i.e. density and

structure – their output power is significantly lower. Nevertheless, QD-VECSELs with up to a few Watts of output power were demonstrated for various operation wavelengths ranging from 654 nm up to 1.3 µm [25-29]. Using second harmonic generation, even emission at wavelengths down to 514 nm were achieved [29]. Up to date, the highest output power for QD-VECSELs has been obtained to be 8.4 W in multi-mode operation from single chip at 1040 nm wavelength [30], while 6 W in fundamental $TEM_{00}$ -mode operation has been demonstrated using a dual-chip device at the same wavelength [31]. Further details regarding the CW operation of SDLs can be found in Refs. [32-34].

In the previous section, we briefly discussed the functionality of VECSELs and the CW operation of these devices. In the next sections, we will review the mode-locked operation and will particularly focus on recent developments of ultrafast SDLs.

## 3. Mode-locking techniques for optically-pumped SDLs

To date, various passive mode-locking techniques for OP-VECSELs have been demonstrated. The first technique employs a semiconductor saturable-absorber mirror (SESAM), with which mode-locking was demonstrated in the year 2000 [9].

For various resonator geometries, a schematic picture of the realized devices is given in Fig. 3, also depicting schematically the layered structure for both a VECSEL chip and a SESAM. Figure 3(a) shows the simplest configuration for SESAM-mode-locked VECSELs in a V-shaped cavity geometry. The SESAM itself consists of one or more QW or QD layers which act as a saturable absorber. These layers are grown on top of a highly reflective DBR to form the complete saturable-absorber mirror. The SESAM design also includes some top layers to control the dispersion and the absorption behavior [35]. Mode-locking operation has been demonstrated for different gain/absorber combinations, i.e QW-gain/QW-absorber [9, 36-52],

QW-gain/QD-absorber [53-58], QD-gain/QW-absorber [59, 60], and QD-gain/QD-absorber [61, 62].

Following the resonator-integrated SESAMs, chip-integrated SESAMs have been demonstrated in order to introduce a more compact mode-locked SDL type with the ability of repetition rate scaling. A mode-locked integrated external-cavity surface-emitting laser (MIXSEL) combines the gain region of the laser with the saturable-absorber region of a SESAM, which results in a single integrated semiconductor chip. Thereby, mode-locking can be achieved in a simple linear cavity. The first MIXSEL has been demonstrated in 2007 by Maas et al [63]. The configuration and the layered structure of the MIXSEL are displayed in Figure 3(b). Mode-locking operation of MIXSELs has been successfully demonstrated for the combination of QW-gain/QD-absorber [63-65] and QW-gain/QW-absorber [66, 67].

Although SESAM-mode-locking is the most prominent technique, several other techniques have been published for VECSELs with respect to mode-locking. For example, a VECSEL was presented in 2013 by Zaugg et al. which was mode-locked by a single-layer graphene saturable-absorber mirror (GSAM) [68]. With this approach, VECSELs were mode-locked with a series of different gain chips over a 46 nm wavelength range (from 935 to 981 nm) with sub 500 fs pulse durations and output powers up to 26 mW. One year later, Husaini et al. presented output power levels of up to 10 W from GSAM mode-locked VECSELs with pulse durations as low as 353 fs [69]. Figure 3(c) shows a schematic view of this technique. In the same year – 2013 – Seger et al. employed single-walled carbon-nanotubes saturable absorbers (SWCNT-SA) for the mode-locking operation of a VECSEL [70] (cf. Figure 3(d)).

Remarkably, within the last few years even saturable-absorber-free mode-locking of VECSELs appeared to be a serious alternative to previously widely used active and passive mode-locking techniques. In this scheme, a hard aperture is inserted into the resonator in front of an output coupler (OC) or highly reflective end mirror, leading to an effect also referred to

as self-mode-locking (SML). Figure 3(e) presents the simplest configuration for such an SML VECSELs, using a straight cavity design. Remarkably, SML operation of VECSELs has been demonstrated for both QW [71-77] and QD-VECSEL chips [78], and first assumptions and preliminary studies regarding the mechanisms behind SML arose [72, 79]

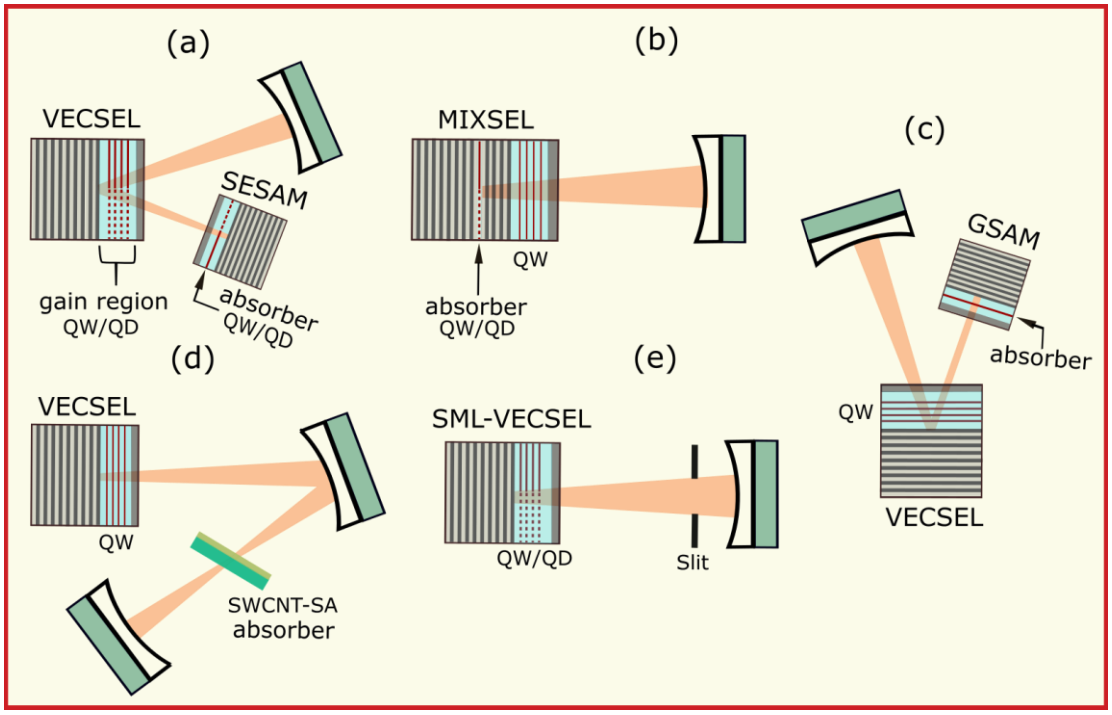


**Figure 3.** Different mode-locking techniques for OP-SDLs. (a) SESAM ML device, (b) MIXSEL, (c) graphene and (d) carbon-nanotube-based saturable absorber ML devices, (e) self-mode-locked VECSEL.

## 4. Mode locking achievements

### 4.1. Overview of the developments

#### *4.1.1. Pulse duration*

Generally, the laser pulse duration is an important parameter. Shorter durations allow higher time resolution in spectroscopic applications and enhance precision in material processing [80]. Ultrashort pulses can be also beneficial for application in terahertz time-domain spectroscopy [81,82]. The demonstration of the first mode-locked VECSEL dates back to the year 2000 and was achieved by Hoogland et al. for a central wavelength of 1 µm with 22 ps

long pulses [9]. It did not take long, and VECSELs were considered becoming compact, cost-efficient alternatives to commercial mode-locked lasers with ever shorter pulses using resonator-integrated SESAMs [36-62], MIXSELs [63-67], GSAMs [68, 69], carbon nanotube saturable absorber [70], as well as SML [71-78]. The pulse durations have been reduced to below 200 fs [45, 83] at sub-Watt-level output powers. However, similar pulse durations have not been achieved at average powers greater than 1 W.

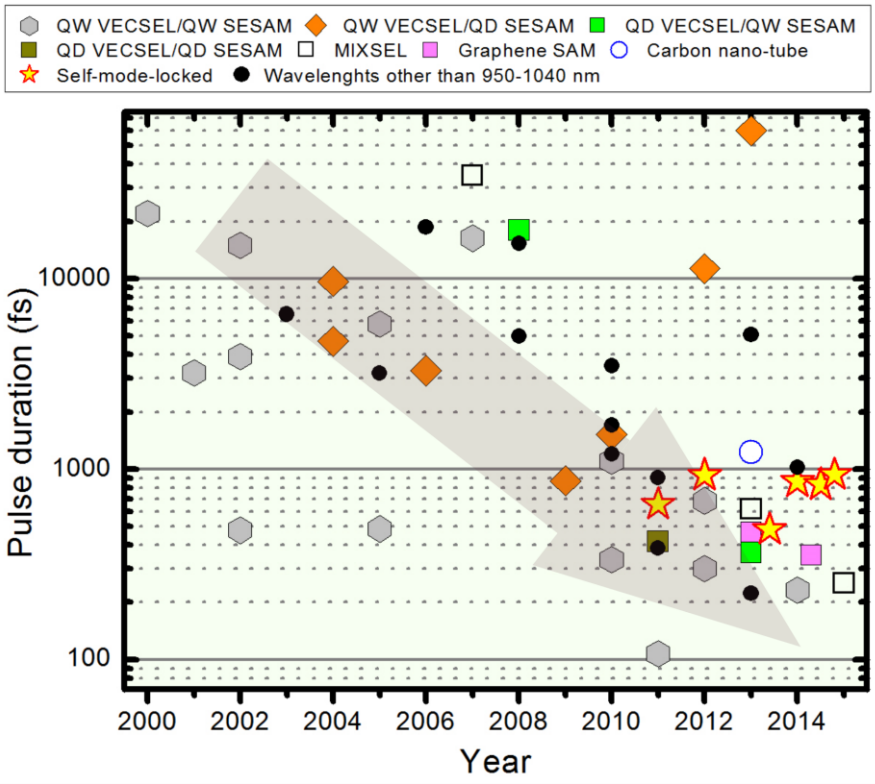


**Figure 4.** Pulse durations of mode-locked optically pumped VECSELs. Devices emitting around a wavelength of 1µm (950-1050 nm) are represented by big symbols, while devices with other wavelengths than 1µm are represented by small black dots.

An overview of pulse durations for various optically pumped mode-locked VECSELs are presented in Figure 4, in which results from all known mode-locking techniques are summarized. In this chart, devices emitting around a wavelength of 1µm (950-1050 nm) are represented by big symbols, while devices with other wavelengths than that range are represented by small black dots.

*4.1.2. Peak power*

Since high peak powers with short pulse durations enable the use of nonlinear processes based applications, significant efforts have been done through the last decade to increase the peak power of mode-locked SDLs. Figure 5(a) shows the increasing spread of achievable peak powers for pulsed VECSELs using different mode-locking techniques. Here, the symbols sort the results by the VECSEL's wavelength region, while the MIXSEL-type 1µm-emitting devices are separately displayed for clarity. Although results with peak powers even in the kW range have been obtained, as shown in Figure 5(b), yet, none of these results featured pulse durations shorter than 200 fs, which are together with high peak powers important for applications such as coherent supercontinuum generation. However, from these results, incoherent supercontinuum generation has been demonstrated only by Wilcox et al. using 4.35 kW peak power pulses with duration of 400 fs [51]. They generated directly from VECSEL without amplification a supercontinuum with a bandwidth of 175 nm and average power of 0.5 W using a 2-m long, 2.2 µm core photonic crystal fiber. In addition, a VECSEL has been also used for incoherent supercontinuum generation in fiber-amplified configurations [84].

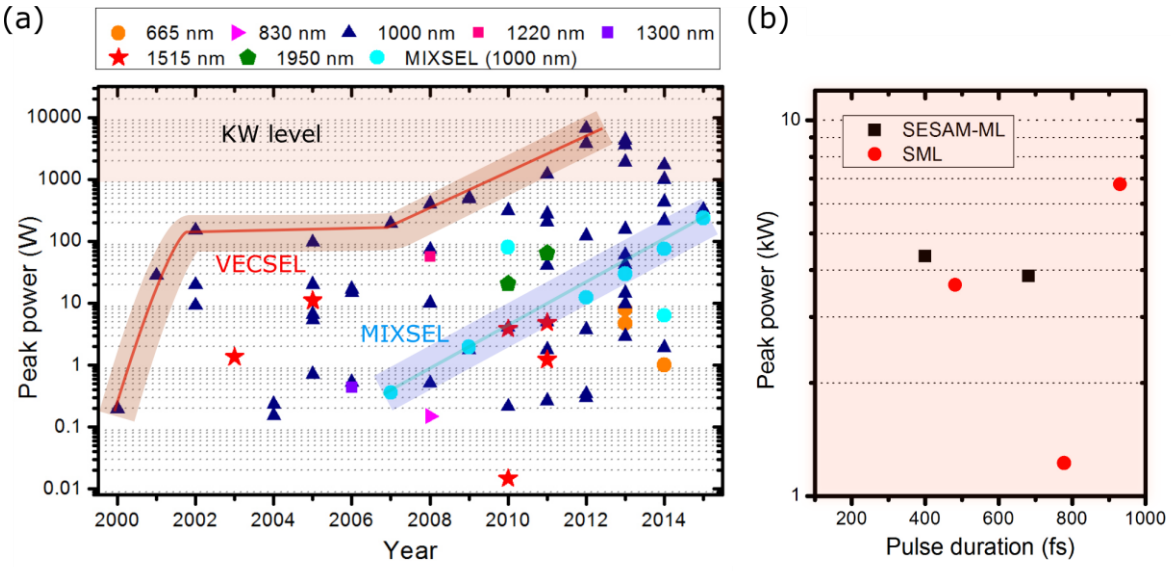


**Figure 5.** (a) Demonstration of the achieved peak powers from mode-locked SDLs over the past 15 years. (b) kW peak power level as a function of the corresponding pulse duration.

Quarterman et al. presented an alternative solution for a high repetition rate pump source for coherent supercontinuum generation in the absence of VECSELs that are capable of direct pumping [85]. In this work, they demonstrated a system based on the spectral broadening and compression of VECSEL pulses. 1.56 GHz trains of either 150 fs pulses at 270 mW average power or 220 fs pulses at 520 mW average power have been achieved.

#### *4.1.3. Repetition rate*

Not only high peak powers and short pulse durations are of importance to applications, as can be sensed by the considerable interest in VECSELs of different, even variable, repetition rates. For example, pulsed sources with low repetition rate will enable the use of SDLs in biomedical applications [86], for instance accounting for long fluorescence times. In contrast, these sources are practically ideally suited to shoot for high repetition rates as their architecture allows for compact cavities --- although not ultimate compact --- and their short upper state lifetimes provide strong suppression of Q-switching instabilities. Thereby, the GHz operation of these sources can facilitate employment of mode-locked VECSELs for applications for example in metrology [87] and high-resolution optical sampling [88].

*Fundamental mode-locking*

The simple cavity geometry of VECSELs and the large gain cross-sections of the semiconductor materials (~ $10^{-14}$ $cm^2$) enabled stable mode-locking at repetition rates starting from 85 MHz [58] up to 50 GHz in fundamental mode-locking operation [54]. Additionally, continuous repetition rate tuning from 2.87 to 7.87 GHz [89] and from 6.5 to 11.3 GHz [90] in femtosecond operation has been demonstrated. With MIXSELs, stable fundamental mode-locking in an extremely wide range of repetition rates between 2.47 GHz and 101.2 GHz has been delivered [63-67]. Figure 6 shows the peak power versus the repetition rate obtained from mode-locked SDLs at different operation wavelengths.

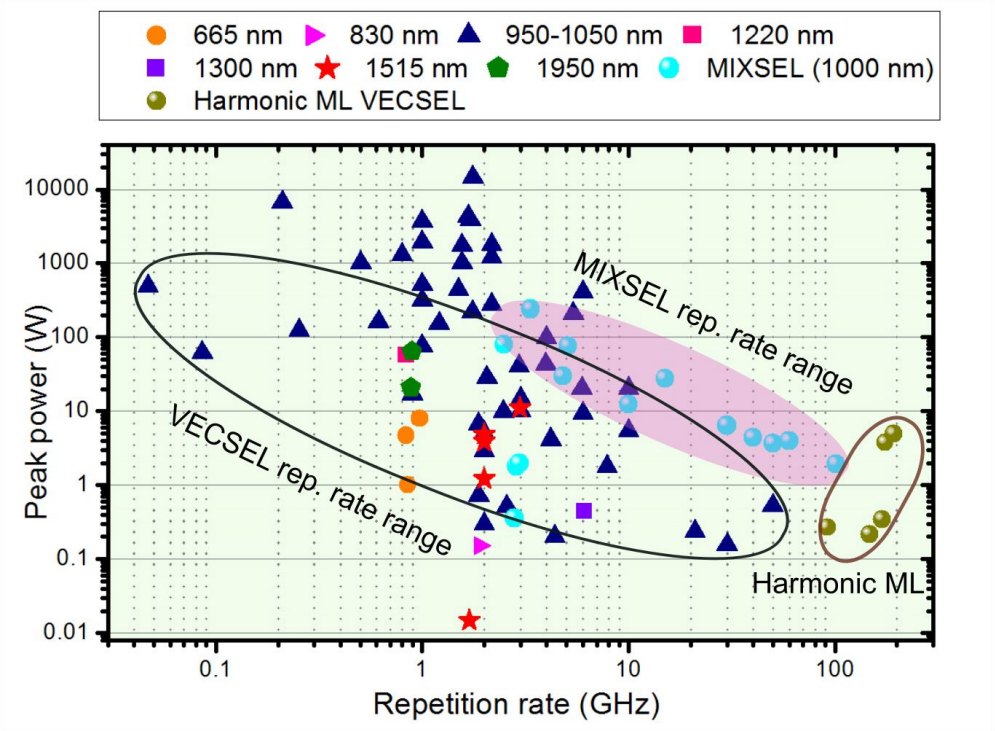


**Figure 6.** Peak power versus repetition rate for mode-locked SDLs

*Harmonic mode-locking*

Aiming for applications such as optical clocking and high bandwidth telecommunications [6, 7], recent publications pushed the boundaries for pulse repetition frequency up beyond the limit of fundamental repetition frequencies. A path to high repetition frequency is provided by harmonic mode-locking (HML), where more than one pulse circulates in the laser cavity, and pulses are emitted at an integer multiple of the fundamental repetition frequency of the laser cavity [91]. Up to date, with HML, diode lasers have achieved pulse repetition frequencies up to 100s of GHz [92, 93], while fiber lasers reached 200 GHz [94]. However, for all of these lasers the average power is limited and the pulse duration is > 1 ps for repetition frequency > 100 GHz.

On the other hand, VECSELs offer the generation of GHz repetition frequency pulse trains with high average power and femtosecond duration. In 2010, Quarterman et al. reported a harmonically mode-locked VECSEL where the SESAM substrate was used as an external

coupled cavity. They demonstrated 147 GHz repetition frequency with 1.1 ps pulses and 40 mW average output power [95]. One year later, HML of VECSELs was demonstrated at 92 GHz with 198 fs pulses and 30 mW average power [45], whereas HML occurred spontaneously driven by the saturable-absorber and gain dynamics. The multi-GHz repetition frequency with pulse duration of sub-200 fs should support interest in using SDLs for communications or frequency comb generation. While, in 2012, Wilcox et al. reported HML-VECSELs using an intracavity etalons to act as both thermal heat spreader and sub-cavity [96]. They observed 400 fs pulses at a repetition frequency 175 GHz with an average output power of 300 mW. The repetition frequency has been pushed beyond 190 GHz for 830 fs pulses with 4.95 W peak power by Saarinen et al. [97]. To our knowledge, this is the highest repetition frequency obtained from a mode-locked VECSEL, as well as the highest peak power above 100 GHz of any mode-locked laser technology. More details about the results achieved with harmonically mode-locked SDLs can be found in Table 1.

**Table 1.** Overview of important results achieved with harmonically mode-locked SDLs.

| Year | Type Gain/SESAM | Rep. Rate GHz | Pulse duration | $P_{avg}$ (mW) | Peak power (W) | λc(nm) | Harmonic number | Ref. |
|---|---|---|---|---|---|---|---|---|
| **2010** | 6 InGaAs QWs / single InGaAs QW | 80 | 1.5 ps | 80 mW | 0.587 | 1039 | $81_{st}$ | [95] |
| | | 147 | 1.1 ps | 40 mW | 0.218 | 1025 | | [95] |
| **2011** | 4 InGaAs QWs / single InGaAs QW | 92 | 198 fs | 30 mW | 0.268 | 1022 | $18_{th}$ | [45] |
| **2012** | 6 InGaAs QWs / single InGaAs QW | 169 | 300 fs | 20 mW | 0.347 | 1030 | $112_{th}$ | [96] |
| | | 175 | 400 fs | 300 mW | 3.77 | 1037.5 | $116_{th}$ | [96] |
| **2012** | 7 InGaAs QWs / two InGaAs QWs | 193 | 830 fs | 900 mW | 4.95 | 1050 | $150_{th}$ | [97] |

### 4.2. Semiconductor saturable absorber mirrors (SESAMs) mode-locked VECSELs

As discussed previously in section 3, the SESAM consists of a highly reflective DBR, one or more QW or QD layers which act as a saturable absorber, and some top layers to control the absorption behavior and dispersion.

*4.2.1. The rise of mode-locked VECSELs based on quantum-well structures*

In 2000, the first demonstration of an OP passively mode-locked VECSEL was achieved using a QW gain structure and a QW SESAM for a central wavelength of 1 µm, obtaining 22 ps short pulses [9]. It did not take long, and femtosecond pulse generation has been achieved from a QW-VECSEL in 2002 [37]. Three years later, the output power of mode-locked VECSELs has been improved from the mW regime to more than 2 W using a strain-compensated gain structure [42]. Up to date, pulse durations down to 107 fs in the fundamentally mode-locked operation [45] or even 60 fs pulse bursts [83] were achieved. In addition, the femtosecond pulse operation with high power-levels was pushed to 5.1 W of average output power with 682 fs pulses [49] or 3.3 W with 400 fs pulses [51] leading to a peak power of 4.35 kW for the SESAM-mode-locked configuration, whereas a record-high 6.8 kW peak power was demonstrated [72] for SESAM-free mode-locked configuration (discussed in Section 4.5). A mode-locked QW-VECSEL utilizing a QD-SESAM with a record-low repetition rate of 85.7 MHz at 989 nm has also been demonstrated [58]. An overview of the record values achieved from SESAM mode-locked QW-VECSELs is shown in Table 2. Please notice, that the record performance was achieved with VECSELs based on InGaAs QWs owing to beneficial properties of this material system such as low lattice mismatch and good thermal conductivity, and access to thin high-reflectivity DBRs. More details about the working principle of SESAMs and the pulse formation mechanisms in SESAM mode-locked VECSELs can be found in Refs. [10,35].

Recently, sub-150-fs pulses have been demonstrated using 10 strain-compensated InGaAs QW-VECSEL in combination with a single InGaAs QW SESAM. However, in this structure, the QWs are placed in pairs symmetrically around the anti-nodes of the electric field. For such a power level of around 100 mWatts, this is the shortest pulse duration reported to date directly from a fundamentally mode-locked VECSEL. Moreover, for such a VECSEL with sub-300-fs pulses, pulse peak powers as high as 328 W were obtained [98].

**Table 2**. Overview of record results achieved with SESAM mode-locked QW-SDLs.

| | Record value | Year | Gain medium | Wavelength | Reference |
|---|---|---|---|---|---|
| **Pulse duration** | 107 fs | 2011 | 4 InGaAs QWs | 1030 | [45] |
| **Average power** | 5.1 W | 2012 | 10 InGaAs QWs | 1030 | [49] |
| **Rep. Rate** | Highest: 50 GHz | 2006 | 7 InGaAs QWs | 958 | [54] |
| | Lowest: 85.7 MHz | 2013 | 16 InGaAs QWs | 989 | [58] |
| **Peak power** | 4.35 kW | 2013 | 10 InGaAs QWs | 1013 | [51] |

*4.2.2. First mode-locked quantum-dot VECSEL*

In the recent years, there has been a growing interest in the development of OP-VECSELs utilizing QD semiconductors. The QD structures are very promising materials that are able to offer a combination of unique features – broad gain bandwidth, ultrafast carrier dynamics, low temperature sensitivity, low threshold current and lower absorption saturation, and thus allow a number of advantages in comparison with the widely used QW structures [2,3].

The first report on the realization of a QD-VECSEL in the CW regime at 1040 nm was published in 2008 [99], and was followed soon by demonstration of QD-VECSELs operating at different wavelengths [100-104, 25, 29]. Recently, QD-VECSELs with output power exceeding 8 W at 1040 nm [30], 7 W at 1180 nm [105] and 3 W at 1250 nm [106] were demonstrated. Also, the broad gain bandwidth of QD materials was explored, and wavelength tunability up to 60 nm around 1040 nm, 69 nm around 1180 nm, and 25 nm around 1260 nm was demonstrated [29].

QD-VECSELs have also attracted considerable attention in mode-locking experiments using QW- and QD-SESAMs. The first mode-locked QD-based VECSEL using a QW-SESAM has been reported at 1059 nm by Hoffmann et al. [59] in 2008. In this work, a VECSEL with 35 QD-layers in the gain region and a standard QW-SESAM have been employed to demonstrate the fundamental mode-locking with an average output power of 27.4 mW with pulse duration of 18 ps at a repetition rate of 2.57 GHz, corresponding to 0.52 W of peak power.

*4.2.3. All-quantum-dot SESAM-mode-locked VECSEL*

The QD-based SESAMs, that provide an independent control of saturation fluence and modulation depth [107] and have shown the potential to support mode-locking in a wide range of repetition rates from 100 MHz to a few GHz [108], were also employed in a number of mode-locked VECSELs. A QD-SESAM was used to mode-lock a QW-VECSEL, resulting in the first of such type of lasers with sub-picosecond pulse widths [55]. In this work, the mode-locking operation with an average power of 45.5 mW and pulse duration of 870 fs at a repetition rate of 895.5 MHz and wavelength of 1027.5 nm was demonstrated. QD-based SESAMs have also allowed a 50-GHz repetition rate QW-VECSEL to be demonstrated at 958 nm with pulse duration of 3.3 ps and an average power of 102 mW, corresponding to 0.54 W of peak power [54]. A QW-VECSEL mode-locked using a QD-SESAM and delivering an average output power of 287 mW, with 1.5 ps pulses at 500 MHz and a central wavelength of 965 nm has been also demonstrated [86].

In 2009, Hoffmann et al. have reported the first all-quantum-dot SESAM-mode-locked VECSEL with an average output power of 22 mW at 1053 nm wavelength in 10-ps pulses with 2.54 GHz repetition rate [109]. Two years later, the first femtosecond all-quantum-dot based VECSEL with 1.05 W of average output power with a pulse duration of 784 fs at a repetition rate of 5.4 GHz and a center wavelength of 970 nm was reported [61]. The shortest pulse duration of 416 fs at a repetition rate of 4.5 GHz with an average output power of 143 mW at 960 nm was also demonstrated in this work. Recently, all-QD mode-locked VECSEL in the red spectral range was also demonstrated with an average power of 1 mW at 651 nm and with pulse duration of 720 fs at a repetition rate of 852 MHz [110]. Very recently, even a leap towards the UV region of the spectrum was accomplished by the demonstration of intra-cavity frequency conversion of light from a red mode-locked VECSEL [111].

### 4.3. Mode-locked integrated external-cavity surface-emitting laser (MIXSEL)

In 2007, Maas et al [63] combined the gain of VECSEL with the saturable absorber of a SESAM in a single integrated semiconductor chip to present the first MIXSEL. Their resonant system design delivered 40 mW of average power in 35-ps pulses at 2.8 GHz. Figure 7 shows a schematic design of a MIXSEL layer stack. The MIXSEL semiconductor layer stack is composed of a DBR for the lasing wavelength and a DBR for the pump wavelength. In between the DBRs, a single saturable absorber (QW or QD) is placed.

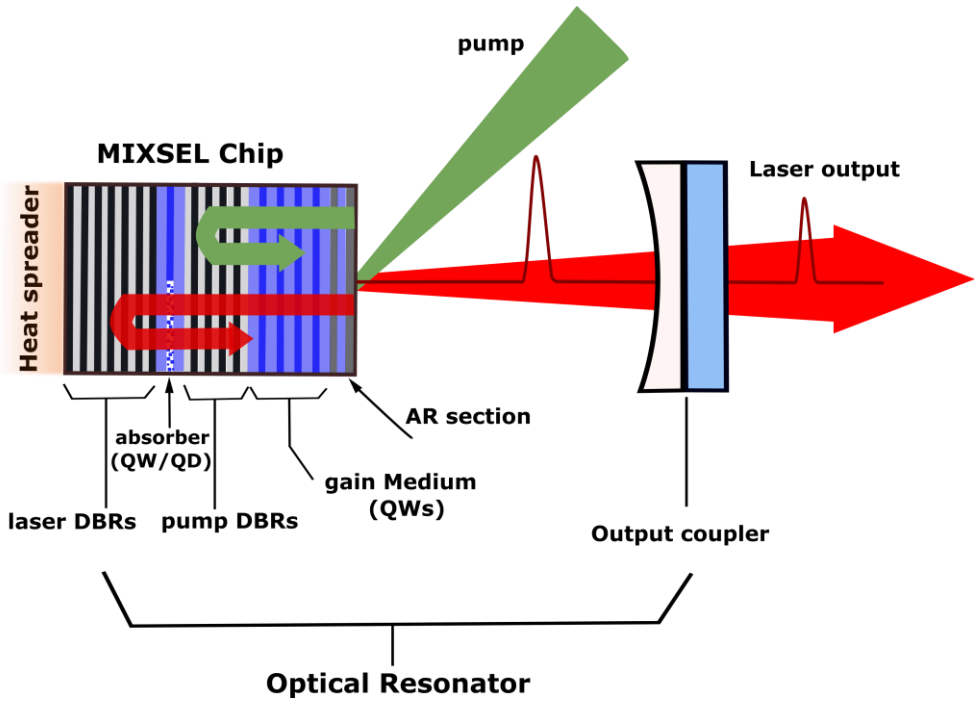


**Figure 7.** A schematic design of an OP-MIXSEL device.

In 2010, a novel MIXSEL design based on a low saturation fluence QD absorber in an antiresonant structure has been demonstrated by Rudin et al. which led to a record high average output power of 6.4 W in 28-ps pulses at 2.5-GHz repetition rate [64]. But the slow recovery dynamics of the QD saturable absorbers prevented shorter pulse generation. Ultimately, using a low-temperature grown single InGaAs QW embedded into AlAs barrier layers, which features fast recovery dynamics and low saturation fluence, this hurdle was stridden. Therefore, the first femtosecond MIXSEL with pulse duration of 620 fs at 4.83 GHz

repetition rate and 101 mW of average output power [66] has been demonstrated. One year later, Mangold et al. showed, that MIXSEL can also support pulse repetition rate scaling from ˜5 GHz up to >100 GHz [67] with the same MIXSEL chip used for femtosecond pulse generation [66]. The structure layout of the MIXSEL chip was used is schematically shown in Figure 8. Recently, even sub-300-fs pulses have been achieved with MIXSELs, using a device with a similar structure to the one described in [67], but with a strain compensated active region [112]. Summary of the record reported results achieved with MIXSEL written in Table 3.

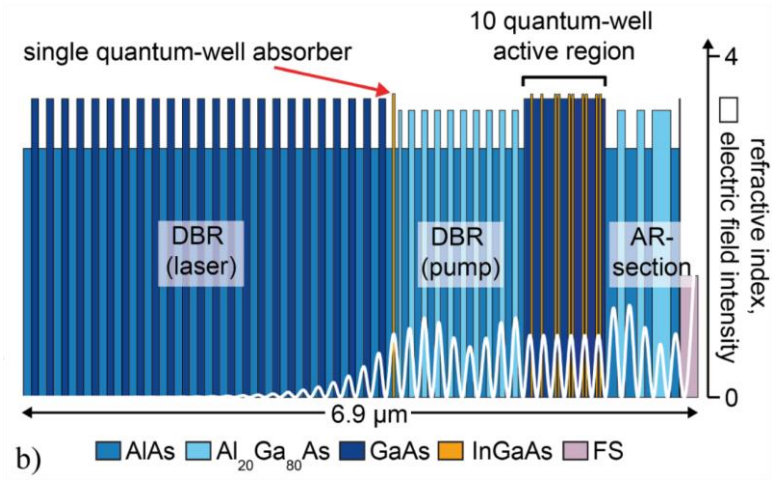


**Figure 8.** The 7-µm-thick MIXSEL semiconductor layer stack used for both the generation of first femtosecond MIXSEL [66] and the pulse repetition rate scaling from 5 GHz up to 100 GHz [67]. It consists of a single InGaAs QW saturable absorber placed inbetween the DBRs. The active region consists of 10 InGaAs QWs. Reproduced with permission.[66] Copyright 2013, Optical Society of America.

**Table 3**. Record reported results achieved with MIXSEL.

| | Record value | Year | Gain/absorber | Wavelength (nm) | Reference |
|---|---|---|---|---|---|
| **Average power** | 6.4 W | 2010 | 7 $In_{0.13}Ga_{0.87}As$ QWs /single layer of InAs QDs | 959 | [64] |
| **Rep. Rate** | Highest: 101.2 GHz | 2014 | 10 compressively strained $In_{0.12}Ga_{0.88}As$ QWs /single InGaAs QW | 964 | [67] |
| | Lowest: 2.47 GHz | 2010 | Same structure as for 6.4 W | 959 | [64] |
| **Pulse duration** | 253 fs | 2015 | Similar to the structure described in [67], but with strain compensated active region | 1044 | [112] |
| **Peak power** | 240 W | 2015 | Same structure as for 253 fs | 1044 | [112] |

### 4.4. Carbon nanotube mode-locked optically-pumped VECSEL

Recent reports showed the potential that single-walled carbon nanotubes (SWCNTs) can be successfully employed as ultrafast saturable absorbers (SAs) for mode-locking solid-state lasers [113-115] and fiber lasers [116-118]. SWCNT-SAs are characterized by broadband absorption which covers the near-IR spectral range from 800 nm up to ~1940 nm and can be fabricated by relatively simple methods.

In the year 2013, Seger et al. showed for the first time that saturable absorbers based on SWCNT with low loss operating in transmission can be used for mode-locking an OP-SDL [70]. They demonstrated a stable fundamental mode-locking at a repetition rate of 613 MHz with a pulse length of 1.23 ps. The system delivered a maximum average output power of 136 mW at 1074 nm. The VECSEL gain region was used composed of 3 GaInAs QWs engineered for the emission wavelength of 1060 nm.

### 4.5. Self-mode-locked optically-pumped VECSELs

Here, we shed the light on recent demonstrations of SESAM-free SDLs which are operated under SML conditions. It was recently demonstrated that the SML scheme is not only applicable to quantum-well SDLs [71-74, 76, 77], but also to quantum-dot devices [78]. Moreover, harmonic mode-locking with sub-ps pulses has been demonstrated at discrete power levels in SML-SDLs [74].

#### *4.5.1. The first results*

The first SESAM-free mode-locked SDL has been reported by Chen et al. in classical straight cavity configuration [71]. In this work the authors suggested that mode-locking results from saturable absorption in the unpumped QWs, by analogy with MIXSEL. Pulses as short as 654 fs has been generated with an average output power of 0.45 W at a repetition rate 2.17 GHz.

One year later, Kornaszewski et al. demonstrated the SML in a folded six-mirror SDL-cavity configuration [72]. However, they attributed the origin of pulsed operation to the intensity

dependent Kerr lens effect arising in the semiconductor gain medium. In that work, the mode-locked operation has been shown in two different configurations. First, stable mode-locking was observed when the cavity operated near its stability limit. In such configuration single pulses with duration of ~ 1.5 ps with an average output power of 700 mW at 200 MHz repetition rate were achieved. Secondly, mode-locked operation was also achieved by operating cavity in its stability region and inserting a hard aperture near the output. Pulses with duration of 930 fs at 210 MHz repetition rate and at 985 nm with average output power of 1.5 W and a record-high 6.8 kW peak power were demonstrated [72]. A schematic drawing of the cavity configuration was used is shown in Figure 9.

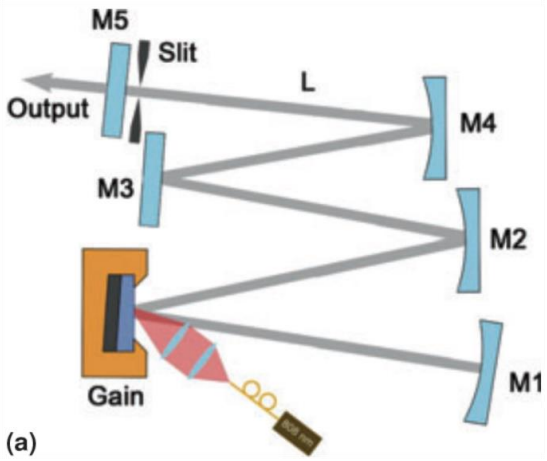


**Figure 9.** A schematic drawing of SESAM-free mode-locked SDL cavity configuration. Reproduced with permission.[72] Copyright 2012, Wiley-VCH.

*4.5.2. Rising controversy*

SML reports have been the source of some controversy, in part due to incomplete or ambiguous characterizations of the laser performance, but also due to the mechanism responsible for the self-mode-locking not having been identified. As discussed before, some authors are suggesting that mode-locking results from saturable absorption in the unpumped QWs [71] while others are suggesting that Kerr lensing in the gain medium is responsible for that [72]. The most prominent controversy is the discussion presented in Refs. [119, 79] triggered by a report on SESAM-free ML-VECSEL [72].

*4.5.3. Self-mode-locking burst*

It did not take long time, and other groups observed the SML phenomenon. Albrecht et al. also demonstrated Kerr-lens mode-locked operation for both soft and hard apertures placed at the optimal intra-cavity positions [73]. Their system delivered pulses with durations of below 500 fs at 1 GHz repetition rate. In their measurements they observed a residual background or pedestal which can be attributed to CW background; in addition the pulse train fluctuates over a time scale of some microseconds.

While in [75] the authors claimed to enhance the Kerr lensing effect with an extra Kerr medium inside the cavity. For this, they utilized an yttrium orthvanadate crystal which exhibits a nonlinear refractive index three times higher than that of titanium sapphire. Pulse duration of about 850 fs sits on a high background pedestal indicating a strong quasi-CW component in the emission has been shown. A schematic drawing of the cavity configuration was used in this experiment is shown in Figure 10.

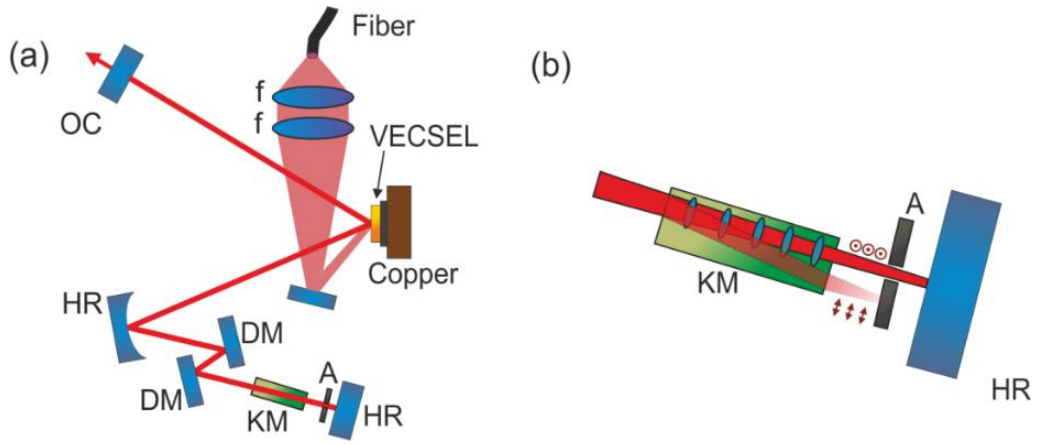


**Figure 10.** (a) Schematics of the laser cavity was used, the Kerr medium (KM) was placed close to the end mirror. (b) The $YVO_4$ crystal provides polarization control: The ordinary laser beam passes the crystal directly while the orthogonal polarization is displaced and is blocked by the aperture (A). Reproduced with permission.[75] Copyright 2014, Optical Society of America.

On the other hand, Liang et al. [76] supposed that the occurrence of SML can be assisted by the existence of high-order transverse modes. Liang et al. observed a threshold for SML which coincided with the threshold of high-order transverse modes. While Gaafar et al. demonstrated an excellent beam quality of SML-VECSEL with fundamental transverse mode profile [77]. They ruled out a dependence of SML on high-order transverse modes. In addition, more detailed set of measurements that has been discussed in Refs. [79, 119] was presented in [77]. In order to unequivocally verify the mode-locked operation in SML-VECSEL, they performed external second harmonic generation (SHG) measurement. A beta barium borate (BBO) crystal was used for frequency doubling of the SML-VECSEL.

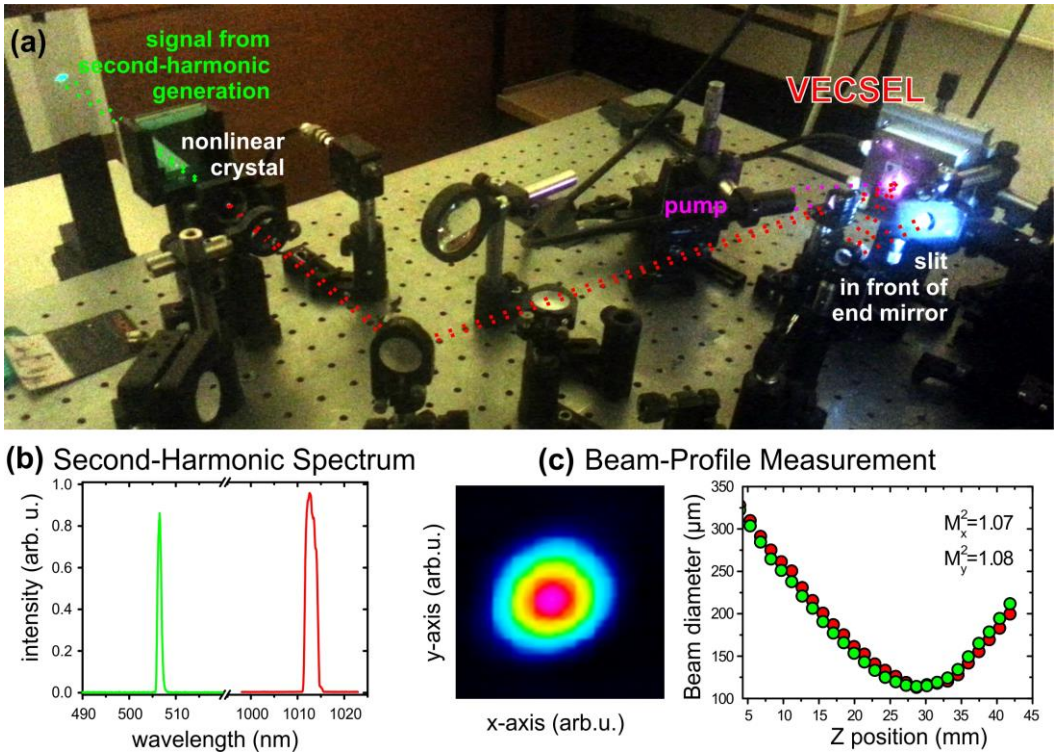


**Figure 11.** Photo of the actual setup was used for external SHG using the original laser output of SML-VECSEL. Colored dotted lines indicate the beam path inside and outside the VECSEL cavity. Top inset: Optical spectrum of SHG signal and the original laser light. Bottom inset: Beam quality measurement.

### *4.5.4. Passively harmonically SML VECSELs*

As seen in Figure 11, green light is produced via SHG with the infrared pulsed laser light. No SHG signal is observed in case of continuous-wave operation whereas a clear spectrum of the SHG signal can be measured if the laser is mode-locked. Figure 11(b) shows the

corresponding optical spectra of the frequency-doubled signal (507 nm) originating from SHG using the original laser output of SML-VECSEL (1014 nm). Figure 11(c) (left: beam profile, right: $M^2$ measurement) presents the beam quality measurement which confirm operation in the fundamental-transverse mode with $M^2$ values less than 1.1 for both axes.

In this section, we will summarize the observation of harmonic SML which was achieved with QW-VECSEL device by Gaafar et al. [74]. In that work, mode-locking was only observed for nearly discrete pump power levels in repeated investigations, up to the third harmonic. Figure 12 shows the dependence of the number of pulses circulating in the cavity on the pump power. In this chart, the error bars represent the pump power range in which a stable ML operation was accomplished.

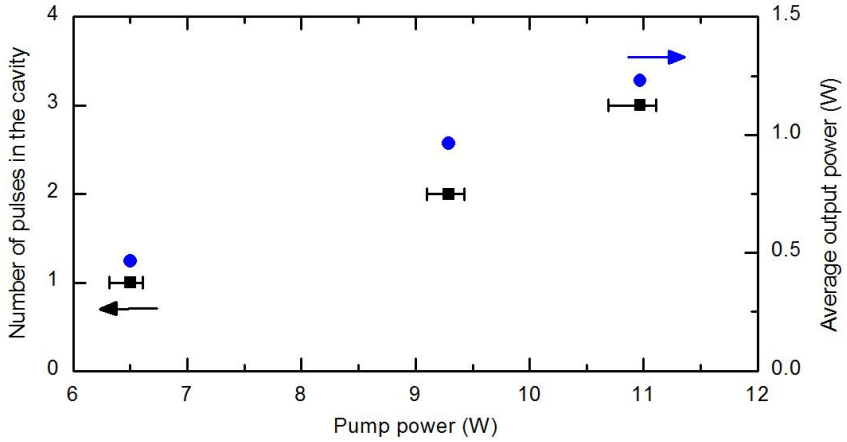


**Figure 12.** Number of pulses in the cavity (black squares, left axis) and the average output power (blue circles) as a function of the optical pump power of the device.

Fundamental mode-locking is observed for the lowest pump level. With increasing the pump level, the obtained repetition rate is doubled and tripled with respect to the fundamental rate, corresponding to two and three pulses circulating in the cavity, respectively. In their observations, ML was not self-starting but can be initiated when the slit is moved or the slit width is narrowed. Figure 13 (a)–(c) present RF spectra for the SML VECSEL in the regimes of fundamental, second-harmonic and third-harmonic mode-locking, respectively. (a′)–(c′) Optical spectra and (a″)–(c″) Autocorrelation traces (black) with $sech^2$ fits (orange)

corresponding to signal shown in (a)–(c), respectively. Peak powers 948 W for the first, 752 W for the second and 754 W for the third harmonic ML has been obtained. The nearly constant peak power for the different power levels indicates that a certain intra-cavity power is needed for the underlying ML mechanism.

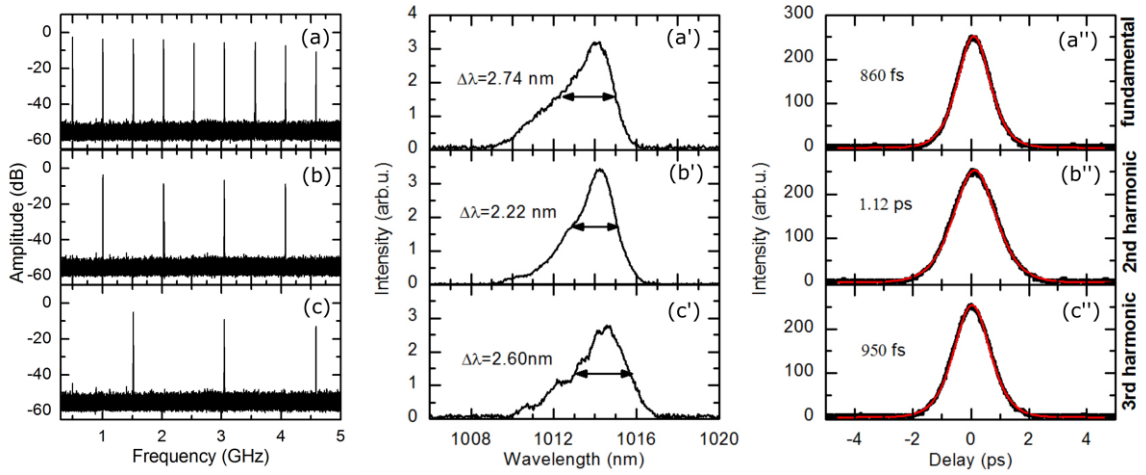


**Figure 13.** (a)–(c) RF spectra for the SML VECSEL in the regimes of fundamental, second-harmonic and third-harmonic mode-locking, respectively. (a′)–(c′) Optical spectra and (a″)–(c″) Autocorrelation traces (black) with sech² fits (orange) corresponding to signal shown in (a)–(c), respectively.

*4.5.5. Self-mode-locking with quantum-dot gain medium*

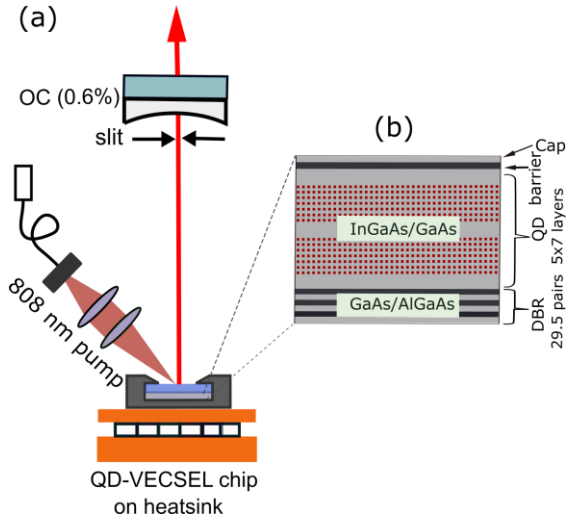


**Figure 14.** (a) Schematic drawing of the optically-pumped SML QD-VECSEL setup. (b) Structure of the QD-VECSEL chip.

The first passively SML optically-pumped QD-VECSEL has been demonstrated by Gaafar et al. in 2014 in a classical straight cavity configuration (cf Figure 14(a)) [78]. The VECSEL

chip was used composed of 35 layers of Stranski–Krastanow grown InGaAs QDs, organized as five stacks of seven QD layers. A ternary 29.5 pairs of GaAs/AlGaAs DBR was also grown. A schematic drawing of the VECSEL chip's structure is shown in Figure 14(b).

Sub-picosecond pulse duration with 750mW average output power at 1.5 GHz repetition rate has been delivered from this system. The measured autocorrelation trace representatively shown in Figure 15(a). The inset shows the corresponding optical spectrum which centered at 1038 nm. Moreover, the RF spectrum of the fundamental repetition rate is presented in Figure 15(b). The inset illustrates the RF spectrum which was measured over a span of 6.5 GHz, showing the first four harmonics.

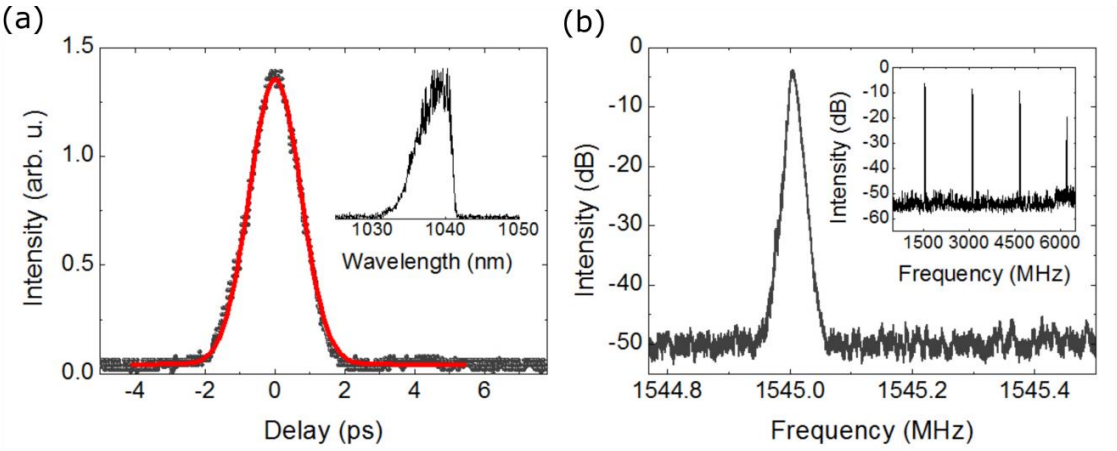


**Figure 15.** (a) Autocorrelation trace of the self-mode-locked QD-VECSEL. Black dotted: experimental data. Red line: fit curve assuming a sech2 pulse. Inset: corresponding optical spectrum. (b) Radio frequency (RF) spectrum measured over a span of 1 MHz and a resolution bandwidth (RBW) of 10 kHz. RF signal centered around 1.545 GHz. Inset: RF spectrum measured over a span of 6.5 GHz and a RBW of 100 kHz, showing the first 4 harmonics.

### 4.6. Graphene saturable absorber mode-locked VECSELs

Due to its ultrafast dynamics (<100 fs) [120, 121] and its wide bandwidth [122-124], graphene based saturable absorbers have considered as a promising saturable absorber for ultrafast pulse generation. In 2013, Zaugg et al. demonstrated for the first time a VECSEL mode-locked with a single layer GSAM [68]. In that work, they mode-locked VECSELs with

a series of different gain chips. Broad tunable operation of 46 nm wavelength range (from 935 to 981 nm) with repetition rates up to 2.48 GHz, and pulse duration down to 466 fs has been presented. However, due to the low damage threshold and the excessive non-saturable losses, the average output power was limited in the milliwatt regime. Average output power up to 26 mW with 2 ps pulses was achieved. The pulse duration and average output power for different emission wavelengths are presented in Figures 16(a) and 16(b), respectively. A tuning range up to 21 nm with a single VECSEL gain chip was achieved with the 970 nm QW VECSEL. Higher output power of up to 10 W has been demonstrated from VECSEL mode-locked with an antiresonant GSAM with low non-saturable losses and high saturation fluence [69]. However, the autocorrelation measurement shows three-peak autocorrelation trace, which suggests the multiple pulse operation. The center autocorrelation peak show a pulse width of 353 fs pulses at 1.76 GHz repetition rate and 1046 nm central wavelength.

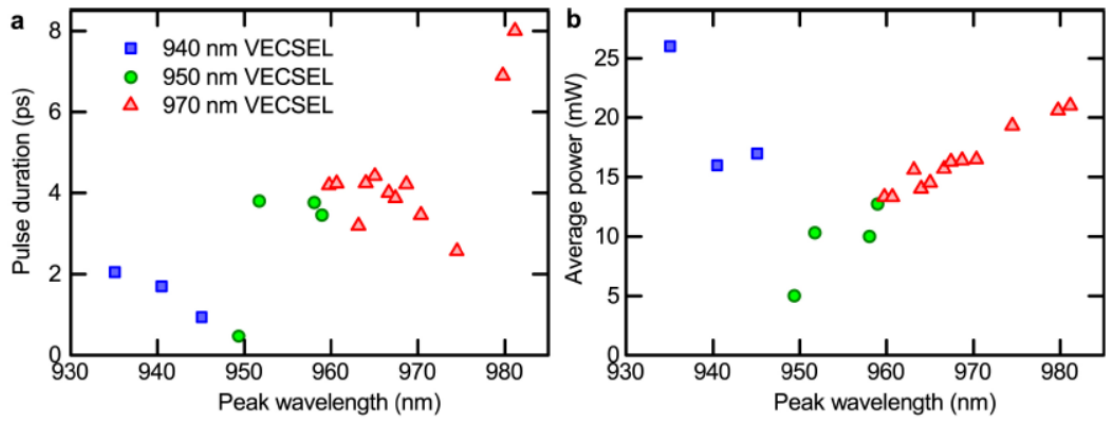


**Figure 16.** Tuning results from GSAM mode-locked VECSEL. (a) Pulse duration and (b) average output power at different emission wavelengths. Reproduced with permission.[68] Copyright 2013, Optical Society of America.

## 5. Applications and Outlook

VECSELs are wavelength-versatile lasers, which are likely suitable for different applications ranging from biophotonics [3] to optoelectronics and spectroscopy [125]. In particular, ultrafast VECSELs are of great interest for nonlinear optical microscopy of biological organisms [86], as they combine key features such as excellent beam quality, output power,

short pulse durations, amplitude stability, and can be made to operate at a large set of wavelengths, while maintaining simplicity and ease of operation. In addition, QD-based VECSELs, due to their high spectral bandwidth [2], are very promising for the development of broadly-swept tunable laser sources for non-invasive medical diagnostics such as optical coherence tomography, allowing tissue imaging with micrometer resolution [3]. Other important applications for SDLs include the generation of coherent radiation in the visible spectral region via second harmonic generation for use in laser projection display technology [126], confocal laser scanning microscopy [127] and ophthalmology [128]. The long-wavelength VECSELs in the 2-3 μm wavelength region are of great importance for remote gas sensing, as a number of atmospheric gases have strong absorption lines in this spectral region [32]. For applications in communications that demand high pulse repetition frequencies, mode-locked VECSELs can cover a wide range of repetition frequencies (from sub-100 MHz to more than 100 GHz in fundamental operation) without the Q-switching instabilities which are challenging for solid state lasers operation in this regime, i.e. with high power and a diffraction limited beam. Remarkably, mode-locked VECSELs have been also employed as a pump laser in the field of quantum optics, where single-photon emission of a QD-microlens chip at a record-high single-photon flux of 143 MHz has been achieved [129]. Further information on progress in the field of mode-locked VECSELs can also be extracted from other reviews on this topic, yet with a different emphasis, for instance focusing on the route towards sub-200-fs pulses with kW peak powers [130].

SML results taken into account in this review clearly emphasize that this quite young technique, even though the mechanism behind the effect has yet not been well understood, is capable of enabling mode-locked operation for different gain media as well as cavity configurations. We believe that mechanism behind it will allow for better improvements. Taking into account that SESAM technology is not well developed for wavelengths above 1.1 μm, the self-mode-locking technology demonstrates the advantage by allowing the

development of ultrafast VECSELs with output power ranging from a few to tens of Watts in the short-wavelength IR and mid-IR spectral range without use of a SESAM and with peak powers not constrained by the limits of intracavity fluencies and non-saturable losses on a SESAM [72]. Such a laser source potentially can find an application in laser micromachining and surface texturing field [5] where femtosecond high-power lasers are required to produce repeatable, precise features down to 10 μm in size, like holes and grooves on surfaces or structures for use in microfluidic devices and a lab-on-a-chip [131].

To omit any power amplifier and compression stages, future work in the field of ultrafast VECSELs will push the limits of mode-locked VECSELs towards 100 fs pulse durations with watt-level average output powers. As mentioned before, both 107 fs pulses [45] and several-kW peak power levels [72, 51] were indeed demonstrated, yet independently. Therefore, we believe that such combination of benchmark features in a single device will pose an important step towards practical application of mode-locked VECSELs in more and more fields, such as the coherent supercontinum generation without pulse compression and power amplifications, or material processing. Also, such development will on-top of that lead to compact and self-referenceable frequency combs.

**Acknowledgment**

The authors acknowledge financial support by the DFG (GRK 1782 and SFB 1083) and EU FP7 program through FAST-DOT project (contract No. 224338). Mahmoud Gaafar acknowledges support from the Yousef Jameel scholarship funds. The authors also would like to thank Fan Zhang, Dalia Al Nakdali, Christoph Möller, Matthias Wichmann, Mohammad Khaled Shakfa, and Bernd Heinen for fruitful discussions.

**Keywords:** mode-locked lasers, semiconductor disk lasers, self-mode-locking, vertical external-cavity surface-emitting lasers, optically-pumped semiconductor lasers.

**References**


[1] D. E. Spence, P. N. Kean, and W. Sibbett, Opt. Lett. **16**, 42–44 (1991).

[2] Ultrafast Lasers Based on Quantum Dot Structures: Physics and Devices, E. U. Rafailov, M. A. Cataluna, E. A. Avrutin, Wiley-VCH, (2011).

[3] The Physics and Engineering of Compact Quantum Dot-based Lasers for Biophotonics, E. U. Rafailov, Wiley-VCH, (2014).

[4] A. H. Zewail, Science **242**, 1645–1653 (1988).

[5] V. Markovic, A. Rohrbacher, P. Hofmann, W. Pallmann, S. Pierrot, H. Ammann, B. Resan, CLEO-Europe 2015, CA-9.1, Munich (2015).

[6] D. A. B. Miller, IEEE J. Sel. Top. Quantum Electron. **6**, 1312–1317 (2000).

[7] L. F. Mollenauer, P. V. Mamyshev, J. Gripp, M. J. Neubelt, N. Mamysheva, L. Grüner-Nielsen, and T. Veng, Opt. Lett. **25**, 704–706 (2000).

[8] M. Kuznetsov, F. Hakimi, R. Sprague, and A. Mooradian, IEEE Photon. Technol. Lett. **9**, 1063–1065 (1997).

[9] S. Hoogland, S. Dhanjal, A. C. Tropper, S. J. Roberts, R. Häring, R. Paschotta, and U. Keller, IEEE Photon. Technol. Lett. **12**, 1135–1137 (2000).

[10] O. G. Okhotnikov, Semiconductor Disk Lasers: Physics and Technology, ED. Weinheim: Wiley-VCH (2010).

[11] M. A. Hadley, G. C.Wilson, K. Y. Lau, J. S. Smith, Appl. Phys. Letters **6**3, 1607-1609 (1993).

[12] J. G. McInerney, A. Mooradian, A. Lewis, A. V. Shchegrov, E. M. Strzelecka, D. Lee, J. P. Watson, M. Liebman, G. P. Carey, B. D. Cantos, W. R. Hitchens, and D. Heald, Electron. Lett. **39**, 523-525 (2003).

[13] P. Zhao, B. Xu, R. V. Leeuwen, T. Chen, L. Watkins, D. Zhou, P. Gao, G. Xu, Q. Wang,

and C. Ghosh, Opt. Lett. **39**, 4766-4768 (2014).

[14] B. Heinen, T. L. Wang, M. Sparenberg, A. Weber, B. Kunert, J. Hader, S. W. Koch, J. V. Moloney, M. Koch, and W. Stolz, Electron. Lett. **48**, 516-517 (2012).

[15] B. Rudin, A. Rutz, M. Hoffmann, DJ. Maas, AR. Bellancourt, E. Gini, T. Südmeyer, and U. Keller, Opt. Lett. **33**, 2719-2721 (2008).

[16] F. Zhang, B. Heinen, M. Wichmann, C. Möller, B. Kunert, A. Rahimi-Iman, W. Stolz, and M. Koch, Opt. Express **22**, 12817-12822 (2014).

[17] J. Chilla, Q.-Z. Shu, H. Zhou, E. Weiss, M. Reed, and L. Spinelli, Proc. SPIE, vol. 6451, 645109-1–645109-10 (2007).

[18] E. Kantola, T. Leinonen, J-P. Penttinen, V-M. Korpijärvi, and M. Guina, Opt. Express **23**, 20280-20287 (2015).

[19] J. E. Hastie, L. G. Morton, A. J. Kemp, M. D. Dawson, A. B. Krysa, and J. S. Roberts, Appl. Phys. Lett. **89**, 061114 (2006).

[20] J. Hastie, S. Calvez, M. Dawson, T. Leinonen, A. Laakso, J. Lyytikäinen, and M. Pessa, Opt. Express **13**, 77–81 (2005).

[21] H. Lindberg, A. Strassner, E. Gerster, and A. Larsson, Electron. Lett. **40**, 601–602 (2004).

[22] M. Rahim, M. Arnold, F. Felder, K. Behfar, and H. Zogg, Appl. Phys. Lett. **91**, 151102 (2007).

[23] Y. Kaneda, J. M. Yarborough, L. Li, N. Peyghambarian, L. Fan, C. Hessenius, M. Fallahi, J. Hader, J. V. Moloney, Y. Honda, M. Nishioka, Y. Shimizu, K. Miyazono, H. Shimatani, M. Yoshimura, Y. Mori, Y. Kitaoka, and T. Sasaki, Opt. Lett. **33**, 1705–1707 (2008).

[24] E. U. Rafailov, M. A. Cataluna, and W. Sibbett, Nat. Photonics **1**, 395–401 (2007).

[25] T. Schwarzbäck, R. Bek, F. Hargart, C. A. Kessler, H. Kahle, E. Koroknay, M. Jetter, and P. Michler, Appl. Phys. Lett. **102**, 092101-1–092101-4 (2013).

[26] A. Rantamäki, J. Rautiainen, L. Toikkanen, I. Krestnikov, M. Butkus, E. U. Rafailov, and O. Okhotnikov, IEEE Photon. Technol. Lett. **24**, 1292–1294 (2012).

[27] J. A. Lott, A. R. Kovsh, N. N. Ledentsov, and D. Bimberg, Pacific Rim conference on lasers and electro-optics, CLEO/Pacific Rim 2005, pp. 160–161 (2005).

[28] M. Butkus, C.J. Hamilton, J. Rautiainen, O.G. Okhotnikov, S.S. Mikhrin, I.L. Krestnikov, and E.U. Rafailov, IET Optoelectron. **5**, 165–167 (2011).

[29] M. Butkus, J. Rautiainen, O. G. Okhotnikov, C. J. Hamilton, G. P. A. Malcolm, S. S. Mikhrin, I. L. Krestnikov, D. A. Livshits, and E. U. Rafailov, IEEE J. Sel. Top. Quantum Electron. **17**, 1763–1771 (2011).

[30] D. Al Nakdali, M. K. Shakfa, M. Gaafar, M. Butkus, K. A. Fedorova, M. Zulonas, M. Wichmann, F. Zhang, B. Heinen, A. Rahimi-Iman, W. Stolz, E. U. Rafailov, and M. Koch, IEEE Photonics Technol. Lett. **26**, 1561–1564 (2014).

[31] J. Rautiainen, I. Krestnikov, J. Nikkinen, and O. G. Okhotnikov, Opt. Lett. **35**, 1935–1937 (2010).

[32] N. Schulz, J. M. Hopkins, M. Rattunde, D. Burns, J. Wagner, Laser Photon. Rev. **2**, 160-181 (2008).

[33] S. Calvez, J. E. Hastie, M. Guina, O. G. Okhotnikov, M. D. Dawson, Laser Photon. Rev. **3**, 407-434 (2009).

[34] A.C. Tropper, and S. Hoogland, Progress in Quantum Electronics **30**, 1–43 (2006).

[35] U. Keller and A.C. Tropper, Physics Reports **429**, 67–120 (2006).

[36] R. Haring, R. Paschotta, E. Gini, F. Morier-Genoud, D. Martin, H. Melchior, and U. Keller, Electron. Lett. **37**, 766–767 (2001).

[37] A. Gamache, S. Hoogland, A. Trooper, I. Sagnes, G. Saint-Girons, and J. S. Roberts, Appl. Phys. Lett. **80**, 3892–3894 (2002).

[38] R. Haring, R. Paschotta, A. Aschwanden, E. Gini, F. Morier-Genoud, and U. Keller, IEEE J. Quantum Electron. **38**, 1268–1275 (2002).

[39] S. Hoogland, A. Garnache, I. Sagnes, J. S. Roberts, and A. C. Tropper, IEEE Photonics Technol. Lett. **17**, 267–269 (2005).

[40] O. Casel, D. Woll, M. A. Tremont, H. Fuchs, R. Wallenstein, E. Gerster, P. Unger, M. Zorn, and M. Weyers, Appl. Phys. B **81**, 443–446 (2005).

[41] H. Lindberg, M. Sadeghi, M. Westlund, S. Wang, A. Larsson, M. Strassner, and S. Marcinkevicius, Opt. Lett. **30**, 2793-2795 (2005).

[42] A. Aschwanden, D. Lorenser, H. J. Unold, R. Paschotta, E. Gini, and U. Keller, Opt. Lett. **30**, 272-274 (2005).

[43] E. J. Saarinen, A. Härkönen, R. Herda, S. Suomalainen, L. Orsila, T. Hakulinen, M. Guina, and O. G. Okhotnikov, Opt. Express **15**, 955-964 (2007).

[44] K. G. Wilcox, A. H. Quarterman, H. Beere, D. A. Ritchie, and A. C. Tropper, IEEE Photonics Technol. Lett. **22**, 1021–1023 (2010).

[45] P. Klopp, U. Griebner, M. Zorn, and M. Weyers, Appl. Phys. Lett. **98**, 071103 (2011).

[46] J. Rautiainen, J. Lyytikainen, L. Toikkanen, J. Nikkinen, A. Sirbu, A. Mereuta, A. Caliman, E. Kapon, and O. G. Okhotnikov, IEEE Photon. Tech. Lett. **22**, 748 – 750 (2010).

[47] A. Härkönen, C. Grebing, J. Paajaste, R. Koskinen, J.-P. Alanko, S. Suomalainen, G. Steinmeyer, and M. Guina, Electron. Lett. **47**, 454–456 (2011).

[48] Z. Zhao, S. Bouchoule, J. Y. Song, E. Galopin, J.-C. Harmand, J. Decobert, G. Aubin, and J.-L. Oudar, Opt. Lett. **36**, 4377–4379 (2011).

[49] M. Scheller, T. L. Wang, B. Kunert, W. Stolz, S. W. Koch, and J. V. Moloney, Electron. Lett. **48**, 588–589 (2012).

[50] R. Bek, H. Kahle, T. Schwarzbäck, M. Jetter, and P. Michler, Appl. Phys. Lett. **103**, 242101 (2013).

[51] K. G. Wilcox, A. C. Tropper, H. E. Beere, D. A. Ritchie, B. Kunert, B. Heinen, and W. Stolz, Opt. Express **21**, 1599–1605 (2013).

[52] C. A. Zaugg, A. Klenner, M. Mangold, A. S. Mayer, S. M. Link, F. Emaury, M. Golling, E. Gini, C. J. Saraceno, B. W. Tilma, and U. Keller, Opt. Express **22**, 1332–1334 (2014).

[53] D. Lorenser, H. J. Unold, D. J. H. C. Maas, A. Aschwanden, R. Grange, R. Paschotta, D. Ebling, E. Gini, and U. Keller, Appl. Phys. B **79**, 927–932 (2004).

[54] D. Lorenser, D. J. H. C. Maas, H. J. Unold, A. R. Bellancourt, B. Rudin, E. Gini, D. Ebling, and U. Keller, IEEE J. Quantum Electron. **42**, 838–847 (2006).

[55] K. G. Wilcox, M. Butkus, I. Farrer, D. A. Ritchie, A. Tropper, and E. U. Rafailov, Appl. Phys. Lett. **94**, 251105 (2009).

[56] M. Hoffmann, O. D. Sieber, D. J. H. C. Maas, V. J. Wittwer, M. Golling, T. Südmeyer, and U. Keller, Opt. Express **18**, 10143–10153 (2010).

[57] C. A. Zaugg, M. Hoffmann, W. P. Pallmann, V. J. Wittwer, O. D. Sieber, M. Mangold, M. Golling, K. J. Weingarten, B. W. Tilma, T. Südmeyer, and U. Keller, Opt. Express **20**, 27915–27921 (2012).

[58] M. Butkus, E. A. Viktorov, T. Erneux, C. J. Hamilton, G. Maker, G. P. A. Malcolm, and E. U. Rafailov, Opt. Express **21**, 25526-25531 (2013).

[59] M. Hoffmann, Y. Barbarin, D. Maas, M. Golling, I. L. Krestnikov, S. S. Mikhrin, A. R. Kovsh, T. Südmeyer, and U. Keller, Appl. Phys. B **93**, 733–736 (2008).

[60] O. D. Sieber, M. Hoffmann, V. J. Wittwer, M. Mangold, M. Golling, B. W. Tilma, T. Südmeyer, and U. Keller, Appl. Phys. B **113**, 133–145 (2013).

[61] M. Hoffmann, O. D. Sieber, V. J. Wittwer, I. L. Krestnikov, D. A. Livshits, Y. Barbarin, T. Südmeyer, and U. Keller, Opt. Express **19**, 8108–8116 (2011).

[62] R. Bek, G. Kersteen, H. Kahle, T. Schwarzbäck, M. Jetter, and P. Michler, Appl. Phys. Lett. **105**, 082107 (2014).

[63] D. J. H. C. Maas, A.-R. Bellancourt, B. Rudin, M. Golling, H. J. Unold, T. Südmeyer, and U. Keller, Appl. Phys. B **88**, 493–497 (2007).

[64] B. Rudin, V. J. Wittwer, D. J. H. C. Maas, M. Hoffmann, O. D. Sieber, Y. Barbarin, M.

Golling, T. Südmeyer, and U. Keller, Opt. Express **18**, 27582–27588 (2010).

[65] V. J. Wittwer, M. Mangold, M. Hoffmann, O. D. Sieber, M. Golling, T. Sudmeyer, and U. Keller, Electron. Lett. **48**, 1144–1145 (2012).

[66] M. Mangold, V. J. Wittwer, C. A. Zaugg, S. M. Link, M. Golling, B. W. Tilma, and U. Keller, Opt. Express **21**, 24904–24911 (2013).

[67] M. Mangold, C. A. Zaugg, S. M. Link, M. Golling, B. W. Tilma, and U. Keller, Opt. Express **22**, 6099 – 6107 (2014).

[68] C. A. Zaugg, Z. Sun, V. J. Wittwer, D. Popa, S. Milana, T. S. Kulmala, R. S. Sundaram, M. Mangold, O. D. Sieber, M. Golling, Y. Lee, J. H. Ahn, A. C. Ferrari, and U. Keller, Opt. Express **21**, 31548–31559 (2013).

[69] S. Husaini, and R. G. Bedford, Appl. Phys. Lett. **104**, 161107 (2014).

[70] K. Seger, N. Meiser, S. Y. Choi, B. H. Jung, D.-I. Yeom, F. Rotermund, O. Okhotnikov, F. Laurell, and V. Pasiskevicius, Opt. Express **21**, 17806–17813 (2013).

[71] Y. F. Chen, Y. C. Lee, H. C. Liang, K. Y. Lin, K. W. Su, and K. F. Huang, Opt. Lett. **36**, 4581–4583 (2011).

[72] L. Kornaszewski, G. Maker, G. P. A. Malcolm, M. Butkus, E. U. Rafailov, and C. J. Hamilton, Laser Photonics Rev. **6**, L20–L23 (2012).

[73] A. R. Albrecht, Y. Wang, M. Ghasemkhani, D. V. Seletskiy, J. G. Cederberg, and M. Sheik-Bahae, Opt. Express **21**, 28801–28808 (2013).

[74] M. Gaafar, C. Möller, M. Wichmann, B. Heinen, B. Kunert, A. Rahimi-Iman, W. Stolz, and M. Koch, Electron. Lett. **50**, 542–543 (2014).

[75] J. V. Moloney, I. Kilen, A. Bäumner, M. Scheller, and S. W. Koch, Opt. Express **22**, 6422–6427 (2014).

[76] H. C. Liang, C. H. Tsou, Y. C. Lee, K. F. Huang, and Y. F. Chen, Laser Phys. Lett. **11**, 105803 (2014).

[77] M. Gaafar, P. Richter, H. Keskin, C. Möller, M. Wichmann, W. Stolz, A. Rahimi-Iman,

and M. Koch, Opt. Express **22**, 28390–28399 (2014).

[78] M. Gaafar, D. Al Nakdali, C. Möller, K. A. Fedorova, M. Wichmann, M. K. Shakfa, F. Zhang, A. Rahimi-Iman, E. U. Rafailov, and M. Koch, Opt. Lett. **39**, 4623–4626 (2014).

[79] L. Kornaszewski, G. Maker, G. P. A. Malcolm, M. Butkus, E. U. Rafailov, and C. J. Hamilton, Laser Photonics Rev. **7**, 555–556 (2013).

[80] X. Liu, D. Du, and G. Mourou, IEEE J. Quantum Electron. **33**, 1706 (1997).

[81] Z. Mihoubi, K. G. Wilcox, S. Elsmere, A. Quarterman, R. Rungsawang, I. Farrer, H. E. Beere, D. A. Ritchie, A. Tropper, and V. Apostolopoulos, Opt. Lett. **33**, 2125-2127 (2008).

[82] K. G. Wilcox, F. Rutz, R. Wilk, H. D. Foreman, J. S. Roberts, J. Sigmund, H. L. Hartnagel, M. Koch, and A.C. Tropper, Electron. Lett. **42**, 1159 (2006).

[83] A. H. Quarterman, K. G. Wilcox, V. Apostolopoulos, Z. Mihoubi, S. P. Elsmere, I. Farrer, D. A. Ritchie, and A. C. Tropper, Nat. Photonics **3**, 729–731 (2009).

[84] C. R. Head, H.-Y. Chan, J. S. Feehan, D. P. Shepherd, S. Alam, A. C. Tropper, J. H. V. Price, and K. G. Wilcox, IEEE Photon. Technol. Lett. **25**, 464–467 (2013).

[85] A. H. Quarterman, L. E. Hooper, P. J. Mosley, and K. G. Wilcox, Opt. Express **22**, 12096-12101 (2014).

[86] R. Aviles-Espinosa, G. Filippidis, C. Hamilton, G. Malcolm, K. J. Weingarten, T. Südmeyer, Y. Barbarin, U. Keller, S. I. C. O. Santos, D. Artigas, and P. Loza-Alvarez, Biomed. Opt. Express **2**, 739–747 (2011).

[87] P. W. Juodawlkis, J. C. Twichell, G. E. Betts, J. J. Hargreaves, R. D. Younger, J. L. Wasserman, F. J. O'Donnell, K. G. Ray, and R. C. Williamson, IEEE Trans. Microw. Theory Tech. **49**, 1840–1853 (2001).

[88] H. R. Telle, G. Steinmeyer, A. E. Dunlop, J. Stenger, D. H. Sutter, and U. Keller, Appl. Phys. B **69**, 327–332 (1999).

[89] K. G. Wilcox, A. H. Quarterman, H. E. Beere, D. A. Ritchie, and A. C. Tropper, Opt.

Express **19**, 23453– 23459 (2011).

[90] O. D. Sieber, V. J. Wittwer, M. Mangold, M. Hoffmann, M. Golling, T. Südmeyer, and U. Keller, Opt. Express **19**, 23538–23543 (2011).

[91] E. J. Saarinen, R. Herda, and O. G. Okhotnikov, J. Opt. Soc. Am. B **24**, 2784 (2007).

[92] Y. K. Chen, and M. C. Wu, IEEE J. Quantum Electron. **28**, 2176–2185 (1992).

[93] D. A. Yanson, M. W. Street, S. D. McDougall, I. G. Thayne, J. H. Marsh, and E. A. Avrutin, IEEE J. Quantum Electron. **38**, 1–11 (2002).

[94] E. Yoshida, and M. Nakazawa, Electron. Lett. **32**, 1370–1372 (1996).

[95] A. H. Quarterman, A. Perevedentsev, K. G. Wilcox, V. Apostolopoulos, H. E. Beere, I. Farrer, D. A. Ritchie, and A. C. Tropper, Appl. Phys. Lett. **97**, 251101 (2010).

[96] K. G. Wilcox, A. H. Quarterman, V. Apostolopoulos, H. E. Beere, I. Farrer, D. A. Ritchie, and A. C. Tropper, Opt. Express **20**, 7040-7045 (2012).

[97] E. J. Saarinen, A. Rantamaki, A. Chamorovskiy, and O. G. Okhotnikov, Electron. Lett. **48**, 1355–1356 (2012).

[98] D. Waldburger, M. Mangold, S. M. Link, M. Golling, E. Gini, B. W. Tilma, and U. Keller, CLEO-SM3F.2, San Jose (2015).

[99] A. Strittmatter, T. D. Germann, J. Pohl, U. W. Pohl, D. Bimberg, J. Rautiainen, M. Guina and O. G. Okhotnikov, Electron. Lett. **44**, 290-291 (2008).

[100] T. D. Germann, A. Strittmatter, U. W. Pohl, D. Bimberg, J. Rautiainen, M. Guina, and O. G. Okhotnikov, Journal of Crystal Growth, **310**, 5182-5186 (2008).

[101] T. D. Germann, A. Strittmatter, J. Pohl, U. W. Pohl, D. Bimberg, J. Rautiainen, M. Guina, and O. G. Okhotnikov, Appl. Phys. Letters, **93**, 051104 (2008).

[102] M. Butkus, K. G. Wilcox, J. Rautiainen, O. G. Okhotnikov, S. S. Mikhrin, I. L. Krestnikov, A. R. Kovsh, M. Hoffmann, T. Sudmeyer, U. Keller, and E. U. Rafailov,

Opt. Lett. **34**, 1672-1674 (2009).

[103] P. J. Schlosser, J. E. Hastie, S. Calvez, A. B. Krysa, and M. D. Dawson, Opt. Express **17**, 21782-21787 (2009).

[104] J. Rautiainen, I. Krestnikov, M. Butkus, E. U. Rafailov, and O. G. Okhotnikov, Opt. Lett. **35**, 694-696 (2010).

[105] D. Al Nakdali, M. Gaafar, M. K. Shakfa, F. Zhang, M. Vaupel, K. A. Fedorova, A. Rahimi-Iman, E. U. Rafailov, and M. Koch, IEEE Photonics Technol. Lett. **27**, 1128-1131 (2015).

[106] A. R. Albrecht, T. J. Rotter, C. P. Hains, A. Stintz, J. V. Moloney, K. J. Malloy, and G. Balakrishnan, Electron. Lett. **46**, 856-857 (2010).

[107] A. A. Lagatsky, C. G. Leburn, C. T. A. Brown, W. Sibbett, S. A. Zolotovskaya, and E. U. Rafailov, Progress in Quantum Electronics **34**, 1-45 (2010).

[108] M. Butkus, G. Robertson, G. Maker, G. Malcolm, C. Hamilton, A. B. Krysa, B. J. Stevens, R. A. Hogg, Y. Qiu, T. Walther, and E. U. Rafailov, IEEE Photon. Technol. Lett. **23**, 1603-1605 (2011).

[109] M. Hoffmann, Y. Barbarin, D. J. H. C. Maas, A.-R. Bellancourt, M. Shafiei, M. Golling, T. Südmeyer, U. Keller, I. L. Krestnikov, S. S. Mikhrin, and A. R. Kovsh, CLEO JThE13, Baltimore, (2009).

[110] R. Bek, G. Kersteen, H. Kahle, T. Schwarzbäck, M. Jetter, and P. Michler, Proc. SPIE 9349, Vertical External Cavity Surface Emitting Lasers (VECSELs) V, 93490G (March 4, 2015).

[111] R. Bek, S. Baumgärtner, F. Sauter, H. Kahle, T. Schwarzbäck, M. Jetter, and P. Michler, Opt. Express **23**, 19947-19953 (2015).

[112] M. Mangold, M. Golling, E. Gini, B. W. Tilma, and U. Keller, Opt. Express **23**, 22043-22059 (2015).

[113] H. R. Chen, Y. G. Wang, C. Y. Tsai, K. H. Lin, T. Y. Chang, J. Tang, and W. F. Hsieh, Opt. Lett. **36**, 1284–1286 (2011).

[114] I. H. Baek, S. Y. Choi, H. W. Lee, W. B. Cho, V. Petrov, A. Agnesi, V. Pasiskevicius, D. I. Yeom, K. Kim, and F. Rotermund, Opt. Express **19**, 7833–7838 (2011).

[115] F. Rotermund, W. B. Cho, S. Y. Choi, I. H. Baek, J. H. Yim, S. Lee, A. Schmidt, G. Steinmeyer, U. Griebner, D.-I. Yeom, K. Kim, and V. Petrov, Quantum Electron. **42**, 663–670 (2012).

[116] M. A. Solodyankin, E. D. Obraztsova, A. S. Lobach, A. I. Chernov, A. V. Tausenev, V. I. Konov, and E. M. Dianov, Opt. Lett. **33**, 1336-1338 (2008).

[117] M. A. Chernysheva, A. A. Krylov, P. G. Kryukov, N. R. Arutyunyan, A. S. Pozharov, E. D. Obraztsova, and E. M. Dianov, Opt. Express **20**, B124-B130 (2012).

[118] M. A. Chernysheva, A. A. Krylov, N. R. Arutyunyan, A. S. Pozharov, E. D. Obraztsova, and E. M. Dianov, IEEE J. Sel. Top. Quantum Electron. **20**, 1101208 (2014).

[119] K. G. Wilcox, and A. C. Tropper, Laser Photonics Rev. **7**, 422–423 (2013).

[120] D. Brida, A. Tomadin, C. Manzoni, Y. J. Kim, A. Lombardo, S. Milana, R. R. Nair, K. S. Novoselov, A. C. Ferrari, G. Cerullo, and M. Polini, Nature Comm. **4**, 1987 (2013).

[121] A. Tomadin, D. Brida, G. Cerullo, A. C. Ferrari, and M. Polini, Phys. Rev. B **88**, 035430 (2013).

[122] F. Bonaccorso, Z. Sun, T. Hasan, and A. C. Ferrari, Nat. Photonics **4**, 611 - 622 (2010).

[123] R. R. Nair, P. Blake, A. N. Grigorenko, K. S. Novoselov, T. J. Booth, T. Stauber, N. M. R. Peres, and A. K. Geim, Science **320**, 1308 (2008).

[124] K. F. Mak, M. Y. Sfeir, Y. Wu, C. H. Lui, J. A. Misewich, and T. F. Heinz, Phys. Rev. Lett. **101**, 196405 (2008).

[125] A. Garnache, A. A. Kachanov, F. Stoeckel, and R. Houdre, Journal of the Optical Society of America B **17**, 1589-1598 (2000).

[126] A. Mooradian, and G. Niven, in: Proceedings of the International Display Workshop, LAD2-2, Otsu, Japan, (2006).

[127] E. Esposito, S. Keatings, K. Gardner, J. Harris, E. Riis, and G. McConnell, Review of Scientific Instruments **79**, 083702 (2008).

[128] S. Hilbich, W. Seelert, V. Ostroumov, C. Kannengiesser, R. v. Elm, J. Mueller, E. Weiss, H. Zhou, and J. Chilla, Proc. SPIE **6451**, Solid State Lasers XVI: Technology and Devices, 64510C (February 19, 2007)

[129] A. Schlehahn, M. Gaafar, M. Vaupel, M. Gschrey, P. Schnauber, J.-H. Schulze, S. Rodt, A. Strittmatter, A. Rahimi-Iman, T. Heindel, M. Koch, and S. Reitzenstein, Appl. Phys. Letters **107**, 041105 (2015).

[130] B. W Tilma, M. Mangold, C. A Zaugg, S. M Link, D. Waldburger, A. Klenner, A. S Mayer, E. Gini, M. Golling, and U. Keller, Light: Science & Applications **4**, e310 (2015).

[131] V. C. Coffey, Optics & Photonics News **25**, 28-35 (2014).

## 4.5 High-Power Quantum-Dot Vertical-External-Cavity Surface-Emitting Laser Exceeding 8 W

D. Al Nakdali, M. K. Shakfa, M. Gaafar, M. Butkus, K. A. Fedorova, M. Zulonas, M. Wichmann, F. Zhang,B. Heinen, A. Rahimi-Iman, W. Stolz, E. U. Rafailov, M. Koch, IEEE Photonics Technology Letters **26**, 15 (2014). DOI: 10.1109/LPT.2014.2329269.

**Abstract** We report on a record-high output power from an optically pumped quantum-dot vertical-external-cavity surface-emitting laser, optimized for high-power emission at 1040 nm. A maximum continuous-wave output power of 8.41 W is obtained at a heat sink temperature of $1.5°C$. By inserting a birefringent filter inside the laser cavity, a wavelength tuning over a range of 45 nm is achieved.

**The author's contribution**

Most of the experimental work for this publication was conducted by D. Al-Nakdali. Mohammad Khaled Shakfa and I helped to carry out the experiments in the laboratory, with other coauthors of the group in Marburg also having strongly supported the experimental achievements. The QD-VECSEL chip was designed and provided by the group of Prof. Dr. E. U. Rafailov, which is currently located at Aston University in the United Kingdom. The manuscript, which was improved by all co-authors, was primarily written by M. K. Shakfa, Dr. A. Rahimi-Iman and D. Al-Nakdali, whom I supported. All co-authors contributed with important ideas and fruitful discussions.

# High-Power Quantum-Dot Vertical-External-Cavity Surface-Emitting Laser Exceeding 8 W

Dalia Al Nakdali, Mohammad Khaled Shakfa, Mahmoud Gaafar, Mantas Butkus, Ksenia A. Fedorova, Modestas Zulonas, Matthias Wichmann, Fan Zhang, Bernd Heinen, Arash Rahimi-Iman, Wolfgang Stolz, Edik U. Rafailov, and Martin Koch

***Abstract*— We report on a record-high output power from an optically pumped quantum-dot vertical-external-cavity surface-emitting laser, optimized for high-power emission at 1040 nm. A maximum continuous-wave output power of 8.41 W is obtained at a heat sink temperature of 1.5 °C. By inserting a birefringent filter inside the laser cavity, a wavelength tuning over a range of 45 nm is achieved.**

***Index Terms*— Quantum-dot (QD) semiconductors, optical pumping, vertical-external-cavity surface-emitting laser (VECSEL), semiconductor disk laser (SDL), wavelength tuning.**

## I. Introduction

VERTICAL-EXTERNAL-CAVITY surface-emitting lasers (VECSELs) which are also known as semiconductor disk lasers (SDLs) have attracted much attention in recent years owing to their ability to combine high output-powers with diffraction-limited spatial beam quality and a widely accessible spectral range starting in the ultraviolet [1], [2] and reaching the mid-infrared [3], [4]. Novel structures based on quantum dots (QDs) embedded in this type of lasers [5] offer a number of the unique features such as broad gain bandwidth, ultrafast carrier dynamics, low temperature sensitivity, low threshold current and lower absorption saturation [6]. Moreover, their open architecture allows for numerous advantages such as passive modelocking using saturable absorbers [7]–[9] as well as even self-starting modelocking [10], [11] and intra-cavity frequency conversion [12]–[14]. Thus, these optically pumped systems have been employed for a variety of applications–scientific as well as industrial– such as spectroscopy, metrology, biophotonics, optical telecommunication, etc. [1], [3], [15]. It has been furthermore shown, that careful thermal management enables very high power operation for single-chip VECSELs with output powers exceeding 100 W [16]. Power scaling is also achieved by employment of multiple gain elements which can be exploited for frequency-doubled 532 nm devices with more than 60 W output power [17].

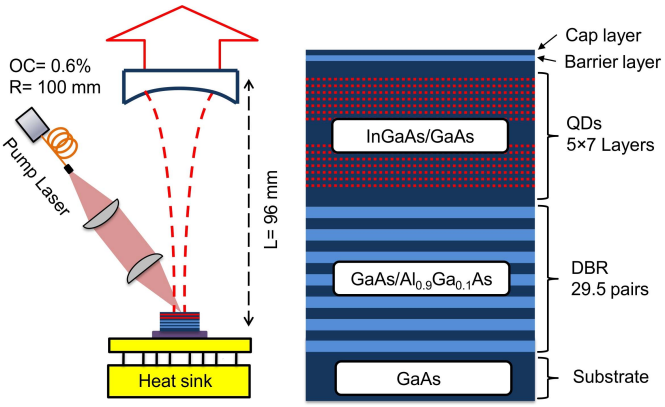


Fig. 1. Schematic illustrations of the OP-VECSEL cavity setup with a linear resonator (left), and the structure of the QD-VECSEL chip (right).

The chips constituting a VECSEL are not limited to periodic gain structures containing numerous quantum wells (QW), but also stacks of QDs layers are used which can be epitaxially grown under self-organization [18]. These QD-VECSELs provide as versatile systems as their similar QW pendants, with an even broader spectral gain and thus better tunability. However, their power output is significantly lower. Nevertheless, QD-VECSELs with up to a few Watts output power were demonstrated for various operation wavelengths in recent years; 1.39 W at 654 nm [19], 2 W at 1200 nm [20], 4.65 W at 1250 nm [21], 5.2 W at 960 nm [22], up to 4 W at 1180 nm [13], and 6 W at 1040 nm [13]. For the last two cases, wavelength tunabilities of 60 and 69 nm are reported, respectively [13].

In this letter, we report on a high performance operation of a QD-VECSEL designed for emission at 1040 nm. The output power is recorded for various pump spot widths and different heat sink temperatures. As a consequence of the optimization of the operation conditions, a maximum continuous-wave

Manuscript received April 29, 2014; revised May 24, 2014; accepted June 2, 2014. Date of publication June 5, 2014; date of current version July 15, 2014. This work was supported in part by the European Union FP7 Programme through the FAST-DOT Project under Contract 224338, and in part by the German Research Foundation through the GRK1782 Project and SFB1083 Project.

D. Al Nakdali, M. K. Shakfa, M. Gaafar, M. Wichmann, F. Zhang, B. Heinen, A. Rahimi-Iman, W. Stolz, and M. Koch are with the Department of Physics and Material Sciences Center, Philipps-University of Marburg, Marburg 35032, Germany (e-mail: dalia.alnakdali@physik.uni-marburg.de; m.k.shakfa@gmx.de; mahmoud.gaafar@physik.uni-marburg.de; matthias.wichmann@physik.unimarburg.de; fan.zhang@physik.uni-marburg.de; bernd.heinen@physik.unimarburg.de; a.r-i@physik.uni-marburg.de; wolfgang.stolz@physik.unimarburg.de; martin.koch@physik.uni-marburg.de).

M. Butkus is with the University of Dundee, Dundee DD1 4HN, U.K. (e-mail: mantas2butkus@gmail.com).

K. A. Fedorova, M. Zulonas, and E. U. Rafailov are with the School of Engineering and Applied Science, Aston University, Birmingham B4 7ET, U.K. (e-mail: k.fedorova@aston.ac.uk; zulonasm@aston.ac.uk; e.rafailov@aston.ac.uk).

Color versions of one or more of the figures in this letter are available online at http://ieeexplore.ieee.org.

Digital Object Identifier 10.1109/LPT.2014.2329269

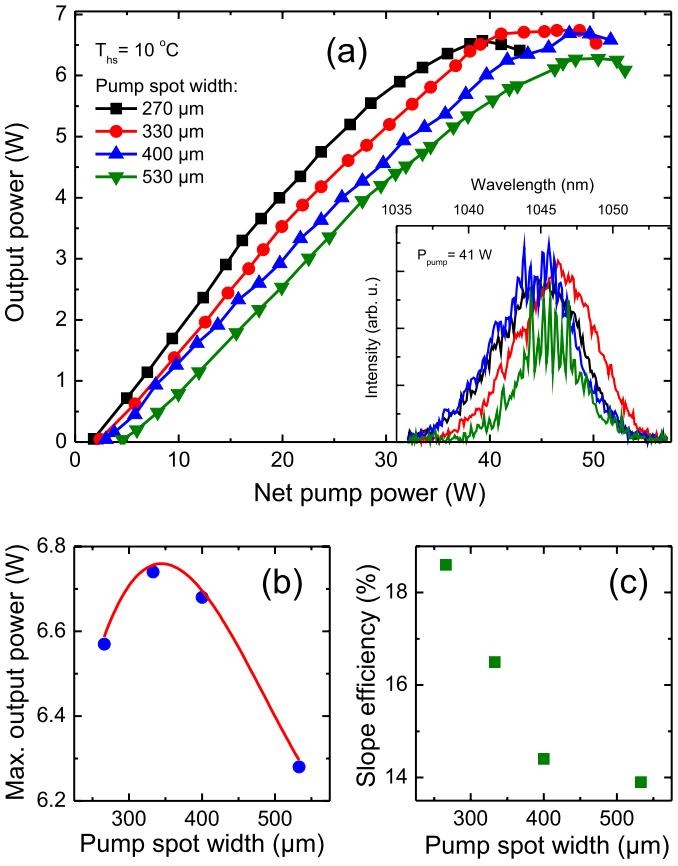


Fig. 2. (a) Input-output power characteristics for different pump spot widths, measured at a heat sink temperature ($T_{hs}$) of 1.5 °C. The inset in (a) shows the optical spectra of the laser for different pump spot widths, recorded at a net pump power ($P_{pump}$) of 41 W. (b) and (c) present the maximum (max.) output power and the slope efficiency as a function of the pump spot width, respectively. The red line in (b) serves as a guide to the eye.

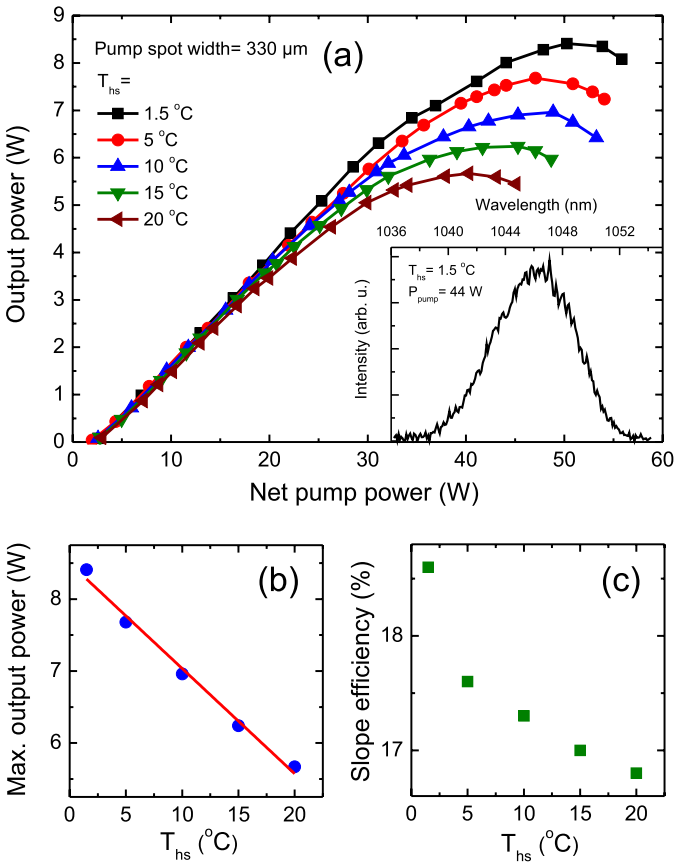


Fig. 3. (a) Input-output power characteristics for different heat sink temperatures, measured for a pump spot width of 330 $\mu$m. The inset in (a) shows the optical spectrum of the laser, recorded at a net pump power of 44 W at a heat sink temperature of 1.5 °C. (b) and (c) show the maximum output power and the slope efficiency as a function of the heat sink temperature, respectively. The red line in (b) denotes to a linear fit of the experimental data.

(CW) output power of 8.41 W is obtained for a pump spot width of 330 $\mu$m at a heat sink temperature of 1.5 °C. To our knowledge, this record output power is to date the highest reported for QD-VECSELs. Besides, a broad wavelength tunability up to 45 nm is achieved using a birefringent filter (BRF) which is inserted inside the laser cavity at Brewster's angle.

## II. Experimental Setup

The VECSEL chip structure exhibits an antiresonant design and was grown on a GaAs substrate by molecular beam epitaxy (MBE) and designed to emit at 1040 nm. After a 500-nm-GaAs buffer, a high reflectivity distributed Bragg reflector (DBR) consisting of 29.5 pairs GaAs/$Al_{0.9}Ga_{0.1}As$ is followed by the active gain medium. The latter consists of 35 layers of Stranski-Krastanow grown InGaAs QDs within GaAs spacer, organized as 5 stacks of each 7 QD layers that are placed at the standing-wave electric field maxima inside the cavity. Finally, the structure is capped by an $Al_{0.9}Ga_{0.1}As$ barrier layer followed by a GaAs layer in order to prevent surface recombination of the excited carriers and to avoid oxidation, respectively. A schematic drawing of the VECSEL chip's structure is shown on the right side of Fig. 1. The VECSEL chip is bonded to an intra-cavity diamond heat-spreader using liquid capillary bonding technique [23], which is employed for thermal management, and mounted on a Peltier-cooled copper heat sink. The excess heat, generated during operation, is dissipated via closed-cycle water cooling.

A linear cavity configuration is used in our study, as shown on the left side of Fig. 1, in which the resonator consists of the VECSEL-chip's DBR and a concave output coupler (OC) mirror with a transmittance of 0.6% and a radius of curvature of 100 mm. The choice of this OC mirror is based on previous investigations, which indicated that by varying the overall output coupling an optimum performance can be obtained. In a study of a linear cavity configuration using three different transmittances of 0.15%, 0.3% and 0.6%, respectively, the best performance was revealed using a 0.6% transmittance. In addition, the optimum performance was obtained at a value of 0.6% in a similar investigation using several OC mirrors with transmittance in the range of 0.2% to 1% in steps of 0.2% in a single-pass V-shaped cavity, wherein the chip serves as an end-mirror such as in the linear configuration. We are confident that even finer tuning of the OC transmittance could still result in an increase of performance. The OC mirror opposes the gain mirror at an optimum distance of approximately 96 mm, resulting in a maximum of the laser output power while the system is operating in a transversal multimode regime.

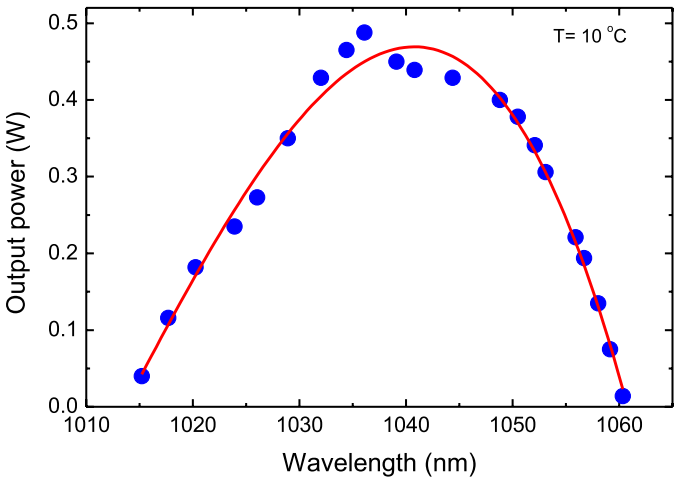


Fig. 4. Wavelength tuning characteristic, measured using a 0.6% output coupler (OC) and a birefringent filter (BRF) at a heat sink temperature of 10 °C. The BRF was inserted inside the cavity at Brewster's angle. The red curve serves as a guide to the eye.

The VECSEL chip is optically pumped (OP) by a 808-nm fiber-coupled diode laser with a maximum continuous-wave (CW) output power of 120 W. The pump laser is focused onto the VECSEL chip under an incidence angle of 35°. While the cavity-mode width at the chip's position and the OC are not changed for all measurements, the pump spot width is varied systematically between 270 $\mu$m and 530 $\mu$m in order to probe different mode matchings and power scaling effects.

## III. Results

In order to optimize the VECSEL's performance we first study the output power of the device for different pump-to-mode matchings which are given by the ratio of the pump spot width to the set cavity-mode width at the chip's position. Fig. 2(a) shows the output power as a function of the net pump power for pump spot widths ranging from 270 $\mu$m to 530 $\mu$m, measured at a heat sink temperature of 10 °C. While the thermal roll-over together with the threshold occur earlier for reduced pump spot widths, the maximum output power (before the occurrence of the thermal roll-over) exhibits a maximum for a pump spot width of 330 $\mu$m, as can be seen in Fig. 2(b). Moreover, the laser's emission wavelength near the thermal roll-over remains independent of the pump spot width (see inset in Fig. 2(a)). However, the slope efficiency, presented in Fig. 2(c), decreases when the pump spot width is increased. For pump spot widths larger than 400 $\mu$m its value remains nearly constant.

Subsequently, for a pump spot width of 330 $\mu$m, we measured the output power of the VECSEL as a function of the net pump power for different heat sink temperatures corresponding to 1.5, 5, 10, 15 and 20 °C, which are plotted in Fig. 3(a). An obvious increase in the maximum output power as well as the slope efficiency is observed when the heat sink temperature is decreased, as is shown in Figs. 3(b) and (c), respectively. A maximum output power and a slope efficiency of 8.41 W and 18.6%, respectively, are recorded at a heat sink temperature of 1.5 °C. The inset in Fig. 3(a) represents the emission spectrum of the laser, which is recorded before the onset of thermal roll-over at a net pump power of 44 W and a heat sink temperature of 1.5 °C. Furthermore, the heat sink temperature dependence of the VECSEL output power is linear in this temperature range, as can be seen in Fig. 3(b), with an absolute slope of 0.15 W/°C. Hence, an output power of about 10 W could be achieved when the heat sink temperature is decreased to −10 °C.

Finally, we characterize the tunability of the output wavelength of our device. A BRF with a thickness of 1 mm is inserted inside the cavity at Brewster's angle in order to tune the wavelength. Fig. 4 shows the wavelength tuning characteristic, measured for a net pump power of 30 W and a pump spot width of 330 $\mu$m at a heat sink temperature of 10 °C. By rotating the BRF in its surface plane, the wavelength can be tuned from 1015 nm to 1060 nm, corresponding to a total range of 45 nm. In this experiment, the highest output power recorded amounts to 0.5 W at 1036 nm due to introduced optical losses.

## IV. Conclusion

To summarize, we demonstrate high-power operation of a QD-VECSEL with optical output powers exceeding 8 W at 1040 nm. The input-output characteristics feature a clear dependence on the matching of the laser mode size on the gain mirror to the pump-spot width as well as a dependence on the chips temperature. Eventually, a maximum output power is obtained in the regime of transversal multimode operation for an optimized linear cavity of 96-mm length with a pump spot width of 330 $\mu$m at 1.5 °C. Moreover, the laser is tunable over a relatively large range of 45 nm when using a birefringent filter inside the cavity.We are confident that with further optimization of our QD-VECSEL device even higher output powers could be achieved in future studies.

## Acknowledgment

The authors would like to thank Innolume GmbH for the fabrication of the VECSEL chip.

## References

[1] S. Calvez, J. E. Hastie, M. Guin, O. G. Okhotnikov, and M. D. Dawson, "Semiconductor disk lasers for the generation of visible and ultraviolet radiation," *Laser Photon. Rev.*, vol. 3, no. 5, pp. 407–434, 2009.

[2] Y. Kaneda *et al.*, "Continuous-wave single-frequency 295 nm laser source by a frequency-quadrupled optically pumped semiconductor laser," *Opt. Lett.*, vol. 34, no. 22, pp. 3511–3513, 2009.

[3] A. Garnache *et al.*, "2-2.7 $\mu$m single frequency tunable Sb-based lasers operating in CW at RT: Microcavity and external cavity VCSELs, DFB," *Proc. SPIE*, vol. 6184, pp. 61840N-1–61840N-15, Apr. 2006.

[4] N. Schulz, J.-M. Hopkins, M. Rattunde, D. Burns, and J. Wagner, "High-brightness long-wavelength semiconductor disk lasers," *Laser Photon. Rev.*, vol. 2, no. 3, pp. 160–181, 2008.

[5] M. Butkus *et al.*, "High-power quantum-dot-based semiconductor disk laser," *Opt. Lett.*, vol. 34, no. 11, pp. 1672–1674, 2009.

[6] E. U. Rafailov, M. A. Cataluna, and W. Sibbett, "Mode-locked quantum-dot lasers," *Nature Photon.*, vol. 1, no. 7, pp. 395–401, 2007.

[7] U. Keller and A. C. Tropper, "Passively modelocked surface-emitting semiconductor lasers," *Phys. Rep.*, vol. 429, no. 2, pp. 67–120, 2006.

[8] M. Scheller, T.-L. Wang, B. Kunert, W. Stolz, S. W. Koch, and J. V. Moloney, "Passively modelocked VECSEL emitting 682 fs pulses with 5.1 W of average output power," *Electron. Lett.*, vol. 48, no. 10, pp. 588–589, May 2012.

[9] M. Butkus *et al.*, "85.7 MHz repetition rate mode-locked semiconductor disk laser: Fundamental and soliton bound states," *Opt. Exp.*, vol. 21, no. 21, pp. 25526–25531, 2013.

[10] L. Kornaszewski, G. Maker, G. P. A. Malcolm, M. Butkus, E. U. Rafailov, and C. J. Hamilton, "SESAM-free mode-locked semiconductor disk laser," *Laser Photon. Rev.*, vol. 6, no. 6, pp. L20–L23, 2012.

[11] M. Gaafar *et al.*, "Harmonic self-mode-locking of optically pumped semiconductor disc laser" *Electron. Lett.*, vol. 50, no. 7, pp. 542–543, Mar. 2014.

[12] M. Scheller, J. M. Yarborough, J. V. Moloney, M. Fallahi, M. Koch, and S. W. Koch, "Room temperature continuous wave milliwatt terahertz source," *Opt. Exp.*, vol. 18, no. 26, pp. 27112–27117, 2010.

[13] M. Butkus *et al.*, "Quantum dot based semiconductor disk lasers for 1–1.3 $\mu$m," *IEEE J. Sel. Topics Quantum Electron.*, vol. 17, no. 6, pp. 1763–1771, Nov./Dec. 2011.

[14] E. Kantola, T. Leinonen, S. Ranta, M. Tavast, and M. Guina, "High-efficiency 20 W yellow VECSEL," *Opt. Exp.*, vol. 22, no. 6, pp. 6372–6380, 2014.

[15] F.-Q. Li *et al.*, "Compact 7.8-W 1-GHz-repetition-rate passively mode-locked $TEM_{00}$ Nd: $YVO_4$ laser under 880 nm diode direct-in-band pumping," *Opt. Commun.*, vol. 284, no. 19, pp. 4619–4622, 2011.

[16] B. Heinen *et al.*, "106 W continuous-wave output power from vertical-external-cavity surface-emitting laser," *Electron. Lett.*, vol. 48, no. 9, pp. 516–517, Apr. 2012.

[17] J. Chilla, Q.-Z. Shu, H. Zhou, E. Weiss, M. Reed, and L. Spinelli, "Recent advances in optically pumped semiconductor lasers," *Proc. SPIE*, vol. 6451, pp. 645109-1–645109-10, Feb. 2007.

[18] T. Germann *et al.*, "Quantum-dot semiconductor disk lasers," *J. Cryst. Growth*, vol. 310, no. 23, pp. 5182–5186, 2008.

[19] T. Schwarzbäck *et al.*, "High-power InP quantum dot based semiconductor disk laser exceeding 1.3 W," *Appl. Phys. Lett.*, vol. 102, no. 9, pp. 092101-1–092101-4, Mar. 2013.

[20] A. Rantamäki *et al.*, "Flip chip quantum-dot semiconductor disk laser at 1200 nm," *IEEE Photon. Technol. Lett.*, vol. 24, no. 15, pp. 1292–1294, Aug. 1, 2012.

[21] A. R. Albrecht *et al.*, "High-power 1.25 Â$\mu$m InAs QD VECSEL based on resonant periodic gain structure," *Proc. SPIE*, vol. 7919, pp. 791904-1–791904-6, Feb. 2011.

[22] M. Hoffmann *et al.*, "All quantum dot based femtosecond VECSEL," *Proc. SPIE*, vol. 7919, pp. 79190X-1–79190X-6, Feb. 2011.

[23] J. E. Hastie *et al.*, "0.5-W single transverse-mode operation of an 850-nm diode-pumped surface-emitting semiconductor laser," *IEEE Photon. Technol. Lett.*, vol. 15, no. 7, pp. 894–896, Jul. 2003.

## 4.6 High-Power Operation of Quantum-Dot Semiconductor Disk Laser at 1180 nm

D. Al Nakdali, M. Gaafar, M. K. Shakfa, , F. Zhang, M. Vaupel, K. A. Fedorova, A. Rahimi-Iman, E. U. Rafailov, M. Koch, IEEE Photonics Technology Letters, 27, 1128 (2015). DOI: 10.1109/LPT.2015.2408619.

**Abstract** In this letter, we report on a high-power operation of an optically pumped quantum-dot semiconductor disk laser designed for emission at 1180 nm. As a consequence of the optimization of the operation conditions, a record-high continuous wave output power exceeding 7 W is obtained for this wavelength at a heat-sink temperature of 2°C. A wavelength tuning over a range of 37 nm is achieved using a birefringent filter inside the cavity.

**The author's contribution**

The major experimental work in this publication was carried out by D. Al-Nakdali and me. The QD-SDL chip designed for emission at 1180 nm was provided by Prof. Dr. E. U. Rafailov's group at Aston-University in the United Kingdom. The manuscript was mainly written by Mohammad Khaled Shakfa, in cooperation with D. Al-Nakdali and me. All co-authors supported the experimental study, data evaluation and contributed with important discussions and corrections to the manuscript.

# High-Power Operation of Quantum-Dot Semiconductor Disk Laser at 1180 nm

Dalia Al Nakdali, Mahmoud Gaafar, Mohammad Khaled Shakfa, Fan Zhang, Max Vaupel, Ksenia A. Fedorova, Arash Rahimi-Iman, Edik U. Rafailov, and Martin Koch

***Abstract*— In this letter, we report on a high-power operation of an optically pumped quantum-dot semiconductor disk laser designed for emission at 1180 nm. As a consequence of the optimization of the operation conditions, a record-high continuous-wave output power exceeding 7 W is obtained for this wavelength at a heat-sink temperature of 2 °C. A wavelength tuning over a range of 37 nm is achieved using a birefringent filter inside the cavity.**

***Index Terms*— Quantum-dot (QD) semiconductors, optical pumping, semiconductor disk laser (SDL), vertical-external cavity surface-emitting laser (VECSEL), wavelength tuning.**

## I. Introduction

AMONG lasers in general, and semiconductor lasers in particular, semiconductor disk lasers (SDLs), also known as vertical-external-cavity surface-emitting lasers (VECSELs) [1], have attracted increasing attention during the last two decades in the scientific community. Beside their compactness, functionalities, and relatively low costs, SDLs are evolving as a key optoelectronic technology that can offer excellent beam quality [2], high brightness [3], and low-noise performance [4]–[6]. Furthermore, SDLs provide not only high-power multi-mode continuous-wave (CW) operation [7], [8], but also ultra-short pulsed emission [9]–[12] across a wide range of the electromagnetic spectrum, i.e, from the ultraviolet [13], [14] to the mid-infrared [15], [16]. The latter is enriched with successful exploitation of SDLs as a secondary source based on intra-cavity frequency-conversion processes. In particular, benefiting from their unique external-cavity geometry, SDLs are utilized for, e.g., the generation of higher harmonics [17], [18] and the difference frequency generation (room-temperature CW terahertz applications [19]–[21]). However, SDLs operating in the high-power regime are typically required for such non-linear intra-cavity applications.

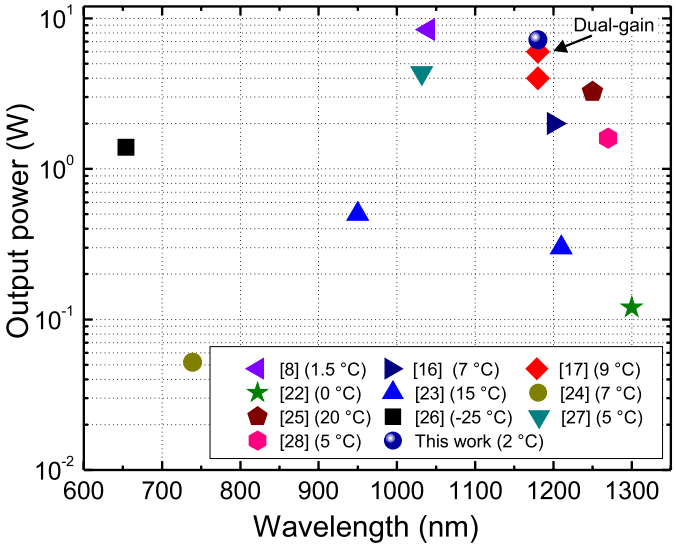


Fig. 1. Fundamental maximum continuous-wave output powers of QD-SDLs to date reported in the literature together with our present work. The corresponding temperatures are presented, each in brackets.

In this context, SDLs with quantum-dots-(QDs)-based active regions have generated an enormous amount of interest due to their potential for long-wavelength applications. In 2005, the first QD-SDL was achieved by Lott et al. [22] emitting near 1300 nm with an average output power of 120 mW. Three years later, QD-SDLs based on InAs/GaAs submonolayer (SML) and InGaAs Stranski-Krastanow (S-K) grown QDs gain material were demonstrated [23]. While for S-K samples, 300 mW output powers at 1040 nm and 1210 nm were reported, output powers of 1.4 W at 1040 nm and 0.5 W at 950 nm were achieved for SML samples. Further work led to an increase in the output power [18] and an extension of spectral coverage by QD-SDLs to red and near-infrared regions with a few tens of milliwatts at 730 nm [24] and multiwatts at 1250 nm [25], respectively. However, the highest output power for QD-SDLs has been recently obtained to be 8.4 W at 1040 nm [8]. A summary of remarkable fundamental maximum CW output powers of QD-SDLs to date is shown in Fig. 1.

In this letter, we report on a high-power operation of an optically pumped SDL based on (InGa)As S-K grown quantum dots and designed for emission at 1180 nm. The impact of the laser-cavity's parameters, i.e., the cavity length, the pump-spot width, and the transmittance of the

Manuscript received December 4, 2014; revised February 17, 2015; accepted February 23, 2015. Date of publication March 3, 2015; date of current version April 29, 2015. This work was supported in part by the European Community's Seventh Framework Programme through the FAST-DOT Project under Contract 224338 and in part by the German Research Foundation under Project GRK1782.

D. Al Nakdali, M. Gaafar, M. K. Shakfa, F. Zhang, M. Vaupel, A. Rahimi-Iman, and M. Koch are with the Material Sciences Center, Department of Physics, Philipps-University of Marburg, Marburg 35037, Germany (e-mail: dalia.alnakdali@physik.unimarburg.de; mahmoud.gaafar@physik.uni-marburg.de; m.k.shakfa@gmx.de; fan.zhang@physik.uni-marburg.de; Vaupelm4@students.uni-marburg.de; a.r-i@physik.uni-marburg.de; martin.koch@physik.uni-marburg.de).

K. A. Fedorova and E. U. Rafailov are with the School of Engineering and Applied Science, Aston University, Aston Triangle, Birmingham B4 7ET, U.K. (e-mail: k.fedorova@aston.ac.uk; e.rafailov@aston.ac.uk).

Color versions of one or more of the figures in this letter are available online at http://ieeexplore.ieee.org.

Digital Object Identifier 10.1109/LPT.2015.2408619

output-coupler (OC) mirror, on the performance of the studied device is systematically investigated to achieve the optimization of the operating conditions. For the optimized aforementioned cavity parameters, the output power is recorded at various heat-sink temperatures. While QD-SDLs at 1180 nm with 4 W and 6 W output powers were previously reported employing a single gain-chip and double gain-chips, respectively [17], [29], we have obtained – using only a single gain chip – a maximum CW output power of 7.22 W at a heat-sink temperature of 2 °C. Moreover, the wavelength tunability is performed using a birefringent filter (BRF). The latter is inserted inside the laser cavity at Brewster's angle.

## II. Experimental Setup

The structure of the SDL chip studied in the present work was grown by molecular beam epitaxy (MBE) on a semi-insulating GaAs substrate. Firstly, a highly reflective distributed Bragg (DBR) reflector consisting of 35 pairs of GaAs/AlAs layers was grown on a 500-nm-thick-GaAs buffer. The active medium was grown on the top of the DBR and consists of 39 layers of S-K grown (InGa)As QDs, which are separated by 35-nm-thick-GaAs spacers. Each QDs-layer has a thickness of 6 nm. The QDs-layers are divided into 13 groups and placed at the anti-nodes of the optical standing wave. In addition, 83.4-nm-thick-GaAs spacer layers are placed between the groups of QDs. Then, the active region is capped by an $(Al_{0.9}Ga_{0.1})As$ window confinement layer with a thickness of 50 nm in order to prevent carrier recombination at the structure's surface. Finally, a 42.6-nm-thick-GaAs layer was grown on the top of the whole structure to avoid any oxidation. The above-described structure was designed for operation in the near-infrared spectral range at a wavelength of 1180 nm. More details on the structure's design can be found in the literature [18], [30].

The SDL chip is capillary bonded to an intra-cavity diamond heat-spreader, which is employed for thermal management, and mounted on a Peltier-cooled copper heat-sink. The excess heat, generated during laser operation, is dissipated via closed-cycle water cooling. The device is operated in a standard linear-cavity configuration, in which the resonator consists of the SDL-chip's DBR and a concave OC mirror. The SDL chip is optically pumped (OP) by a 808-nm fiber-coupled diode laser with a maximum CW output power of 120 W. The pump laser is focused onto the SDL chip under an incidence angle of 30°. At the aforementioned pump launch angle, the reflectivity from the diamond top surface and from the semiconductor-diamond interface for the pump wavelength was measured to be almost 10%. In this letter, we used four OC mirrors of an equal radius of curvature of −100 mm and different transmissions of 0.15%, 0.3%, 0.7%, and 1%. Also, the pump spot width is varied systematically in order to find the optimum operation condition for obtaining high output power.

## III. Results

In spite of the emission wavelength of an SDL, a critical parameter which can significantly affect the SDL devices performance is the mode-matching, i.e, the ratio, of the pump-spot width to cavity-mode width at the chips position. Besides, the transmittance of the OC mirror should be carefully chosen for the purpose of high-power operation. The cavity-mode width is typically determined from the cavity length in the case of a linear cavity as well as $TEM_{00}$ laser mode for a given radius of curvature of the OC mirror. However, at the conditions of high-power SDL operation, a transversal multimode emission is expected [31] and, hence, the cavity-mode width cannot be directly estimated. Therefore, in the following, we introduce the impact of the variation of the cavity length, instead of the cavity-mode width, on the SDL's performance.

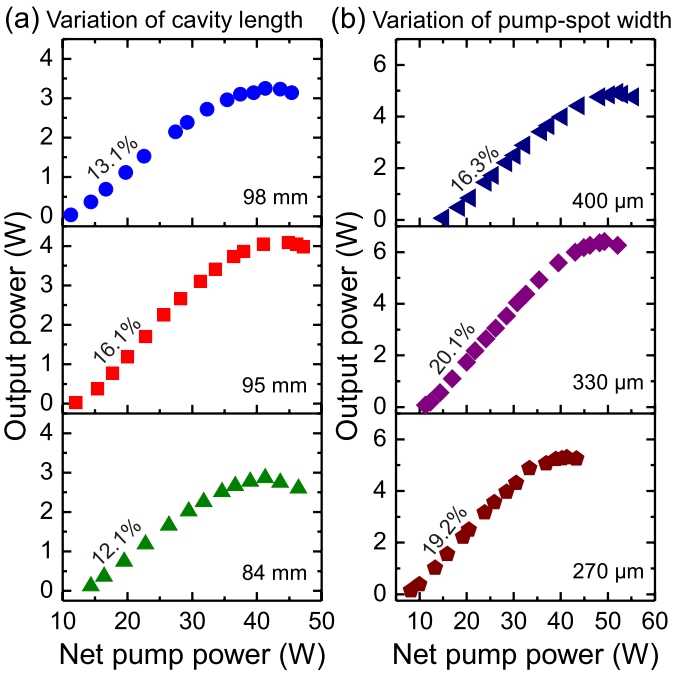


Fig. 2. (a) Output power characteristics measured for different cavity lengths, a pump-spot width of about 330 $\mu$m, and a heat-sink temperature of 15 °C. (b) Output power characteristics measured for different pump-spot widths, cavity length of 95 mm, and a heat-sink temperature of 5 °C. An OC mirror with 0.7%-transmission is used for all presented measurements. The inclined number in each subfigure in (a) as well as (b) represents the slope efficiency.

Fig. 2(a) shows the output power as a function of the net pump power for different cavity lengths and an OC mirror with a transmission of 0.7% at a heat-sink temperature of 15 °C. Here, the pump-spot width is set to about 330 $\mu$m and the cavity lengths are varied between 84 mm and 98 mm. The maximum output power of about 4.1 W, corresponding to the highest slope efficiency of 16.1%, is obtained for a cavity length of 95 mm. For the latter, on the other hand, the output power against the net pump power is shown in Fig. 2(b) for different pump-spot widths at a heat-sink temperature of 5 °C. In this case, the best performance of the studied device is observed for the pump-spot width of about 330 $\mu$m.

Next, we study the influence of the transmission of the OC mirror on the SDL's performance. Considering our above-mentioned findings, the cavity length and the pump-spot width are set to 95 mm and about 330 $\mu$m, respectively. However, the transmission of the OC mirror is varied between 0.15% and 1%. The corresponding experimental results are shown in Fig. 3, where the heat-sink temperature is set to 5 °C

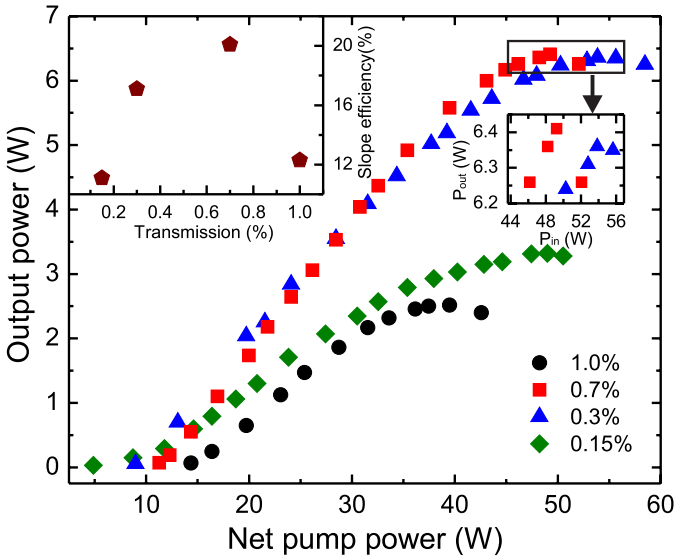


Fig. 3. Output power characteristics measured for for different OC mirrors, a pump-spot width of about 330 $\mu$m, a cavity length of 95 mm, and a heat-sink temperature of 5 °C. All OC mirrors have an equal curvature radius of −100 mm, but different transmissions. The left-hand inset shows the slope efficiency as a function of the transmission of the OC mirror. The right-hand inset shows a magnification of the encased area.

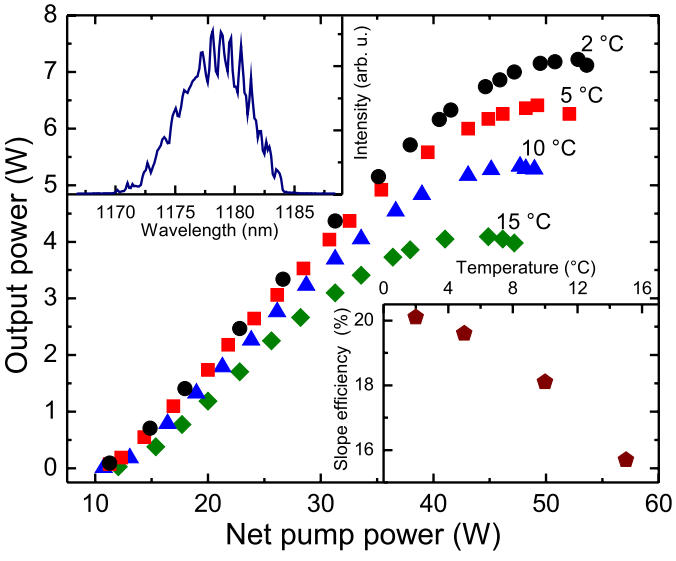


Fig. 4. Output power characteristics measured at various heat-sink temperatures for for a pump-spot width of about 330 $\mu$m, a cavity length of 95 mm, and an OC mirror with 0.7%-transmission. The bottom-right inset represents the slope efficiency as a function of the heat-sink temperature. The top-left inset shows the optical spectrum of the laser measured at an output power of 6.5 W at 2 °C.

for all measurements. Although the thermal roll-over of our device in the case of an OC mirror with 0.3%-transmission sets in later than for 0.7%, a maximum output power of 6.41 W as well as the highest slope efficiency of 20.1% is obtained for the second case, cf. the insets of Fig. 3.

Subsequently, the impact of the heat-sink temperature on the performance of our studied device is investigated. Here, the above-determined optimal parameters for our cavity are used, i.e., the cavity length of 95 mm, the pump-spot width of about 330 $\mu$m, and the OC mirror with 0.7%-transmission. A clear enhancement in the SDL's performance is observed when the heat-sink temperature is decreased from 15 °C down to 2 °C, as it is shown in Fig. 4. This is represented by the variation of the corresponding slope efficiency which is plotted against the heat-sink temperature in the bottom-right inset of Fig. 4. Remarkably, we obtain a maximum output power of 7.22 W at a heat-sink temperature of 2 °C. To our knowledge, this record output power is to date the highest reported for QD-SDLs emitting in the wavelength region of 1180 nm. However, owing to the different gain medium and chip structure, this result cannot be compared to record output powers in excess of 20 W obtained for quantum-well SDLs emitting at similar wavelengths [32]. The top-left inset of Fig. 4 shows the optical spectrum of the laser, which is centered at 1180 nm, recorded at an output power of 6.5 W and 2 °C heat-sink temperature. The distinct periodically spaced peaks in the output spectrum are caused by an etalon effect introduced by the intracavity diamond heat spreader.

Finally, in order to tune the laser wavelength of our device, an 1-mm-thick BRF is inserted inside the cavity at Brewster's angle. By rotating the BRF, the wavelength is tuned over 37 nm around its central wavelength for an OC mirror with 0.15%-transmission. This is shown in Fig. 5. The output

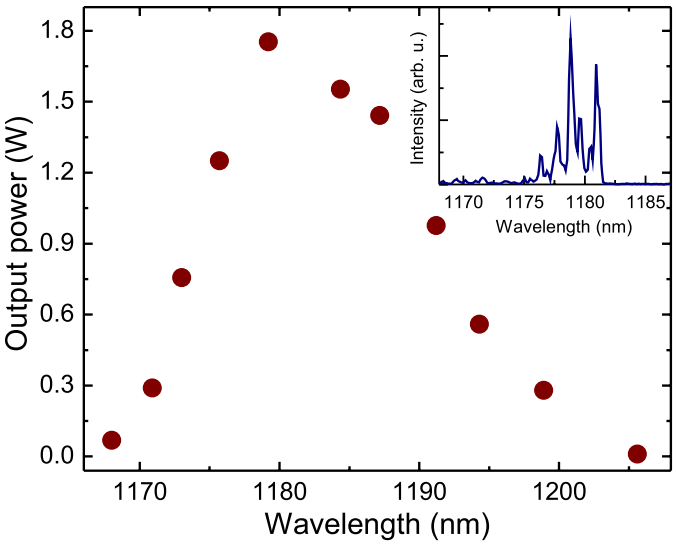


Fig. 5. Wavelength tuning characteristic measured using an 1-mm-thick BRF for an OC mirror with 0.15%-transmission at a heat-sink temperature of 10 °C. The inset shows the optical spectrum of the laser measured after having inserted the BRF inside the cavity.

power at the central wavelength is almost 1.7 W and reduced at the wings of the tuning range. An example of the optical spectrum obtained after having inserted the BRF inside the cavity is presented in the inset of Fig. 5.

## IV. Conclusion

High-power operation of an optically pumped QD-SDL emitting at 1180 nm has been demonstrated. The cavity's parameters, i.e., the cavity length, the pump-spot width, and the OC mirror's transmittance, were systematically varied in order to reach the optimal performance of the studied device.

The best performance is achieved for a cavity length of 95 mm, a pump-spot width of about 330 $\mu$m, and an OC mirror with 0.7%-transmission. The corresponding maximum continuous-wave output power up to 7.22 W is recorded at a heat-sink temperature of 2 °C. Besides, by rotating a birefringent filter inside the laser cavity, the emission wavelength became tunable over a range of 37 nm.

## ACKNOWLEDGMENT

The authors would like to thank Dr. D. A. Livshits from Innolume GmbH for the fabrication of the QD structure and Prof. O. G. Okhotnikov from Tampere University of Technology for the preparation of the VECSEL.

## REFERENCES

[1] M. Kuznetsov, F. Hakimi, R. Sprague, and A. Mooradian, "High-power (>0.5-W CW) diode-pumped vertical-external-cavity surface-emitting semiconductor lasers with circular $TEM_{00}$ beams," *IEEE Photon. Technol. Lett.*, vol. 9, no. 8, pp. 1063–1065, Aug. 1997.

[2] L. Fan *et al.*, "Over 3 W high-efficiency vertical-external-cavity surface-emitting lasers and application as efficient fiber laser pump sources," *Appl. Phys. Lett.*, vol. 86, no. 21, p. 211116, 2005.

[3] L. Fan *et al.*, "Tunable high-power high-brightness linearly polarized vertical-external-cavity surface-emitting lasers," *Appl. Phys. Lett.*, vol. 88, no. 2, p. 021105, 2006.

[4] S. Kaspar *et al.*, "Linewidth narrowing and power scaling of single-frequency 2.X $\mu$m GaSb-based semiconductor disk lasers," *IEEE J. Quantum Electron.*, vol. 49, no. 3, pp. 314–324, Mar. 2013.

[5] A. Laurain, C. Mart, J. Hader, J. V. Moloney, B. Kunert, and W. Stolz, "15 W single frequency optically pumped semiconductor laser with sub-megahertz linewidth," *IEEE Photon. Technol. Lett.*, vol. 26, no. 2, pp. 131–133, Jan. 15, 2014.

[6] F. Zhang *et al.*, "A 23-watt single-frequency vertical-external-cavity surface-emitting laser," *Opt. Exp.*, vol. 22, no. 11, pp. 12817–12822, Jun. 2014.

[7] B. Heinen *et al.*, "106 W continuous-wave output power from vertical-external-cavity surface-emitting laser," *Electron. Lett.*, vol. 48, no. 9, pp. 516–517, Apr. 2012.

[8] D. Al Nakdali *et al.*, "High-power quantum-dot vertical-external-cavity surface-emitting laser exceeding 8 W," *IEEE Photon. Technol. Lett.*, vol. 26, no. 15, pp. 1561–1564, Aug. 1, 2014.

[9] U. Keller and A. C. Tropper, "Passively modelocked surface-emitting semiconductor lasers," *Phys. Rep.*, vol. 429, no. 2, pp. 67–120, Jun. 2006.

[10] E. U. Rafailov, M. A. Cataluna, and W. Sibbett, "Mode-locked quantum-dot lasers," *Nature Photon.*, vol. 1, no. 7, pp. 395–401, 2007.

[11] M. Gaafar *et al.*, "Self-mode-locked quantum-dot vertical-external-cavity surface-emitting laser," *Opt. Lett.*, vol. 39, no. 15, pp. 4623–4626, 2014.

[12] M. Gaafar *et al.*, "Self-mode-locking semiconductor disk laser," *Opt. Exp.*, vol. 22, no. 23, pp. 28390–28399, Nov. 2014.

[13] S. Calvez, J. E. Hastie, M. Guina, O. G. Okhotnikov, and M. D. Dawson, "Semiconductor disk lasers for the generation of visible and ultraviolet radiation," *Laser Photon. Rev.*, vol. 3, no. 5, pp. 407–434, 2009.

[14] Y. Kaneda *et al.*, "Continuous-wave single-frequency 295 nm laser source by a frequency-quadrupled optically pumped semiconductor laser," *Opt. Lett.*, vol. 34, no. 22, pp. 3511–3513, Nov. 2009.

[15] N. Schulz, J.-M. Hopkins, M. Rattunde, D. Burns, and J. Wagner, "High-brightness long-wavelength semiconductor disk lasers," *Laser Photon. Rev.*, vol. 2, no. 3, pp. 160–181, Jul. 2008.

[16] A. Rantamäki *et al.*, "Flip chip quantum-dot semiconductor disk laser at 1200 nm," *IEEE Photon. Technol. Lett.*, vol. 24, no. 15, pp. 1292–1294, Aug. 1, 2012.

[17] J. Rautiainen, I. Krestnikov, J. Nikkinen, and O. G. Okhotnikov, "2.5 W orange power by frequency conversion from a dual-gain quantum-dot disk laser," *Opt. Lett.*, vol. 35, no. 12, pp. 1935–1937, Jun. 2010.

[18] M. Butkus *et al.*, "Quantum dot based semiconductor disk lasers for 1–1.3 $\mu$m," *IEEE J. Sel. Topics Quantum Electron.*, vol. 17, no. 6, pp. 1763–1771, Nov./Dec. 2011.

[19] M. Scheller, J. M. Yarborough, J. V. Moloney, M. Fallahi, M. Koch, and S. W. Koch, "Room temperature continuous wave milliwatt terahertz source," *Opt. Exp.*, vol. 18, no. 26, pp. 27112–27117, Dec. 2010.

[20] M. Scheller *et al.*, "Heterodyne detection of intracavity generated terahertz radiation," *IEEE Trans. Terahertz Sci. Technol.*, vol. 2, no. 3, pp. 271–277, May 2012.

[21] M. Wichmann, M. Stein, A. Rahimi-Iman, S. W. Koch, and M. Koch, "Interferometric characterization of a semiconductor disk laser driven terahertz source," *J. Infr. Millim. Terahertz Waves*, vol. 35, nos. 6–7, pp. 503–508, Jul. 2014.

[22] J. A. Lott, A. R. Kovsh, N. N. Ledentsov, and D. Bimberg, "GaAs-based InAs/InGaAs quantum dot vertical cavity and vertical external cavity surface emitting lasers emitting near 1300 nm," in *Proc. Pacific Rim Conf. Lasers Electro-Opt. (CLEO/Pacific Rim)*, Aug. 2005, pp. 160–161.

[23] T. D. Germann *et al.*, "Quantum-dot semiconductor disk lasers," *J. Cryst. Growth*, vol. 310, no. 23, pp. 5182–5186, Nov. 2008.

[24] P. J. Schlosser, J. E. Hastie, S. Calvez, A. B. Krysa, and M. D. Dawson, "InP/AlGaInP quantum dot semiconductor disk lasers for CW $TEM_{00}$ emission at 716–755 nm," *Opt. Exp.*, vol. 17, no. 24, pp. 21782–21787, Nov. 2009.

[25] A. R. Albrecht *et al.*, "Multi-watt 1.25 $\mu$m quantum dot VECSEL," *Electron. Lett.*, vol. 46, no. 12, pp. 856–857, Jun. 2010.

[26] T. Schwarzbäck *et al.*, "High-power InP quantum dot based semiconductor disk laser exceeding 1.3 W," *Appl. Phys. Lett.*, vol. 102, no. 9, p. 092101, 2013.

[27] M. Butkus *et al.*, "High-power quantum-dot-based semiconductor disk laser," *Opt. Lett.*, vol. 34, no. 11, pp. 1672–1674, Jun. 2009.

[28] M. Butkus, J. Rautiainen, O. G. Okhotnikov, S. S. Mikhrin, I. L. Krestnikov, and E. U. Rafailov, "1270 nm quantum dot based semiconductor disk lasers," in *Proc. 22nd IEEE Int. Semiconductor Laser Conf. (ISLC)*, Sep. 2010, pp. 71–72.

[29] J. Rautiainen, I. Krestnikov, M. Butkus, E. U. Rafailov, and O. G. Okhotnikov, "Optically pumped semiconductor quantum dot disk laser operating at 1180 nm," *Opt. Lett.*, vol. 35, no. 5, pp. 694–696, Mar. 2010.

[30] E. U. Rafailov, Ed., *The Physics and Engineering of Compact Quantum Dot-based Lasers for Biophotonics*. Hoboken, NJ, USA: Wiley, 2013.

[31] M. Wichmann *et al.*, "Evolution of multi-mode operation in vertical-external-cavity surface-emitting lasers," *Opt. Exp.*, vol. 21, no. 26, pp. 31940–31950, Dec. 2013.

[32] S. Ranta, M. Tavast, T. Leinonen, N. Van Lieu, G. Fetzer, and M. Guina, "1180 nm VECSEL with output power beyond 20 W," *Electron. Lett.*, vol. 49, no. 1, pp. 59–60, Jan. 2013.

## 4.7 Single-photon emission at a rate of 143 MHz from a deterministic quantum-dot microlens triggered by a mode-locked vertical-external-cavity surface-emitting laser

A. Schlehahn, M. Gaafar, M. Vaupel, M. Gschrey, P. Schnauber, J.-H. Schulze, S. Rodt, A. Strittmatter, W. Stolz, A. Rahimi-Iman, T. Heindel, M. Koch, S. Reitzenstein, Applied Physics Letters 107, 041105 (2015). Doi: 10.1063/1.4927429.

**Abstract** We report on the realization of a quantum dot (QD) based single-photon source with a recordhigh single-photon emission rate. The quantum light source consists of an InGaAs QD which is deterministically integrated within a monolithic microlens with a distributed Bragg reflector as back-side mirror, which is triggered using the frequency-doubled emission of a mode-locked vertical-external-cavity surface-emitting laser (ML-VECSEL). The utilized compact and stable laser system allows us to excite the single-QD microlens at a wavelength of 508 nm with a pulse repetition rate close to 500 MHz at a pulse width of 4.2 ps. Probing the photon statistics of the emission from a single QD state at saturation, we demonstrate single-photon emission of the QD-microlens chip with $g^{(2)}(0) < 0.03$ at a record-high single-photon flux of $(143 \pm 616)$ MHz collected by the first lens of the detection system. Our approach is fully compatible with resonant excitation schemes using wavelength tunable ML-VECSELs, which will optimize the quantum optical properties of the single-photon emission in terms of photon indistinguishability.

**The author's contribution**

The study, which is the subject of this publication, was planned by Prof. Dr. S. Reitzenstein together with Dr. T. Heindel, and Dr. A. Rahimi-Iman. The experimental work was then prepared parallely in Berlin and Marburg by the two involved teams around Prof. Dr. S. Reitzenstein and Prof. Dr. M. Koch. In this context, the required VECSEL setup for ultrafast excitation of quantum-dot microlenses was designed and realized primarily by myself, with the help of M. Vaupel. The VECSEL chip was provided by Prof. Dr. W. Stolz. The quantum-dot microlenses where fabricated and characterized in Berlin in the group of Prof. Dr. S. Reitzenstein. All the experiments regarding the demonstration of single-photon emission triggered by a mode-locked VECSEL were carried out in Berlin by A. Schlehahn and me, together with the help of M. Vaupel. All co-authors contributed with important ideas and helped to discuss as well as interpret the data and to improve the manuscript, which was mainly written by Dr. T. Heindel and me.

# Single-photon emission at a rate of 143 MHz from a deterministic quantum-dot microlens triggered by a mode-locked vertical-external-cavity surface-emitting laser

A. Schlehahn,[1] M. Gaafar,[2] M. Vaupel,[2] M. Gschrey,[1] P. Schnauber,[1] J.-H. Schulze,[1] S. Rodt,[1] A. Strittmatter,[1,a)] W. Stolz,[2] A. Rahimi-Iman,[2] T. Heindel,[1,b)] M. Koch,[2] and S. Reitzenstein[1]

[1]*Institut für Festkörperphysik, Technische Universität Berlin, Berlin 10623, Germany*
[2]*Department of Physics and Materials Science Center, Philipps-Universität Marburg, 35032 Marburg, Germany*

(Received 28 May 2015; accepted 15 July 2015; published online 27 July 2015)

We report on the realization of a quantum dot (QD) based single-photon source with a record-high single-photon emission rate. The quantum light source consists of an InGaAs QD which is deterministically integrated within a monolithic microlens with a distributed Bragg reflector as back-side mirror, which is triggered using the frequency-doubled emission of a mode-locked vertical-external-cavity surface-emitting laser (ML-VECSEL). The utilized compact and stable laser system allows us to excite the single-QD microlens at a wavelength of 508 nm with a pulse repetition rate close to 500 MHz at a pulse width of 4.2 ps. Probing the photon statistics of the emission from a single QD state at saturation, we demonstrate single-photon emission of the QD-microlens chip with $g^{(2)}(0) < 0.03$ at a record-high single-photon flux of $(143 \pm 16)$ MHz collected by the first lens of the detection system. Our approach is fully compatible with resonant excitation schemes using wavelength tunable ML-VECSELs, which will optimize the quantum optical properties of the single-photon emission in terms of photon indistinguishability. © *2015 AIP Publishing LLC*. [http://dx.doi.org/10.1063/1.4927429]

A light source emitting single photons at high repetition rates is highly desirable with respect to future applications in the field of quantum information technology.[1] Single semiconductor quantum dots (QDs) turned out to be promising candidates for the realization of such non-classical light sources.[2] In particular, the engineering of electrically operated devices has been actively pursued within the nanophotonics community[3–7] and recently, even the feasibility of quantum-key distribution within a 500 m free-space experiment using electrically triggered QD single-photon sources (SPSs) has been demonstrated.[8] Using suitable pulse-generators such SPSs can be triggered electrically with frequencies up to the GHz range[9,10] in order to maximize the single photon flux. On the other hand, quasi-resonant[11,12] or strict-resonant[13–15] excitation is highly desirable with respect to the generation of indistinguishable photons due to reduced temporal jitter and dephasing. These excitation schemes, however, are not easily compatible with electrical current injection schemes[16–18] as in most cases the charge carriers are injected above-band via p-i-n diode structures. Recently, we tackled this issue by utilizing an integrated electrically driven microlaser on the same chip as the non-classical light source,[19] but a very sophisticated device technology is required in this approach. Therefore, in most quantum optics experiments QDs are excited optically using commercial laser systems based on mode-locked Ti:sapphire lasers, which offer ps- or fs-pulse-widths and can be tuned over a broad spectral range. These widely used laser systems, however, are rather bulky, expensive and most importantly have limited repetition rates of typically ~80 MHz, restricting the achievable single photon flux for a given photon extraction efficiency.

In this work, we realize an ultra-bright SPS by optically exciting a deterministically integrated single-QD microlens using a frequency-doubled mode-locked vertical-external-cavity surface-emitting laser (ML-VECSEL). The compact and stable laser system allows us to overcome the limited repetition rates of commercial mode-locked (ML) Ti:sapphire lasers and to excite the single-QD microlens with a pulse repetition rate close to 500 MHz and a pulse width of 4.2 ps at a wavelength of 508 nm. Probing the photon statistics of the emission of a single QD-state at saturation, we demonstrate single-photon emission of the QD microlens with $g^{(2)}(0) < 0.03$ at a record-high single-photon flux of $(143 \pm 16)$ MHz collected by the first lens of the detection system.

The sample used for the fabrication of deterministic QD microlenses was grown by metal-organic chemical vapor deposition on GaAs (001) substrate. After a 300 nm thick GaAs buffer layer, a distributed Bragg reflector (DBR) consisting of 23 alternating $\lambda/4$-thick layers of AlGaAs (77.0 nm) and GaAs (65.7 nm) is grown. Next, 65 nm of GaAs is deposited followed by a low-density layer of self-organized InGaAs QDs which are realized in the Stranski-Krastanow growth mode. Finally, the QDs are capped by 400 nm of GaAs. The thickness of the GaAs capping layer is optimized for the realization of microlenses with high photon

a)Present address: Abteilung für Halbleiterepitaxie, Otto-von-Guericke Universität, 39106 Magdeburg, Germany.
b)Author to whom correspondence should be addressed. Electronic mail: tobias.heindel@tu-berlin.de

 

extraction efficiency. The actual QD microlens is then fabricated deterministically onto a single pre-selected InGaAs QD via a recently established *in-situ* electron beam lithography technique.[20,21] Here, cathodoluminescence spectroscopy in combination with 3D *in-situ* electron-beam writing and subsequent plasma etching is used to precisely define a monolithic microlens on top of the pre-selected QD. The overall alignment accuracy is 34 nm.[22] The resulting QD microlenses (cf. Fig. 1(c)) feature enhanced photon extraction efficiencies as reported recently in Ref. 21.

To optically excite the QD microlens with high pulse repetition rates, we implemented a compact laser system emitting 508-nm ps-pulses based on a ML-VECSEL (see Fig. 1(a)) into a standard micro-photoluminescence ($\mu$PL) spectroscopy setup (Fig. 1(b)). The laser system itself is mainly composed of an optically pumped VECSEL chip in combination with a semiconductor saturable-absorber mirror (SESAM) and a nonlinear crystal made out of beta-barium borate (BBO) for frequency conversion via second-harmonic generation (SHG). The VECSEL chip consists of 10 (InGa)As quantum wells equally spaced by $\lambda/2$ (GaP)As barrier layers. The DBR consists of $24\frac{1}{2}$ pairs of quarter wavelength GaAs/(AlGa)As layers. Details of the semiconductor layer structure can be found in Ref. 23. Such a chip is then mounted to a water-cooled heat-sink and optically pumped by a continuous-wave (CW) diode laser emitting at 808 nm.[24,25] The frequency-doubled emission of the ML-VECSEL is coupled to the $\mu$PL setup via a cold mirror. Here, a microscope objective (MO) with a numerical aperture of 0.4 focuses the laser light onto the QD microlens,

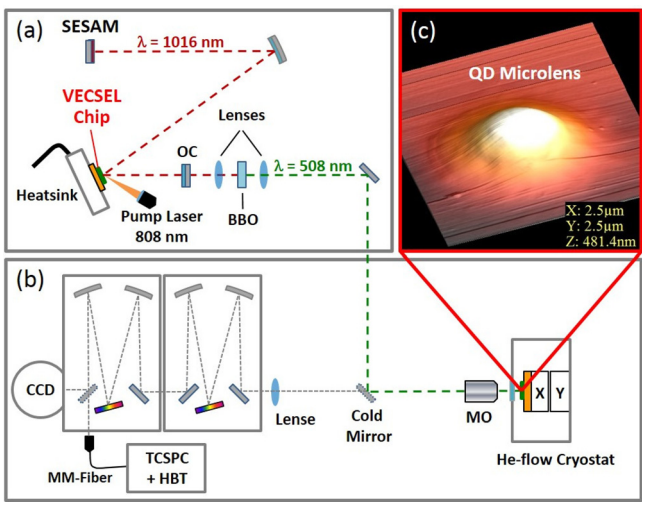


FIG. 1. Schematic of the experimental setup used to operate a quantum dot (QD) single-photon source at high repetition rates of 494 MHz using a mode-locked vertical-external-cavity surface-emitting laser (ML-VECSEL). (a) The laser system comprises an optically pumped VECSEL chip operating at 1016 nm in combination with a semiconductor saturable-absorber mirror (SESAM) and a nonlinear crystal (BBO) for second-harmonic generation of 508 nm light pulses (OC: output coupler). (b) Micro-photoluminescence setup: Emission of the QD sample is collected via a microscope objective (MO) serving as first lens of the detection system and spectrally analyzed using a double-grating spectrometer. Time-resolved and Hanbury-Brown and Twiss (HBT) type measurements can be performed at a second output port of the spectrometer. (c) Atomic force microscopy image of a QD microlens fabricated via *in-situ* 3D electron beam lithography. In the experiments, a deterministic single QD microlens with a base diameter of 2 $\mu$m acted as single-photon emitter.

which is mounted onto the cold-finger of a liquid-helium-flow cryostat for cooling the sample to a temperature of 20 K. The same MO serves as the first lens of the detection system and collects the emission of the QD-microlens chip. The collimated emission is then spectrally analyzed using a double-grating spectrometer with attached charge-coupled device (CCD) camera enabling a spectral resolution down to 25 $\mu$eV. To perform time-resolved (TR) measurements, a multi-mode (MM) fiber attached to a second output port of the spectrometer is coupled to a Si-based avalanche photodiode (APD) with a timing resolution of 40 ps. The photon statistics of the QD emission is analyzed by means of photon-autocorrelation measurements using a 50:50 MM fiber-coupled beam-splitter (BS) and two Si-APDs in a Hanbury-Brown and Twiss (HBT) type setup with an overall timing resolution of 380 ps. Both the HBT and TR setup utilize time-correlated single-photon counting (TCSPC) electronics for coincidence measurements.

Prior to single QD experiments, the utilized laser system was analyzed in terms of its spectral and temporal emission features. Fig. 2(a) displays the spectrum of the ML-VECSEL emission after SHG, which shows a full width at half maximum of 0.2 nm. The maximum output power of the laser after the BBO crystal was measured to be 5 $\mu$W. A TR measurement of the ML laser emission recorded via a Si-APD with a timing resolution of 40 ps is depicted in Fig. 2(b). Here, a pulse train with equidistant pulse separations of 2.025 ns can be observed corresponding to a pulse repetition rate of 494 MHz. The shape of a single laser pulse of the 1016 nm VECSEL emission recorded with a commercial intensity autocorrelator is shown in Fig. 2(c), which exhibits a pulse width of 4.2 ps. Next, the ML-VECSEL was used to optically excite the QD sample. Fig. 3(a) shows a $\mu$PL spectrum of a single-QD microlens under ML-VECSEL excitation at a laser power of 1.3 $\mu$W. The spectrum is dominated by the emission of the positively charged trion state $X^+$ at an emission energy of 1.335 eV. The assignment of the emission to a specific QD state was carried out via polarization and power dependent measurements as described in Ref. 26. At lower energies around 1.331 eV, the emission of other excitonic states of the same QD is visible. The exceedingly bright emission of the $X^+$ state (maximum count rate of 65 kHz per CCD-pixel) in comparison to other QD states is

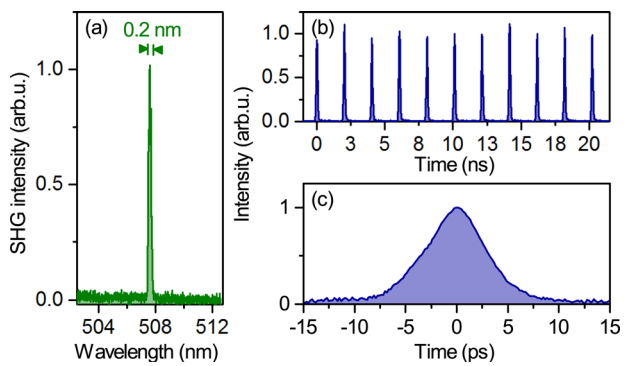


FIG. 2. (a) SHG spectrum of the frequency-doubled VECSEL emission under mode-locked operation at 494 MHz. (b) Corresponding time-resolved measurement on a laser pulse train. (c) Autocorrelation measurement of the 1016 nm VECSEL emission revealing a pulse width of 4.2 ps.

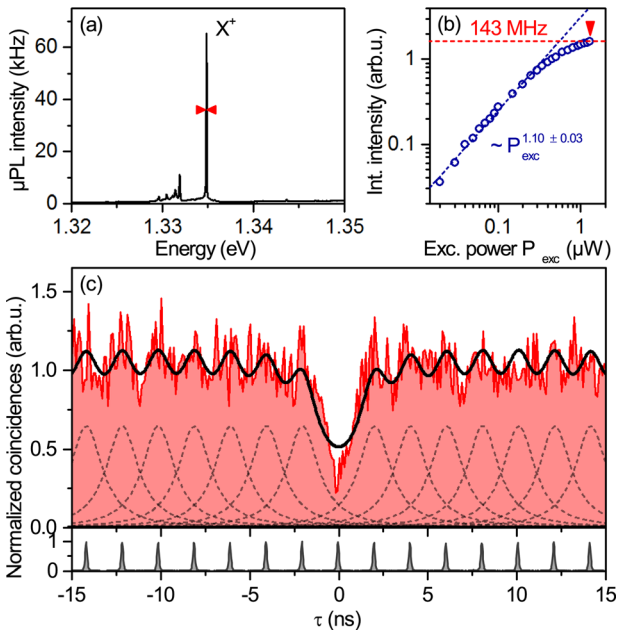


FIG. 3. Analysis of the emission of a deterministic QD microlens excited by a frequency-doubled ML-VECSEL at a repetition rate of 494 MHz. (a) $\mu$PL spectrum of the single QD microlens, revealing bright emission of a positively charged exciton state ($X^+$) at an excitation power of $P_{exc} = 1.3\,\mu$W. (b) Spectrally integrated $\mu$PL intensity of the $X^+$ emission in dependence on the ML-VECSEL excitation power. The dashed blue line corresponds to a linear fit to the experimental data. The maximum $X^+$ emission intensity is reached at 1.3 $\mu$W corresponding to saturation of the QD state (dashed horizontal line). At this working point, the single-photon flux emitted by the QD into the first lens of the setup amounts to 143 MHz. (c) Photon-autocorrelation histogram measured on the $X^+$ emission at saturation (spectral filtering is indicated by arrows in (a) as well as the working point in (b)). The coincidence data reach a minimal value of 0.22. The model curve (solid black line) reveals an upper bound to the antibunching value of $g^{(2)}(0) < 0.03$, clearly proving single-photon emission. The lower panel shows for comparison the photon-autocorrelation histogram measured on the ML-VECSEL emission.

attributed to an intrinsic p-type background doping during growth, which is typically observed in this type of QD sample.[20,26] To probe the achievable occupation of the $X^+$ state, excitation-power dependent $\mu$PL spectra have been evaluated. In Fig. 3(b), the integrated intensity of the $X^+$ emission is depicted as a function of the ML-VECSEL excitation power at 508 nm in logarithmic scaling. An almost linear excitation power dependence with a slope of $1.10 \pm 0.03$ is observed up to an excitation power of 0.3 $\mu$W. Further increasing the excitation power results in saturation of the $X^+$ state, until the maximum emission intensity is reached at $P_{exc} = 1.3\,\mu$W (indicated by red arrow in Fig. 3(b)). In order to gain insight into the photon statistics of the QD emission under these excitation conditions, we performed measurements of the second-order photon-autocorrelation $g^{(2)}(\tau)$. For this purpose, the spectrally filtered emission of the $X^+$ state (indicated by red arrows in Fig. 3(a)) was coupled to the fiber-based HBT setup. The excitation power of the ML-VECSEL was set to 1.3 $\mu$W for saturation of the QD state, resulting in a combined detection rate of 71.5 kHz at the APDs. The resulting coincidence histogram of $g^{(2)}(\tau)$ is presented in the upper panel of Fig. 3(c). A strongly reduced number of coincidences with a measured value of 0.22 can be observed at zero time delay ($\tau = 0$), which indicates single-photon emission of the QD microlens. Furthermore, coincidence maxima with a periodicity of 2.025 ns, corresponding to the pulse repetition rate of the ML-VECSEL, can be clearly identified at finite time delays. This gets even more evident by comparing the data with the $g^{(2)}(\tau)$ histogram measured directly on the frequency-doubled emission of the ML-VECSEL, which is shown as a reference in the lower panel of Fig. 3(c). The strongly overlapping coincidence peaks observed in this measurement are due to the high repetition rate of the excitation laser generating pulses with a separation close to the lifetime (~1.5 ns) of the QD state. To quantitatively extract the suppression of two-photon emission events, we modeled the data with equidistant photon pulses represented by Lorentzian profiles with 2.3 ns full-width at half maximum and a pulse separation according to the 494 MHz repetition rate of the exciting laser. The area of the pulses was assumed to be constant, except for the zero-delay peak. The fitted model function (cf. Fig. 3(c)) nicely retraces the experimental data and allows to deduce an upper bound for the antibunching of $g^{(2)}(0) < 0.03$ by dividing the area of the almost vanishing zero-delay peak by the area of the exemplarily displayed peak at finite time delay. Such strong suppression of two-photon emission events unambiguously proves the triggered emission of single-photons from the deterministic QD microlens even at saturation of the QD state.

A major advantage of using a ML-VECSEL for the excitation of a single quantum emitter, as demonstrated in this work, is given by the prospect and achievement of significantly higher excitation repetition rates compared to conventional laser systems such as Ti:sapphire lasers. To quantitatively analyze the emission of the QD microlens in terms of the single-photon flux, we experimentally determined the detection efficiency $\eta_{setup}$ of our experimental setup.[21] This was achieved by focusing a CW diode laser tuned to the emission wavelength of the $X^+$ state onto a gold mirror mounted in the cryostat. The laser was attenuated using neutral-density filters in front of the monochromator to achieve APD count-rates at the HBT setup similar to those observed for the QD emission. Taking into account the laser power, the reflection of the gold mirror, the transmission of the cryostat window, the attenuation of the density filters, and the maximal count-rates on the APDs, we determined our setup efficiency to $\eta_{setup} = (0.50 \pm 0.06) \times 10^{-3}$. The $X^+$ state excited at saturation ($P_{exc} = 1.3\,\mu$W) showed a combined detection rate on the APDs of $R_{det} = (71.5 \pm 2.0)$ kHz, which corresponds to a single-photon flux $F_{SPS}$ emitted into the microscope objective of $F_{SPS} = R_{det}/\eta_{setup} = (143 \pm 16)$ MHz. Taking into account the repetition rate of the ML-VECSEL of 494 MHz, this corresponds to a photon extraction efficiency of the deterministic single QD microlens of $(29 \pm 3)$%. The demonstrated single-photon flux of 143 MHz represents a significant improvement compared to the previous reports on SPSs based on tapered nanowires[27] as well as optically[28] and electrically[29] triggered QD micropillar cavities.

In summary, we realized an ultra-bright QD SPS by using a frequency-doubled ML-VECSEL operating at 494 MHz pulse repetition rate to excite a single QD deterministically integrated within a monolithically fabricated

microlens. This compact and long-term-stable laser system allows us to overcome the repetition rate limit of standard commercial ML Ti:sapphire lasers and to achieve record-high single-photon fluxes of $(143 \pm 16)$ MHz collected by the first lens of the setup, which corresponds to a photon extraction efficiency of $(29 \pm 3)\%$. Probing the photon statistics of the emission of a single QD-state at saturation, we demonstrate triggered single-photon emission of the microlens with $g^{(2)}(0) < 0.03$. This first proof of principle experiment carried out under above-band excitation points out the high potential of our approach, which can be extended in the future towards resonant excitation of QD-microlenses or other QD based nanophotonic devices. This could be accomplished by deterministically matching the wavelength of respective QD transitions to the emission of a ML-VECSEL, or by exploiting wavelength-tunable ML-VECSELs in the future. In this light, even the generation of indistinguishable photons at unprecedented emission rates seems to be feasible. Further improvements towards practical SPSs might include spectral tuning via piezoelectric actuators[30] or the integration of microlenses onto arrays of site-controlled QDs.[31,32] Moreover, it would be interesting to combine our approach with materials providing stable room-temperature operation,[33,34] or alternatively by utilizing compact table-top cryocoolers.[26]

This work was financially supported by the German Federal Ministry of Education and Research (BMBF) through the VIP-project QSOURCE (Grant No. 03V0630) and the German Science Foundation (Deutsche Forschungsgemeinschaft, abbreviated as DFG) within the Collaborative Research Center SFB 787 "Semiconductor Nanophotonics: Materials, Models, Devices." M. Gaafar acknowledges financial support from the Yousef Jameel scholarship funds, and W. Stolz, A. Rahimi-Iman, and M. Koch acknowledge support from the German Science Foundation (DFG: GRK 1782, SFB 1083). We gratefully acknowledge expert QD sample preparation by R. Schmidt as well as VECSEL chip processing by C. Möller, B. Heinen, and the NAsP III/V GmbH.

[1]E. Knill, R. Laflamme, and G. J. A. Milburn, Nature **409**, 46 (2001).
[2]P. Michler, A. Kiraz, C. Becher, W. V. Schoenfeld, P. M. Petroff, L. Zhang, E. Hu, and A. Imamoğlu, Science **290**, 2282 (2000).
[3]J. Kim, O. Benson, H. Kan, and Y. Yamamoto, Nature **397**, 500 (1999).
[4]Z. Yuan, B. E. Kardynal, R. M. Stevenson, A. J. Shields, C. J. Lobo, K. Cooper, N. S. Beattie, D. A. Ritchie, and M. Pepper, Science **295**, 102 (2002).
[5]D. J. P. Ellis, A. J. Bennett, S. J. Dewhurst, C. A. Nicoll, D. A. Ritchie, and A. J. Shields, New J. Phys. **10**, 043035 (2008).
[6]W. Unrau, D. Quandt, J.-H. Schulze, T. Heindel, T. D. Germann, O. Hitzemann, A. Strittmatter, S. Reitzenstein, U. Pohl, and D. Bimberg, Appl. Phys. Lett. **101**, 211119 (2012).
[7]T. Heindel, C. Schneider, M. Lermer, S. H. Kwon, T. Braun, S. Reitzenstein, S. Höfling, M. Kamp, and A. Forchel, Appl. Phys. Lett. **96**, 011107 (2010).
[8]M. Rau, T. Heindel, S. Unsleber, T. Braun, J. Fischer, S. Frick, S. Nauerth, C. Schneider, G. Vest, S. Reitzenstein, M. Kamp, A. Forchel, S. Höfling, and H. Weinfurter, New J. Phys. **16**, 043003 (2014).
[9]A. Lochmann, E. Stock, J. Töfflinger, W. Unrau, A. Toropov, A. Bakarov, V. Haisler, and D. Bimberg, Electron. Lett. **45**, 566 (2009).
[10]F. Hargart, C. A. Kessler, T. Schwarzbäck, E. Koroknay, S. Weidenfeld, M. Jetter, and P. Michler, Appl. Phys. Lett. **102**, 011126 (2013).
[11]C. Santori, D. Fattal, J. Vučković, G. S. Solomon, and Y. Yamamoto, Nature **419**, 594 (2002).
[12]P. Gold, A. Thoma, S. Maier, S. Reitzenstein, C. Schneider, S. Höfling, and M. Kamp, Phys. Rev. B **89**, 035313 (2014).
[13]A. Muller, E. B. Flagg, P. Bianucci, X. Y. Wang, D. G. Deppe, W. Ma, J. Zhang, G. J. Salamo, M. Xiao, and C. K. Shih, Phys. Rev. Lett. **99**, 187402 (2007).
[14]C. Matthiesen, A. N. Vamivakas, and M. Atatüre, Phys. Rev. Lett. **108**, 093602 (2012).
[15]Y.-M. He, Y. He, Y.-J. Wei, D. Wu, M. Atatüre, C. Schneider, S. Höfling, M. Kamp, C.-Y. Lu, and J.-W. Pan, Nat. Nanotechnol. **8**, 213 (2013).
[16]L. Turyanska, A. Baumgartner, A. Chaggar, A. Patanè, L. Eaves, and M. Henini, Appl. Phys. Lett. **89**, 092106 (2006).
[17]A. Baumgartner, E. Stock, A. Patanè, L. Eaves, M. Henini, and D. Bimberg, Phys. Rev. Lett. **105**, 257401 (2010).
[18]M. J. Conterio, N. Sköld, D. J. P. Ellis, I. Farrer, D. A. Ritchie, and A. J. Shields, Appl. Phys. Lett. **103**, 162108 (2013).
[19]P. Munnelly, T. Heindel, M. M. Karow, S. Höfling, M. Kamp, C. Schneider, and S. Reitzenstein, IEEE J. Sel. Top. Quantum Electron. **21**, 1900609 (2015).
[20]M. Gschrey, F. Gericke, A. Schüßler, R. Schmidt, J.-H. Schulze, T. Heindel, S. Rodt, A. Strittmatter, and S. Reitzenstein, Appl. Phys. Lett. **102**, 251113 (2013).
[21]M. Gschrey, A. Thoma, P. Schnauber, M. Seifried, R. Schmidt, B. Wohlfeil, L. Krüger, J.-H. Schulze, T. Heindel, S. Burger, F. Schmidt, A. Strittmatter, S. Rodt, and S. Reitzenstein, Nat. Commun. **6**, 7662 (2015).
[22]M. Gschrey, R. Schmidt, J.-H. Schulze, A. Strittmatter, S. Rodt, and S. Reitzenstein, J. Vac. Sci. Technol., B **33**, 021603 (2015).
[23]M. Gaafar, C. Möller, M. Wichmann, B. Heinen, B. Kunert, A. Rahimi-Iman, W. Stolz, and M. Koch, Electron. Lett. **50**, 542 (2014).
[24]B. Heinen, T. L. Wang, M. Sparenberg, A. Weber, B. Kunert, J. Hader, S. W. Koch, J. V. Moloney, M. Koch, and W. Stolz, Electron. Lett. **48**, 516 (2012).
[25]F. Zhang, B. Heinen, M. Wichmann, C. Möller, B. Kunert, A. Rahimi-Iman, W. Stolz, and M. Koch, Opt. Express **22**, 12817 (2014).
[26]A. Schlehahn, L. Krüger, M. Gschrey, J.-H. Schulze, S. Rodt, A. Strittmatter, T. Heindel, and S. Reitzenstein, Rev. Sci. Instrum. **86**, 013113 (2015).
[27]J. Claudon, J. Bleuse, N. S. Malik, M. Bazin, P. Jaffrennou, N. Gregersen, C. Sauvan, P. Lalanne, and J.-M. Gérard, Nat. Photonics **4**, 174–177 (2010).
[28]O. Gazzano, S. Michaelis de Vasconcellos, C. Arnold, A. Nowak, E. Galopin, I. Sagnes, L. Lanco, A. Lemaître, and P. Senellart, Nat. Commun. **4**, 1425 (2013).
[29]T. Heindel, C. Schneider, M. Lermer, S. Höfling, S. Reitzenstein, L. Worschech, and A. Forchel, J. Phys.: Conf. Ser. **245**, 012005 (2010).
[30]J. Zhang, F. Ding, E. Zallo, R. Trotta, B. Höfer, L. Han, S. Kumar, Y. Huo, A. Rastelli, and O. G. Schmidt, Nano Lett. **13**, 5808 (2013).
[31]C. Schneider, T. Heindel, A. Huggenberger, T. A. Niederstrasser, S. Reitzenstein, A. Forchel, S. Höfling, and M. Kamp, Appl. Phys. Lett. **100**, 091108 (2012).
[32]A. Strittmatter, A. Schliwa, J.-H. Schulze, T. D. Germann, A. Dreismann, O. Hitzemann, E. Stock, I. A. Ostapenko, S. Rodt, W. Unrau, U. W. Pohl, A. Hoffmann, D. Bimberg, and V. Haisler, Appl. Phys. Lett. **100**, 093111 (2012).
[33]O. Fedorych, C. Kruse, A. Ruban, D. Hommel, G. Bacher, and T. Kümmell, Appl. Phys. Lett. **100**, 061114 (2012).
[34]S. Deshpande, T. Frost, A. Hazari, and P. Bhattacharya, Appl. Phys. Lett. **105**, 141109 (2014).

## 4.8 Recent advances in the field of vertical-external-cavity surface-emitting lasers

A. Rahimi-Iman, M. Gaafar, D. Al Nakdali, C. Möller, F. Zhang, M. Wichmann, M. K. Shakfa, K. A. Fedorova, W. Stolz, E. U. Rafailov, M. Koch, in Proceedings of SPIE 9349, Vertical External Cavity Surface Emitting Lasers (VECSELs), volume 934906, (2015). DOI: 10.1117/12.2079182.

**Abstract** Vertical-external-cavity surface-emitting lasers (VECSELs) have proved to be versatile lasers which allow for various emission schemes which on the one hand include remarkably high-power multi-mode or single-frequency continuous wave operation, and on the other hand two-color as well as mode-locked emission. Particularly, the combination of semiconductor gain medium and external cavity provides a unique access to high-brightness output, a high beam quality and wavelength flexibility. Moreover, the exploitation of intra-cavity frequency conversion further extends the achievable radiation wavelength, spanning a spectral range from the UV to the THz. In this work, recent advances in the field of VECSELs are summarized and the demonstration of self-mode-locking (SML) VECSELs with sub-ps pulses is highlighted. Thereby, we present studies which were not only performed for a quantum-well-based VECSEL, but also for a quantum-dot VECSEL.

**The author's contribution**

The manuscript primarily written by me and Dr. A. Rahimi-Iman is based on recent experimental work which was performed in the research group at the Philipps-University of Marburg, with the help of our cooperation partners. The topics highlighted are mainly re-

lated to recent achievements in the course of my doctoral studies, thus I could contribute significantly to the presented results with the help of the co-authors. In this context, I contributed to the experimental work related to mode-locked VECSELs and helped to write the corresponding sections in the manuscript. All co-authors contributed to this publication and helped to write and improve the manuscript.

# Recent Advances in the Field of Vertical-External-Cavity Surface-Emitting Lasers

Arash Rahimi-Iman,*[a] Mahmoud Gaafar,[a] Dalia Al Nakdali,[a] Christoph Möller,[a] Fan Zhang,[a] Matthias Wichmann,[a] Mohammad Khaled Shakfa,[a] Ksenia A. Fedorova,[b] Wolfgang Stolz,[a,c] Edik U. Rafailov,[b] and Martin Koch[a]

[a]Department of Physics and Material Sciences Center, Philipps-Universität Marburg, Renthof 5, D-35032 Marburg, Germany;
[b]Optoelectronics and Biomedical Photonics Group, School of Engineering and Applied Science, Aston University, Aston Triangle, Birmingham B4 7ET, UK;
[c]NAsP III/V GmbH, Am Knechtacker 19, 35041 Marburg, Germany;
*arash.rahimi-iman@physik.uni-marburg.de

## ABSTRACT

Vertical-external-cavity surface-emitting lasers (VECSELs) have proved to be versatile lasers which allow for various emission schemes which on the one hand include remarkably high-power multi-mode or single-frequency continuous-wave operation, and on the other hand two-color as well as mode-locked emission. Particularly, the combination of semiconductor gain medium and external cavity provides a unique access to high-brightness output, a high beam quality and wavelength flexibility. Moreover, the exploitation of intra-cavity frequency conversion further extends the achievable radiation wavelength, spanning a spectral range from the UV to the THz. In this work, recent advances in the field of VECSELs are summarized and the demonstration of self-mode-locking (SML) VECSELs with sub-ps pulses is highlighted. Thereby, we present studies which were not only performed for a quantum-well-based VECSEL, but also for a quantum-dot VECSEL.

**Keywords:** Semiconductor disk lasers, vertical-external-cavity surface-emitting laser, self-mode-locking, mode-locked lasers.

## 1. INTRODUCTION

Vertical-external-cavity surface-emitting lasers (VECSELs), also known as semiconductor disk lasers (SDLs), are versatile lasers which serve as an excellent platform for the realization of various emission schemes. Following the first demonstration in 1997 by Kuznetsov et al. [1], a wide range of modifications and improvements towards more specific applications were conducted. Optimizations based on microscopic modeling [2] and a detailed analysis of the thermal impedance [3, 4] have pushed the output power of SDLs beyond 100W [5]. Owing to their remarkable design flexibility and features, not only the realization of high-power multi-mode [5, 6] or single-frequency [7] continuous-wave operation schemes have been pushed forward in recent years, but also the accomplishment of dual-color [8] as well as mode-locked [9, 10] operation. Moreover, in order to expand the accessible wavelength range drastically, their external resonator is well exploited for intra-cavity frequency conversion processes via nonlinear elements: while second-harmonic generation pushes the boundaries of the emission wavelength into the UV [11], terahertz frequencies can be reached by difference-frequency generation inside a two-color VECSEL [12, 13]. This is to name a few important achievements in this field.

VECSELs have particularly attracted much attention within the last decade as alternative sources of pulsed laser light, since they can typically provide both a high output power and an outstanding beam quality. The demonstration of the first mode-locked (ML) VECSEL, which was achieved by Hoogland et al. for a central wavelength of 1 μm with 22 ps long pulses [14], dates back to the year 2000 and kicked off a movement towards an entering of the fs-pulse-regime. Additionally, the exploration of pulsed operation for a variety of wavelength has been on the agenda. It did not take long

Vertical External Cavity Surface Emitting Lasers (VECSELs) V, edited by Mircea Guina, Proc. of SPIE
Vol. 9349, 934906 · © 2015 SPIE · CCC code: 0277-786X/15/$18 · doi: 10.1117/12.2079182

that VECSELs—devices which are also compact and robust—were considered becoming cost-efficient alternatives to commercial mode-locked lasers with short pulses, high peak powers and enhanced tenability.

Up-to-date, mode-locking of VECSELs required using resonator-integrated [9, 15] or chip-integrated [16] semiconductor saturable-absorber mirrors (SESAMs). Indeed, besides semiconductor materials, saturable absorbers as graphene [17, 18] and carbon nanotubes [19] have also been employed for ML operation of VECSELs. However, the power-sensitive, complex and costly absorber mirrors, which have to be carefully designed for a certain wavelength range, naturally impose limitations on the device's performance. Fortunately, on the other hand, mode-locking has also been reported to take place without any additional saturable absorber in the system—an effect called self-mode locking (SML) [20–25].

In this context, we highlight recent demonstrations of SESAM-free VECSELs which are operated under SML conditions in this work. Thereby, SML operation is not only presented for a quantum-well VECSEL [22, 25], but also for a quantum-dot device [23]. Furthermore, passively harmonically self-mode-locked devices with sub-ps-pulsed operation are shown which run at discrete power levels up to the third harmonic [22]. However, it is worth to note that the mechanism behind this effect has not been fully understood, yet, and future investigations will provide a broader picture with respect to this feature.

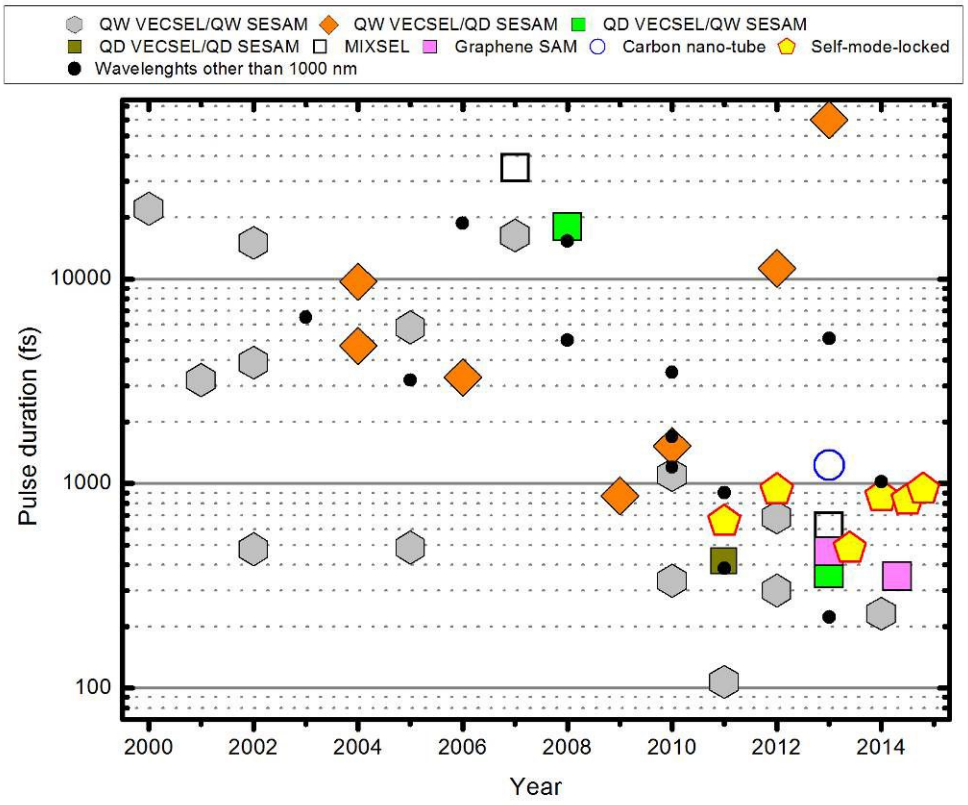


Figure 1. Pulse durations of mode-locked optically pumped VECSELs. Big symbols represent devices emitting around a wavelength of 1µm, while small black dots represent devices with wavelengths other than 1µm.

## 2. GAIN MIRROR DESIGNS

In the following, a brief overview on the design of the employed chip structures is given. *Structure 1* is a MOVPE grown VECSEL chip with 10 (InGa)As quantum wells (QWs) equally spaced by λ/2 (GaP)As barrier layers. The distributed Bragg reflector (DBR) consists of 24½ pairs of λ/4 GaAs/(AlGa)As layers and is transparent to the wavelength of the fibre-coupled 808 nm diode pump laser. The structure was grown "bottom-

up" and flip-chip bonded with Au–In solid–liquid interdiffusion onto a 350 µm-thick CVD diamond heat spreader. Originally, the chip was designed as a resonant chip and exhibits the micro-cavity resonance at the quantum well gain peak at 1010 nm. For the purpose of mode-locking, the cap layer thickness was reduced from λ/2 to λ/4 via wet etching in order to obtain an anti-resonant micro-cavity with minimized group delay dispersion (GDD) and a spectrally broadened effective gain of the structure. A schematic drawing of the VECSEL chip's structure is shown in Fig. 2(a).

*Structure 2* was grown by molecular-beam epitaxy. It consists of 35 layers of Stranski–Krastanow grown InGaAs QDs within GaAs spacers, organized as five stacks of seven QD layers. These stacks are distributed within the cavity to be located at standing-wave electric field antinodes of the optical mode for an optimum gain. As in *structure 1*, a ternary DBR was grown, which consists of 29.5 pairs of GaAs/(AlGa)As and is transparent to the wavelength of the fiber-coupled 808 nm pump laser. Both, the QDs and the DBR, are designed for an emission wavelength of 1040 nm. A schematic drawing of the VECSEL chip's structure is shown in Fig. 2(b). The VECSEL chip is capillary bonded to an intra-cavity diamond heat spreader which exhibits an anti-reflection coating. The anti-reflection coating is also minimizing the GDD at the design wavelength.

Table 1. Overview of the semiconductor disk laser gain mirrors used in this work.

| | **Structure 1** | **Structure 2** |
|---|---|---|
| **Wavelength (nm)** | 1010 | 1040 |
| **Gain type** | QW | QD |
| **Gain layers** | 10 single QWs | 35 QD layers, in stacks of 7 |
| **Mirror pairs per DBR** | 24.5 | 29.5 |
| **Resonance** | Anti-resonant | Anti-resonant |
| **Heat management** | Flip-chip bonded onto diamond heat spreader | "Top emitter" with intra-cavity diamond heat spreader |

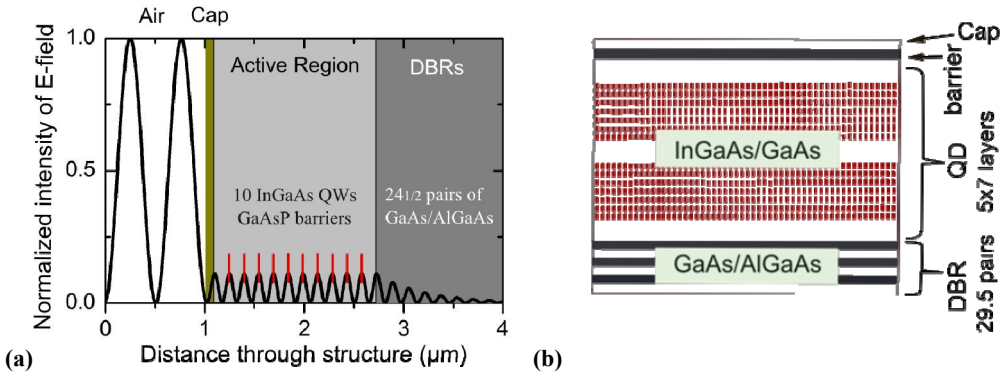


Figure 2. (a) Electric-field distribution of a standing optical wave inside the near-antiresonant gain structures normalized to the input intensity in the case of the QW-gain mirror (*structure 1*). The position of the quantum wells are represented by the vertical red lines. (b) Scheme of the QD-gain mirror structure. 5 Stacks consisting of 7 layers Stransky-Krastanow-grown QDs are incorporated into the active region of the chip (*structure 2*).

## 3. EXPERIMENTAL SETUPS

Pulsed VECSELs, similar to cw ones, employ the gain mirror in combination with an external cavity, which is defined by at least one mirror. While the cavity geometry of the presented SML VECSELs varies slightly, the principle which

allows for mode-locking remains the same, as mentioned later. Here, the laser setups for a quantum well (QW) and quantum dot (QD) VECSEL are schematically shown in Fig. 3.

As the diamond heat spreader of the QW-VECSEL is attached to the chip's DBR structure, the VECSEL chip is directly mounted on a water-cooled copper heat sink. The laser resonator can be seen as a Z-shaped cavity, which is formed by a flat output coupler (OC) with a transmittance of 1.6%, the gain chip itself, and a highly reflective (HR) curved mirror (CM) with a radius of curvature (RC) of 150 mm as well as a plane HR mirror. With a total cavity length amounting to 30 cm, a free spectral range of approximately 0.5 GHz is determined. The angle of incidence on the curved mirror was kept below 10° in order to avoid excessive astigmatism. The cavity is optimized for mode-locked operation assuming Kerr-lensing inside the VECSEL chip structure. Therefore, a variable slit is placed directly in front of the HR end mirror (cf Fig. 3(a)). An 808 nm fiber-coupled diode laser which can deliver up to 35W output power is used to pump the system.

For the QD-VECSEL setup, the copper heat sink is attached to both the outer region of the intracavity diamond heat spreader on the top of the gain mirror and the DBR structure on the reverse side of the VECSEL chip. A thermoelectric cooler is employed to extract excess heat from the copper heat sink to the closed-cycle cooling water. To complete the laser cavity, a concave (RC=100 mm) OC mirror with a transmittance of 0.6% is placed at a position 97 mm away from the gain chip. Thereby, a linear cavity is formed with a free spectral range of approximately 1 GHz. Similar to the QW-VECSEL setup, a variable slit is inserted close to the external mirror in this linear cavity (cf. Fig. 3(b)). The pump laser system is the same as used in the QW-VECSEL setup.

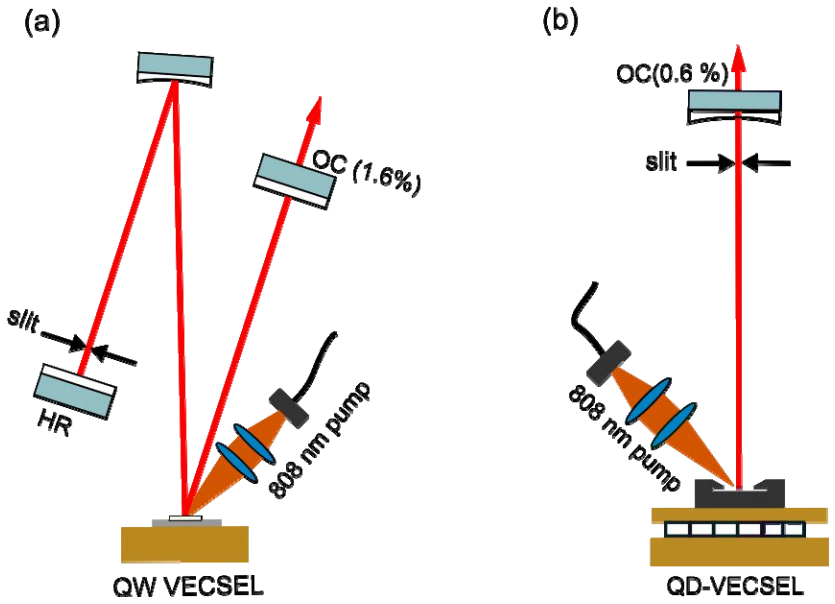


Figure 3. Schematic drawing of the setups used to realize SML (a) for a QW-VECSEL and (b) a QD-VECSEL. These two designs represent the common cavity configurations known as z-cavity and linear cavity, respectively.

## 4. RESULTS

### 4.1 Quantum well VECSEL chip

Self-mode-locking, which can be also named saturable-absorber-mirror-free mode-locking, is initiated in the VECSEL system when the slit in front of the HR end mirror is moved or the slit width is narrowed. Moreover, to stabilize SML operation, the cavity length was fine-tuned (see also [21, 22] for more details on the systems). The long-time-span pulse train of the SML QW VECSEL reveals stable operation on the microsecond scale (see Fig. 4(a)), with a repetition rate

faster, while also on the order of Ti:Sapphire oscillators: A 500-MHz repetition rate is demonstrated for the fundamental mode in a close-up of the pulse train, shown in Fig. 4(b). Another indicator of stable pulsed operation can be obtained from RF spectra, of which an example is shown in Fig. 4(c) for the signal of the fundamental repetition rate. Here, the RF linewidth is less than 30 kHz, indicating stable SML operation. The mode-locked pulse duration was measured with a self-made intensity autocorrelator with a scan range of ~130 ps. Figure 4(d) presents a long-delay autocorrelation trace for fundamental mode-locking measured with a self-made intensity autocorrelator with a scan range of ~130 ps, confirming single-pulse operation. This measurement also demonstrates the absence of a pedestal. Typical short-delay autocorrelation traces, from which pulse durations are estimated, are shown in the following section (cf. Fig. 8(a'-c')).

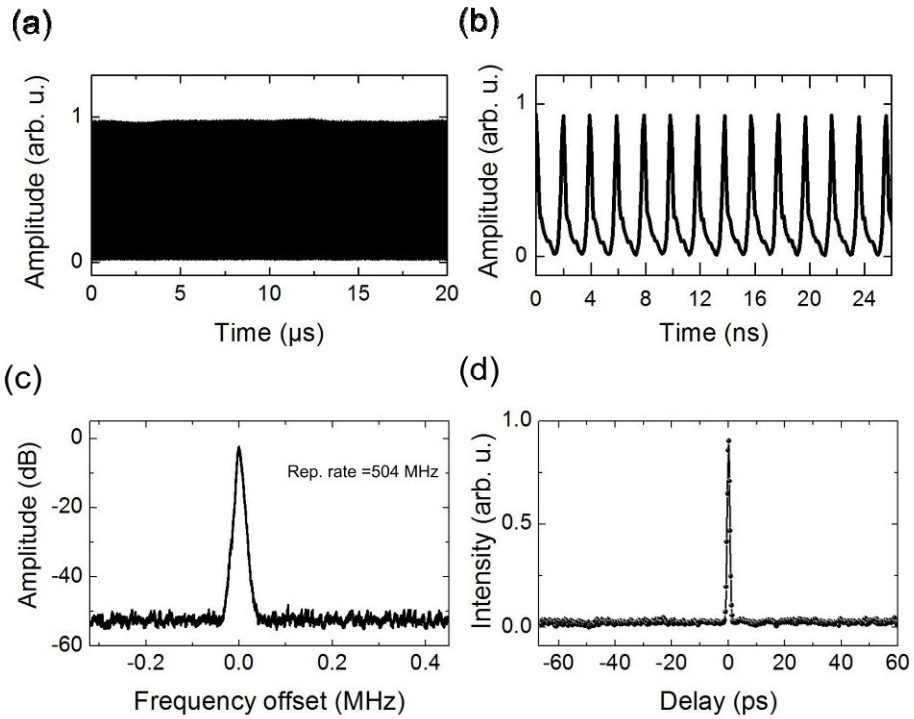


Figure 4. (a) Diagram of the long-time-span pulse train of the SML QW device. (b) A 500-MHz repetition rate is revealed for the fundamental mode in a close-up of the pulse train. (c) RF spectrum of the fundamental repetition rate. The RF linewidth is less than 30 kHz, indicating stable SML operation. (d) Single pulse operation is confirmed by a long-delay autocorrelation trace for fundamental mode-locking.

To provide further evidence of a mode-locked operation, a nonlinear frequency conversion in a BBO crystal is performed using the SML QW VECSEL. By directing the out-coupled laser beam of the VECSEL into the nonlinear crystal, green light is externally produced via second-harmonic generation (SHG) with the infrared pulsed laser light. While a clear spectrum of the SHG signal can be measured if the laser is mode-locked, in the case of continuous-wave operation no SHG signal is observed, owing to the fact that SHG is an intensity-dependent nonlinear effect. Depicted in Fig. 5, the experimental setup of the self-mode-locked QW VECSEL shows how SHG is utilized to produce green light externally. In the top inset of Fig. 5, a spectrum of the frequency-doubled SHG signal together with the spectrum of the original laser output is presented. Finally, a beam quality measurement confirms operation in the fundamental-transverse mode with $M^2$ values less than 1.1 for both axes, as shown by the bottom insets of Fig. 5 (left: beam profile, right: $M^2$ measurement). It is worth mentioning, that whenever a new mode-locking technique is demonstrated, the confirmation of mode-locked operation requires different measurements to be carried out, particularly beyond standard characterization methods which typically can't serve as an unambiguous evidence of mode-locking. Indeed, this has motivated part of our experiments and further discussion of the performed investigations and obtained results can be found in Ref. [25].

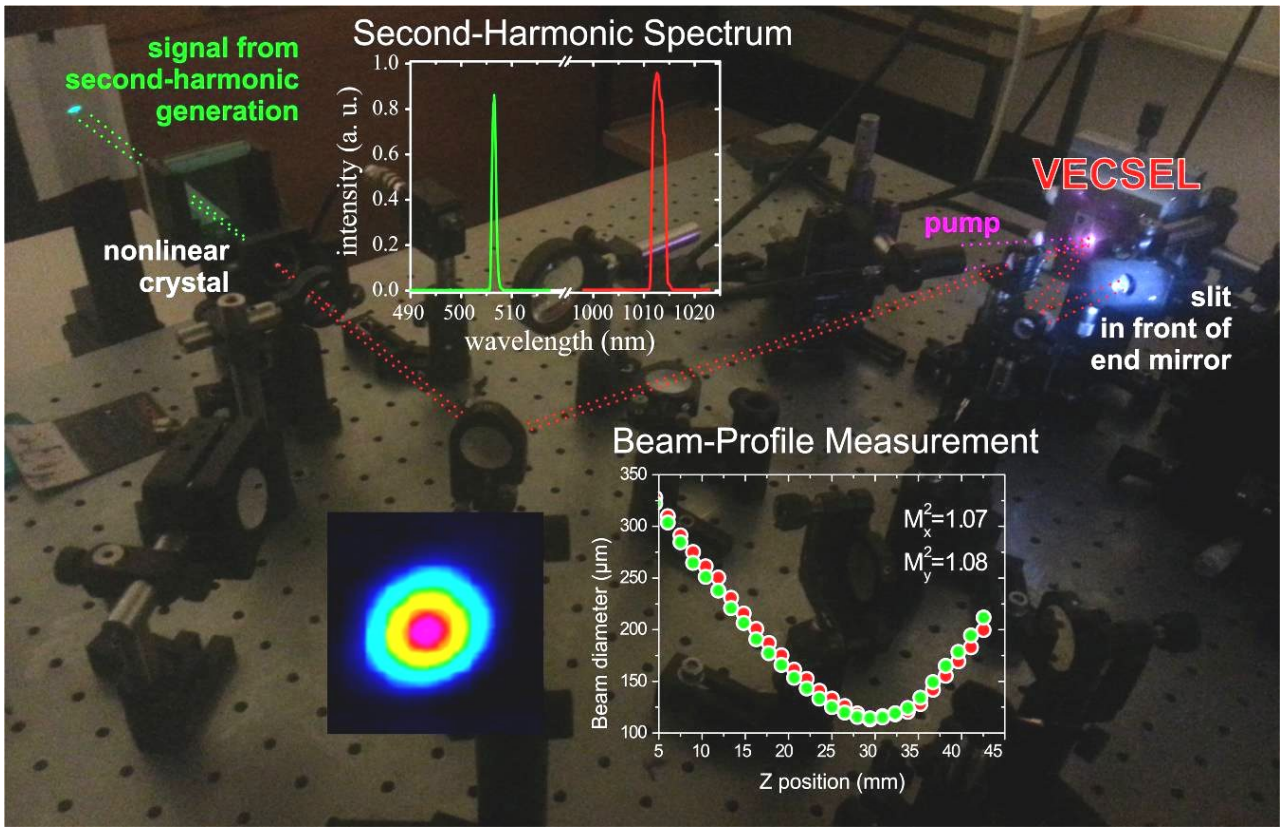


Figure 5. The experimental setup of the self-mode-locked QW VECSEL shows how second-harmonic generation is utilized to produce green light externally via the infrared pulsed laser light. Top inset: Spectrum of the frequency-doubled SHG signal and the original laser light. Bottom inset: Beam quality measurement confirming operation in fundamental-transverse mode with $M^2$ values less than 1.1 for both axes.

### 4.2 Harmonic mode-locking

Next, we want to summarize the observation of harmonic self-mode-locking which can be achieved with the presented QW device. Interestingly, mode-locking is only observed for nearly discrete pump levels. The error bars in Fig. 6 represent the pump regions in which a stable ML operation was accomplished in repeated investigations. For the lowest pump level, fundamental mode-locking is observed. For the higher pump levels the repetition rate is doubled and tripled, corresponding to two and three equally spaced pulses in a single cavity roundtrip, respectively. In our observations, ML is not self-starting but can be initiated when the slit width is narrowed or the slit is moved. However, the fundamental mode-locked operation is self-sustaining and the slit can be opened completely without disturbing the ML process. In harmonic operation, a self-sustaining ML is only achieved with the slit partially closed.

In order to confirm stable mode-locking, an RF spectrum (cf. Fig. 7), an optical spectrum and an autocorrelation trace (cf. Fig. 8) was performed. The resulting time bandwidth products of 0.69 (first), 0.73 (second) and 0.72 (third) reveal that the pulses are not transform limited which can be attributed to a remaining GDD caused by the VECSEL chip. Also, we obtain the peak powers 948 W for the first, 752 W for the second and 754 W for the third harmonic ML. The nearly constant peak power for the different power levels indicates that a certain intra-cavity power is needed for the underlying ML mechanism.

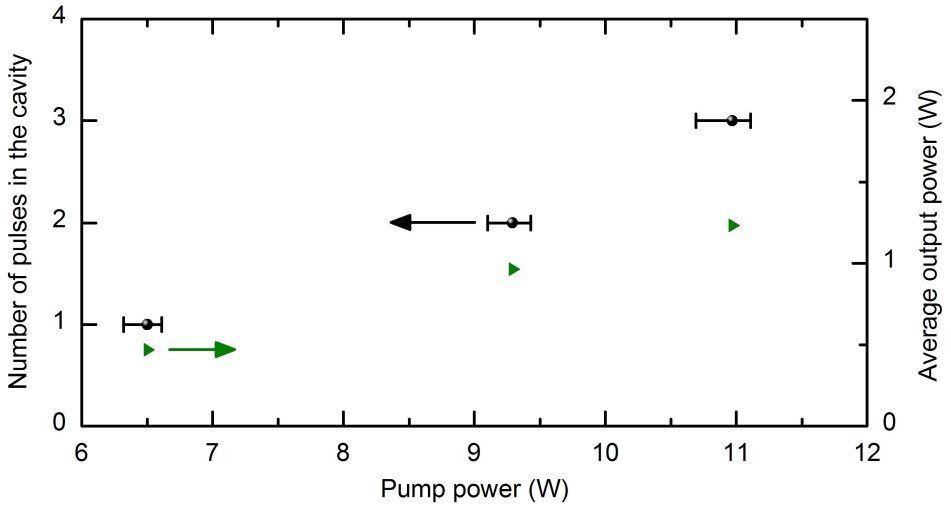


Figure 6. Number of pulses in the cavity as a function of the optical pump power (black squares, left axis). The average output power of the device is plotted with respect to the right axis (green circles).

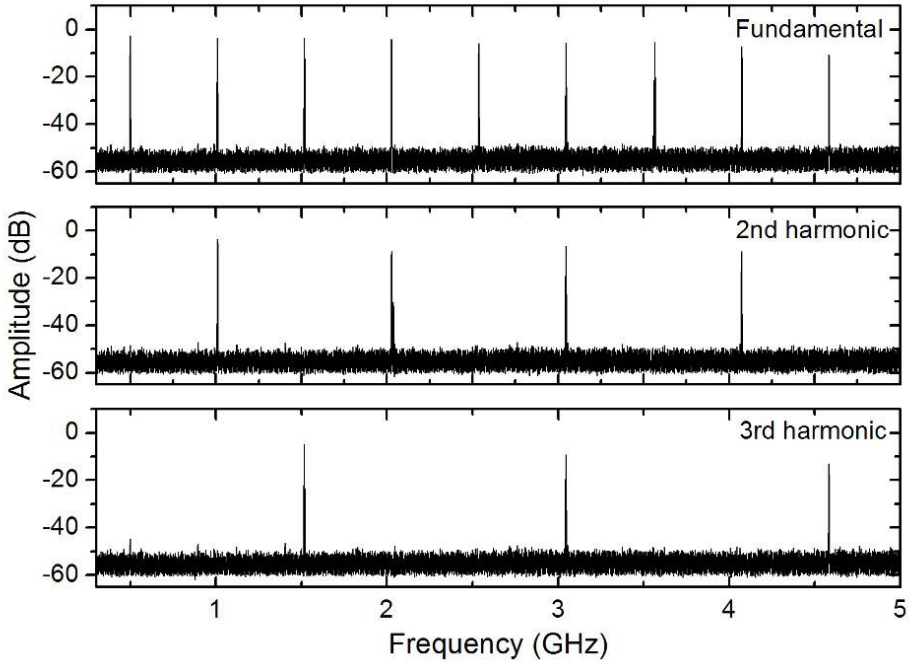


Figure 7. RF spectra reveal fundamental (top row), second harmonic (center) and third harmonic (bottom) mode-locking.

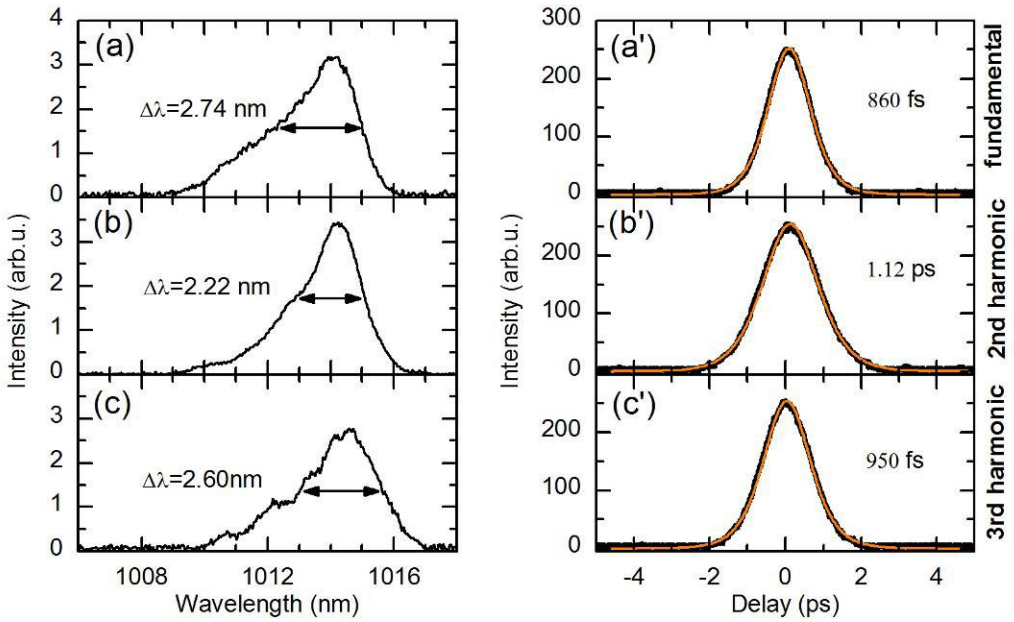


Figure 8. (a)–(c) Optical spectra for the SML VECSEL in the regimes of fundamental, second-harmonic and third-harmonic mode-locking, respectively. (a′)–(c′) Autocorrelation traces (black) with sech² fits (orange) corresponding to signal shown in (a)–(c), respectively.

### 4.3 Quantum dot VECSEL chip

In this section, we present the first passively-self-mode-locked optically-pumped QD-VECSEL. The measurements indicated sub-picosecond duration of the laser pulses in the mode-locked regime with 750mW average output power at 1.5 GHz repetition rate. The RF spectrum which was measured over a span of 6.5 GHz using a 100 kHz resolution bandwidth (RBW), is shown in Fig. 9(a). Moreover, Fig. 9(b) shows an RF spectrum of the fundamental repetition rate measured over a span of 1 MHz using a RBW of 10 kHz. Here, a clear peak at 1.5 GHz with a signal to noise ratio of about 45 dB is observed.

Fig. 10(a) presents the corresponding optical spectrum of the SML QD-VECSEL at room temperature centered at 1038 nm. The mode-locked pulse duration is yielded assuming sech² shaped pulses in the autocorrelation trace representatively shown in Fig. 10 (b). In a temperature dependence study, pulse durations varied between approximately 0.8 and 1.0 ps.

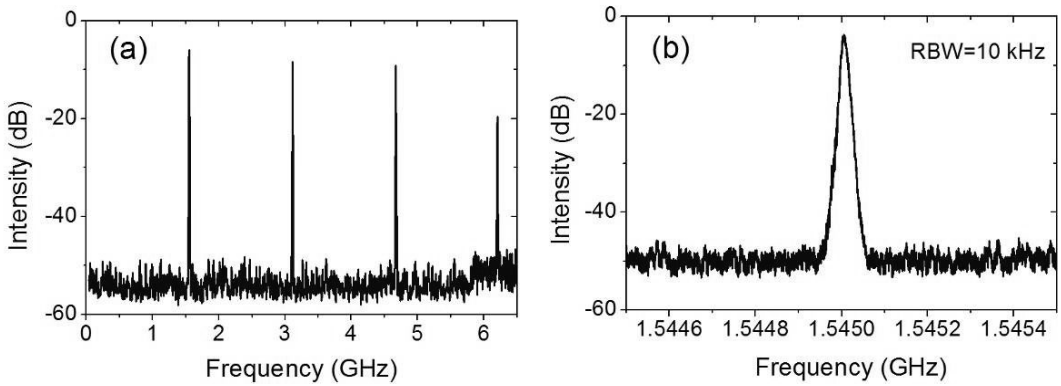


Figure 9. RF spectra measured over (a) a span of 6.5 GHz and a RBW of 100 kHz, showing the first 4 harmonics, and (b) a span of 1 MHz and a RBW of 10 kHz, with the RF signal centered around 1.545 GHz.

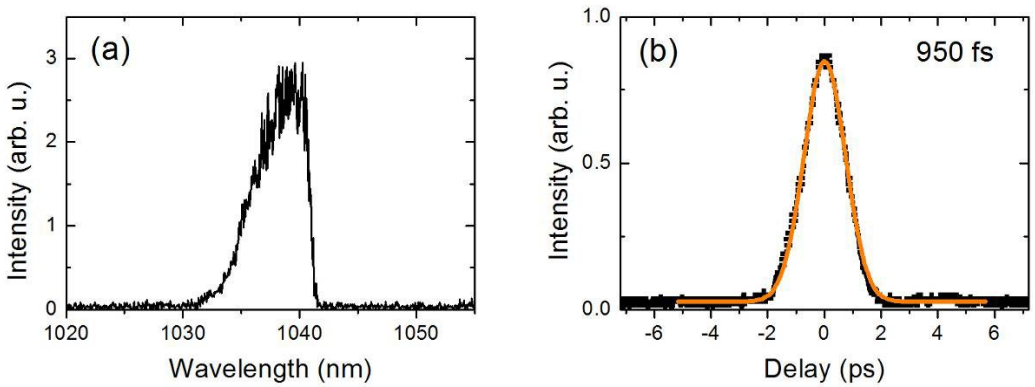


Figure 10. (a) Optical spectrum of the SML QD-VECSEL. (b) Corresponding autocorrelation trace. Black dotted: experimental data. Orange line: fit curve assuming a $sech^2$ pulse.

## 5. CONCLUSIONS

In summary, we presented recent developments in the field of semiconductor disk lasers, well known as VECSELs, which provide access to various operation modes and features for a broad wavelength range. In addition to high-power operation, frequency stabilization and frequency conversion techniques, the field of mode-locking of VECSELs gained much attraction in recent years, with the efforts of the community leading towards an alternative source for pulsed lasers. In this context, we highlight the demonstration of self-mode-locking VECSELs as a variation of mode-locked VECSELs which do not require a saturable absorber mirror for pulsed operation, and thus circumvent some limitations set by saturable absorbers. Results are presented for a quantum well and a quantum dot device to emphasize that this quite young technique, even though the mechanism behind the effect has yet not been well understood, is capable of enabling mode-locked operation for different gain media as well as cavity configurations.

## ACKNOWLEDGEMENTS

The authors acknowledge financial support by the DFG (GRK 1782 and SFB 1083) and EU FP7 program through FAST-DOT project (contract No. 224338). M. Gaafar acknowledges support from the Yousef Jameel scholarship funds. The authors would like to thank Innolume GmbH for the fabrication of the QD structures and Prof. O.G. Okhotnikov from Tampere University of Technology for the preparation of the QD-VECSELs.

## REFERENCES

[1] Kuznetsov, M., Hakimi, F., Sprague, R. and Mooradian, A., "High-power (>0.5-W CW) diode-pumped vertical-external-cavity surface-emitting semiconductor lasers with circular TEM00 beams," IEEE Photonics Technol. Lett. 9, 1063-1065 (1997).

[2] Wang, T.-L., Heinen, B., Hader, J., Dineen, C., Sparenberg, M., Weber, A., Kunert, B., Koch, S. W., Moloney, J. V., Koch, M., and Stolz, W., "Quantum design strategy pushes high-power vertical-external-cavity surface-emitting lasers beyond 100 W," Laser Photonic Rev., 6(5), L12–L14 (2012)

[3] Hader, J., Wang, T.-L., Moloney, J. V., Heinen, B., Koch, M., Koch, S. W., Kunert, B., and Stolz, W., "On the measurement of the thermal impedance in vertical-external-cavity surface-emitting lasers," J. Appl. Phys., 113(15), 153102 (2013).

[4] Heinen, B., Zhang, F., Sparenberg, M., Kunert, B., Koch, M., and Stolz, W., "On the Measurement of the Thermal Resistance of Vertical-External-Cavity Surface-Emitting Lasers (VECSELs)," IEEE J. Quantum Electron., 48(7), 934–940 (2012).

[5] Heinen, B., Wang, T. L., Sparenberg, M., Weber, A., Kunert, B., Hader, J., Koch, S. W., Moloney, J. V., Koch, M. and Stolz, W., "106 W continuous-wave output power from vertical-external-cavity surface-emitting laser," Electron. Lett. 48 (9), 516-517 (2012).
[6] Al Nakdali, D., Shakfa, M. K., Gaafar, M., Butkus, M., Fedorova, K. A., Zulonas, M., Wichmann, M., Zhang, F., Heinen, B., Rahimi-Iman, A., Stolz, W., Rafailov, E. U., and Koch M., "High-Power Quantum-Dot Vertical-External-Cavity Surface-Emitting Laser Exceeding 8 W," IEEE Photonics Technol. Lett. 26(15), 1561 (2014)
[7] Zhang, F., Heinen, B., Wichmann, W., Möller, C., Kunert, B., Rahimi-Iman, A., Stolz, W. and Koch, M., "A 23-watt single-frequency vertical-external-cavity surface-emitting laser," Opt. Express 22, 12817-12822 (2014).
[8] Wichmann, M., Shakfa, M. K., Zhang, F., Heinen, B., Scheller, M., Rahimi-Iman, A., Stolz, W., Moloney, J. V., Koch, S. W. and Koch, M., "Evolution of multi-mode operation in vertical-external-cavity surface-emitting lasers," Opt. Express 21(26) 31940 (2013).
[9] Keller, U. and Tropper, A. C., "Passively modelocked surface-emitting semiconductor lasers," Physics Reports 429, 67–120 (2006).
[10] Moloney, J.V., Kilen, I., Bäumner, A., Scheller, M., and Koch, S.W., "Nonequilibrium and thermal effects in mode-locked VECSELS," Opt. Express 22(6), 6422–6427 (2014).
[11] Chen, Y. F., Lee, Y. C., Liang, H. C., Lin, K. Y., Su, K. W. and Huang, K. F., "Femtosecond high-power spontaneous mode-locked operation in vertical-external cavity surface-emitting laser with gigahertz oscillation," Opt. Lett. 36(23), 4581–4583 (2011).
[12] Scheller, M., Yarborough, J. M., Moloney, J. V., Fallahi, M., Koch, M., and Koch, S. W., "Room temperature continuous wave milliwatt terahertz source," Opt. Express 18(26), 27112–27117 (2010).
[13] Wichmann, M., Stein, M., Rahimi-Iman, A., Koch, S. W., and Koch, M., "Interferometric Characterization of a Semiconductor Disk Laser driven Terahertz Source," J. Infrared Milli. Terahz. Waves 35(6-7), 503–508 (2014).
[14] Hoogland, S., Dhanjal, S., Tropper, A. C., Roberts, S. J., Häring, R., Paschotta, R., and Keller, U., "Passively mode-locked diode-pumped surface-emitting semiconductor laser," IEEE Photon. Technol. Lett. 12(9), 1135–1137 (2000).
[15] Wilcox, K.G., Tropper, A.C., Beere, H.E., Ritchie, D.A., Kunert, B., Heinen, B., Stolz, W., "4.35 kW peak power femtosecond pulse mode-locked VECSEL for supercontinuum generation," Opt. Express 21(2), 1599–1605 (2013)
[16] Mangold, M., Wittwer, V. J., Zaugg, C. A., Link, S. M., Golling, M., Tilma, B. W., and Keller, U., "Femtosecond pulses from a modelocked integrated external-cavity surface emitting laser (MIXSEL)," Opt. Express 21(21), 24904–24911 (2013).
[17] Zaugg, C. A., Sun, Z., Wittwer, V. J., Popa, D., Milana, S., Kulmala, T. S., Sundaram, R. S., Mangold, M., Sieber, O. D., Golling, M., Lee, Y., Ahn, J. H., Ferrari, A. C., and Keller, U., "Ultrafast and widely tuneable vertical-external-cavity surface-emitting laser, mode-locked by a graphene-integrated distributed Bragg reflector," Opt. Express 21(25), 31548–31559 (2013).
[18] Husaini, S., and Bedford, R. G., "Graphene saturable absorber for high power semiconductor disk laser mode-locking," Appl. Phys. Lett. 104(16), 161107 (2014).
[19] Seger, K., Meiser, N., Choi, S. Y., Jung, B. H., Yeom, D.-I., Rotermund, F., Okhotnikov, O., Laurell, F., and Pasiskevicius, V., "Carbon nanotube mode-locked optically-pumped semiconductor disk laser," Opt. Express 21(15), 17806–17813 (2013).
[20] Kornaszewski, L., Maker, G., Malcolm, G. P. A., Butkus, M., Rafailov, E. U. and Hamilton, C. J., "SESAM-free mode-locked semiconductor disk laser," Laser Photonics Rev. 6(6), L20–L23 (2012).
[21] Albrecht, A. R., Wang, Y., Ghasemkhani, M., Seletskiy, D. V., Cederberg, J. G. and Sheik-Bahae, M., "Exploring ultrafast negative Kerr effect for mode-locking vertical external-cavity surface-emitting lasers," Opt. Express 21(23), 28801–28808 (2013).
[22] Gaafar, M., Möller, C., Wichmann, M., Heinen, B., Kunert, B., Rahimi-Iman, A., Stolz, W. and Koch, M., "Harmonic self-mode-locking of optically pumped semiconductor disc laser," Electron. Lett. 50(7), 542–543 (2014).
[23] Gaafar, M., Al Nakdali, D., Möller, C., Fedorova, K. A., Wichmann, M., Shakfa, M. K., Zhang, F., Rahimi-Iman, A., Rafailov, E. U. and Koch, M., "Self-mode-locked quantum-dot vertical-external-cavity surface-emitting laser," Opt. Lett. 39(15), 4623–4626 (2014).
[24] Liang, H. C., Tsou, C. H., Lee, Y. C., Huang, K. F. and Chen, Y. F., "Observation of self-mode-locking assisted by high-order transverse modes in optically pumped semiconductor lasers," Laser Phys. Lett. 11, 105803 (2014).
[25] Gaafar, M., Richter, P., Keskin, H., Möller, C., Wichmann, M., Stolz, W., Rahimi-Iman, A. and Koch, M., "Self-mode-locking semiconductor disk laser," Opt. Express 22(23), 28390–28399 (2014).

# Bibliography


[1] T. H. Maiman: *Stimulated Optical Radiation in Ruby*. Nature **187** (1960) 4736, 493-494.

[2] O. Svelto: Principles of Lasers. Boston, MA: Springer US 2010.

[3] L. A. Coldren, S. W. Corzine, M. L. Mašanović: Diode Lasers and Photonic Integrated Circuits. Hoboken, NJ, USA: John Wiley & Sons 2012.

[4] W. Koechner and M. Bass: Solid-State Lasers: A Graduate Text. New York, USA: Springer 2003.

[5] W. Koechner: Solid-State Laser Engineering. New York, USA: Springer 2006.

[6] G. P. Agrawal and N. K. Dutta: Long-Wavelength Semiconductor Lasers. Van Nostrand Reinhold Co., New York 1986.

[7] W. Chow, S. W. Koch: Semiconductor Laser Fundamentals. Berlin: Springer 1999.

[8] M. A. Hadley, G. C. Wilson, K. Y. Lau, J. S. Smith: *High single-transverse mode output from external-cavity surface-emitting laser diodes*. Applied Physics Letters **63** (1993), 1607-1609.

[9] M. Kuznetsov, F. Hakimi, R. Sprague, A. Mooradian: *High-power (> 0.5-W CW) diode-pumped vertical-external-cavity surface-emitting semiconductor lasers with circular $TEM_{00}$ beams*. IEEE Photonics Technology Letters **9** (1997), 1063-1065.

[10] B. Heinen, T. L. Wang, M. Sparenberg, A. Weber, B. Kunert, J. Hader, S. W. Koch, J. V. Moloney, M. Koch, W. Stolz: *106 W continuous-wave output power from vertical-external-cavity surface-emitting laser*. Electronics Letters **48** (2012) 9, 516-517.

[11] B. Rudin, A. Rutz, M. Hoffmann, DJ. Maas, AR. Bellancourt, E. Gini, T. Südmeyer, U. Keller: *Highly efficient optically pumped vertical emitting semiconductor laser with more than 20-W average output power in a fundamental transverse mode*. Optics Letters **33** (2008) (22), 2719-2721.

[12] F. Zhang, B. Heinen, M. Wichmann, C. Möller, B. Kunert, A. Rahimi-Iman, W. Stolz, M. Koch: *A 23-watt single-frequency vertical-external-cavity surface-emitting laser*. Optics Express **22** (2014), 12817-12822.

[13] J. E. Hastie, L. G. Morton, A. J. Kemp, M. D. Dawson, A. B. Krysa, J. S. Roberts: *Tunable ultraviolet output from an intracavity frequency-doubled red vertical-external-cavity surfaceemitting laser*. Applied Physics Letters **89** (2006), 061114.

[14] J. Hastie, S. Calvez, M. Dawson, T. Leinonen, A. Laakso, J. Lyytikäinen, M. Pessa: *High power CW red VECSEL with linearly polarized $TEM_{00}$ output beam*. Optics Express **13** (2005), 77-81.

[15] H. Lindberg, A. Strassner, E. Gerster, A. Larsson: *0.8 W optically pumped vertical external cavity surface emitting laser operating CW at 1550 nm*. Electronics Letters **40** (2004), 601-602.

[16] M. Rahim, M. Arnold, F. Felder, K. Behfar, H. Zogg: *Midinfrared lead-chalcogenide vertical external cavity surface emitting laser with 5 mm wavelength*. Applied Physics Letters **91** (2007), 151102.

[17] U. Keller: *Recent developments in compact ultrafast lasers*. Nature **424** (2003), 831-838.

[18] A. H. Zewail: *Laser femtochemistry*. Science **242** (1988), 1645-1653.

[19] D. J. Jones, S. A. Diddams,J. K. Ranka, A. Stentz, R. S. Windeler, J. L. Hall, and S. T. Cundiff: *Carrier-envelope phase control of femtosecond modelocked lasers and direct optical frequency synthesis*. Science **288** (2000), 635-639.

[20] A. Apolonski, A. Poppe, G. Tempea, C. Spielmann, T. Udem, R. Holzwarth, T. W. Hänsch, and F. Krausz: *Controlling the phase evolution of few-cycle light pulses*. Physical Review Letter **85** (2000), 740-743.

[21] L. F. Mollenauer, P. V. Mamyshev, J. Gripp, M. J. Neubelt, N. Mamysheva, L. Grüner-Nielsen, T. Veng: *Demonstration of massive wavelength-division multiplexing over transoceanic distances by use of dispersion-managed solitons*. Optics Letters **25** (2000), 704-706.

[22] D. A. B. Miller: *Optical interconnects to silicon*. IEEE Journal of Selected Topics in Quantum Electronics **6** (2000), 1312-1317.

[23] S. Hoogland, S. Dhanjal, A. C. Tropper, S. J. Roberts, R. Häring, R. Paschotta, and U. Keller: Passively modelocked diode-pumped surface-emitting semiconductor laser . IEEE Photonics Technology Letters **12** (2000), 1135-1137.

[24] R. Haring, R. Paschotta, E. Gini, F. Morier-Genoud, D. Martin, H. Melchior, U. Keller: Picosecond surface-emitting semiconductor laser with $>$ 200 mW average power. Electronics Letters **37** (2001) 12, 766-767.

[25] A. Gamache, S. Hoogland, A. Trooper, I. Sagnes, G. Saint-Girons, J. S. Roberts: Sub-500-fs soliton-like pulse in a passively mode-locked broadband surface-emitting laser with 100 mW average power. Applied Physics Letters **80** (2002) 21, 3892-3894.

[26] R. Haring, R. Paschotta, A. Aschwanden, E. Gini, F. Morier-Genoud, U. Keller: High-power passively mode-locked semiconductor lasers. IEEE Journal of Quantum Electronics **38** (2002) 9, 1268-1275.

[27] S. Hoogland, A. Garnache, I. Sagnes, J. S. Roberts, A. C. Tropper: 10-GHz train of sub-500-fs optical soliton-like pulses from a surface-emitting semiconductor laser. IEEE Photonics Technology Letters **17** (2005) 2, 267-269.

[28] O. Casel, D. Woll, M. A. Tremont, H. Fuchs, R. Wallenstein, E. Gerster, P. Unger, M. Zorn, M. Weyers: Blue 489-nm picosecond pulses generated by intracavity frequency doubling in a passively mode-locked optically pumped semiconductor disk laser. Applied Physics B **81** (2005) 4, 443-446.

[29] H. Lindberg, M. Sadeghi, M. Westlund, S. Wang, A. Larsson, M. Strassner, S. Marcinkevicius: Mode locking a 1550 nm semiconductor disk laser by using a GaInNAs saturable absorber. Optics Letters **30** (2005) 20, 2793-2795.

[30] A.Aschwanden, D. Lorenser, HJ. Unold, R. Paschotta, E. Gini, U. Keller: 2.1-W picosecond passively mode-locked external-cavity semiconductor laser. Optics Letters **30** (2005), 272-274.

[31] P. Klopp, U. Griebner, M. Zorn, M. Weyers: Pulse repetition rate up to 92 GHz or pulse duration shorter than 110 fs from a mode-locked semiconductor disk laser. Applied Physics Letters **98** (2011) 7, 071103-071103.

[32] J. Rautiainen, J. Lyytikainen, L. Toikkanen, J. Nikkinen, A. Sirbu, A. Mereuta, A. Caliman, E. Kapon, O. G. Okhotnikov: 1.3 $\mu$m Mode-Locked Disk Laser with Wafer Fused Gain and SESAM Structures. IEEE Photonics Technology Letters **22** (2010) 11, 748-750.

[33] Z. Zhao, S. Bouchoule, J. Y. Song, E. Galopin, J.-C. Harmand, J. Decobert, G. Aubin,

J.-L. Oudar: Subpicosecond pulse generation from a 1.56 $\mu$m mode-locked VECSEL. Optics Letters **36** (2011) 22, 4377-4379.

[34] M. Scheller, T. L. Wang, B. Kunert, W. Stolz, S. W. Koch, J. V. Moloney: Passively mode-locked VECSEL emitting 682 fs pulses with 5.1 W of average output power. Electronics Letters **48** (2012) 10, 588-U123.

[35] R. Bek, H. Kahle, T. Schwarzbäck, M. Jetter, P. Michler: Mode-locked red-emitting semiconductor disk laser with sub-250 fs pulses. Applied Physics Letters **103** (2013), 242101.

[36] K. G. Wilcox, A. C. Tropper, H. E. Beere, D. A. Ritchie, B. Kunert, B. Heinen, W. Stolz: 4.35 kW peak power femtosecond pulse mode-locked VECSEL for supercontinuum generation. Optics Express **21** (2013) 2, 1599-1605.

[37] C. A. Zaugg, A. Klenner, M. Mangold, A. S. Mayer, S. M. Link, F. Emaury, M. Golling, E. Gini, C. J. Saraceno, B. W. Tilma, U. Keller: Gigahertz self-referenceable frequency comb from a semiconductor disk laser. Optics Express **22** (2014) 13, 1332-1334.

[38] D. Lorenser, H. J. Unold, D. J. H. C. Maas, A. Aschwanden, R. Grange, R. Paschotta, D. Ebling, E. Gini, U. Keller: Towards wafer-scale integration of high repetition rate passively mode-locked surface-emitting semiconductor lasers. Applied Physics B **79** (2004) 8, 927-932.

[39] D. Lorenser, D. J. H. C. Maas, H. J. Unold, A. R. Bellancourt, B. Rudin, E. Gini, D. Ebling, U. Keller: 50-GHz passively mode-locked surface-emitting semiconductor laser with 100-mW average output power. IEEE Journal of Quantum Electronics **42** (2006) 7, 838-847.

[40] K. G. Wilcox, M. Butkus, I. Farrer, D. A. Ritchie, A. Tropper, E. U. Rafailov: Subpicosec-

ond quantum dot saturable absorber mode-locked semiconductor disk laser. Applied Physics Letters **94** (2009) 25, 251105.

[41] M. Hoffmann, O. D. Sieber, D. J. H. C. Maas, V. J. Wittwer, M. Golling, T. Südmeyer, U. Keller: Experimental verification of soliton-like pulse-shaping mechanisms in passively mode-locked VECSELs. Optics Express **18** (2010) 10, 10143-10153.

[42] C. A. Zaugg, M. Hoffmann, W. P. Pallmann, V. J. Wittwer, O. D. Sieber, M. Mangold, M. Golling, K. J. Weingarten, B. W. Tilma, T. Südmeyer, U. Keller: Low repetition rate SESAM modelocked VECSEL using an extendable active multipass-cavity approach. Optics Express **20** (2012) 25, 27915-27921.

[43] M. Butkus, E. A. Viktorov, T. Erneux, C. J. Hamilton, G. Maker, G. P. A. Malcolm, E. U. Rafailov: 85.7 MHz repetition rate mode-locked semiconductor disk laser: fundamental and soliton bound states. Optics Express **21** (2013) 21, 25526-25531.

[44] M. Hoffmann, Y. Barbarin, D. Maas, M. Golling, I. L. Krestnikov, S. S. Mikhrin, A. R. Kovsh, T. Südmeyer, U. Keller: Modelocked quantum dot vertical external cavity surface emitting laser. Applied Physics B **93** (2008) 4, 733-736.

[45] O. D. Sieber, M. Hoffmann, V. J. Wittwer, M. Mangold, M. Golling, B. W. Tilma, T. Südmeyer, U. Keller: Experimentally verified pulse formation model for high-power femtosecond VECSELs. Applied Physics B **113** (2013) 1, 133-145.

[46] M. Hoffmann, O. D. Sieber, V. J. Wittwer, I. L. Krestnikov, D. A. Livshits, Y. Barbarin, T. Südmeyer, U. Keller: Femtosecond high-power quantum dot vertical external cavity surface emitting laser. Optics Express **19** (2011) 9, 8108-8116.

[47] R. Bek, G. Kersteen, H. Kahle, T. Schwarzbäck, M. Jetter, P. Michler: All quantum dot mode-locked semiconductor disk laser emitting at 655 nm. Applied Physics Letters **105** (2014), 082107.

[48] D. J. H. C. Maas, A.-R. Bellancourt, B. Rudin, M. Golling, H. J. Unold, T. SÃijdmeyer, U. Keller: Vertical integration of ultrafast semiconductor lasers. Applied Physics B **88** (2007) 4, 493-497.

[49] B. Rudin, V. J. Wittwer, D. J. H. C. Maas, M. Hoffmann, O. D. Sieber, Y. Barbarin, M. Golling, T. Südmeyer, U. Keller: High-power MIXSEL: an integrated ultrafast semiconductor laser with 6.4 W average power. Optics Express **18** (2010) 26, 27582-27588.

[50] V. J. Wittwer, M. Mangold, M. Hoffmann, O. D. Sieber, M. Golling, T. Südmeyer, U. Keller: High-power integrated ultrafast semiconductor disk laser: multi-Watt 10 GHz pulse generation. Electronics Letters **48** (2012) 18, 1144-1145.

[51] M. Mangold, V. J. Wittwer, C. A. Zaugg, S. M. Link, M. Golling, B. W. Tilma, U. Keller: Femtosecond pulses from a modelocked integrated external-cavity surface emitting laser (MIXSEL). Optics Express **21** (2013) 21, 24904-24911.

[52] M. Mangold, C. A. Zaugg, S. M. Link, M. Golling, B. W. Tilma, U. Keller: Pulse repetition rate scaling from 5 to 100 GHz with a high-power semiconductor disk laser. Optics Express **22** (2014) 5, 6099-6107.

[53] C. A. Zaugg, Z. Sun, V. J. Wittwer, D. Popa, S. Milana, T. S. Kulmala, R. S. Sundaram, M. Mangold, O. D. Sieber, M. Golling, Y. Lee, J. H. Ahn, A. C. Ferrari, U. Keller: Ultrafast and widely tunable vertical-external-cavity surface-emitting laser, mode-locked by a graphene-integrated distributed Bragg reflector. Optics Express 21 (2013) **25**, 31548-31559.

[54] S. Husaini, R. G. Bedford: Graphene saturable absorber for high power semiconductor disk laser mode-locking. Applied Physics Letters **104** (2014) 16, 161107.

[55] K. Seger, N. Meiser, S. Y. Choi, B. H. Jung, D.-I. Yeom, F. Rotermund, O. Okhotnikov,

F. Laurell, V. Pasiskevicius: Carbon nanotube mode-locked optically-pumped semiconductor disk laser. Optics Express 21 (2013) **15**, 17806-17813.

[56] Y. F. Chen, Y. C. Lee, H. C. Liang, K. Y. Lin, K. W. Su, K. F. Huang: *Femtosecond high-power spontaneous mode-locked operation in vertical-external cavity surface-emitting laser with gigahertz oscillation*. Optics Letters **36** (2011) 23, 4581-4583.

[57] L. Kornaszewski, G. Maker, G. P. A. Malcolm, M. Butkus, E. U. Rafailov, C. J. Hamilton: *SESAM-free mode-locked semiconductor disk laser*. Laser and Photonics Review **6** (2012) 6, L20-L23 .

[58] A. R. Albrecht, Y. Wang, M. Ghasemkhani, D. V. Seletskiy, J. G. Cederberg, M. Sheik-Bahae: *Exploring ultrafast negative Kerr effect for mode-locking vertical external-cavity surface-emitting lasers*. Optics Express **21** (2013) 23, 28801-28808 .

[59] M. Gaafar, C. Möller, M. Wichmann, B. Heinen, B. Kunert, A. Rahimi-Iman, W. Stolz, M. Koch: *Harmonic self-mode-locking of optically pumped semiconductor disc laser*. Electronics Letters **50** (2014) 7, 542-543.

[60] J. V. Moloney, I. Kilen, A. Bäumner, M. Scheller, S. W. Koch: *Nonequilibrium and thermal effects in modelocked VECSELS*. Optics Express **22** (2014) 6, 6422-6427.

[61] H. C. Liang, C. H. Tsou, Y. C. Lee, K. F. Huang, Y. F. Chen: *Observation of self-mode-locking assisted by high-order transverse modes in optically pumped semiconductor lasers*. Laser Physics Letters **11** (2014), 105803.

[62] M. Gaafar, P. Richter, H. Keskin, C. Möller, M. Wichmann, W. Stolz, A. Rahimi-Iman, M. Koch: *Self-mode-locking semiconductor disk laser*. Optics Express **22** (2014) 23, 28390âĂŞ28399.

[63] M. Gaafar, D. Al Nakdali, C. Möller, Ksenia A. Fedorova, M. Wichmann, M. K. Shakfa,

F. Zhang, A. Rahimi-Iman, E. U. Rafailov, M. Koch: *Self-mode-locked quantum-dot vertical-external-cavity surface-emitting laser*. Optics Letters **39** (2014) 15, 4623-4626.

[64] K. G. Wilcox, A. C. Tropper: *Comment on SESAM-free mode-locked semiconductor disk laser*. Laser and Photonics Review **7** (2013) 3, 422-423.

[65] L. Kornaszewski, G. Maker, G. P. A. Malcolm, M. Butkus, E. U. Rafailov, C. J. Hamilton: *Reply to comment on SESAM-free mode-locked semiconductor disk laser*. Laser and Photonics Review **7** (2013) 4, 555-556.

[66] M. Kuznetsov, F. Hakimi, R. Sprague, A. Mooradian: *Design and characteristics of high-power (>0.5-W CW) diode-pumped vertical external- cavity surface emitting semiconductor lasers with circular $TEM_{00}$ beams*. IEEE Journal of Selected Topics in Quantum Electronics **5** (1999), 561-573.

[67] L. J. Mawst, A. Bhattacharya, J. Lopez, D. Botez, D. Z. Garbuzov, L. DeMarco, J. C. Connolly, M. Jansen, F. Fang, R. F. Nabiev: *8 W continuous wave front-facet power from broad-waveguide Al-free 980 nm diode lasers*. Applied Physics Letters **69** (1996), 1532-1534.

[68] A. Al-Muhanna, L. J. Mawst, D. Botez, D. Z. Garbuzov, R. U. Martinelli, J. C. Connolly: *High-power (> 10 W) continuous-wave operation from 100 $\mu$m aperture 0.97 $\mu$m emitting Al-free diode lasers*. Applied Physics Letters **73** (1998), 1182-1184.

[69] A. Haglund, J. S. Gustavsson, J. Vukusic, P. Modh, A. Larsson: *Single fundamental-mode output power exceeding 6 mW from VCSELs with a shallow surface relief*. IEEE Photonics Technology Letters **16** (2004), 368-370.

[70] E. Innerhofer, T. Sudmeyer, F. Brunner, R. Häring, A. Aschwanden, R. Paschotta, C. Honninger, M. Kumkar, U. Keller: *60-W average power in 810-fs pulses from a thin-disk Yb:YAG laser*. Optics Letters **28** (2003), 367-9.

[71] A. Giesen, H. Hügel, A. Voss, K. Wittig, U. Brauch, H. Opower: *Scalable concept for diode-pumped high-power solid-state lasers*. Applied Physics B: Lasers and Optics **58** (1994) 5, 365-372.

[72] A. Giesen, J. Speiser: *Fifteen years of work on thin-disk lasers: results and scaling laws*. IEEE Journal of Selected Topics in Quantum Electronics **13** (2007) 3, 598-609.

[73] M. Arrigoni, B. Morioka, A. Lepert: *Optically pumped semiconductor lasers: Green OPSLs poised to enter scientific pump-laser market*. Laser FocusWorld, Oct. 2009.

[74] E. U. Rafailov, M. A. Cataluna, W. Sibbett: *Mode-locked quantum-dot lasers*. Nature Photonics **1** (2007), 395-401.

[75] T. Schwarzbäck, R. Bek, F. Hargart, C. A. Kessler, H. Kahle, E. Koroknay, M. Jetter, P. Michler: *High-power InP quantum dot based semiconductor disk laser exceeding 1.3 W*. Applied Physics Letters **102** (2013) 9, 092101-1-092101-4.

[76] A. Rantamäki, J. Rautiainen, L. Toikkanen, I. Krestnikov, M. Butkus, E. U. Rafailov, O. Okhotnikov: *Flip chip quantum-dot semiconductor disk laser at 1200 nm*. IEEE Photonics Technology Letters **24** (2012) 15, 1292-1294.

[77] J. A. Lott, A. R. Kovsh, N. N. Ledentsov, D. Bimberg: *GaAs-based InAs/InGaAs quantum dot vertical cavity and vertical external cavity surface emitting lasers emitting near 1300 nm*. Pacific Rim conference on lasers and electro-optics, CLEO/Pacific Rim (2005), 160-161.

[78] M. Butkus, C.J. Hamilton, J. Rautiainen, O.G. Okhotnikov, S.S. Mikhrin, I.L. Krestnikov, E.U. Rafailov: *Broadly tunable 1250 nm quantum dot-based semiconductor disk laser*. IET Optoelectronics **5** (2011), 165-167.

[79] M. Butkus, J. Rautiainen, O. G. Okhotnikov, C. J. Hamilton, G. P. A. Malcolm, S. S. Mikhrin, I. L. Krestnikov, D. A. Livshits, E. U. Rafailov: *Quantum dot based semiconductor*

*disk lasers for 1-1.3 $\mu m$*. IEEE Journal of Selected Topics in Quantum Electronics, **17** (2011) 6, 1763-1771.

[80] D. Al Nakdali, M. K. Shakfa, M. Gaafar, M. Butkus, K. A. Fedorova, M. Zulonas, M. Wichmann, F. Zhang, B. Heinen, A. Rahimi-Iman, W. Stolz, E. U. Rafailov, M. Koch: *High-power quantum-dot vertical-external-cavity surface-emitting laser exceeding 8 W*. IEEE Photonics Technology Letters **26** (2014) 15, 1561-1564.

[81] J. Rautiainen, I. Krestnikov, J. Nikkinen, O. G. Okhotnikov: *2.5 W orange power by frequency conversion from a dual-gain quantum-dot disk laser*. Optics Letters **35** (2010) 12, 1935-1937.

[82] N. Schulz, JM. Hopkins, M. Rattunde, D. Burns, J. Wagner: High-brightness long-wavelength semiconductor disk lasers. Laser and Photonics Review **2** (2008) 3, 160-181.

[83] S. Calvez, J. E. Hastie, M. Guina, O. G. Okhotnikov, M. D. Dawson:*Semiconductor disk lasers for the generation of visible and ultraviolet radiation*. Laser and Photonics Review **3** (2009), 407-434.

[84] O. G. Okhotnikov: Semiconductor Disk Lasers: Physics and Technology, ED. Weinheim: Wiley-VCH 2010.

[85] A. Härkonen: Optically-Pumped Semiconductor Disk Lasers for Generating visible and Infrared Radiation, Ph.D. dissertation, Tampere University of technology, Tampere, Finland, 2008.

[86] M. Butkus: Quantum Dot Based Semiconductor Disk Lasers, Ph.D. dissertation, University of Dundee, England, 2012.

[87] D. Babic, S. Corzine: *Analytic expressions for the reflection delay, penetration depth, and ab-*

*sorptance of quarter-wave dielectric mirrors*. IEEE Journal of Quantum Electronics **28** (1992) 2, 514-524.

[88] A. C. Tropper, S. Hoogland: *Extended cavity surface-emitting semiconductor lasers*. Progress in Quantum Electronics **30** (2006), 1-43.

[89] C. Borgentun, J. Bengtsson, A. Larsson, F. Demaria, A. Hein, P. Unger: *Optimization of a broadband gain element for a widely tunable high-power semiconductor disk laser*. IEEE Photonics Technology Letters **22** (2010) 13, 978-980.

[90] R. Bedford, M. Kolesik, J. Chilla, M. Reed, T. Nelson, J. Moloney: *Power-limiting mechanisms in VECSELs*. Proc. SPIE, **5814** (2005), 199-208.

[91] E. Kuhn, A. Thranhardt, C. Buckers, S. W. Koch, J. Hader, J. Moloney: *Numerical study of the influence of an antireflection coating on the operating properties of vertical-external-cavity surface-emitting lasers*. Journal of Applied Physics **106** (2009) 6, 063105.

[92] N. Schulz, M. Rattunde, C. Ritzenthaler, B. Rosener, C. Manz, K. Kohler, J. Wagner: *Effect of the cavity resonance-gain offset on the output power characteristics of GaSb-based VECSELs*. IEEE Photonics Technology Letters **19** (2007) 21, 1741-1743.

[93] T.-L. Wang, Y. Kaneda, J. Hader, J. Moloney, B. Kunert, W. Stolz, S. Koch: *Strategies for power scaling VECSELs*. Proceedings of SPIE, **8242** (2012), 8242091-8242098.

[94] Z. Liau: *Semiconductor wafer bonding via liquid capillarity*. Applied Physics Letters **77** (2000) 5, 651âĂŞ653.

[95] T. Udem, R. Holzwarth, T. W. Hänsch: *Optical frequency metrology*. Nature(2002)

[96] F. J. McClung, R. W. Hellwarth: *Giant optical pulsations from ruby*. Applied Optics (1962)

[97] M. DiDomenico: *Small-Signal Analysis of Internal (Coupling-Type) Modulation of Lasers*. Journal Of Applied Physics (1964).

[98] L. E. Hargrove, R. L. Fork, M. A. Pollack: *Locking of NeNe laser modes induced by synchronous intracavity modulation*. Applied Physics Letters **5** (1964).

[99] A. Yariv: *Internal modulation in multimode laser oscillators*. Journal Of Applied Physics (1965)

[100] U. Keller, A. C. Tropper: *Passively modelocked surface-emitting semiconductor lasers*. Physics Reports **429** (2006), 67-120.

[101] U. Keller, G. W. Hooft, W. H. Knox, J. E. Cunningham: *Femtosecond Pulses from a Continuously Self-Starting Passively Mode-Locked Ti:Sapphire Laser*. Optics Letters **16** (1991),1022-1024.

[102] T. Brabec, C. Spielmann, P. F. Curley, F. Krausz: *Kerr lens mode locking*. Optics Letters **17** (1992), 1292-1294.

[103] R. Ell, U. Morgner, F. X. Kärtner, J. G. Fujimoto,E. P. Ippen, V. Scheuer, G. Angelow, T. Tschudi, M. J. Lederer, A. Boiko, B. Luther-Davies: *Generation of 5-fs pulses and octave-panning spectra directly from a Ti:sapphire laser*. Optics Letters **26** (2001), 373-375.

[104] L. Gallmann, D. H. Sutter, N. Matuschek, G. Steinmeyer, U. Keller, C. Iaconis, I. A. Walmsley: *Characterization of sub-6-fs optical pulses with spectral phase interferometry for direct electric field reconstruction*. Optics Letters **24** (1999), 1314-1316.

[105] R. Paschotta, U. Keller: *Passive mode locking with slow saturable absorbers*. Applied Physics B **73** (2001), 653âĂŞ662.

[106] A. Agnesi, A. Greborio, F. Pirzio, G. Reali, J. Aus der Au, A. Guandalini: *40-fs Yb3+:CaGdAlO4 laser pumped by a single-mode 350-mW laser diode*. Optics Express **20** (2012), 10077-10082.

[107] R. Paschotta, R. H**a**ring, U. Keller, A. Garnache, S. Hoogland, A. C. Tropper: *Soliton-like pulse-shaping mechanism in passively mode-locked surface-emitting semiconductor lasers*. Applied Physics B **75** (2002), 445-451.

[108] A. H. Quarterman, K. G. Wilcox, V. Apostolopoulos, Z. Mihoubi, S. P. Elsmere, I. Farrer, D. A. Ritchie, A. Tropper: *A passively mode-locked external-cavity semiconductor laser emitting 60-fs pulses*. Nature Photonics **3** (2009), 729-731.

[109] K. G. Wilcox, A. H. Quarterman, Harvey Beere, D. A. Ritchie, A. C. Tropper: *High Peak Power Femtosecond Pulse Passively Mode-Locked Vertical-External-Cavity Surface-Emitting Laser*. IEEE Photonics Technology Letters 22 (2010) 14, 1021-1023.

[110] S. Hoogland, A. Garnache, I. Sagnes, J. S. Roberts, A. C. Tropper: *10-GHz train of sub-500-fs optical soliton-like pulses from a surface-emitting semiconductor laser*. IEEE Photonics Technology Letters **17** (2005),267-269.

[111] P. Klopp, U. Griebner, M. Zorn, A. Klehr, A. Liero, M. Weyers, G. Erbert: *Mode-locked InGaAs-AlGaAs disk laser generating sub-200-fs pulses, pulse picking and amplification by a tapered diode amplifier*. Optics Express **17** (2009) 13, 10820-10834.

[112] E. Saarinen, A. Härkonen, R. Herda, S. Suomalainen, L. Orsila, T. Hakulinen, M. Guina, O. G. Okhotnikov: *Harmonically mode-locked VECSELs for multi-GHz pulse train generation*. Optics Express **15** (2007) 3, 955-964.

[113] E. Saarinen, R. Herda, O. G. Okhotnikov: *Dynamics of pulse formation in mode-locked semiconductor disk lasers*. Journal of the Optical Society of America B **24** (2007) 11, 2784-2790.

[114] D. Lorenser, H.J. Unold, D.J.H.C. Maas, A. Aschwanden, R. Grange, R. Paschotta, D. Ebling, E. Gini, U. Keller: *Towards wafer-scale integration of high repetition rate passively mode-locked surface-emitting semiconductor lasers*. Applied Physics B **79** (2004) 8, 927-932.

[115] C. H. Henry: *Theory of the linewidth of semiconductor lasers*. IEEE Journal of Quantum Electronics **18** (1982), 259-264.

[116] O. SIEBER: Scaling high-power ultrafast VECSELs into the femtosecond regime, Ph.D. dissertation, ETH Zurich, 2013.

[117] M. Hoffmann, O. D. Sieber, D. J. H. C. Maas, V. J. Wittwer, M. Golling, T. Südmeyer, U. Keller: *Experimental verification of soliton-like pulse-shaping mechanisms in passively mode-locked VECSELs*. Optics Express **18** (2010), 10143-10153.

[118] O. D. Sieber, M. Hoffmann, V. J. Wittwer, M. Mangold, M. Golling, B. W. Tilma, T. Südmeyer, U. Keller: *Experimentally verified pulse formation model for high-power femtosecond VECSELs*. Applied Physics B, **27** (2013), 1-13.

[119] A. H. Quarterman, M. A. Tyrk, K. G. Wilcox: *Z-scan measurements of the nonlinear refractive index of a pumped semiconductor disk laser gain medium*. Applied Physics Letters **106** (2015), 011105.

# Scientific carrier

## Personal data

| | |
|---|---|
| Name | Mahmoud Gaafar |
| Date of birth | 08.09.1987 |
| Place of birth | Beheira-Egypt |

## Education

*May 2012-November 2015*

PhD at the department of Physics and material sciences center, Philipps-University of Marburg, Marburg-Germany.

*September 2009-March 2012*

M. Sc. at the department of Physics, Menoufiya University-Shebin El Kom, Egypt.

*September 2010-December 2011*

Diploma at Bogoliubov Laboratory of Theoretical Physics (BLTP), Dubna, Moscow region, Russia.

*September 2004-May 2008*

B. Sc. at the department of Physics, Menoufiya University-Shebin El Kom, Egypt.